INTERACTION OF QUINOLONE ANTIBIOTICS
WITH THE HUMAN INTESTINAL CACO-2 CELL MODEL

MANJINDER SINGH KANG

Doctor of Philosophy

ASTON UNIVERSITY

March 2001

1

Aston University

INTERACTION OF QUINOLONE ANTIBIOTICS
WITH THE HUMAN INTESTINAL CACO-2 CELL MODEL
by
Manjinder Singh Kang
Submitted for the degree of Doctor of Philosophy, 2001

THESIS SUMMARY

The transport of a group of quinolone antibiotics across the human intestinal model, Caco-2 cells, was investigated. It was found that the transport of the quinolones generally correlated with the lipophilicity of the compounds, indicating that passive diffusional transcellular processes were involved. However, it was observed that the transport in both directions apical-to-basolateral and basolateral-to-apical was not equivalent, and polarised transport occurred. For all the quinolones studied except, BMS-284756-01, it was found that the basolateral-to-apical transport was significantly greater than the apical-to-basolateral transport. This finding suggested that the quinolones underwent a process of active secretion.

The pK_as and logPs for the quinolones were determined using potentiometric titrations. The measured logP values were compared with those determined using theoretical methods. The theoretical methods for calculating logP including the Moriguchi method correlated poorly with the measured logP values.

Further investigations revealed that there maybe an active transporter involved in the apical-to-basolateral transport of quinolones as well. This mechanism was sensitive to competing quinolones, but, it was unaffected by the metabolic inhibitor combination of sodium azide (15 mM) with 2-deoxy-D-glucose (50 mM).

The basolateral-to-apical transport of quinolones was found to be sensitive to inhibition by a number of different inhibitors. The metabolic inhibitors, sodium azide (15 mM) with 2-deoxy-D-glucose (50 mM) and 2,4-dinitrophenol (1 mM), were able to reduce the basolateral-to-apical transport of the quinolones. A reduction in temperature from 37°C to 2°C caused an 80-fold decrease in the transport of gatifloxacin in both directions, however, this effect was not sufficient to abolish the greater basolateral-to-apical secretion. As with apical-to-basolateral transport, it was found that quinolones competed with gatifloxacin for basolateral-to-apical transport, both ofloxacin (100 µM) and norfloxacin (100 µM) significantly (P<0.003) decreased the basolateral-to-apical transport of gatifloxacin; however, ciprofloxacin (100 µM and 300 µM) had no effect.

A number of inhibitors of various transport systems were also investigated. It was found that the anion transport inhibitor, probenecid (100 µM) had a significant inhibitory effect on the basolateral-to-apical transport of ciprofloxacin (P=0.039), while the cation transport inhibitor cimetidine (100 µM and 500 µM) had no effect. The organic anion exchange inhibitor 4,4'-diisothiocyanostilbene-2-2'-disulphonic acid DIDS (400 µM) also had a significant inhibitory effect (P=0.013). The PgP inhibitor and anion exchange inhibitor verapamil (400 µM) was able to completely abolish the basolateral-to-apical secretion of gatifloxacin and bring it into line with the apical-to-basolateral flux. In conclusion, the apical-to-basolateral and basolateral-to-apical transport of quinolones involved an active component. The basolateral-to-apical secretion was abolished by a verapamil (400 µM), a bisubstrate for PgP and the anion transporter.

Keywords: Quinolones, Caco-2 cells, active secretion; PgP, BMS-284756-01, gatifloxacin, lipophilicity, logP, pK_a, molecular modelling.

ਮੇਰੇ ਪਿਆਰੇ ਮਾਤਾ ਅਤੇ ਪਿਤਾ ਵਾਸਤੇ

To my beloved parents

ACKNOWLEDGEMENTS

TABLE OF CONTENTS

TABLE OF FIGURES

TABLE OF TABLES

ABBREVIATIONS

%	Percentage
°C	Degrees Celsius
Å	Angstrom
ABC	ATP Binding cassette
ANOVA	Analysis of variance
ATP	Adenosine triphosphate
ATTC	American Type Tissue Culture Collection
C_d	Concentration in donor compartment
CFTR	Cystic Fibrosis Transmembrane Receptor
cm^2	$(centimetre)^2$
cMOAT	canalicular multispecific organic anion transporter
CO_2	Carbon dioxide
CSF	Cerebrospinal fluid
CYP3A	Cytochrome P450 3A
Da	Daltons
DIDS	4,4'-Diisothiocyanostilbene-2-2'-disulphonic acid
DMEM	Dulbecco's modified Eagle's medium
DMSO	Dimethylsulphoxide
DNA	Deoxyribonucleic acid
DPM	Disintegrations *per* minute
DTS	Di-tri-peptide transporter
EDTA	Ethylenediaminetetraacetic acid
FBS	Foetal bovine serum
$g.L^{-1}$	Grams *per* litre
H_2O	Water
HCl	Hydrochloric acid
HEPES	N-2-hydroxyethylpiperazine-N'-2-ethansulphonic acid
HPLC	High-Performance Liquid Chromatography
IS	3,4,-dimethoxybenzaldehyde
IV	Intravenous
K	Retention Capacity
K_d	Diffusion rate constant
kDa	Kilo Daltons
K_m	Michaelis-Menton constant
K_o	Corrected Retention Capacity
KOH	Potassium hydroxide
LLC-PK$_1$	Pig-kidney epithelial cell line
LogD	Partition coefficient at a particular pH
LogK_o	Partition coefficient based on corrected retention capacity
LogP	Partition coefficient
LPS	Lipopolysaccharides
M	Molar
MBq	Mega Bequeral
MDCKI	Dog-renal epithelial cell line
MDCKII	Dog-renal epithelial cell line
mdr1	Multidrug resistance gene one
mdr2	Multidrug resistance gene two

MES	2-[N-morpholino]ethanesulphonic acid
MIC	Minimum inhibitory concentration
mL	Millilitre
mM	Millimolar
mol	Mole
MRP1	Multiple drug resistance protein
NEAA	Non-essential amino acids
nM	Nanomolar
ODS	Octadecyl-silane
P450	Cytochrome P450
P_{app}	Apparent permeability
PBS	Phosphate buffered saline
PgP	P-glycoprotein
pH	Negative logarithm of hydrogen ion concentration
P_i	Isoelectric point
PK_a	Negative logarithm of dissociation constant
p_sK_a	Apparent negative logarithm of dissociation constant
QSAR	Quantitative Structure Activity Relationship
r^2	Correlation coefficient
SD	Standard deviation
SEM	Scanning electron microscopy
SI	3,4,-dimethoxybenzoic acid
TEER	Transepithelial electrical resistance
UWL	Unstirred water layer
V_{max}	Maximum rate of transport
ΔH_f	Enthalpy of formation
Ω	Ohm
μM	Micromolar
μm	Micrometre

CHAPTER 1 GENERAL INTRODUCTION

1.1 SUMMARY

This chapter provides an overview of the absorption processes involved in the uptake of drugs delivered orally. An initial outline of the physiology of the gastrointestinal tract and the transport mechanisms found within it, for absorption and efflux of drug compounds are described. The role of different cellular models is discussed in the context of oral drug delivery, as well as the different modes of transport an orally absorbed drug compound may use. The focus then moves to the use of Caco-2 cell culture models as a model of oral drug absorption. The remainder of the chapter discusses the quinolones, a group of antibiotics, the absorption of these compounds was investigated as well as the active intestinal secretion using the Caco-2 cells models.

1.2 BACKGROUND

The discovery and development of novel orally active compounds is usually a lengthy process taking 10 to 15 years and is very expensive costing as much as $250 million. The search for new pharmacologically active compounds in drug discovery programmes places much emphasis upon optimising activity. Potential problems, such as absorption, may frequently cause compounds to be rejected. As a result, compounds which are poorly absorbed constitute a major reason for the low success rate for drug candidates in clinical development. Since the cost of drug development is significantly larger than the cost of drug discovery, predictive methodologies aiding in the selection of orally bioavailable drug candidates at the drug discovery stage would have significant cost and time-saving implications (Palm and Luthman, 1996). The early identification of drug delivery problems have led to an interest in the use of *in vitro* systems to assess the potential for drug absorption (Rubas and Cromwell, 1996).

Factors affecting bioavailability of drugs generally fall into three categories:

(I)   Physiological factors which include gastric motility, surface area of administration site, intestinal secretions, enzymes (cytochrome P450),

membrane permeability, efflux mechanisms (PgP), disease-state and presence of food.

(II)   Physicochemical properties of the drug which include, solubility, pK_a, lipophilicity and particle size.

(III)   Performances of the dosage form, for example the effectiveness of a controlled-release formulation and the rate of dissolution of an oral dosage form.

In order to understand the problems of oral drug absorption, knowledge of the barriers which drug compounds must overcome needs to be established together with an understanding of the function and structure of the gastrointestinal tract.

1.3   PHYSIOLOGY OF THE GASTROINTESTINAL TRACT

1.3.1   INTRODUCTION

The gastrointestinal tract consists of the mouth, pharynx and oesophagus, stomach, small intestine, large intestine and rectum. Normally little absorption takes place in the mouth, the pharynx and oesophagus or the stomach (See figure 1.1). The exceptions to the general case include sublingual and buccal formulations of glyceryl trinitrate which are absorbed from the mouth. Glyceryl trinitrate is absorbed across the buccal mucosa because it has appropriate physicochemical properties, which include high solubility and a logP of 1.62 (Chen *et al.*, 1999).

The gastrointestinal tract is a hollow tube approximately 9 m long, which is continuous with the external environment. The wall of the digestive tract has the same general structure through-out most of its length from the oesophagus to the anus, with specific modifications in certain regions to aid the digestive and absorptive processes. The gastrointestinal tract circulation is the largest of the systemic regional vasculature receiving nearly a third of the cardiac output, with approximately 10 % of the gastrointestinal tract circulation supplying the small intestine. The distribution of blood flow varies on the metabolic demands of the different areas. The *villi* receive 60 % of the blood flow to the mucus layer while the muscle layer receives only 20 % of the blood flow. The blood flows from the intestine into the hepatic portal vein, which goes

on to the liver. The liver has the highest drug metabolising capacity of any organ in the body and in a single pass can metabolise a large proportion of absorbed compounds; this is referred to as first-pass metabolism. Although this is not a physical barrier, the metabolic process acts as a significant barrier to drug absorption. The gastrointestinal tract is richly supplied with lymphatic vessels. The lymphatic system is important in the absorption of nutrients, especially fat from the gastrointestinal tract; it also provides a route for the return of electrolytes and proteins back into circulation from the intestinal spaces (Sherwood, 1997).

1.3.2 THE SMALL INTESTINE

The small intestine is the main absorptive region for nutrients and drugs along the gastrointestinal tract. It is the site where most digestion and absorption of nutrients and drugs occurs, no significant digestion occurs when the luminal contents have passed beyond the small intestine. Water and salt absorption occurs in the large intestine but the majority of drug and nutrient absorption occurs in the small intestine. It is made up of the *duodenum, jejunum* and *ileum* (see figure 1.1).

Most absorption occurs in the *duodenum* and *jejunum*, with very little occurring in the *ileum*. The lining of the small intestine is well adapted for its function of absorption, it has a large surface area of approximately 470 m^2. This is achieved by folding of the intestinal wall to produce *villi* and *microvilli* and the epithelial cells (Daugherty and Mrsny, 1999).

Since the surface of the small intestine is designed for absorption of compounds required by the body and at the same time excludes toxins, an understanding of its structure is beneficial in the use of any models mimicking it. Enterocytes, the absorptive cells, make up 90 % of the epithelial cell population and are the most important barrier against drug absorption. The apical or brush-border membrane, which is densely packed with *microvilli*, is their most distinctive feature. It has a fuzzy coat, which is a glycoprotein produced by the enterocyte, extending 0.1 µm from the *microvilli* tips, aiding in the digestive process and protecting the intestinal mucosa (MacAdam, 1993).

21

Figure 1.1 – The organs involved in the digestive processes (adapted from Sherwood, 1997).

The cells that lie between the *villi* form crypts. The functions of the cells within the crypts are renewal, water and ion exchange, as well as endocrine and exocrine secretions. There are at least four different cell types, the Paneth cells, goblet cells, undifferentiated cells and endocrine cells. The Paneth cells secrete protein-rich material and contain lysozymes. The goblet cells secrete mucus, the undifferentiated cells are involved in the constant renewal of the epithelial. Together these cells form a continuous single sheet. The epithelial cells are produced from a cell population, which is located at the crypts of Lieberkuhn. Cells divide and migrate towards the tips of the *villi*, differentiating into different cell types on their journey, the cells have a life span of three to five days. Division and migration of the precursor cells in the crypts is a continuous process, replenishing the daily cell losses, and repairing the damage incurred to the epithelium during the digestive process (Berne and Levy, 1993). Mature cells

forming the *villi* and *microvilli* are the most effective at adsorption and have active uptake mechanisms present which the other cells will not posses until maturity.

The digestive tract wall is composed of four major tissue layers. They are the *mucosa*, *submucosa*, *muscularis externa* and *serosa*. The *mucosa* lines the luminal surface to the digestive tract and can be divided into three sections, the mucus membrane, *lamina propria*, *muscularis mucosa* (see figure 1.2). The outermost layer of the gastrointestinal tract is a covering of flattened mesothelial cells with underlying loose connective tissue known as the serosal layer. The *serosa* secretes a watery fluid which lubricates, preventing friction between the digestive organs and the surrounding viscera (Sherwood, 1997; Berne and Levy, 1993).

Aston University

Illustration removed for copyright restrictions
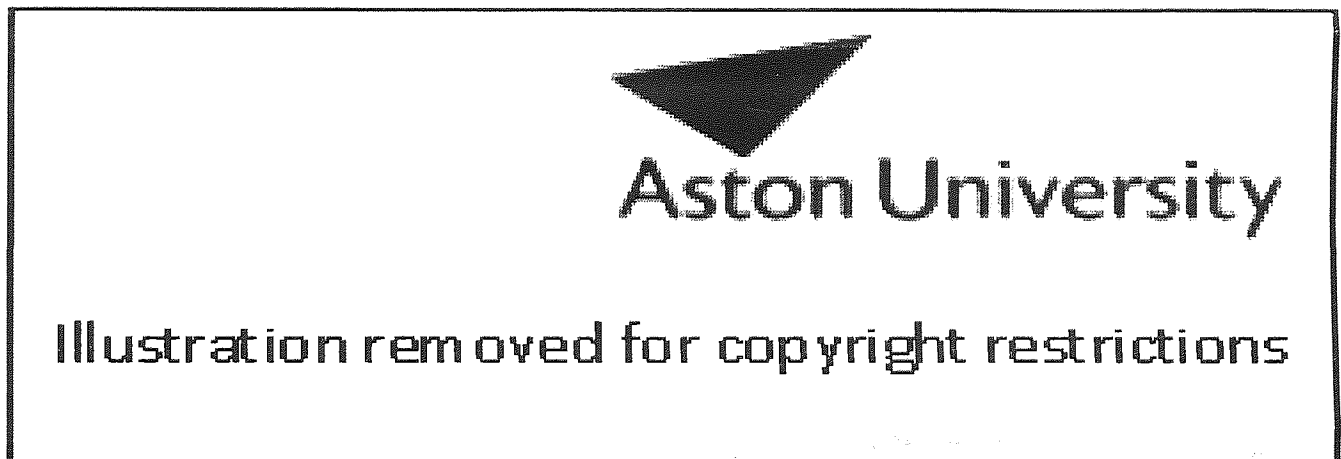
Figure 1.2 – Physiology of the gastrointestinal tract, clearly showing the *mucosa*, *submucosa*, *muscularis externa* and *serosa* (taken from Sherwood, 1997).

The absorptive efficiency varies down the gastrointestinal tract, with maximal absorption occurring in the small intestine (Ungell, 1997).

Minimal drug absorption occurs in the stomach as mentioned earlier, however, it can influence drug absorption in a number of ways. The pH of the stomach normally ranges from pH 2 to 4; degradation mainly in the form of acid hydrolysis can occur as well as

enzymatic attack. Binding of drug molecules to the luminal contents may also take place, for example, the complexation of antacid salts with drug molecules. Gastric emptying significantly alters the absorption of drug molecules in the intestine (MacAdam, 1993). Gastric emptying is affected by the presence of food in the stomach; in-turn, this can affect absorption by reducing the time the drug spends in the stomach.

The epithelium is not a continuous layer and divisions exist between cells. Generally, there are three kinds of divisions between cells: tight junctions, gap junctions and desmosomes. An understanding of cellular junctions can lead to an appreciation of why some compounds are absorbed and others are not.

Tight junctions are present at the apical region of the cells, below the brush-border membrane, forming a tight 'seal' between neighbouring epithelial cells. Tight junctions separate the contents of the intestinal lumen from the contents of the intercellular spaces. These limit passive diffusion through the intercellular spaces, therefore controlling the interchange between the luminal contents and the circulation. They play a crucial role in maintaining the selective barrier function of cell. Functionally, the tight junctions are not sealed but are permeable to water and electrolytes and other molecules. The size of these pores varies along the length of the gastrointestinal tract, the usual upper limit is 200 Daltons (Da) (Artursson and Hochman, 1994).

The commonest type of cellular junction is the gap junction. They are characterised by regions where cell membranes are separated by 2 to 3 nm gaps. The gap is crossed by cytoplasmic filaments, which allow intracellular cytoplasm to transfer between cells. Molecules up to 1200 Da can pass freely between cells (Karali *et al.*, 1989; Sherwood, 1997).

Goblet cells are cup-shaped secretory cells found in the crypts. They possess a system used for mucus production. Mucus is a complex mixture of glycoproteins, water, serum, cellular macromolecules, electrolytes and sloughed cells. The mucus protects the gastrointestinal tract mucosa from acid, enzymes and other luminal substances. It also lubricates the surface of the epithelium. The mucus layer adjacent to the colonic mucosa provides a stable pH environment as well as a barrier to absorption. The epithelium of the intestine is covered with mucus; it is primarily composed of mucin, a

large polysaccharide of approximately 500,000 Da. It serves as a lubricant and a protective layer and it is a viscoelastic compound which enables it to act as a mechanical barrier which can flow. Mucin provides an acidic microclimate close to the cell surface. The estimate of the pH microclimate in the unstirred water layer is 5.5 in the *duodenum*, with slightly higher values in the *jejunum* and *ileum* (Hunter and Hirst, 1997). The physical presence of mucus and the acidic microclimate can hinder drug absorption. Basic drugs such as cimetidine, are ionised in the acidic microclimate and therefore may have problems with transcellular permeability. Colonic bacteria degrade mucins. Therefore, changes in intestinal flora can affect the mucosal environment, such as during a course of antibiotics. The mucus layer can also be affected by prostaglandins and disease states such as cystic fybrosis (MacAdam, 1993).

1.3.3 THE LARGE INTESTINE

The large intestine is responsible for the conservation of water and electrolytes, unlike the small intestine, which is designed for absorption. The residence time in the colon can vary from hours to days depending on the individual dietary habit and level of physical activity. The colon extends from the *ileo-caecal* junction to the anus and is approximately 125 cm long. It can be divided into the *caecum*, ascending, traverse, descending and sigmoidal colon, rectum and anus (Bieck, 1993; Sherwood, 1997). The absorptive capacity of the colon is much less than that of the small intestine, and this is mainly due to a lower surface area and the lack of *microvilli*. The mucosal surface of the colon is a flat mucosa with deep crypts. The colon has a large capacity for the absorption of water, electrolytes and short-chain fatty acids formed during fermentation of carbohydrates by colonic bacteria. Approximately 1.5 L of water enters the colon and only 200 mL *per* day is eliminated (Bieck, 1993).

1.3.4 GASTROINTESTINAL TRACT MEMBRANE

The cellular membrane is composed of a phospholipid bilayer containing lipoidal molecules, including, sphingolipids and sterols as well as phospholipids. The amphipathic phospholipids are aligned to form bilayers with hydrophilic head groups on

the outer surface exposed to aqueous solutions. The hydrophobic fatty acid chains form the interior. The surface of the membrane is composed of tightly packed phospholipids interdispersed with proteins, the proteins in specific conformations act as structural elements as well as transporters and participants in cellular signalling (see figure 1.3).

Aston University

Illustration removed for copyright restrictions

Figure 1.3 – Artist's impression of the phospholipid membrane (adapted from Herbette, 1999).

The lipid composition of the intestinal membrane could be a factor regulating the fluidity of the membrane and thereby affecting the transcellular transport characteristics and modulate cellular responses and enzymatic activity. The lipid composition of the membrane is known to be affected by different disease states and diet (Ungell *et al.*, 1998).

It is believed that most drugs are absorbed through the epithelium from the gastrointestinal tract by a simple diffusion mechanism. However, if this was the sole case, it does not explain how ionised and hydrophilic compounds and macromolecules can effectively traverse the epithelial membrane. The principal permeability barriers to drug absorption are the epithelial cells and the tight junctions between epithelial cells.

Transport of drugs across the gastrointestinal tract epithelial cells is only viable if the biological and physical barriers presented by the gastrointestinal tract can be overcome. The intestinal epithelium acts as a physical barrier by restricting the movement of molecules along the paracellular and transcellular routes, and as a biochemical barrier due to metabolism *via* enzyme systems and transports back into the gastrointestinal tract lumen *via* efflux mechanisms (Pauletti *et al.*, 1996).

Orally administered drugs have to pass through epithelial cell layers to reach their target tissues or organs. Drugs which exert a local effect formulated as creams or ointments still have to penetrate into the skin and thereby have to traverse epithelial cells. Epithelial barriers delineate the outer margins of organs and possess structural, secretory and absorptive elements. Passage through the cells of the absorbing epithelium involves permeation across the brush-border, the intracellular space and the basolateral membrane. Provisions are made for the supply and retention of substrates from extracellular sources and the secretion of waste products. These functions lead to the plasma membrane being a selectively permeable membrane. Various regions of the gastrointestinal tract are normally exposed to a large range of different molecules and micro-organisms. Therefore, the intestine has to protect the body from systemic exposure by minimising absorption of various toxins, antigens and micro-organisms as well as carry out its major role in digestion and uptake of nutrients.

Several factors can influence the bioavailability of a drug when given orally. Aqueous solubility and aqueous dissolution rates are important, degradation within the gastrointestinal lumen could be due to instability in acidic pH or metabolism by luminal digestive enzymes, or by luminal micro-organisms. Although first-pass metabolism of drugs is the greatest form of metabolism, the role of intestinal enterocytes should not be underestimated in controlling absorption. Phase 2 metabolic reactions also occur in enterocytes. Another potential site of pre-synaptic metabolism is the intestinal luminal brush-border membrane, with its associated hydrolases.

The major bioavailability problem for most compounds is poor membrane permeation, however, there are exceptions such as taxol where efflux is a major problem (Anderle *et al.*, 1998).

1.3.5 BARRIERS TO ORAL DRUG DELIVERY

The barriers to oral drug delivery can be broken down into a number of steps. The drug compound must firstly cross the gastrointestinal tract wall where it faces a number of obstacles including enzymatic degradation and mucus. Once it has been transported into cell, it must enter the systemic circulation prior to distribution to sites of action (see figure 1.4).

Intestinal permeability and physicochemical properties of a drug determine the absorption from the intestine. The rate of drug absorption from the intestine is determined by factors such as solubility, dissolution rate, luminal complexation, degradation, transit time, efflux and metabolism.

For a compound to be absorbed, it needs to be soluble in an aqueous environment; this can cause problems with highly lipophilic compounds. The rate of dissolution will affect the bioavailability of a compound. Drugs with a slow dissolution rate may be incompletely absorbed because, by the time they go into solution, they could be too far down the gastrointestinal tract for complete absorption. Luminal complexation with salts can reduce the amount of drug available for the systemic circulation; for example, Ca^{2+} ions can form salts with quinolones, which reduces their bioavailability (Ross and Riley, 1993).

Additionally there are those physical barriers which exist because of physico-chemical properties of the dosage form as well as the physical environment of the gastrointestinal tract. These include dissolution and degradation of the dosage form. The pH and enzymatic environment of the gastrointestinal tract also have their own roles to play.

The unstirred water layer (UWL) adjacent to the cells may have a significant effect on drug absorption. The drug molecule must diffuse through this layer where it may undergo binding to cell surface components, electrostatic attraction or repulsion.

The unstirred water layer is a stagnant layer of water, mucus and glycocalyx adjacent to the intestinal wall that is created by incomplete mixing of the luminal contents near the intestinal mucosal surface. The rate-limiting step in the transmucosal uptake of low permeability compounds is the transport across the apical membrane, rather than the

diffusion through the unstirred water layer. The intestinal absorption in humans appears to be membrane-controlled for both low and high permeability compounds. In conclusion, the resistance of the UWL to intestinal absorption of highly permeable drugs has been overestimated and efficient stirring in the Caco-2 cell model would lead to permeability which was similar to human *in vivo jejunal* permeability (Wilson and Washington, 1989).
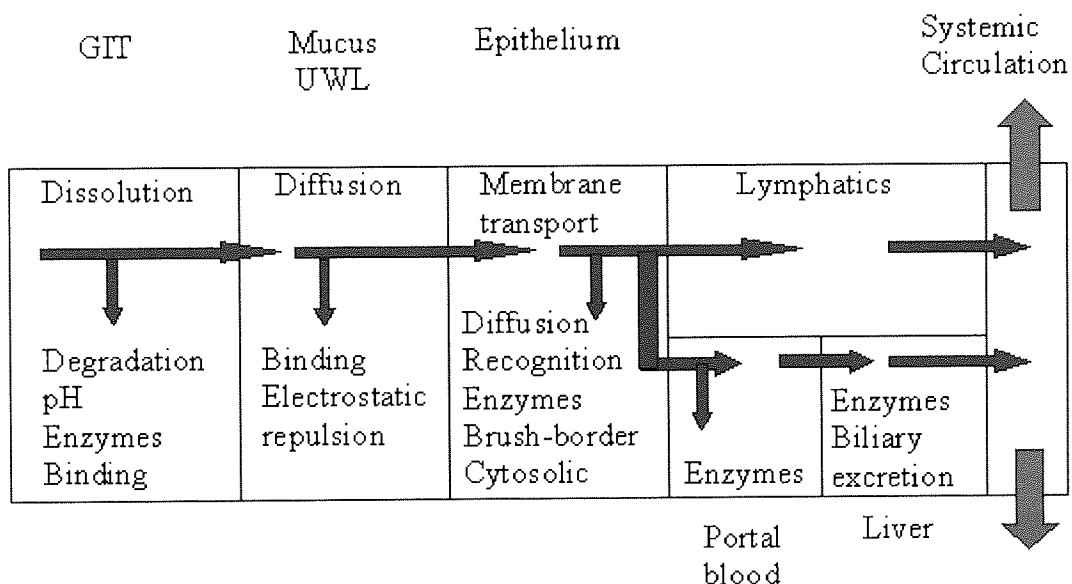
Figure 1.4 – Illustrating the barriers to absorption of oral drugs.

Once the drug molecule has passed through the UWL, it then faces the epithelium where depending on its physicochemical properties, there are a number of different mechanisms for its transport across the membrane. Once within the cell, the compound must make its way into the systemic circulation, avoiding degradation and cellular entrapment.

Drugs which are absorbed from the gastrointestinal tract enter the portal blood supply from where they find their way to the liver and may undergo extensive first-pass metabolism. This can have beneficial as well as detrimental effects; for example, pro-drugs can be used to exploit this first-pass metabolism.

1.4 MECHANISMS OF TRANSPORT

1.4.1 INTRODUCTION

There are a number of pathways that a compound can utilise in order to traverse the epithelial membrane. These include active as well as passive processes. An understanding of these is useful in predicting drug permeability. These mechanisms will be discussed in more detail in the following sections and are represented in figure 1.5.
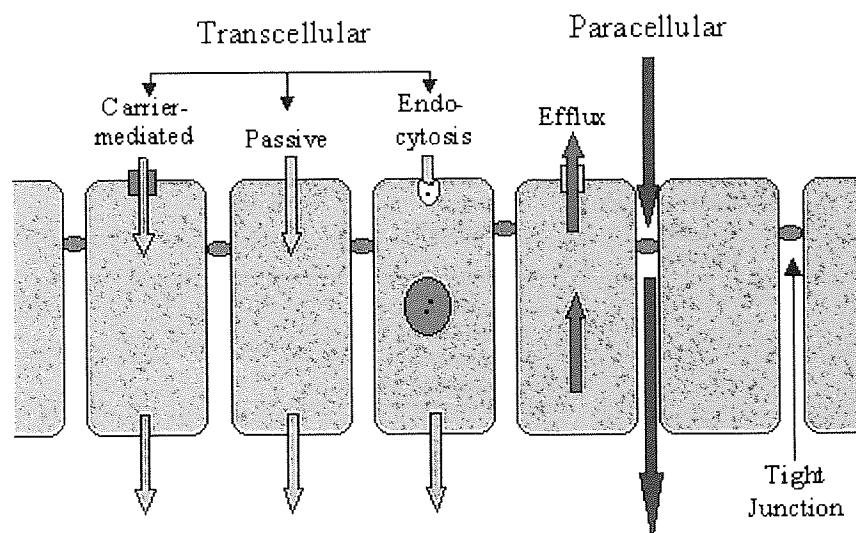
Figure 1.5 - Different routes a compound may use to traverse the epithelial membrane.

The selective nature of the intestinal barrier to drugs is borne from the necessity of the intestinal epithelium to facilitate absorption of nutrients and other essential constituents of the diet, including sugars, amino acids, small peptides, nucleosides, vitamins and trace elements. Absorption of other luminal contents, including bile salts, is also facilitated. There are numerous specific membrane transporters located on both apical and basolateral membranes of absorptive enterocytes; these will be discussed later. The intercellular tight junctions that connect together adjacent epithelial cells are not static structures and the exploitation of the dynamic nature of these junctional complexes, has led to the concept of enhancing absorption of certain hydrophilic drugs by modulation of junction permeability.

A drug molecule may cross from the intestinal lumen into the circulation or the lymphatic system *via* two major pathways, the transcellular and the paracellular route. The transcellular route can be further subdivided into passive, carrier-mediated and endocytotic pathways. There are active transport mechanisms such as the di-tri-peptide transporter and endocytotic pathways, which include pinocytosis, these are outlined in figure 1.6.
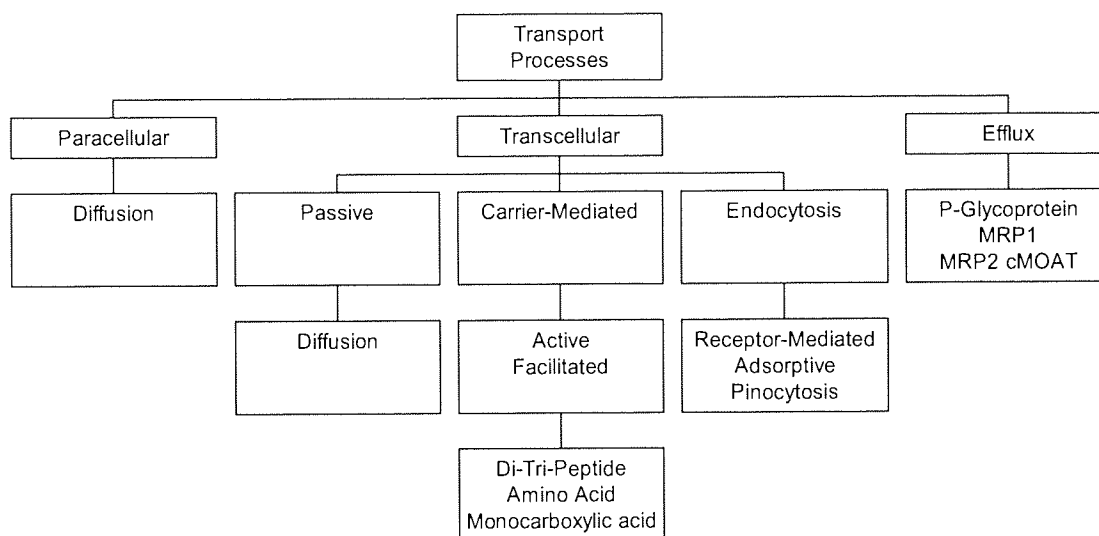
Figure 1.6 – Mechanisms of permeation of compounds.

1.4.2 TRANSCELLULAR MECHANISMS

1.4.2.1 PASSIVE TRANSCELLULAR

Passive transport is the diffusion of a solute along its concentration and electrical gradient. The chemical potential difference between the solute concentration on either side of the membrane provides the driving force for the diffusion of the molecule. Absorption of hydrophobic drugs principally occurs by the transcellular route (Karali *et al.*, 1989). The diffusion of molecules with molecular weights of less than 200 Da occurs in this way *via* diffusion through aqueous channels in the membrane and *via* the tight junctional complexes.

For passive transcellular flux, the molecule must have an appropriate set of physicochemical properties. Size, lipophilicity, hydrogen bonding and conformation

determine whether the compound will be able to cross the lipophilic cellular barrier (Hunter and Hirst, 1997).

For hydrophobic compounds, an inconsistent pattern in regional absorption and permeability exists. This inconsistency between different areas of the gastrointestinal tract may be related to the differences in physiological properties of the membrane in various regions along the intestine such as active uptake mechanisms. The intestinal permeability, for low permeability drugs such as terbutaline, decreased in the order jejunum > ileum > colon while, for the high permeability drugs such as propranolol, the converse was seen.

The 'rule of 5' is a general rule of thumb based on physicochemical properties of a compound which can be used to estimate a drugs permeability. Lipinski, (1997), analysed a large number of compound libraries and created the 'rule of 5' which defines a poorly absorbed compound as, one with five or more hydrogen bond donors, a molecular weight greater than 500, Moriguchi logP over 4.15 and the sum of nitrogens and oxygens to be greater than ten.

Lipid-partitioning is part of passive transcellular transport and involves the incorporation of a hydrophobic drug molecule into the lipid membrane of the cell and then partitioning of the molecule into the cell. The lipid bilayer is highly impermeable to charged molecules, where charge and a high degree of hydration prevent them from entering the hydrocarbon phase of the bilayer. The absorption rate of drugs through biological membranes is directly proportional to the value of the partition coefficient until an optimal value of 3.5 (Ungell *et al.*, 1998). At low LogP values, a drug cannot penetrate the lipid membrane. However, at high LogP values, the drug becomes so lipophilic that diffusion through the unstirred water layer will become the rate-limiting step for absorption.

1.4.2.2   ACTIVE TRANSPORT MECHANISMS

There is a huge amount of interest in active transporters or carrier-mediated systems in order to provide a better understanding of the mechanisms involved and to identify

specific chemical motifs required for recognition by receptors. The information provided could be used in the design of new drugs and prodrugs to aid oral absorption of compounds.

Facilitated diffusion involves the reversible binding of specific substrates to proteins in the cell membrane to assist the transport of a substance across the membrane (Karali *et al.*, 1989). Compounds which under go carrier-mediated transport such as ACE-inhibitors showed higher permeability values in the upper small intestine than in the colon (Ungell *et al.*, 1998), this occurs because the uptake mechanisms are located in the upper small intestine.

Active transport involves the binding of specific substrates to membrane-located proteins. Transport can occur against a concentration gradient and therefore, requires energy. The energy can be supplied in two ways, either involving a coupled transport process such as the Na^+-dependant amino acid transporter, whereby a second substrate is transported down its concentration gradient, releasing energy. The alternative is that the substrate binds to a transporter as with the di-tri-peptide transporter, with energy being released from the hydrolysis of adenosine tri-phosphate, (ATP). The transporter protein is then phosphorylated resulting in a conformational change in the pump bringing the active site with its ligand to the other side of the membrane and thus translocation into the cell. Active transport processes are sensitive to metabolic inhibitors, such as 2,4-dinitrophenol and sodium azide. Substrate analogues of the transported compound can also inhibit transport by competing for the active site on the transporter (Karali *et al.*, 1989). The transport of a substrate by the transporter protein can be subject to inhibition by another compound, which can either be competitive or non-competitive. Competitive inhibitors compete with the substrate for the active site of the transporter protein. A competitive inhibitor combines reversibly with the active site, and therefore, increasing the substrate concentration can reverse inhibition.

There are a number of active uptake transporters, which can be found in the gastrointestinal tract. These include the amino-acid transporters, two of which are facilitated transporters and one an active transporter. There is also a specific transport system present for small peptide consisting of 2 to 4 amino acids known as the di-tri-peptide transporter (DTS); free amino acids do not serve as a substrate for this system.

The pharmacological relevance of this transporter has become evident in recent years because, this transporter mediates the absorption of orally active β-lactam antibiotics and other peptide-like drugs such as ACE-inhibitors (Tsuji and Tamai, 1996). Carbohydrates are transported by four general mechanisms, which are active, facilitated and passive diffusional or paracellular transport. There is a facilitated transport system for D-fructose transport, monosaccharides accumulated in enterocytes are transported by facilitation across the basolateral membrane (Mizuma *et al.*, 1994). Benzoic acid is transported *via* a carrier-mediated transport system thought to be the mono-carboxylic acid transporter (Tsuji and Tamai, 1996). Carrier-mediated transport of phosphates also occurs in the brush-border of intestinal cells (Tsuji and Tamai, 1996). These mechanisms have the potential to be exploited as drug transport systems, especially if the drug was to be modified to mimic the natural substrate, or as a prodrug with the natural substrate attached to it. Although none of these transporters mentioned have been exploited as of yet, some drugs as mentioned earlier use these transporters.

1.4.2.3   ENDOCYTOSIS

Larger molecules, over 500 Da, may be absorbed by endocytosis. Pinocytosis is a process in which the cell membrane produces a deep in-folding which detaches as an intracellular vesicle. Pinocytosis involves the capture of extracellular liquid and is a common function of most nucleated cells. Endocytosis has a minimal absorptive effect in adults. Receptor-mediated transcytosis involves the binding of membrane-located receptors to macromolecules which are then transported across the cell in endocytosed vesicles. Fluid-phase endocytosis involves the incorporation of extracellular fluid which contains dissolved substances into the endocytosed vesicle, which is then transported through the cell (Artursson and Hochman, 1994). Transcytosis is an important pathway for specialised intestinal cells such as M cells of the immune system (Hunter and Hirst, 1997).

Persorption is a process of drug absorption, which occurs during the continual renewal of the intestinal wall. During digestion, the cells are sloughed off the intestinal wall leaving temporary gaps, through which large particles can enter the circulation as shown in figure 1.7 (Wilson and Washington, 1989).

Figure 1.7 - Potential epithelial spaces opened up which would
be used by large molecules to gain access to the circulation
(Wilson and Washington, 1989).

The intestine absorbs approximately 10 litres of water *per* day; this water absorption could aid the absorption of drugs such as metoclopramide which has a logP of 2.62. In general the absorption of acidic and basic drugs increases as the water absorption increases, this phenomenon is referred to as solvent drag (Wilson and Washington, 1989).

1.4.3 PARACELLULAR MECHANISMS

Paracellular transport across healthy intestinal membrane is minimal due to the presence of the tight junctions. Only small hydrophilic molecules can use the cellular tight junctions (Hunter and Hirst, 1997).

Drugs with low permeability such as terbutaline are incompletely absorbed due to their hydrophilicity and high desolvation energy and consequently show low partitioning into the lipid phase of the membrane. These compounds are thought to be transported through the paracellular route across the tight junctions in the intercellular spaces; compounds with a molecular weight greater than 200 Da are not able to utilise this route effectively.

The paracellular route involves diffusion through the junctional complexes or the transient gaps between cells at the extrusion zones on the *villus* tips, while the transcellular route involves the movement of a molecule through the epithelial cell. The paracellular route exclusively involves passive transport.

1.4.4 EFFLUX MECHANISMS

1.4.4.1   INTRODUCTION

Additional to active uptake mechanisms present in the epithelium, active secretory mechanisms have also been identified which are able to secrete compounds that were originally passively absorbed (see figure 1.6). These mechanisms act as barriers by providing a resistance to drug absorption.

These efflux mechanisms include PgP, which is a product of the *mdr1* gene, multiple drug resistance protein (MRP) and the canalicular multispecific organic anion transporter (cMOAT) (Tsuji and Tamai, 1996).

1.4.4.2   P-GLYCOPROTEIN (PgP)

A drug being absorbed must traverse the apical membrane, make its way through the cell and then get past the basolateral membrane, resulting in the observed unidirectional transepithelial flux. PgP acts as an additional barrier to permeability by contributing to the outward flux across the apical membrane. This results in the transepithelial flux in the secretory direction which acts to reduce net absorptive flux and, in some cases, may exceed that in the absorptive direction. The transepithelial permeability of a substrate for PgP will be dependent not only on the passive permeability of the apical membrane to the substrate, but also on its affinity for the active transport site and the maximal capacity of PgP contained in the apical membrane. PgP can behave as a simple pump leak at the apical membrane or a significant efflux system depending on the compound (Hunter and Hirst, 1997).

The function of PgP may explain divergence from the predicted permeability based upon drug octanol-water partition coefficients. Limitations of absorptive uptake will be most pronounced with PgP substrates when diffusional influx is low and when ATP-dependent drug efflux is not limiting with respect to diffusional input. This condition is met if the drug has a high affinity with respect to ATP-dependent export and the cytosolic drug concentrations are non-saturating (Hunter and Hirst, 1997).

PgP is a 170 kDa protein originally found to cause multidrug resistance in cancer chemotherapy, upon treatment with anticancer drugs such as vinblastine, antinomycin and daunomycin. PgP also affects noncytostatic drugs, such as β-blockers and peptides. The PgP transporter secretes drug at low concentrations out of the epithelium back into the intestinal space. However, at high intestinal concentrations, this transporter is saturated. Therefore PgP may not have a significant clinical effect on compounds where passive absorption is significantly high, because the efflux mechanism will have a small, insignificant effect. Conversely, for compounds with low absorption which are substrates, it can have a highly significant effect. PgP is expressed in the liver, pancreas, kidneys, and reproductive organs as well as the endothelia lining the brain, testes and adrenal glands (Anderle *et al.*, 1998). These organs are responsible for the elimination of toxicants from the body, suggesting that it maintains the clearance of toxic material from the entire body. PgP also transports polycyclic aromatic hydrocarbons. Expression of PgP has also been correlated to resistance to environmental pollutants (Ueda *et al.*, 1997).

PgP functions as an ATP-dependent drug efflux pump thereby reducing the accumulation of various intracellular chemotherapeutic agents. Since the expression of PgP is at the apical epithelial cell border, transepithelial secretion of PgP substrates is predicted. PgP may function in detoxification and to limit intestinal permeation of natural toxic compounds found as normal constituents of diet (Hunter *et al.*, 1993).

The molecular weight of the known substrates for PgP ranges between 300 and 2000 Da. Many molecules with high hydrophobicity interact with PgP; human PgP transports cortisol, aldosterone and dexamethasone. A slight difference in structure or some other characteristic of the steroid determines whether or not PgP transports it.

PgP substrates are structurally so diverse that it is difficult to identify any common structural features (see table 1.1). Ueda *et al.*, (1997) suggested the minimum set of structural features for compounds interacting with PgP were a basic nitrogen atom and two planar aromatic domains, in addition to a molecular weight greater than 300 and less than 2000, moderate lipophilicity and a positive charge at physiological pH. These structural features may be important, however compounds such as cyclosporin A lack these structural features and are still PgP substrates. Another exception to the rule is methotrexate which has a negative charge at physiological pH. It appears that PgP may have more than one drug binding site, which would go someway to explain the diverse number of compounds that are substrates or inhibitors (Ueda *et al.*, 1997).

Ueda *et al.*, (1997) found that, as lipophilicity increased for a homologous series of pesticides, the binding to PgP increased to a maximum logP of approximately 4.5; beyond this, increasing lipophilicity reduced the ability of the pesticide to inhibit PgP and those pesticides with a logP less than 2.5, could not inhibit PgP (Bain and LeBlanc, 1996). There was a correlation between the hydrophobicity of steroid hormones and their ability to inhibit drug binding and efflux mediated by PgP (Ueda *et al.*, 1997). Progesterone is the most hydrophobic steroid, and it inhibits PgP most strongly, without itself being transported. A possible mechanism for the lack of transport is that, due to its high hydrophobicity, it binds extremely tightly to PgP and is not released.

SUBSTRATES	INHIBITORS
Digoxin	Bepridil
Doxorubicin	Chlorpromazine
Ethidium bromide	Cyclosporin A
FK506	Nifedipine
Paclitaxel	Quinidine
Vinblastine	Progesterone
Vincristine	Verapamil

Table 1.1 - Some common PgP substrates and inhibitors (Hunter and Hirst, 1997; Kusuhara *et al.*, 1998).

PgP expression has been found to be primarily associated at the *villus* epithelium of the small intestine as stated earlier, and displays complementary expression with cystic fibrosis transmembrane receptor (CFTR) another member of the ABC gene family.

CFTR expression is observed in the crypts but switches to PgP expression as enterocytes differentiate and move up the crypt-*villi* axis to the maximal at the *villus* tips (Hunter and Hirst, 1997).

In humans there are two genes that encode for PgP, termed *mdr1* and *mdr2*, only *mdr1* appears to encode for a functional transporter. PgP contains 12 transmembrane domains and consists of two subclasses, *mdr1* and *mdr2*; the former confers multidrug resistance to tumour cells, while the latter acts as a translocator for phospholipids (Kusuhara *et al.*, 1998).

The exact mechanism of action of PgP is currently unknown although several theories have been put forward. Three of the popular models include aqueous pore, the hydrophobic vacuum model and the flippase model (Hunter and Hirst, 1997). The aqueous pore is the simplest model, with PgP forming a transmembrane pore through which substrates from within the cell are pumped out into the aqueous environment on the outside of the cell (Higgins *et al.*, 1997). With the hydrophobic model, PgP substrates are transported from the cellular membrane to the outside of the cell, this action referred to as the hydrophobic vacuum cleaner (Hunter and Hirst, 1997). The flippase model also transports substrates from within the membrane to the outer side of the cell.

The human *mdr2* (PgP) supports the flippase model; it is a phosphatidylcholine-specific translocase in the bile canalicular membrane of hepatocytes. All of the amino acids reported to alter the substrate specificity of *mdr1* were conserved between *mdr1* and *mdr2*. Based on these results, *mdr1* may work as a flippase like *mdr2*, so that *mdr1* interacts with a substrate in the inner leaflet of the lipid bilayer and flips them to the outer leaflet. This flippase model may explain the unusually broad substrate specificity of *mdr1* (Ueda *et al.*, 1997). In *mdr2* knock-out mice, abnormalities such as scattered hepatocyte necrosis, proliferation of bile ducts and portal inflammation was observed. These pathological conditions may be accounted for by the lack of phosphatidylcholine actions. *mdr2* translocates phosphatidylcholine from the inner leaflet of the lipid bilayers, phosphatidylcholine in the outer leaflet forms aggregates with bile salts excreted into the bile, preventing the cytotoxic detergent affect of bile salts acting on

cells. However, overexpression of *mdr2* in drug-sensitive cells does not confer MDR (Kusuhara *et al.*, 1998).

PgP is expressed in Caco-2 cells to varying degrees, the variation can be due to the time in culture as well as the culturing conditions (Anderle *et al.*, 1998). Caco-2 cells are used as a model of intestinal absorption for compounds; therefore PgP expression has to be taken into account. Cases could arise where the PgP expression in the model is higher than the PgP expression in humans and may lead to the risk of an underestimation of human intestinal permeability. Conversely, if PgP expression is lacking a compound which could be a PgP substrate may not be so determined until much later in development. PgP expression levels in Caco-2 cells are dependent on the time in culture as well as the conditions of culture, as cell passage number increases, PgP expression increases. It can be expressed by a stepwise exposure to cytotoxic compounds such as doxorubicin (Anderle *et al.*, 1998). There is a drop-off in PgP expression as the cells in culture age in passage number. However, trypsinsing the cells before reaching confluence, approximately at 70 % confluence resulted in a significant increase in PgP expression. A stable transfected cell line may show less variation, but eventually leads to a change of expression levels due to selection pressures (Anderle *et al*, 1998; Hoskins *et al*, 1993).

A number of compounds such as verapamil and reserpine inhibit the active drug efflux mechanism in cell-culture models. Verapamil, at a concentration of 100 μM, was able to inhibit the net transport of vinblastine sulphate across the epithelial cell layers by about 50 % (Hunter *et al.*, 1993). The effects of temperature on the activity of PgP have not been documented.

1.4.4.3 MULTIPLE DRUG RESISTANCE ASSOCIATED PROTEIN (MRP) AND CMOAT

PgP and multidrug resistance associated protein MRP1 are both efflux transporters, with a molecular weight of 190 kDa. They are primary active transporters and members of the ABC ATP-binding cassette superfamily. Their drug resistance profiles resemble

each other closely, however, their amino acid sequence shows only 15 % similarity (Kusuhara *et al.*, 1998; Hunter and Hirst, 1997).

Another transporter, whose specificity resembles MRP1 is cMOAT, a canalicular multispecific organic anion transporter, which is responsible for the excretion of xenobiotics across the bile canalicular membrane (Kusuhara *et al.*, 1998).

It has been established that the transport of several organic anions is mediated by MRP1. Substrates of MRP1 include glutathione conjugates and sulphated conjugates. MRP1 will also accept glutathione conjugates such as cadmium and cisplatin. It has been hypothesised that the role of MRP1 is to play a part in the detoxification of xenobiotics that can act as electrophilies, which are able to attack DNA. These can be metabolised to glutathione conjugates, which are then extruded from the cell by MRP1 (Kusuhara *et al.*, 1998).

MRP1 and cMOAT are responsible for the transport of organic anions across the bile canalicular membrane. cMOAT is also referred to as MRP2 because of the similarity in the function and structure between cMOAT and MRP1. Irrespective of its relatively similar substrate specificity to MRP1, cMOAT is distinct from MRP1, since the hepatic expression of MRP1 is minimal and restricted to the basolateral membrane. Substrates for cMOAT include anionic xenobiotics such as β-lactams, pravastatin and methotrexate (Kusuhara *et al.*, 1998).

Many of the modulators of PgP including verapamil and cyclosporin A also inhibit MRP but to a lesser extent (Kusuhara *et al.*, 1998).

In summary, the transepithelial permeability of a substrate for an efflux mechanism will be dependent not only on the passive permeability of the substrate, but also the affinity for the active transport site and the maximal capacity of the efflux mechanism contained in the apical membrane. Limitations of absorptive uptake will be most pronounced with efflux substrates when diffusional influx is low and when ATP-dependent drug efflux is not limiting with respect to diffusional input (Hunter *et al.*, 1993).

1.4.5 METABOLIC FACTORS

Drug absorption from the small intestine is mainly regulated by membrane permeability. However, the effects of phase I metabolism in the epithelial cell and the secretion to the intestinal lumen just after uptake must not be ignored. It must be remembered that compounds that are absorbed by passive transcellular mechanisms may be substrates for enterocytic intracellular metabolism. They may also have the same general characteristics, which are likely to make them substrates for apically polarised efflux mechanisms such as PgP or cMOAT (Hunter and Hirst, 1997). There is a growing awareness of the potential for intestinal metabolism of drugs, which in-effect acts as a barrier to drug absorption. Cytochromes P450 phase I enzymes found in the liver are also distributed in the intestine and there is some concordance of PgP and CYP3A substrates and modulators, including verapamil and cyclosporin A. However, there is very little evidence to support this (Hunter and Hirst, 1997; Emi *et al.*, 1998). PgP can re-expose compounds to CYP3A which were passively absorbed. This, in effect, increases the contact time with the enzyme.

1.4.6 PROCESSES OF DRUG TRANSPORT

The mechanisms involved in the absorption of a compound do not act as individual components. A compound traversing the cellular membrane does not solely utilise the paracellular or transcellular routes, but uses a combination of these as well as active uptake and secretion mechanisms, which maybe located in the apical or basolateral membranes.

The major factor affecting the transport of a compound across cellular membranes is lipophilicity. Primarily it will determine whether a compound utilises the paracellular or transcellular routes. However, at intermediate logP values a compound is able to use a combination of both of these. Lipophilicity, logP and ionisation constants pK_a are introduced and discussed in depth in chapter 3.

For compounds that undergo active transport or secretion, this transport may not play a significant role if the passive components are significantly large. In such cases the

active component is swamped by the passive component which could be transcellular, paracellular or a combination of both.

Changes in the environment can lead to alterations in the route of transport. If the most favourable transport route is closed off, then the less favourable routes may still be in use. For example a compound which is actively transported, uses a transporter which may be inhibited by metabolic inhibitors. The compound is then still able to utilise the passive routes of transport.

1.5   CELL CULTURE MODELS

1.5.1 INTRODUCTION

Studying transport through the intestine is difficult because it displays complex geometry with considerable cellular heterogeneity. Access to the serosal side is limited by the impairment of subjacent tissues. The use of human tissue for drug absorption studies has other limitations due to problems with availability and poor viability (Freshney, 1994). Numerous other methods are available for investigating internal absorption mechanism and for assessing oral bioavailabilities of drug compounds these include *in vivo*, *in situ*, and *in vitro* models.

1.5.2 IN VIVO MODELS

In vivo techniques involve the use of intact animals. The absolute bioavailabilities of drug formulations can be determined after oral and intravenous dosing with these methods. The effects on drug absorption of pH, peristalsis in the gastrointestinal tract and the presence of food in the stomach and intestine can be assessed (Karali *et al.*, 1989). *In situ* methods include the modified Doluisio technique used to study rat intestinal absorption (Merino *et al.*, 1995).

1.5.3 IN VITRO MODELS

In vitro methods available for the study of drug absorption include intestinal preparations, ring slices, brush-border membrane vesicles, isolated membranes of mucosal cells and isolated enterocytes (Freshney, 1994).

The advantages of cell culture models include the rapid assessment of epithelial permeability and metabolism of drugs. They provide the opportunity to study mechanisms of drug transport or pathways of degradation under controlled conditions and enable the evaluation of methods to enhance drug absorption and drug targeting. They also provide the opportunity to perform studies on human cells. Cell culture can effectively be characterised before experimental work begins. It can allow the screening of a number of compounds without the legal, moral and ethical questions of animal experimentation. There is a reduction in the time-consuming, expensive and often controversial animal experiments and environmental control can be achieved over pH, temperature, osmotic pressure, O_2 and CO_2 levels.

Although *in vitro* cell culture models have their merits, these models do have certain shortcomings; cell culture techniques must be performed under strict aseptic conditions, requiring a high level of skill in the part of the operator and a potentially high initial capital investment. A high expenditure of effort is required to produce a small amount of material; beyond small-scale work, cell culture may no longer be economically viable. Phenotypic characteristics of the tissue can be lost from isolated cells, probably due to de-differentiation, a process occurring by the overgrowth of undifferentiated cells. If differentiated properties are lost, it becomes difficult to relate cultured cells to functional cells from the original tissue they were derived from. Genetic instability is also a major problem with continuous cell-lines, this can lead to variations in the cell population from passage to passage. There can also be a lack of correlation with *in vivo* techniques. The usefulness of these models often relies on establishing a correlation of the *in vitro* findings (such as permeability) with *in vivo* models (such as bioavailability) (Ribadeneira and Aungst, 1996; Freshney, 1994).

1.5.4 CACO-2 CELL LINE

1.5.4.1   INTRODUCTION

The Caco-2 cell-line was established using the explant culture technique, from a moderately well differentiated colon adenocarcinoma obtained from a 72 year Caucasian male membrane (Pinto *et al.*, 1983). When grown under standard culture conditions, these cells spontaneously differentiate exhibiting enterocyte-like properties, expressing morphological and biochemical features of adult differentiated absorptive cells. They form polarised monolayers with apical and basolateral domains, with brush-border *microvilli* extending perpendicular to the surface from the apical membrane (Pinto *et al.*, 1983). The cells are separated by tight junctions and form confluent monolayers (Grasset *et al.*, 1984). The functional differentiation of the cells is a growth-related phenomenon. There is evident from the analysis of enzyme activities in relation to the formation of domes, brush-border *microvilli* and tight junctions present in Caco-2 cells thereby this model exhibiting appropriate barrier properties (Grasset *et al.*, 1984; Pinto *et al.*, 1983). The functional differentiation of the cells corresponds to a maturation process resembling the situation that is found in the intestine membrane. Caco-2 cells have been used as a screening tool for a number of compounds (Yee, 1997).

The reason why Caco-2 cells, originating from the colon, should spontaneously differentiate into enterocytes representing the intestine is not clear. One possible explanation is the similarity which exists between foetal and cancer cells. By measuring levels of enzymes present in Caco-2 cells and foetal colon of different age, it is believed that Caco-2 cells correspond to intestine cells of a 15-week old foetus (Pinto *et al.*, 1983; Yee, 1997).

Human GI epithelial cells are the most suitable and comparable cells to assess transport of drugs across the gastrointestinal tract. The establishment of primary cell cultures of intestinal cells is a difficult and tedious process. The cell-lines can undergo loss of attachment and generally have short life-spans. They grow as islands of cells consisting of centrally dividing regions and external differentiated areas. Cell-lines from a primary, non-continuous, tissue source can be propagated in an unaltered form for a

limited number of generations beyond which they die, or give rise to immortal cell lines, which can then be used for cellular experiments (Artursson and Hochman, 1994).

A primary cell culture is usually a very heterogeneous group of cells, containing many of the cell types present in the original tissue. Through the process of sub-culturing, a more homogeneous cell-line emerges. This change in the cell types of the culture has advantages and disadvantages; the diversity of the original culture is lost, loss of differentiated properties, trauma of desegregation, enzymatic and mechanical damage. None-the-less, the culture can be propagated, characterised and stored; the loss of diversity leads to an increase in uniformity which can be useful in conducting experiments (Freshney, 1994).

1.5.4.2   SUITABILITY OF THE CACO-2 CELL LINE AS A DRUG TRANSPORT MODEL

The major difference seen between Caco-2 cell models and human perfusion studies results from difference in absorptive area between the flat monolayers and folded human *jejunum*. Permeability values of the low permeability compounds, such as creatinine, atenolol and terbutaline, are on average 50 times lower in Caco-2 cells monolayers than in human *jejunum*. The lower permeability in Caco-2 cells may be due to a lower paracellular and/or a larger area available *in vivo* in humans. It is assumed that the absorption of hydrophilic compounds is so slow that a larger surface area of *intervillous* space is exposed. Thus, the permeability values of hydrophilic compounds in the Caco-2 cells are closer to those seen in the human colon (Lennernas, 1998).

The Caco-2 cell model was assessed as an *in vitro* intestinal absorption and metabolism model using a number of compounds transported *via* different processes (Palm *et al.*, 1997). Results showed that it is an excellent tool for distinguishing passive diffusion from carrier-mediated active transport, and also for identifying paracellular and transcellular transport pathways (Conradi and Hilger, 1992). For passively absorbed drugs, the Caco-2 cell line is an excellent model, as a good correlation between permeability coefficients in Caco-2 cells and oral bioavailability in humans has been demonstrated (Artursson and Hochman, 1994). However, several studies investigating

the transport of actively absorbed drugs have found that the permeability is under-estimated in the Caco-2 cell model. The barrier functions of the tight junctional complexes in the Caco-2 cell model have been reported to be comparable to that of the intact human intestine (Artursson and Hochman, 1994). This highlights the usefulness of the Caco-2 cell model for drug absorption studies (Artursson and Hochman, 1994; Burton *et al.*, 1996; Werner *et al.*, 1997).

The integrity of the cellular monolayer can be assessed by measuring the transepithelial electrical resistance TEER ($\Omega.cm^2$) across the confluent Caco-2 cells. It is a direct measure of the epithelial resistance to passive ion flow, the Caco-2 cells had a TEER of 420 ± 26 $\Omega.cm^2$ (Artursson *et al.*, 1993). Although Caco-2 cell lines can have significantly different TEERs, their permeability to marker molecules can show no significant difference (Artursson *et al.*, 1993). Values for TEER reported in the literature from different sources can show significant differences; for example, Artursson *et al.* (1993) reported TEERs to be 420 ± 26 $\Omega.cm^2$ for the original Caco-2 cell line and an isolated clone Caco-2cl.40 cells having a TEER of 662 ± 42 $\Omega.cm^2$.

There are a number of commercially available systems designed to provide a support to Caco-2 cells which are then used for transport experiments (see section 2.2.1).

The Caco-2 cells cell model does suffer from variations as any cellular model would, these can result from conditions in culture and length of time in culture. Therefore these variations have to be considered when results from different sources are being compared. A number of steps can be taken to try and account for this variation. Firstly paracellular markers can concurrently be run with compound of interest in transport models. The transport of the marker can given an indication to the integrity of the cellular membrane, examples of such markers include D-[1-^{14}C]mannitol. These compounds are widely used in cell culture and often a specific level of transport (for D-[1-^{14}C]mannitol, less than 0.5 % over half an hour) determines that the cellular monolayer was intact for transport studies. The TEER can also be used to determine monolayer integrity, however, this measurement can also show significant variations over time. The use of such markers cannot tell whether a transporter present in the cell culture model has changed. Most active transport or uptake mechanisms found in cell

culture vary with passage number. For example, with PgP, as cellular passage number increases the level of expression also increases. Therefore ideally experiments should be conducted in a small passage number window, this can not be carried out in most laboratory settings. When experiments are conducted over a wide passage numbers, adequate controls should be run with each set of experiments, for example running a control compound in apical-to-basolateral and basolateral-to-apical directions for transport studies (Artursson *et al.*, 1993).

1.6 TRANSPORT MODELS

1.6.1 TRANSCELLULAR PASSIVE TRANSPORT MODELS

The transcellular processes can be modelled using mathematical equations based on Fick's law of diffusion.

The mass of a compound transported across a membrane under passive diffusion is mainly influenced by the thickness of the membrane, the contact area and the donor concentration. If all other terms are kept constant, the mass transported is mostly affected by the donor concentration assuming sink conditions in the receiver (see equation 1.1).

EQUATION 1.1

$$M_t = \frac{D.P.A.C_d.t}{h}$$

Equation 1.1 can be modified to give the rate of transport *i.e.* the mass transported *per* unit time (see equation 1.2).

A more useful term is the apparent permeability coefficient (P_{app}, see equation 1.3). This term provides the permeability of a compound as the distance the compound travels *per* unit time. Since this value is independent of concentration or surface area it allows different compounds to be compared irrespective of the donor concentrations and surface areas used in the model.

EQUATION 1.2

$$\frac{dM}{dt} = \frac{D.P.A.C_d}{h}$$

D	Diffusion coefficient ($cm^2.s^{-1}$)
P	Partition coefficient
A	Area of contact (cm^2)
C_d	Concentration in donor (μM)
P_{app}	Apparent permeability coefficient ($cm.s^{-1}$)
h	Thickness of barrier (cm)

EQUATION 1.3

$$P_{app} = \frac{D.P}{h} = \frac{\frac{dM}{dt}}{A.C_d}$$

1.6.2 TRANSCELLULAR CARRIER-MEDIATED MODELS

The binding of a substrate to a carrier-mediated system can be described by the relationship between enzyme-substrate reactions. Therefore, the kinetic processes which describe such interactions can be extrapolated to active transporter-substrate interactions. When the transporter protein is saturated, the rate of uptake is at a maximum and is referred to as (V_{max}). The binding constant for a substrate to the carrier is referred to as the Michaelis constant (K_m). K_m is equivalent to the concentration of the substrate when uptake is half its maximum possible value (Swaan *et al.*, 1995). The relationship of the process follows the Michaelis-Menten model (see equation 1.4).

EQUATION 1.4

$$V = \frac{V_{max}.C_d}{K_m + C_d}$$

The uptake of a compound from the gastrointestinal tract is usually a mixture of different forms of uptake involving both a passive component as well as a carrier-mediated component. Equation 1.5 accounts for the passive component as well.

EQUATION 1.5

$$V = \frac{V_{max}.C_d}{K_m + C_d} + K_d.C_d$$

V	Rate of transport (nmol.min^{-1}.mg protein^{-1})
V_{max}	Maximum rate of transport (nmol.min^{-1}.mg protein^{-1})
K_m	Michaelis constant (mM)
K_d	Diffusion rate constant (nmol.min^{-1}.mgprotein^{-1}.mM^{-1})
C_d	Concentration in donor (μM)

1.7 QUINOLONES

1.7.1 INTRODUCTION

The quinolones are a group of antibiotics with a wide spectrum of action. Their name is determined from their chemical structure (see figure 1.8 and tables 1.2a, 1.2b and table 1.3). The newer quinolones are also known as the fluoroquinolones because of the additional fluorine atom attached to the quinolone ring structure. They also possess both a carboxylic group and a cationic amine group.

Early quinolones such as nalidixic acid, cinoxacin and pipemidic acid had poor antimicrobial activity. In humans, the bioavailability of numerous quinolones is greater than 90 %, which is evidence for good absorption (Rabbaa *et al.*, 1997), they are also rapidly absorbed, the time required to reach maximal plasma concentration (C$_{max}$) for absorption is 2 hours (Nightingale, 1994).

Both nalidixic acid and norfloxacin showed poor absorption profiles in comparison to other quinolones and they were used in the treatment of urinary tract infections and local application in the gastrointestinal tract (Nightingale, 1994). The absorption of nalidixic acid from the gastrointestinal tract was found to be pH-dependent and faster in the non-ionised form (Othman and Muti, 1988).

During the 1980s, a new series of quinolones appeared which contained a 6-fluoro,-7-piperazinyl feature (see figure 1.8). The new quinolones reach high intracellular concentrations in human phagocytic cells and have been shown to be active against most intracellular pathogens (Rispal *et al.*, 1996). These compounds had a greater activity than the first generation compounds. Not only were these compounds active against Gram-negative bacteria, but they also showed activity against Gram-positive organisms and *Pseudomonas aeruginosa*. These compounds also appear to be active against *Chlamydiae, Legionellae,* and *Mycobacterium* (Greenwood, 1995).
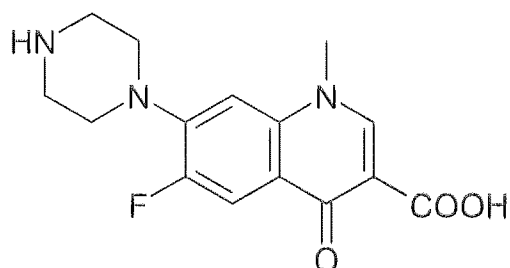
Figure 1.8 - Common structure of new quinolones, 6-fluoro, 7-piperazinyl feature.

Fluoroquinolones are usually administered *via* the oral route; IV preparations are available for ciprofloxacin and ofloxacin. Since quinolones are not nephrotoxic, they are suitable alternatives to aminoglycoside therapy in patients with renal insufficiency. Lomefloxacin absorption and distribution are not significantly altered by changes in renal function. Lomefloxacin clearance appears to decline in parallel with decreasing renal function (Blum, 1992).

Ciprofloxacin is active *in vitro* against a wide range of pathogenic bacteria, including most Gram-positive bacteria and some which are Gram-negative. It exhibits excellent activity against Gram-negative aerobes, moderate activity against Gram-positive aerobes and very poor activity against most anaerobic organisms. Ciprofloxacin achieves cerebrospinal fluid concentrations (CSF) concentrations which are greater than the MIC of most enterobacteriaceae that cause acute bacterial meningitis. At present, the utility of treating bacterial CSF infections with ciprofloxacin is questionable, pending further investigation. Four metabolites of ciprofloxacin have been isolated from urine, three of these metabolites are also excreted in faeces, most likely from bile (Vance-Bryan *et al.*, 1990). Ciprofloxacin, lomefloxacin, and norfloxacin are

metabolised to a greater extent than ofloxacin. The quinolone 4-oxometabolite has been associated with some interference with xanthene alkaloids such as theophylline and caffeine (Nightingale, 1994). Faecal recovery of ciprofloxacin accounts for about 15 % of the dose following intravenous administration and may be the result of elimination directly through the intestinal mucosa (Vance-Bryan *et al.*, 1990).

Fluoroquinolones are generally well tolerated, the main side-effects include rashes, gastrointestinal disturbances and photophobia. They can also cause cartilage deposition in animals and therefore are used with caution in children and pregnant women (Greenwood, 1995; Vance-Bryan *et al.*, 1990). Due to the higher level of penetration they have a number of CNS side-effects such as confusion, hallucinations, anxiety, depression and convulsive seizures. These side-effects occur because of distribution of the quinolones into the CNS and CSF which leads to them interacting with the GABA receptor (Ooie *et al.*, 1997; Jaehde *et al.*, 1992; Jaehde *et al.*, 1993).

Due to the wide spectrum of action and high potency of the quinolone antibiotics, they are used for a number of different conditions. Initially they were used for urinary tract infections (UTI), but the second and third generation quinolones have increased their place in chemotherapy (Hooper and Wolfson, 1993; Wilson and Gruneberg, 1997). Currently, quinolone antibiotics are used for the treatment of UTI, chronic bacterial prostatitis, sexually transmitted disease, bacterial gastro-intestinal infections, respiratory tract infections, ear-nose and throat infections, osteomeylitis and septic arthritis, bacterial meningastrointestinal tractis, bacterial endocarditis, skin and soft tissue infections, eye infections and prophylactic use in immunocompromised patients (Hooper and Wolfson, 1993; Wilson and Gruneberg, 1997).

1.7.2 STRUCTURAL CHARACTERISTICS

Most quinolones contain a pyridone ring and associated carboxyl group, this is the minimum required for interaction with the DNA gyrase enzyme (Hooper and Wolfson, 1993).
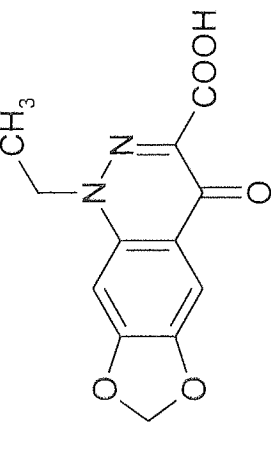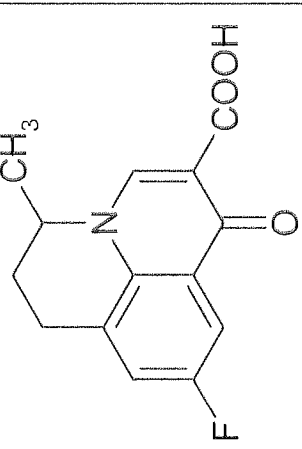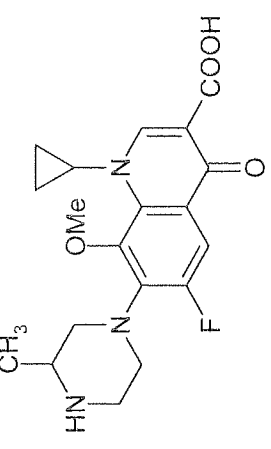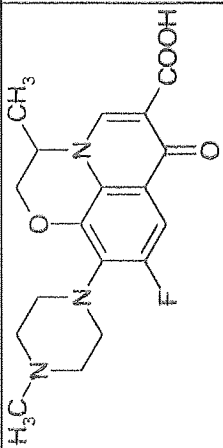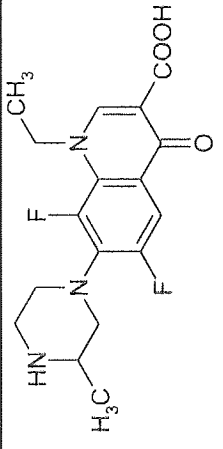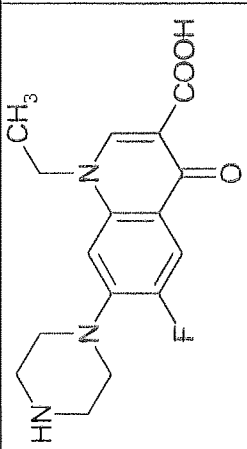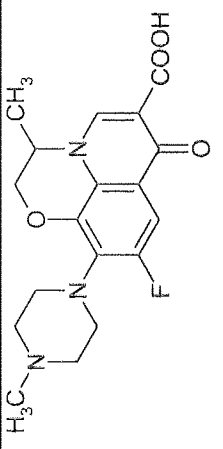
BMS-284756-01	Cinoxacin	Flumequine	Gatifloxacin

Levofloxacin	Lomefloxacin	Norfloxacin	Ofloxacin

Table 1.2a - Structures of quinolones.

53

Sparfloxacin	Ciprofloxacin	Methyl-Ciprofloxacin	Ethyl-Ciprofloxacin
Propyl-Ciprofloxacin	Butyl-Ciprofloxacin	Pentyl-Ciprofloxacin	Grepafloxacin
Fleroxacin	Enoxacin		

Table 1.2b – Structures of quinolones.

QUINOLONE	STRUCTURAL FORMULA	MOLECULAR WEIGHT
BMS-284756-01	$C_{23}H_{20}F_2N_2O_4$	426.42
Cinoxacin	$C_{12}H_{10}N_2O_5$	262.22
Flumequine	$C_{14}H_{12}FNO_3$	261.26
Gatifloxacin	$C_{19}H_{22}FN_3O_4$	375.40
Levofloxacin	$C_{18}H_{20}FN_3O_4$	361.38
Lomefloxacin	$C_{17}H_{19}F_2N_3O_3$	351.36
Norfloxacin	$C_{16}H_{18}FN_3O_3$	319.34
Ofloxacin	$C_{18}H_{20}FN_3O_4$	361.38
Sparfloxacin	$C_{19}H_{23}F_2N_4O_3$	393.42
Ciprofloxacin	$C_{17}H_{18}FN_3O_3$	331.35
Methyl-ciprofloxacin	$C_{18}H_{20}FN_3O_3$	345.38
Ethyl-ciprofloxacin	$C_{19}H_{22}FN_3O_3$	359.40
Propyl-ciprofloxacin	$C_{20}H_{24}FN_3O_3$	373.43
Butyl-ciprofloxacin	$C_{21}H_{26}FN_3O_3$	387.46
Pentyl-ciprofloxacin	$C_{22}H_{28}FN_3O_3$	401.49
Grepafloxacin	$C_{19}H_{22}FN_3O_3$	359.40
Fleroxacin	$C_{18}H_{20}F_3N_3O_3$	383.37

Table 1.3 – Structural formula and molecular weight for quinolones.

1.7.3 MECHANISM OF ACTION

Antibiotics need to exert selective toxicity towards microbial cells. They need to be toxic to microbial cells while having a limited toxicity towards mammalian cells. Current antibiotics can exploit five different molecular mechanisms to achieve this selective toxicity. The targets are the cell wall, protein synthesis, nucleotide synthesis, cytoplasmic membrane and cellular replication (Hugoi and Russell, 1998). Quinolones exert their selective antimicrobial toxicity by targeting cellular replication.

To inhibit replication, quinolones must be able to traverse both the outer and the inner membrane of bacterial cells in order to interact with DNA gyrase, a key enzyme in cellular replication. The route of penetration of the outer membrane is not fully understood, but it is hypothesised that diffusion occurs through the porin channel. Lipopolysaccharides (LPS) in the outer membrane appears to be a barrier to more hydrophobic quinolones. It has also been suggested that, because they chelate Mg^{2+} which is necessary for LPS integrity, quinolones may promote their own diffusion through the outer membrane (Hooper and Wolfson, 1993). Other mechanisms have

been suggested but there is a lack of evidence at this point (Hooper and Wolfson, 1993). Cellular permeability of the quinolones is most likely based on their lipophilicity.

Uptake of quinolones in *S. pneumoniae* occurs by simple diffusion. Sparfloxacin was found to accumulate at twice the level seen for the more hydrophilic compounds such as ciprofloxacin, norfloxacin and ofloxacin. This increased distribution across the membrane might play a role in the better *in vitro* activity of sparfloxacin against *S. pneumoniae*, although its activity for the topoisomerase target is probably the major factor (Zeller *et al.*, 1997).

The target for the quinolones is DNA gyrase (DNA topoisomerase II). Replication of the bacterial chromosome, circular duplex DNA molecule, requires separation of the two highly intertwined strands from one another. However, separation of strands wound in a helix, generates loops, termed positive supercoils. Unless prevented, positive supercoils would increase until the rising torsional strain prevented further unwinding of parental DNA. DNA gyrase relaxes positively supercoiled DNA by periodically breaking a phosphodiester bond in one of the strands of the double helix, then introducing negative supercoils and finally resealing the nick (see figure 1.9). DNA gyrase is composed of four subunits: two gyrase A subunits and two gyrase B subunits. The A subunits of gyrase are involved in the DNA breakage and resealing events associated with supercoiling while the B subunits are responsible for ATP hydrolysis. The enzyme is a heart-shaped structure, interactions occur in the upper portion of the heart with tyrosine residues forming transient phosphotyrosine lineages with broken DNA strands. Binding of ATP to the gyrase B subunit causes conformational change in the protein accompanied by a single round of negative supercoiling. Hydrolysis of ATP returns DNA gyrase to its original conformation. Strand passage followed by further rounds of negative supercoiling and eventual resealing then occurs. Various genetic studies, involving the generation of conditional lethal mutations in *gyrA* and *gyrB*, indicate that DNA gyrase is essential for DNA replication (Ruelle and Kesselring, 1998; Franklin and Snow., 1989; Wilson and Gruneberg, 1997; see figure 1.9).

DNA gyrase stimulates the binding of quinolones to double stranded DNA. The gyrase cleaves the double stranded DNA, which is then vulnerable to binding by the quinolone.

56

The unpaired DNA bases participate in H-bonding to the 3-carboxy and 4-oxo groups, leading to the formation of the quinolone-DNA-gyrase complex, which leads to cell death. The cell death would not result directly from inhibition of gyrase activity, but would be a secondary consequence of inhibition of transcription or DNA replication. Eukaryotic enzymes differ in overall structure from bacterial gyrase, being a dimer of two identical subunits (Ruelle and Kesselring, 1998; Franklin and Snow, 1989; Wilson and Gruneberg, 1997).

Aston University

Illustration removed for copyright restrictions
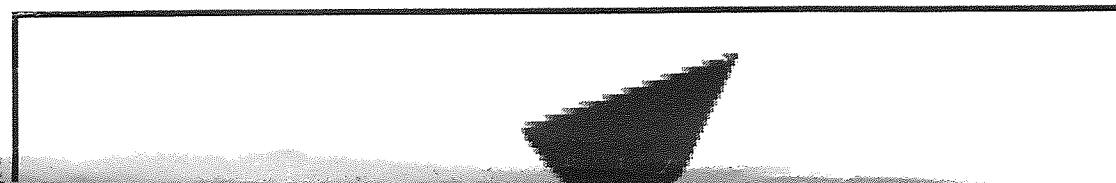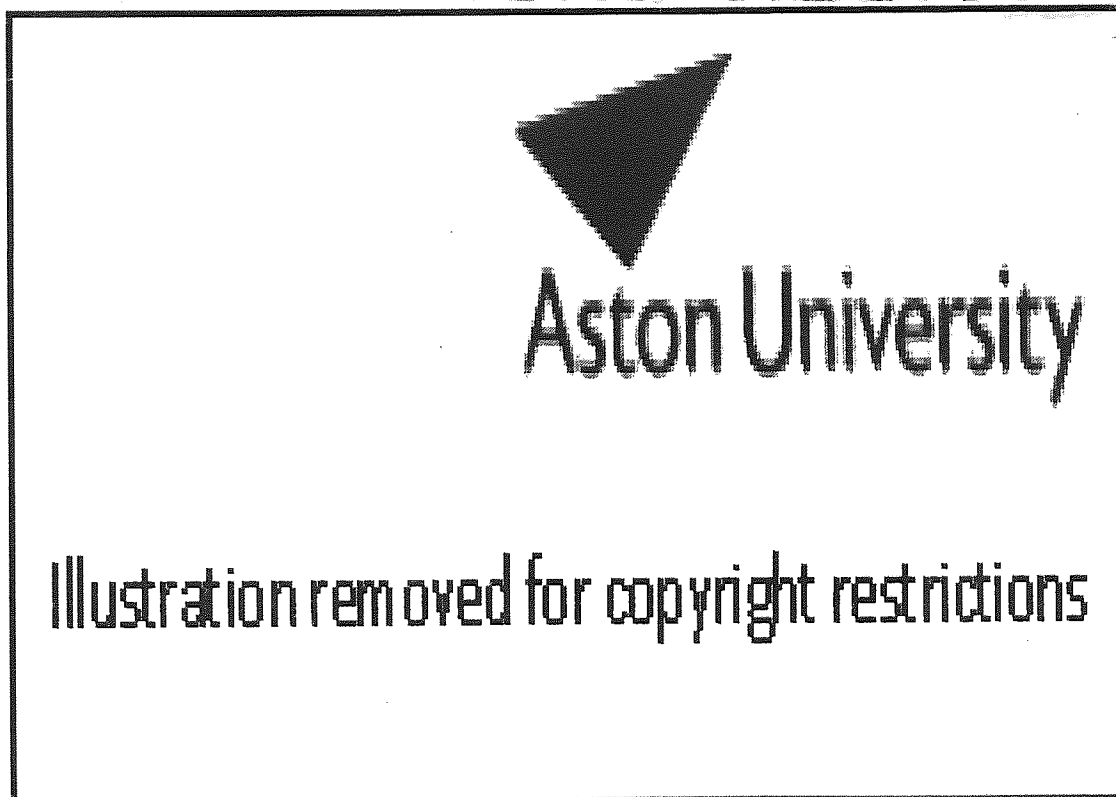
Figure 1.9 – An illustration of the actions of DNA gyrase (taken from Reece and Maxwell, 1991).

1.7.4 MECHANISMS OF BACTERIAL RESISTANCE

Bacteria do not acquire resistance to quinolones through mechanisms that are plasmid mediated, the quinolones do not appear to be vulnerable to degradation by bacterial inactivation mechanisms. Bacterial resistance to the quinolones occurs through chromosomal mutations in the target enzyme or through mutations which alter drug permeability into the cells (Vance-Bryan *et al.*, 1990).

Transport mechanisms including efflux mechanisms are utilised by prokaryotic and eukaryotic cells in many situations, including acquisition of essential nutrients, establishment of charge and pH gradients across cytoplasmic membranes and extrusion of potentially toxic compounds. Mechanisms of resistance to quinolones by *Staphylococcus aureus* include mutational alterations of DNA gyrase. Quinolones interact with the A subunit or the DNA gyrase DNA complex. Several point mutations in *gyrA* confer high levels of quinolone resistance. Another mechanism of resistance is the efflux of quinolones from the cells, which offers lower level of resistance than mutations in *gyrA*. *S. aureus* shows active efflux of the drugs, mediated by a transmembrane protein *NorA*, which is dependent on H^+ gradients and sensitive to compounds such as 2,4-dinitrophenol. Uptake of norfloxacin in resistant strains is also normalised after addition of 2,4-dinitrophenol that disrupts energy processes. The *tet* genes encode for an integral membrane polypeptide antiporter, which acts to pump antimicrobials out of the organism, the function of which is dependent upon the proton gradient. The *NorA*1199 encoded set of proteins form an integral membrane polypeptide 389 amino acids long. This protein mediates the efflux of structurally unrelated compounds and is capable of effluxing quinolones. The function of the protein is inhibited by reserpine and verapamil, compounds that also inhibit the function of PgP (Kaatz *et al.*, 1993). Arsenate was able to inhibit the efflux of ciprofloxacin, thus the drug export system in *S. pneumoniae* could be mediated directly by ATP hydrolysis or *via* the proton motive force. There are several transport systems in the *S. pneumoniae* which are members of the ATP-binding cassette transporter family (Zeller *et al.*, 1997).

1.7.5 PHARMACOKINETICS

In general, quinolones are rapidly absorbed, within 2 hours of oral administration and have a high bioavailability.

In healthy volunteers, oral ciprofloxacin is rapidly absorbed, peak serum concentrations are reached within 2 hours with a bioavailability ranging from 50 to 85 %. Intestinal absorption occurs mainly in the *duodenum* and the *jejunum*, mostly *via* passive-diffusion mechanisms (Nouaille-Degorce *et al.*, 1998). The first-pass effect through the liver is thought to be unimportant (approximately 5 %). Ciprofloxacin diffuses into most body tissues (with particular affinities for the lungs and the prostate), with protein binding of approximating 16 to 40 %. The volume of distribution is large with a steady state range after oral or intravenous dosing of 1.74 to 5.0 $L.kg^{-1}$, reflecting penetration of the drug into most tissues (Nightingale, 1994; Nouaille-Degorce *et al.*, 1998; Vance-Bryan *et al.*, 1990).

Lomefloxacin and ofloxacin have higher serum concentrations and longer half-lives than ciprofloxacin and norfloxacin. The bioavailability among quinolones differs somewhat, norfloxacin 40 %, ciprofloxacin 69 %, and lomefloxacin and ofloxacin are virtually 100 %. The area under the serum concentration time curve, a measure of drug bioavailability is highest for ofloxacin, followed by lomefloxacin (Nightingale, 1994).

The systemic clearance of many quinolones is mainly by metabolism and urinary excretion. However, grepafloxacin and sparfloxacin have biliary clearance which exceeds the renal clearance. Hepatic uptake determines the level of biliary clearance, metabolism and distribution. A number of multispecific transport systems are known to be involved in the hepatic uptake of cationic drugs (Sasabe *et al.*, 1997).

Ciprofloxacin is mainly eliminated *via* the kidneys, with 40-45 % of an administered dose being recovered in the urine in the unchanged form. Both glomerular filtration and active tubular secretion appear to be involved (Nouaille-Degorce *et al.*, 1998). For patients with severe renal failure, the ciprofloxacin half-life doubled, as a consequence of drastically reduced clearance. It was accompanied by an increase in the elimination in faeces of both ciprofloxacin and its metabolites. Despite producing a marked

decrease in clearance, renal failure does not alter the pharmacokinetic profile of ciprofloxacin administered parentally (Nouaille-Degorce *et al.*, 1998).

Non-renal clearance accounts for 33 % of the elimination of ciprofloxacin, with faecal recovery of ciprofloxacin being approximately 15 % of an intravenous dose. Non-renal elimination includes metabolic degradation, biliary excretion and transluminal secretion across the enteric mucosa (Nouaille-Degorce *et al.*, 1998). Gastrointestinal secretion into the intestinal lumen is a quantitatively important route of elimination. In humans, 18 % of an IV ciprofloxacin dose is eliminated by intestinal secretion (Griffiths *et al.*, 1994). About 18 % of the dose is found in the faeces and 71 % is found in the urine. About 15 % of the dose in the faeces is metabolites and 13 % in urine, this leaves about 10 % of an intravenous dose excreted into the faeces by an unknown mechanism. Using radiolabelled quinolones it was found that radioactivity could be detected in the lower parts of the gastrointestinal tract shortly after injection and before any biliary excretions, this indicate the presence of gastrointestinal secretion in that part of the gut. The quantification of gastrointestinal secretion of ciprofloxacin including the absence of complete re-absorption suggests that at least 11 % of the intravenously administered dose is taken up by epithelial cells of the gut and secreted into the gut lumen (Sorgel *et al.*, 1989).

The concomitant oral administration of magnesium-, aluminium-, or calcium-containing antacids, sucralfate, iron preparations and multivitamins containing zinc significantly reduces the absorption of ciprofloxacin. It is not known that if the effects of antacids on the biopharmaceutical properties of the quinolones are due to metal ion complexation, shifts in pH of intestinal fluid, urine or both (Ross and Riley, 1992). However, concomitant administration of food does not hinder absorption. (Vance-Bryan *et al.*, 1990).

The quinolones show a significant level of faecal elimination, even after intravenous administration (Rabbaa *et al.*, 1996). Faecal recovery of ciprofloxacin accounts for about 15 % of the dose following intravenous administration and may be the result of elimination directly through the intestinal mucosa (Vance-Bryan *et al.*, 1990). This elimination is mostly due to gastrointestinal secretion rather than secretion into bile. Substrates for the sodium-independent liver bile acid transporter were found not to

inhibit ciprofloxacin secretion indicating that biliary secretion was not a major contributor.

Clinical studies carried out with patients with renal failure demonstrated a less pronounced decrease in ciprofloxacin total clearance than would have been expected from creatinine clearance values. This suggests the existence of a compensatory mechanism to ciprofloxacin renal elimination. Renal failure did not alter the biliary excretion of ciprofloxacin, however, intestinal secretion was increased in a compensatory manner (Dautrey *et al.*, 1999).

Although some of this work appeared while this project was underway, it is presented here to provide a full picture of quinolone absorption. Gatifloxacin is a new quinolone, which has recently been shown to undergo predominate renal elimination with approximately 60 to 80 % of the dose being recovered unchanged in the urine (Aminimanizani *et al.*, 2001). It has a t_{max} of 1.5 hours and an elimination half-life of 6.5 hours (Lubasch *et al.*, 2000).

1.7.6 MECHANISMS OF QUINOLONE TRANSPORT

The compensatory increase in intestinal elimination following renal failure led to the formation of the rationale that there maybe an active mechanism that was present in the intestine responsible for the secretion of quinolones.

The transport of a number of different quinolones has been studied using different *in vitro* models and varying results have been obtained. Models representing the blood-brain-barrier, renal elimination, hepatic elimination, intestinal secretion and human models have all been used in the investigation of quinolone secretion (Sorgel *et al.*, 1989; Ooie *et al.*, 1996; Cavet *et al.*, 1997a; Sasabe *et al.*, 1997; Dautrey *et al.*, 1999; Ito *et al.*, 1999). These models have produced mixed findings and in many cases findings from one model have been extrapolated across to another which may not be a valid procedure.

Some of the results indicated the presence of active secretion while others indicated that the process was passive and transport of the quinolones is based on lipophilicity (Jaehde *et al.*, 1993). Models which have indicated an active secretory mechanism were in most cases unable to elucidate the exact nature of the mechanism involved and therefore a number of mechanisms have been proposed. The mechanisms suggested for the active secretion of the quinolones included PgP, anion and cation transporters (Yano *et al*, (1997; Cavet *et al*, (1997a), cMOAT (Sasabe *et al.*, 1997) and as yet unknown transporters or a combination of these transporters (Griffiths *et al.*, 1994).

Clinical studies were conducted to explore the renal secretion and the effects of renal insufficiency by Sorgel *et al*, (1989) and Jaehde *et al*, (1995). Sorgel *et al*, (1989) found that at least 10.6 % of an 200 mg IV dose of ciprofloxacin was excreted into the gastrointestinal tract by an unknown mechanism in humans. Jaehde *et al*, (1995) investigated the effects of probenecid on the distribution and elimination of ciprofloxacin in humans. It was found that the probenecid-sensitive active transport in the kidney tubules was the major elimination pathway for ciprofloxacin. A number of other renal models have produced mixed findings some of which are in agreement with the observation made by Jaehde *et al*, (1995) while others are contradictory.

A large proportion of the work investigating quinolone secretion has used renal models, being the principal elimination route for a number of quinolones including ciprofloxacin and gatifloxacin. The most commonly used renal models have included cell lines such as LLC-PK$_1$, cortical slices and perfused kidney models. These methods have produced mixed results which could be attributed to the differences within the models used and the different quinolones investigated.

During the course of this work, Dautrey *et al*, (1999) investigated the influence of renal failure on the intestinal clearance of ciprofloxacin in nephrectomised and control rats. It was found that the intestinal elimination increased in a compensatory manner to the loss observed in renal function and that this intestinal elimination was not due to an increase in biliary excretion. The exact mechanism underlying the increased intestinal elimination of ciprofloxacin in renal failure was not determined. Recently Nouaille-Degorce *et al*, (1998) studied the influence of simulated renal failure on ciprofloxacin pharmacokinetics in the rat. It was found that intestinal secretion increased in a

compensatory manner to account for the renal insufficiency as seen earlier. Once again the mechanism involved was not identified.

Ito *et al*, (1997) used the LLC-PK$_1$ renal cell line and a transfected derivative cell line which over-expresses human PgP within the apical membrane, to study the transcellular transport of levofloxacin. It was found that both anion and cation transport inhibitors had no significant inhibitory effect on the secretion of levofloxacin, however, the PgP inhibitors, cyclosporin A and quinidine, had a significant inhibitory effect. The transfected cell line also secreted significantly more levofloxacin than that observed with the wild-type cell line. It was concluded that PgP might contribute to the renal tubular secretion of levofloxacin. More recently further work conducted on the distribution of levofloxacin in the rat kidney using renal cortical slices by the same group revealed that, typical substrates for the organic anion and cation transporters (*p*-aminohippurate and cimetidine) did not cause a significant effect on the renal secretion. As observed for the LLC-PK$_1$ cell line (Ito *et al.*, 1999). However, as before the PgP inhibitor quinidine had a significant effect. It was concluded that the basolateral-to-apical transport of levofloxacin was mediated by a specific transporter, distinct from the organic cation and anion transport system in the kidney. Even though the PgP inhibitors cyclosporin A and quinidine significantly inhibited the renal secretion, PgP was not proven to be the transporter involved (similar findings were made using the perfused rat model (Ito *et al.*, 2000)).

While this work was in progress Yano *et al*, (1997) characterised the *in vivo* renal tubular secretion of levofloxacin in rats and investigated the effects of cationic and anionic drugs on the renal excretion. It was found that the excretion of levofloxacin was significantly reduced by cimetidine and the tetraethylammonium ion; both of which are cationic. The author concluded that the renal tubular secretion was inhibited by cimetidine, a finding contradictory to that observed by Ito *et al*, (2000) using the perfused rat model.

Recently Matsuo *et al*, (1998) also characterised the secretion of levofloxacin using the kidney epithelial cell line LLC-PK$_1$. The author found that various quinolones were able to inhibit the basolateral-to-apical secretion of levofloxacin. Cimetidine and quinidine also decreased the secretion of levofloxacin. The author concluded that the

quinolones could be transported by a specific mechanism that was distinct from the H^+-organic cation antiport system. As stated earlier, Ito *et al*, (1997) also used the LLC-PK$_1$ renal cell-line and found that cimetidine was ineffective in reducing the secretion of levofloxacin, a finding contradictory to that observed by Matsuo *et al*, (1998).

Most of the quinolones undergo a significant level of renal elimination, however grepafloxacin and sparfloxacin undergo significant hepatic metabolism followed by biliary excretion. During the course of this work Sasabe *et al*, (1997) studied the carrier-mediated hepatic uptake of grepafloxacin in the rat. The transport of grepafloxacin was investigated to determine whether the transporter involved was the conjugated bile acid, organic anion, organic cation or the neutral steroid transporter. It was found that grepafloxacin inhibited the uptake of pravastatin, cimetidine and ouabain at a concentration of 200 μM. Quinidine and verapamil were also able to inhibit the uptake of grepafloxacin; these compounds are inhibitors of PgP and are also amphipathic cations. It was concluded that the hepatic uptake of grepafloxacin was carried out by a Na^+-independent carrier-mediated transport system which was distinct from that involved in the transport of bile acids, organic anions, cations or neutral steroids. Subsequently the carrier-mediated biliary excretion of grepafloxacin and its glucuronide metabolite was also studied in rats (Sasabe *et al.*, 1998). The excretion was compared in two different populations of rats: those with a functional cMOAT and those with a hereditary defect in their cMOAT. It was found that the excretion in rats with functional cMOAT was three times greater than those that had a deficiency with cMOAT. The author concluded that cMOAT contributed to the biliary excretion of grepafloxacin.

For a number of quinolones, such as ciprofloxacin and norfloxacin, intestinal elimination is secondary to renal elimination and, in cases where renal insufficiency occurs, elimination using the intestinal route increases in a compensatory fashion. The exact mechanism of intestinal elimination is not yet clear. Work has been carried out in this area however, using a small number of quinolones, which include ofloxacin, ciprofloxacin, norfloxacin and sparfloxacin using cellular models such as Caco-2 cells and other intestinal models (Griffiths *et al*, (1993); Cavet *et al*, (1997a); Cormet-Boyaka *et al*, (1998)).

Rabbaa *et al*, (1996) studied the intestinal elimination of ofloxacin enantiomers in the rat. It was found that ciprofloxacin could decrease the secretion of both ofloxacin enantiomers. Both verapamil and quinidine were also able to reduce the secretion of both enantiomers of ofloxacin. The author concluded that a stereoselective and saturable mechanism was involved in the intestinal secretion of ofloxacin and was most likely to be PgP (Rabbaa *et al.*, 1997).

Indications that secretion could be observed in the intestinal models was obtained when Griffiths *et al*, (1993) characterised the active secretion of ciprofloxacin with the Caco-2 cell line. The basolateral-to-apical secretion of ciprofloxacin was abolished in the presence of sodium azide with 2-deoxy-D-glucose. It was concluded that the secretion was mediated by an unknown active transport system. The active secretion mechanism was further investigated using ciprofloxacin, norfloxacin and pefloxacin (Griffiths *et al.*, 1994). It was found that norfloxacin and ciprofloxacin were subject to basolateral-to-apical active secretion and cross-competition was observed between the quinolones, indicating the presence of a common secretory mechanism, the exact identity of which could not be elucidated by the author.

A further study on ciprofloxacin secretion in Caco-2 cells found that the secretion of ciprofloxacin was inhibited by DIDS (400 µM) (Cavet *et al.*, 1997a). The secretion of ciprofloxacin was also partially inhibited by verapamil (100 µM). However, the secretion of ciprofloxacin was not subject to inhibition by probenecid or other anion inhibitors. This led to the conclusion that a novel transport mechanism, sensitive to DIDS and verapamil, was responsible for the secretion and the involvement of PgP in the basolateral-to-apical secretion was excluded due to the use of inhibitory PgP monoclonal antibodies, which had no effect on the basolateral-to-apical secretion.

Subsequently Cormet-Boyaka *et al*, (1998) compared the secretion of sparfloxacin with that of the PgP substrate vinblastine. The secretion of both compounds was significantly reduced by the presence of the PgP inhibitor verapamil. It was concluded that PgP was likely to be involved in the intestinal elimination of sparfloxacin, a finding contradictory to that of Cavet *et al*, (1997a). Ooie *et al*, (1996) used the rat choroid plexus, an epithelial tissue which forms the blood-CSF barrier, to investigate a possible active efflux mechanism which moves fleroxacin from the CSF into the blood. It was

found that the transport of fleroxacin was mediated by a sodium-independent efflux mechanism that was also implicated in the transport of other organic anions such as benzylpenicillin. However, Jaehde *et al*, (1993) found that transport of quinolones across the blood-brain-barrier was carried out by a mixture of passive paracellular and transcellular flux and carrier-mediated processes were not involved. This finding is in contradiction to that of Ooie *et al*, (1996).

Currently, there is no clear picture of the mechanism involved in the secretion of the quinolones; it may not even exist. If it exists, it could be an anion transporter, cation transporter, cMOAT, PgP or a new unknown transporter.

This present study will investigate the transport of a number of quinolones through Caco-2 cells, a well established model for the human intestine. Much of the reported work has been carried out using levofloxacin, ciprofloxacin, grepafloxacin and sparfloxacin. This work will be using a series of quinolones which include some of these older quinolones as well as the new quinolones BMS-284756-01 and gatifloxacin. The quinolones used will have a varied physicochemical properties including lipophilicity and molecular weight. Which should help to determine whether the basolateral-to-apical secretion of quinolones is a class effect, or dependent on specific properties of the quinolone. Previous studies have used small numbers of quinolones and have extrapolated observations made using non-intestinal models to the intestinal model used. As this work will exclusively use Caco-2 cell model, this will prevent extrapolation of results from one model to the next, as seen for the involvement of cMOAT in the potential intestinal secretion of quinolones, where most of the data was generated using renal models.

Traditional molecular modelling is usually carried out to determine structure-activity relationships. It is hoped that these molecular modelling techniques can be applied to determine descriptors that could then be used to predict the cellular permeability of the quinolones. A vast amount of work has been carried out on structure activity relationships for the quinolones, focusing on the binding of the quinolones with the DNA-gyrase target (Hooper and Wolfson, 1993), however, very little work has been carried out investigating their absorption. It is hoped that the cellular permeability can be modelled, which in turn could be related to absorption and bioavailability.

This study will investigate the apical-to-basolateral and basolateral-to-apical flux of a range of quinolones across Caco-2 cells to firstly identify if an active secretion mechanism is present, if it exists then to examine the inhibition of this secretory mechanism and whether any physicochemical dependence can be established. Gatifloxacin, a new quinolone, will be used as a primary 'probe' for the active secretion mechanism.

1.8   OBJECTIVES OF THESIS

The objectives of this thesis are to investigate the *in vitro* transport of a group of quinolone antibiotics in terms of their physicochemical parameters and, secondly, to determine descriptors to characterise the physicochemical properties of the quinolones investigated. This will involve:

- Investigation of the mechanisms involved in the apical-to-basolateral and basolateral-to-apical transport for a large group of quinolones, using the intestinal Caco-2 cell model.

- Determination of the mechanism or mechanisms involved in the active transport or secretion of the quinolones, by logically eliminating possible transport mechanisms with inhibitors.

- Attempting to prediction the cellular permeability for the quinolones based on their physicochemical descriptors such as lipophilicity, molecular weight and pK_a, and relating the cellular permeability to *in vivo* absorption.

- Investigation of fluorescein sodium as an appropriate marker for paracellular transport.

It is hoped that this work will help eliminate the confusion in this area regarding the bi-directional transport of quinolones.

CHAPTER 2 MATERIALS AND METHODS

2.1 SUMMARY

This chapter provides an overview of the experimental techniques used and focuses especially on the HPLC methodology. Where specific application methods varied from the general method, these changes are highlighted in the appropriate chapter and section. In most cases, results are expressed as the mean ± the standard deviation of at least three values. Statistical tests performed include the unpaired t-test and one-way analysis of variance (ANOVA) using the Primer of Biostats version 4.0 software by McGraw Hill.

2.2 MATERIALS

2.2.1 CELL CULTURE REAGENTS

Caco-2 cells, passages number 26, were obtained from Astra-Zeneca, Loughborough; the original cells were Caco-2 cells (passage 18/19), purchased from the American Type Tissue Culture Collection (ATTC) (Rockville, MD, USA).

Dulbecco's modified Eagle's medium (DMEM) and N-2-hydroxyethylpiperazine-N'-2-ethansulphonic acid (HEPES) buffer without phenol red, foetal bovine serum (FBS), L-glutamine (200 mM), non-essential amino acids (NEAA), penicillin, streptomycin and trypsin/EDTA were all from Gibco. The 75 cm^2 culture flasks, 24-well plates and 6-well plates were purchased from Costar Corning. FBS, L-glutamine, penicillin, trypsin and streptomycin were stored at -20°C and thawed prior to use in a water-bath at 37°C. DMEM, HEPES 1 M buffer solution and NEAA were stored at 4°C. All other chemicals were stored at room temperature. Transwell inserts, with a clear polycarbonate membrane, 3 μm pore size, were obtained from Costar Corning. D-[1-^{14}C]Mannitol with a specific activity of 9.25 MBq, which was used for assessment of the paracellular permeability, was obtained from Amersham. Phosphate-buffered saline (PBS) tablets and ethylenediaminetetratraacetic acid (EDTA) were purchased from Sigma Chemical Company.

2.2.2 TRANSPORT STUDIES

2-Deoxy-D-glucose, (±)-verapamil hydrochloride, probenecid, 4,4'-diisothiocyanato-stilbene-2,2'-disulphonic acid (DIDS), Kreb's-Ringer bicarbonate buffer, MES (2-[N-morpholino]ethanesulphonic acid) and sodium azide were all purchased from Sigma Chemical Company. Tris-hydroxymethyl-aminomethane was purchased from ICN Biomedicals Inc. [^{3}H]Testosterone with a specific activity of 9.25 MBq was purchased from NEN/Dupont. The quinolones and internal standard used for HPLC are listed in the HPLC section. Black 96-well fluorescence plates were obtained from Life Science Technology, the Wallac Victor^2, a fluorescence plate-reader, was used. Optiphase HiSafe III scintillation fluid purchased from Wallac was used for scintillation counting on the Packard 1900TR liquid scintillation analyser.

2.2.3 GENERAL EQUIPMENT

The microscope used was a Nikon TMS, with a Nikon F-series camera. The pH meter used was a Corning 240. The scanning UV was a Unicam Heλios β. The TEER were measured using World Precision Instruments EVOM chop-stick electrodes.

2.3 CELL CULTURE METHODS

2.3.1 CELLULAR STOCK CULTURES

The cells were maintained in a growth medium comprising of DMEM supplemented with 10 % v/v FBS, 1 % v/v NEAA, 1 % v/v L-glutamine (2 mM), 100 UmL^{-1} penicillin, 100 µg.mL^{-1} streptomycin and 0.5 % w/v HEPES buffer solution (1 M). The media were prepared under aseptic conditions, stored at 4°C and used within 14 days of preparation.

Cells were grown in plastic tissue-culture T-flasks, with a non-wetting 0.22 µm hydrophobic microporous membrane vent, and an area of 75 cm^2. The cultures were maintained in growth medium, which was replaced every 2 days. Cells were grown in an atmosphere of 5 % carbon dioxide and 90 % relative humidity, at 37°C. The cultures

were passaged by trypsinisation when confluent, every 4-5 days, and the flasks were seeded usually using a splitting of 1:3 which gave approximately 8×10^6 cells *per* flask.

The growth medium was aspirated and the cells were washed with 5 mL of PBS pH 7.4 (0.01 M phosphate)/EDTA (6.72 mM) for 5 minutes. The PBS/EDTA was aspirated, the cells were then washed with trypsin/EDTA (0.25 % w/v, 5 mL) for 30 seconds, after which the trypsin/EDTA solution was aspirated. The flask was left at room temperature for 4-5 minute in the hood, after which the cells were observed under the light microscope, if they had not started to separate the flask was tapped gently to dislodge the cell monolayer. Then, 7 mL of growth medium was added to the flask to deactivate the remaining trypsin and the cells were sucked up and down 15-20 times using a 5 mL pipette to achieve a single-cell suspension. The cell suspension was used to seed three flasks (2 mL *per* flask, which was approximately 3 million cells) to which 11 mL of growth media was then added.

In order to check viable-cell density, a trypan-blue exclusion test was performed when seeding 24-well plates and inserts. Trypan blue 100 μL (0.4 %) was added to 400 μl of cell suspension following trypsinisation. 100 μL was then added to the counting chamber of a Neubauer haemocytometer. The cells in 5 large squares of the haemocytometer were counted using a conventional light microscope. Viable cells appeared with clear cytoplasm, whereas dead cells absorb the stain and appeared blue. In most cases cell were found to be more than 80 % viable.

2.3.2 SEEDING 24-WELL PLATES FOR TOXICITY STUDIES

Cells were seeded in 24-well plates and used to assess the toxicity of different concentrations of verapamil. The 24-well plate was seeded with 100,000 cells *per* well and the media were changed every other day and replaced with 1 mL of fresh media. The cells were ready 6 days post-seeding, to be used for toxicity studies. The cells were washed twice using PBS, the PBS was aspirated and replaced with the appropriate concentration of verapamil: 100 μM through to 500 μM (1 mL). The cells were incubated with the verapamil for one hour. The verapamil was aspirated and the cells were trypsinised as described in section 2.3.1, using 200 μL of PBS/EDTA and 200 μL

of trypsin/EDTA. The cells were then counted using the standard procedure described in section 2.3.1. The total numbers of cells were counted as well as those unable to exclude trypan blue, the number of viable cells was expressed as a percentage of total cells.

2.3.3 SEEDING OF INSERTS

The cells were counted and an appropriate amount of medium was added to the flask, to give 400,000 cells *per* 2 mL. The 6-well Transwell inserts were seeded in the following way; 2 mL of growth medium was added to the basolateral compartment and 2 mL of media containing the appropriate number of cells was added drop-wise to the donor compartment. The cultures were then incubated at 37°C, in an atmosphere of 5 % CO_2, 95 % relative humidity. The growth medium was renewed every 2 days and the inserts were used 21-28 days post-seeding, once they were confluent following a visual inspection and measurement of TEERs.

2.3.4 BUFFERS USED FOR TRANSPORT STUDIES

The incubation medium for transport studies was Hank's balanced salt solution without phenol red (HBSS) (9.8 g.L^{-1}) and 25 mM HEPES, adjusted to pH 7.4 with 1 M sodium hydroxide or 1M hydrochloric acid. This was the standard transport medium in which quinolones or inhibitors or other compounds were made up and is subsequently referred to as the transport medium.

For experiments where the pH was varied, the buffers were used:

Buffer pH 8.5

Kreb's-Ringer buffer pH 8.5 (9.8 g.L^{-1} Kreb's Ringer) and 10 mM TRIS base, pH adjusted to pH 8.5 with 1 M sodium hydroxide.

Buffer pH 5.5

Hank's balanced salt solution (HBSS) (9.8 g.L^{-1}) and 25 mM MES adjusted to pH 5.5, with 1 M sodium hydroxide or 1 M hydrochloric acid.

2.4   TRANSPORT STUDIES

2.4.1   GENERAL METHODS

The growth medium was aspirated from the inserts containing the confluent cells, between 21 to 28 days post-seeding. The inserts were washed twice using 2 mL of transport medium. The TEER was measured for the inserts in the presence of the transport medium. The TEER was measured using chop-stick electrodes. Washings were then aspirated and the inserts were transferred to fresh 6-well plates with 2.6 mL of transport medium in the basolateral compartment and 1.5 mL in the apical compartment, the cells were allowed to equilibrate in the medium for 15 minutes. The experiment was initiated by aspirating the medium from both apical and basolateral chambers and transferring the inserts into a new 6-well plate. Blank transport medium or transport medium containing the compound of interest was added to the apical or basolateral sides in volumes of 1.5 mL and 2.6 mL respectively. The plates were incubated at 37°C with agitation within an Amersham hybridisation oven for the duration of the experiment. All experiments were performed in triplicate and results are quoted as the average ± standard deviation (SD) unless otherwise stated.

Samples of 150 μL were taken from each basolateral or apical well at time 5 through to 40 minutes at 5 minute intervals (see figure 2.1). Blank transport medium (containing no drug substance) 150 μL was used to replace the volume removed, subsequent calculations were carried out accounting for the loss of volume (see equation 2.1 and appendix A3). The samples were analysed using HPLC or scintillation counting for radiolabelled compounds or the 96-well plate reader in Victor^2 which was used for fluorescein followed by retrieval of the sample for HPLC.
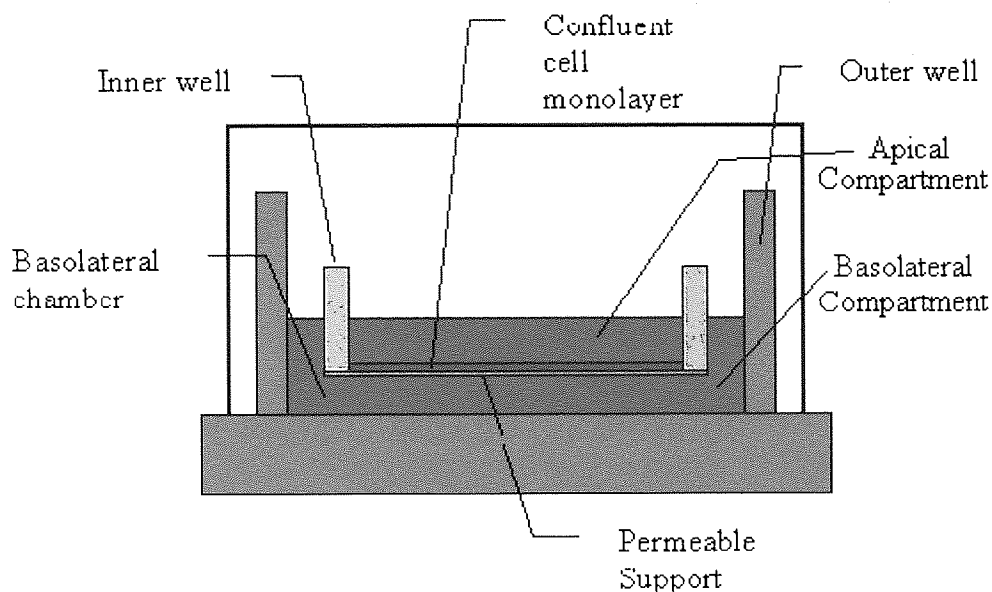
Figure 2.1 - Diagrammatic representation of Corning Costar transport setup.

2.4.1.1 TRANSPORT STUDIES USING INHIBITORS

When an inhibitor was used in the transport experiment together with the various quinolones, the following modifications were made to the general experimental procedure. After the inserts had been washed twice, they were allowed to equilibrate in transport medium containing the appropriate inhibitor for 15 minutes. This medium was then aspirated and replaced with fresh transport medium containing the quinolone and inhibitor and blank transport medium was added to the contralateral chamber. The remainder of the experimental procedure was as stated earlier in section 2.4.1.

2.4.1.2 TRANSPORT STUDIES USING FLUORESCEIN AS A PARACELLULAR MARKER

Fluorescein sodium (10 μg.mL^{-1}) was used as a potential paracellular marker and it was also investigated as an inhibitor of quinolone efflux. When it was used as a paracellular marker, the inserts were incubated in blank transport medium. However, when it was used as an inhibitor, the inserts were incubated with fluorescein for 15 minutes. The equilibration medium was removed and replaced with medium containing quinolone

and fluorescein and blank medium was used in the contralateral chamber. As stated earlier, 150 µL samples were removed every 5 minutes for 40 minutes, these samples were directly transferred to black 96-well plates and measured at an excitation wavelength of 485 nm and emission wavelength of 525 nm. The sample was then recovered and used for HPLC analysis of the quinolone.

2.4.1.3   USE OF RADIOLABELLED COMPOUNDS

With the transport studies using D-[1-^{14}C]mannitol or [^{3}H]testosterone, the following modifications were made to the general experimental procedure for transport studies. Samples of 150 µL were taken from the receiver chamber at 5 minute intervals and directly transferred to scintillation vials. Blank transport media (150 µL) was used to replace the volume removed. To the sample (150 µL), 5 mL of Optiphase HiSafe III fluid was added. The scintillation vial was then vortexed to ensure adequate mixing and then the vials were measured using a liquid scintillation analyser with a 10 minute count-time. Decays *per* min (DPM) were used in calculations (example calculation in appendix A3.1).

2.4.2 CALCULATIONS

To account for the sample removed at each time point and calculate the cumulative amount transported equation 2.1 was used (see appendix A3.3).

EQUATION 2.1

$$M_t[n] = V_r.C[n] + V_s.\sum_{m=1}^{n-1} C[m]$$

$M_t[n]$	Current cumulative mass (µg)
V_r	Volume in receiver (mL)
$C[n]$	Current concentration receiver (µg.mL^{-1})
V_s	Sample volume removed (mL)
$\Sigma C[m]$	Summed total of previous concentrations (µg.mL^{-1})

2.5 SCANNING ELECTRON MICROSCOPY

Scanning electron microscope (SEM) Cambridge Stereoscan 590B was used at Aston University.

2.5.1 MATERIALS

Glutaraldehyde, sodium cacodylate and hexamethyldiazolazone were supplied by Sigma Chemical Company, ethanol was supplied by Fisher. A stock solution of 0.2 M sodium cacodylate buffer was prepared using distilled water and the pH was adjusted to 7.2 using 0.1 M HCl. The cacodylate buffer was stored in at 4°C. The fixative needed to be freshly prepared as follows: sodium cacodylate buffer 0.2 M (50 %), 25 % v/v glutaraldehyde (10 %) and distilled water (40 %).

2.5.2 METHOD

The growth medium was removed from the Caco-2 cells growing on inserts. The surface of each insert was covered with 2 mL of fixative and left for 1 hour to permeate into the tissue.

The fixative was then removed and replaced with 2 mL of 20 % v/v ethanol, this solution was left on the insert for 15 minutes, after which it was replaced with 30 % v/v ethanol. A sequential dehydration procedure was then carried out by replacing alcohol with solutions of increasing concentration for 15 minutes each *i.e.* 40 %, 50 %, 60 %, 70 %, 90 %, 95 % and 100 %. The 100 % ethanol was removed and replaced with hexamethyldiazolazone for 5 minutes after which the insert was allowed to dry. The insert was then mounted on a metallic stud, gold-coated twice for 10 minutes and viewed using the SEM.

2.6 MINIMUM INHIBITORY CONCENTRATIONS MIC MEASUREMENTS

2.6.1 INTRODUCTION

The minimum inhibitory concentration MIC, is the minimum concentration of an antibiotic required to inhibit growth of a test organism. This may be measured by exposing standardised test organisms to different concentrations of the compound being investigated.

2.6.2 MATERIALS

Nutrient broth was purchased from Oxoid. DC0 *E.coli* and *Staphylococcus aureus* test organisms were supplied by Microbiology, Aston University. Sterile disposable plastic was used and all manipulations were conducted under aseptic conditions. The nutrient broth had been autoclaved to sterilise it.

2.6.3 METHOD

Nutrient broth (100 mL) was inoculated with the appropriate organism and incubated for 12 hours to give approximately 10^9 cells.mL^{-1}. Fresh nutrient broth 100 mL was inoculated with 0.1 mL of broth containing organisms to give approximately 10^6 cells.mL^{-1}.

Each solution of quinolone 1 mg.mL^{-1} was filter-sterilised using a 0.2 μm syringe filter. These stock solutions were then serially diluted in 96-well plates to give a concentration range of 128 μg.mL^{-1} to 0.125 μg.mL^{-1}. Nutrient broth (50 μL) containing organisms was added to each well. Control wells containing no antibiotic were also present. The plates were incubated for 12 hours and they were visually inspected for growth.

2.7 COMPUTATIONAL METHODS

The computational methods are outlined in individual chapters and sections 3.3.3.3 and 3.4.

2.8 HPLC TECHNIQUES

The method used for the assay of the quinolones undergoing cellular transport studies was developed from a HPLC method for measuring ciprofloxacin in human serum (Jim *et al.*, 1992).

2.8.1 MATERIALS

Ofloxacin, lomefloxacin, norfloxacin, cinoxacin and 3,4-dimethoxybenzaldehyde, 3,4-dimethoxybenzoic acid, sodium dihydrogen phosphate, triethylamine, HEPES and Hank's balanced salt solution, fluorescein sodium were purchased from Sigma Chemical Company. Ciprofloxacin was purchased from Bayer. Methyl-ciprofloxacin, ethyl-ciprofloxacin, propyl-ciprofloxacin, butyl-ciprofloxacin, pentyl-ciprofloxacin and flumequine were donated by Gloria Sanchez and Teresa M Garrigues, Farmacia y Technologia Farmaceutica, Valencia, Spain. BMS-284756-01 was donated by Bristol-Myers Squibb, Merseyside, UK. Fluorescence-grade acetonitrile and ortho-phosphoric acid was purchased from Fisher. All chemicals were reagent grade and used as received without further purification, double-distilled water was used in the preparation of mobile phase and reagent solutions.

A Waters HPLC column, Nova-Pak C18, reversed-phase, 60 Å pore size, 4 μm particles, 3.9 mm internal diameter by 150 mm length, cartridge column, packed with dimethyloctadecylsilyl-bonded amorphous silica was used. A guard column, 1 cm in length packed with octadecyl-silane ODS spherical coated stationary phase, was used to protect the column throughout the studies. The column, silica particles and ODS were all purchased from HPLC Technology (Macclesfield, Cheshire, UK).

2.8.2 METHODS

A stock solution of 500 mL of Hank's Balanced Salt Solution (9.8 g.L^{-1}) containing 25 mM HEPES was prepared, 1 M sodium hydroxide was used to adjusted the pH to 7.4.

Stock solutions of each quinolone were prepared by dissolving 10 mg of each in transport medium with a few drops of 1 M sodium hydroxide added to enhance solubility of quinolones; volumes were made up to 10 mL with transport media. The solutions were shaken by hand and then sonicated for 10 minutes using an ultrasound bath to aid dissolution. With subsequent dilutions with transport media the pH of the solution for the experiment was restored to pH 7.4, 5.5 or 8.5.

The internal standard used was 3,4,-dimethoxybenzaldehyde (IS) or 3,4,-dimethoxybenzoic acid (SI) of varying concentrations was used (see table 2.1), depending on the quinolone. All quinolones and internal standard solutions were stored in glass vials covered with foil or in amber Eppendorf tubes. Samples were stored at 4°C and stock solutions were stored at -20°C and kept for no longer than one week, this was the length of time over which the stability of the solutions was checked.

The HPLC system consisted of a Cecil dual-reciprocating pump (Series 1000), a Gilson auto-injector (231 XL), Shimadzu fluorescence detector (RF 535XL) and Shimadzu integrator (CR 6A). A chart recorder (Gallenkamp Euroscribe) was also used during the development procedure. A 50 μL loop was used for all injections and a complete loop-fill technique was used, with mobile phase washing out the injection port between injections.

Data were generated by the integrator, which was then manually entered into Microsoft Excel 97 and underwent appropriate manipulations to generate calibration curves and process sample results.

The detector was operated at the various wavelengths depending on the quinolone in use (see table 2.1). These were determined by using a scanning UV spectrophotometer to determine excitation wavelengths λ_{max} and then various emission wavelengths were

obtained by using the Shimadzu detector. The internal standard used and concentration range of quinolones and mobile phase composition can all be found in table 2.1.

These wavelengths are valid for the system in use here (mobile phase and pH conditions) and compare favourably with those found in the literature (Wright *et al.*, 1998; Mehta *et al.*, 1992; Shibl and Tawfik, 1991).

The mobile phases used consisted of 15 to 30 % acetonitrile depending on the quinolone (see table 2.1), 1 % triethylamine and made up to 100 % with 0.01 M sodium dihydrogen phosphate. The pH of the mobile phase was adjusted to pH 3.00 with orthophosphoric acid. The mobile phase was filtered using a 0.45 µm filter and sonicated for 20 minutes before use to ensure that it was effectively degassed. It was delivered at a flow-rate of 1.0 mL.min^{-1}.

Calibration standards were prepared for each assay and run with each assay. Calibration curves were determined by direct linear regression, constructed to relate the peak area ratios of sample quinolone and internal standard. Adequate chromatographic separation was observed for all compounds and total run time was kept below 10 minutes *per* sample injection.

Calibration curves for each quinolone with sample chromatographs are illustrated in appendix A1.1 and A1.2.

With all the quinolones that were assayed, it was possible to detect 1ng.ml^{-1} of the quinolone; after this, the base-line noise caused significant problems. The system was reproducible (see appendix A1) and there was no interference with successive injections. Initially, there was a problem of carry-over with the more lipophilic quinolones, butyl and pentyl-ciprofloxacin. This was resolved by adding a needle flush command to the HPLC system and increasing the volume of mobile phase used to clean the needle. There were small day-to-day variations in the system, most likely from small changes in mobile phase and temperature. To account for these changes at least a five-point calibration was run with the unknown samples.

	Excitation Wavelength (nm)	Emission Wavelength (nm)	Internal Standard	Concentration on Internal Standard (μg.mL^{-1}) [*]	Concentration range of Quinolone (ng.mL^{-1})	Acetonitrile Composition (%)
BMS-284756-01	280	415	SI	20	50-500	23
Butyl-Ciprofloxacin	280	440	SI	50	50-900[+]	18
Cinoxacin	265	420	SI	2.5	1-40	18
Ciprofloxacin	280	440	SI	12.5	1-30	18
Ethyl-Ciprofloxacin	280	440	SI	250	15-400[+]	18
Flumequine	325	365	IS	100	30-700[+]	30
Gatifloxacin	295	495	SI	500	3-180	18
Levofloxacin	295	495	SI	250	4-20	18
Lomefloxacin	295	445	SI	62.5	1-75	18
Methyl-Ciprofloxacin	280	440	SI	500	10-300[+]	18
Norfloxacin	280	440	SI	31.25	1-20	18
Ofloxacin	295	495	SI	100	1-100	18
Pentyl-Ciprofloxacin	280	440	SI	10	50-1500[+]	23
Propyl-Ciprofloxacin	280	440	IS	250	20-720[+]	18

Table 2.1 – Summarised HPLC conditions for the quinolones assayed.

[*] Concentration of internal standard (10 μL) added to 150 μL of quinolone sample.

[+] These samples had to be diluted (1 in 100) before HPLC analysis.

The presence of cell-culture medium DMEM caused a large solvent front which posed a problem with those quinolones with a short retention time. To avoid this, transport experiments were run in HBSS, which did not pose any such problems.

High-performance liquid chromatography (HPLC) assays were developed, with a high level of sensitivity allowing quinolones to be detected in the nano-molar concentration range; a very small sample volume 50 μL is required. Microbiological methods to determine the quinolone levels have been reported in the literature. But, the highly specific and sensitive HPLC methods are preferable to the more time-consuming and less specific microbiological methods. With the latter, active metabolites or other antimicrobial compounds present in the sample can interfere to give falsely high results. The vast majority of quinolone assays currently available are designed for the evaluation of samples in biological fluids such as serum, urine and hair (Uematsu *et al.*, 1993; Wright *et al.*, 1998). Many HPLC assays have been designed to measure a specific quinolone and often require complicated sample preparations, the lack of internal standard is also reflected in some published methods (Shibl and Tawfik, 1991; Mehta *et al.*, 1992).

Calibration curves were used for the calibration and calculation purposes of the assay, the order of injection of the sample did not affect the results, *i.e.* a low concentration sample preceding a high concentration sample was not adversely affected.

In conclusion, the assay developed is suitable for studying quinolone flux through Caco-2 cells, the analytical method described is rapid, sensitive, adaptive and reproducible. This method could be modified and used for other quinolones.

2.8.3 USE OF HPLC FOR LIPOPHILICITY DETERMINATION LOGK

HPLC retention capacity factor K was determined using the above-mentioned HPLC system (see section 2.8.2) at different percentages of acetonitrile. The capacity factors were determined at 10 %, 14 % and 18 % acetonitrile. Not all of the quinolones could be run at these percentages of acetonitrile, which included BMS-284756-01, enoxacin,

flumequine, lomefloxacin, nalidixic acid and sparfloxacin. The retention times of each of the quinolones was converted to capacity factors by using equation 2.2.

EQUATION 2.2

$$K = \frac{t_r - t_m}{t_m}$$

Where t_r is the retention time of the peak for the quinolone and t_m is solvent front. The capacity factor is the relationship between the length of the column and the retention of a compound. The Ks were plotted against the percentage of acetonitrile and a second order polynomial fit was used to extrapolate back to 0 % acetonitrile, this value was known as K_o (Escribano *et al.*, 1997).

CHAPTER 3 PHYSICOCHEMICAL PROPERTIES

3.1 SUMMARY

This chapter investigates the physicochemical properties of quinolones. The pK_as determined using potentiometric titrations were in line with those found in the literature. An in-depth study into lipophilicity was carried including an investigation into the different methods used to measure and calculate lipophilicity. It was found that different methods for calculating logP did not produce comparable values or trends. Molecular modelling techniques were used to correlate lipophilicity with cellular permeability it was found that calculated descriptors cross-correlated with lipophilicity and each other.

3.2 pK$_a$

3.2.1 INTRODUCTION

Knowing the pK_a of a compound can be useful in determining its bioavailability. It can aid prediction of whether a compound will be able to cross a biological membrane. Many drugs are weak acids or weak bases and therefore their partitioning between membranes and aqueous environment can be affected by pH. As previously stated (see section 1.4.1) there are two major routes which a molecule can take to traverse the cellular membrane. The transcellular route is utilised by neutral lipophilic compounds while small hydrophilic charged compounds use the paracellular route. The extent of ionisation at physiological pH is related to pK_a of a compound so this parameter should be known.

The dissociation of a weak acid can be described by equation 3.1

EQUATION 3.1

$$H_2O + HA \rightleftharpoons H_3O+ + A^-$$
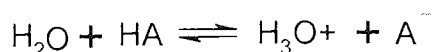
The equilibrium constant for the above expression is the following (see equation 3.2):

EQUATION 3.2

$$K_a = \frac{[H_3O^+].[A^-]}{[HA]}$$

K_a includes an adjustment for the $[H_2O]$ as it is in large excess and therefore is effectively constant.

The following equation (equation 3.3) shows the relationship between K_a and pK_a.

EQUATION 3.3

$$pK_a = -\log K_a$$

The pK_a of a compound can be determined in a number of ways including the use of solubility measures and potentiometric titrations. In the same way, the complementary determinations of pK_b can be made but this term is seldom used, because the information provided by the pK_a term can tell whether a base is weak or strong and by convention pK_a is used. The pK_b can be related to pK_a using equation 3.4.

EQUATION 3.4

$$pK_w = pK_a + pK_b$$

Küster coined the word zwitterion in 1897. A zwitterionic compound has one fully ionised acidic group and one fully ionised basic group in each molecule. These molecules are different from amphoteric substances. A compound can have both acidic and basic groups, but these cannot form an internal salt unless both groups are simultaneously ionised and this depends on the magnitude of their pK_a values (Albert and Serjeant, 1983). In highly acidic solutions, only cations are present and in highly alkaline solutions only anions are present, as with an amphoteric compound. The differences occur at intermediate pH values where the majority of molecules have both groups ionised. Zwitterions often have pK_a values which differ considerably from those of simpler analogues, this occurs when the basic and acidic groups are physically near

each other or are separated by conjugated systems. The ionisation of the basic group creates a positive charge which attracts electrons and thereby strengthens a nearby acidic group so that the pK_a of this group decreases. Conversely, the ionisation of an acidic group releases electrons which strengthen the basic group (Albert and Serjeant, 1983).

The pK_a values of amphoteric substances are readily determined using potentiometric titration. Titration of a compound with an acid result in the proton being added to the basic group and the reverse is true when titration occurs with a base, proton is removed from the acidic group. With a zwitterionic compound both acidic and basic groups may be ionised, therefore, when titrating with an acid the proton will not be added to the basic group but will attach to the cation (which was the acidic ionised group) (Albert and Serjeant, 1983).

A substance is often suspected to be a zwitterion when it is more soluble in water, has a higher melting point than related compound with only one ionisable group. This is a general rule and can apply to a number of non-zwitterionic compounds as well. Albert and Serjeant, (1983), stated that for every molecule which has an acidic pK_a numerically lower than the basic pK_a it is a zwitterion, it has acidic and basic groups strong enough to neutralise one another.

The pK_a values determined experimentally for zwitterions are referred to as macroscopic constants. The macroscopic constants are composites of the microscopic constants. Usually the macroscopic constants are more than enough for purposes required, but when two pK_a values lie within 3 units of one another the microscopic constants can be useful. To solve the microscopic constants one of them most be known. This is a very complex procedure which is seldom required (Albert and Serjeant, 1983; see figure 3.1). The isoelectric point is defined as the sum of the two pK_as for a compound divided by two (see equation 3.5). For a zwitterionic compound when the pH is equal to the P_i the compound exists solely as the zwitterion.

EQUATION 3.5

$$P_i = \frac{pK_a1 + pK_a2}{2}$$
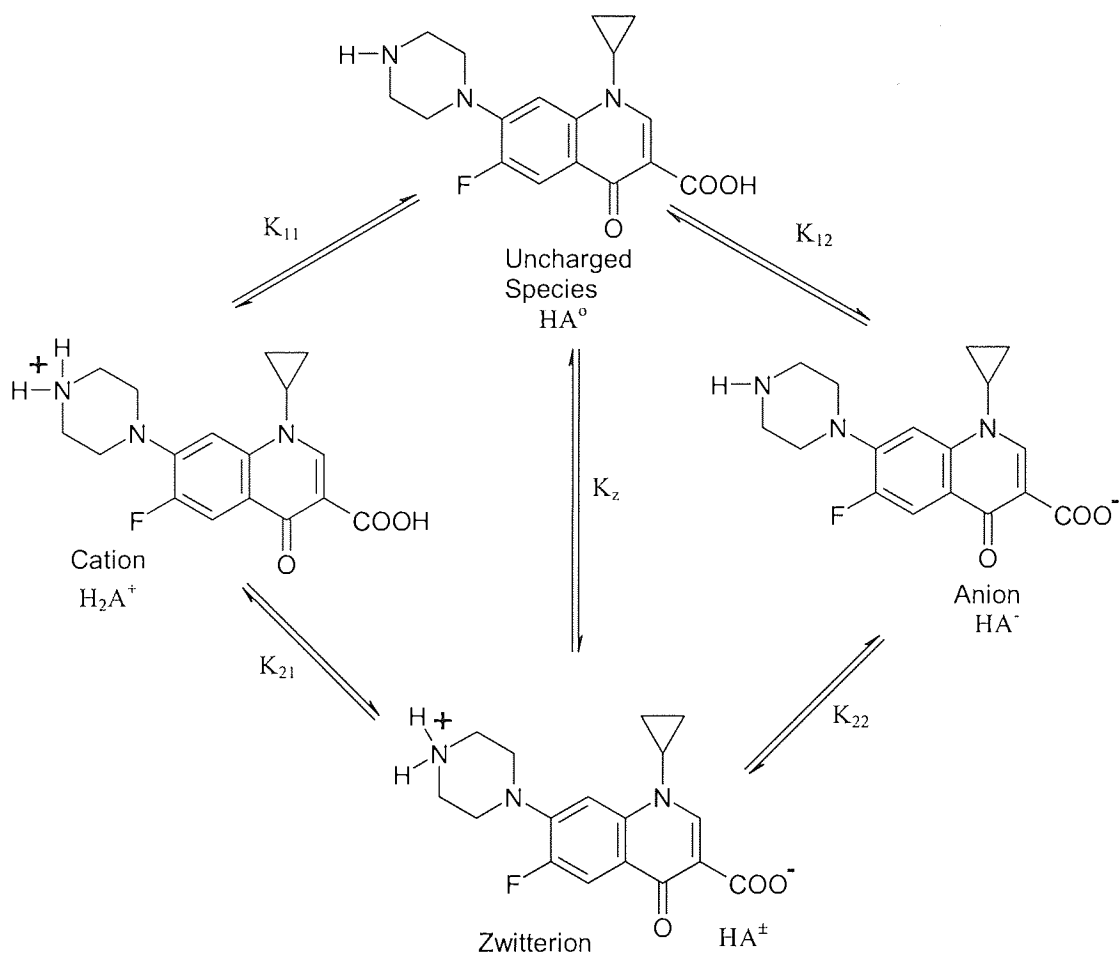
Figure 3.1 – Illustrating relationship between macro and microscopic constants, using ciprofloxacin.

Potentiometery is the most rapid, economical and usually the best method for determination of ionisation constants. Potentiometric titrations involve the precise addition of known volumes of a standardised strong acid such as HCl (1 M) or base such as KOH (1 M), added to a solution of the compound of interest, during which the pH is continuously measured. The compound being measured is dissolved in water or a co-solvent system if it is insoluble in water. The shape of the pH against the volume of titrant added can be used to determine the pK_a of the compound. The inflection point where the slope is at a maximum magnitude designates the endpoint; while the region of maximum buffering known as the half-neutralisation point is provided where the slope is at a minimum. At this point the compound is present in two states of protonation of equal concentrations. The pH at that point is equal to the pK_a. Titrations should be carried out at 0.01 M concentrations whenever solubility allows. At this low concentration, activity effects are minimal, if higher concentrations are used then corrections for activity should be made. The potentiometric titration for a single non-

overlapping pK_a can be described by equation 3.6, a correction for activity would have to be added if high concentration solutions were used. The range over which the titration can occur depends on the electrode, loss of electrode precision at low pH (<2) and at high pH values (>13) occurs. Misleading estimations of pK_a can be made if the negative logarithm of the concentration is greater than the pK_a. Based on this, the reliability of any pK_as less than 2 have to be questioned when a concentration of less than or equal 0.01 M is used (Albert and Serjeant, 1983).

EQUATION 3.6

$$pK_a = pH + \log\left[\frac{a - [H_3O^+] + [OH^-]}{b + [H_3O^+] - [OH^-]}\right]$$

a	Conjugate acid
b	Conjugate base
$[H_3O^+]$	Concentration of protons
$[OH^-]$	Concentration of hydroxyl ions

The ionisation of a monobasic acid, such as flumequine can be described by equation 3.7

EQUATION 3.7

$$HA \underset{H_2O}{\overset{K_a}{\rightleftharpoons}} H_3O+ \ + A^-$$
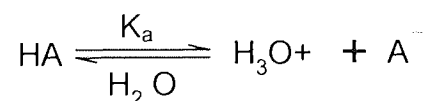
The concentrations of the two species involved in the ionisation at different pH values can be calculated if the pK_a is known. If a C_o value of 100 is used the values of the anion $[A^-]$ and the neutral species [HA] will be equivalent to percentage values (see equations 3.8, 3.9).

EQUATION 3.8

$$[HA] = \frac{C_o[H_3O^+]}{[H_3O^+] + K_a}$$

EQUATION 3.9

$$[A^-] = \frac{C_o K_a}{[H_3O^+] + K_a}$$

In a similar manner the ionisation of a dibasic acid can be described by equation 3.10, this equation can also be used to define the ionic species present for zwitterionic compounds at particular pH values.

EQUATION 3.10

$$H_2A \underset{H_2O}{\overset{K_1}{\rightleftharpoons}} HA^- + H_3O^+ \underset{H_2O}{\overset{K_2}{\rightleftharpoons}} A^{2-} + H_3O^+$$
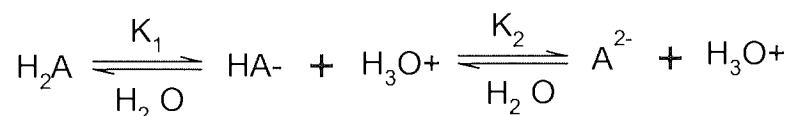
The concentrations of the three species involved in the ionisation can be calculated by equations 3.11 to 3.13. $[H_2A^+]$ is the cationic species, with $[HA^\pm]$ the neutral species and $[HA^-]$ being the anion.

EQUATION 3.11

$$[H_2A^+] = \frac{C_o[H_3O^+]^2}{[H_3O^+]^2 + K_1[H_3O^+] + K_1K_2}$$

EQUATION 3.12

$$[HA^\pm] = \frac{C_o K_1[H_3O^+]}{[H_3O^+]^2 + K_1[H_3O^+] + K_1K_2}$$

EQUATION 3.13

$$[HA^-] = \frac{C_o K_1 K_2}{[H_3O^+]^2 + K_1[H_3O^+] + K_1K_2}$$

These equations can be used to determine the percentages of the different ionic species present at physiologically relevant pH.

3.2.2 MATERIALS AND METHODS

The pK_as were determined using the Sirius equipment (GlpKa from Sirius Analytical Instruments Ltd) by Dr N Bonham at OSI Pharmaceuticals, Birmingham, UK.

A sample of compound of known weight approximately 5 mg was placed in a vial. The Sirius instrument added a predefined volume of methanol/water, depending on the quinolone used and the solubility of the quinolone. The pH of the sample was checked and acid or base (HCl 1 M and KOH 1 M) was added to bring the pH to the requested initial pH value of 2. It was then titrated with base or acid until the requested final pH value (pH 10) was reached, at which point data collection was terminated. Multiple titrations were carried out in this way to obtain aqueous pK_a values by the mixed-solvent technique. With the multi-titrations, the titration was started at pH 2 to minimise the absorption of carbon dioxide and the sample was then titrated up to pH 10 and then back down and back up.

Methanol was used as the co-solvent because its effects on pK_as has been extensively studied (Albert and Serjeant, 1983). Carbon dioxide is also poorly soluble in methanol, which also leads to better titration data.

The co-solvent titrations allow the calculation of the apparent pK_a (p_sK_a). The data-sets were combined to create a multi-set where the values were extrapolated to zero co-solvent (see table 3.1) to obtain the pK_a using the Yasuda-Shedlovsky procedure (Winiwarter *et al.*, 1998).

There was not a large difference in the apparent pK_a values with the different percentages of methanol used in the co-solvent system. For the first apparent pK_a (p_sK_{a1}), which is for the ionisation of the carboxylic acid, as the percentage of methanol increases the apparent pK_a increases. For the second apparent pK_a (p_sK_{a2}) the apparent pK_a decreases as the percentage of methanol is increased. As long as the percentage of methanol is kept under 40 % a reasonable extrapolation can be carried out, the apparent pK_as for a classical zwitterion should diverge as the percentage of methanol increases as seen in this case (Winiwarter *et al*, 1998; Albert and Serjeant, 1983).

Quinolone	% Methanol	p_sK_{a1}	p_sK_{a2}
Ciprofloxacin	39.09	6.790	8.129
	30.01	6.588	8.212
	24.18	6.496	8.261
Ofloxacin	38.96	6.630	7.738
	29.89	6.463	7.830
	24.07	6.345	7.894
Flumequine	39.11	7.056	
	30.10	6.887	
	24.48	6.796	
Propyl-Ciprofloxacin	38.72	6.699	7.494
	29.48	6.594	7.587
	23.62	6.491	7.629

Table 3.1 – Examples of data-sets which were extrapolated to 0 % methanol to determine pK_as.

3.2.3 RESULTS AND DISCUSSION

Potentiometric titrations were carried out to determine pK_as for some of the quinolones studied and fluorescein (see table 3.2). The pK_as obtained for the quinolones were comparable to those reported in the literature (Ross and Riley, 1992).

The pK_{a1} value is the pK_a for the dissociation of the carboxylic acid group and the pK_{a2}, is the pK_a for protonation of the piperazinyl function (see figure 3.1) for the quinolones. The pK_as for fluorescein were 4.28 and 6.26 ± 0.01 for the ionisation of the carboxylic acid group and phenol groups respectively (see figure 5.28). For sparfloxacin the pK_{a1} was 6.10 and pK_{a2} was 8.43, pK_{a1} is for the carboxylic acid group and pK_{a2} is for the protonation of the NH within the piperazinyl function. For BMS-284756-01 pK_{a1} was 5.56 for the carboxylic acid group and pK_{a2} was 8.78 for the ionisation of the NH group part of the substituted pyrrole (see figure 1.2a).

Quinolone	pK$_{a1}$	pK$_{a2}$	SD	P$_i$	SD
Butyl-Ciprofloxacin	6.33	7.74	0.03	7.04	0.01
Cinoxacin	4.42		0.01		
Ciprofloxacin	6.03	8.39	0.01	7.21	0.01
Ethyl-Ciprofloxacin	6.18	7.73	0.02	6.96	0.04
Flumequine	6.47		0.01		
Gatifloxacin	6.09	9.01	0.02	7.55	0.01
Levofloxacin	5.99	8.08	0.01	7.04	0.01
Methyl-Ciprofloxacin	6.06	7.50	0.02	6.78	0.01
Nalidixic Acid	6.19		0.01		
Norfloxacin	6.30	8.57	0.01	7.44	0.01
Ofloxacin	6.01	8.05	0.01	7.03	0.01
Pentyl-Ciprofloxacin	6.33	7.73	0.01	7.03	0.01
Propyl-Ciprofloxacin	6.22	7.77	0.02	7.00	0.01

Table 3.2 - The pK$_a$s for the quinolones studied.

Relating the dissociation constant to structure may prove useful in drug design studies in the explanation of the biopharmaceutical properties of the quinolones. At physiological pH the dominant Bjerrum species are the zwitterion and the neutral form of the drug. The zwitterion species and the neutral species are likely to have different distribution properties (Ross and Riley, 1992).
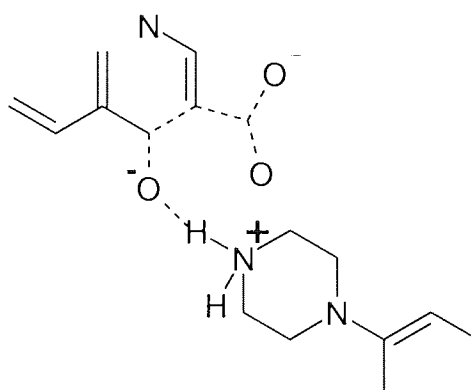
Figure 3.2 – Intramolecular hydrogen bonding of *keto* function to stabilise neighbouring protonated species.

The values for pK$_{a1}$ were higher than what is generally observed with aromatic carboxylic acids such as benzoic acid which has a pK$_a$ of 4.2. This decrease in acidity can be attributed to an intramolecular hydrogen bond formation with the neighbouring

keto function resulting in stabilisation of the protonated species (see figure 3.2). The dissociation constants may also be affected by electron-donating or electron-withdrawing groups, which stabilise or destabilise the charged species. The fluorine atoms, which were conjugated to the carboxylic acid functional group, would affect the dissociation constant. Any oxygens attached to the ring would exert an electron-withdrawing effect, thereby reducing pK_{a1} as would the presence of a secondary fluorine, which would also exert an electron-withdrawing inductive effect and thereby stabilise the carboxylic acid anion resulting in a decrease in pK_{a1}. The spatial separation of the ionisable groups on the quinolones resulted in the charge on one functional group not affecting the dissociation constant of the other ionisable group. Nalidixic acid which did not contain a piperazinyl moiety had a pK_a which was comparable with pK_{a1} for the quinolones (Ross and Riley, 1992).

3.3 LogP

3.3.1 INTRODUCTION

The partition coefficient measures the molecule's affinity for partitioning from an aqueous phase into an organic phase. LogP is simply a logarithm of the ratio of a molecule's concentration in the aqueous and organic phases (see equation 3.14). Lipophilicity was the first quantitative structure-activity relationship QSAR descriptor; it is probably also the most important descriptor with other QSAR descriptors such as molecular refractivity and connectivity indices cross-correlating with it (Ruelle and Kesselring, 1998). Lipophilicity often plays a significant role in determining the biological activity of organic molecules. This can be due to the hydrophobic interactions between ligand and receptor, transport across a membrane or other pharmacokinetic interactions, such as cellular uptake, bioavailability, receptor affinity, protein binding, pharmacological activity and toxicity. In most pharmaceutical cases, lipophilicity is measured as the partition of a compound between organic and aqueous phase, the partition coefficient of a molecule in n-octanol and water solvent system has been recognised to model its transport across biological membranes (Gombar and Enslein., 1996). n-Octanol is used as the organic phase; it was chosen because it has a polar head-group and hydrocarbon chain representing the lipid domain of the membrane

barrier. It is a good solvent for many drug compounds, being stable, commercially available and UV transparent. Other partitioning systems are also available, these include, olive oil, hexane, chloroform, alkane, cells and liposomes; they are used depending on the hydrogen bonding characteristics required.

EQUATION 3.14

$$LogP = log\left(\frac{[HA]_{Octanol} + [A^-]_{Octanol}}{[HA]_{Water} + [A^-]_{Water}}\right)$$

LogP as mentioned earlier is defined as the partition of the neutral molecule. Another useful parameter logD, which is defined as the partition coefficient at a particular pH, at which the compound involved maybe ionised. LogD can be particularly useful to investigate the partitioning of a compound at physiological pH.

In principle, experimental measurements of logP of a compound are straight forward, but there can be problems in developing an assay for measuring the amount of compound in the different phases. Then there can also be other potential problems including compound instability, assay sensitivity, the presence of impurities and the wide variation in the lipophilicity of the compounds being tested. Therefore in order to eliminate such problems and screen a wider range of compounds several theoretical methods have been proposed.

3.3.1.1 PREDICTION OF LOGP

It is desirable to predict the logP of a complex molecule from physicochemical parameters or, ideally, from its molecular structure. Methods which allow the calculation of logP have the advantage that the compound does not have to be synthesised or assayed (Lombardo *et al.*, 1996).

A number of methods have been developed for the prediction of logP from chemical structure. There are generally three types of methods, those, which use group or atomic contributions and capitalise on the additive nature of logP. Regression methods which quantify the weights of different structure descriptors on the principle of least square

deviation and finally the theoretical methods which use desolvation energies (Gombar and Enslein, 1996).

The most common methods for estimating logP are the atomic or molecular fragment based group additivity method. Limitations of this approach include the reliance on experimental data for fragment or atomic contributions and thereby missing fragments can pose a problem (Reynolds, 1995). Hansch and Leo (1979) divided compounds into basic fragments and calculated logP by the summation of the hydrophobic contributions of these fragments. However, this method fails to work for complex compounds and correction factors were included to improve the accuracy of the calculations (Leo *et al.*, 1971). Similar methods based on fragment constants have been put forward by Rekker, Suzuki and Kudo, Moriguchi, and Klopman (Suzuki and Kudo, 1990; Rekker and Laak., 1993). These methods cannot deal with charged compounds or zwitterions or make corrections for them; therefore, their use is limited with the quinolones of interest here.

With the additive atomic contribution methods, the atoms are classified into different types according to the topological environment, which contribute differently to the global logP value. Although atomic contribution techniques are simple to automate, they cannot deal with long-range interactions. It must be remembered that the whole is greater than the sum of its parts and any method of calculating logP of a molecule from its parts has limitations. Among all the current approaches for logP calculations, the group or atomic contribution methods are widely used because they are conceptually simple and fast, although the accuracy of the estimations is questionable. Examples of such methods include XlogP, ClogP and Ghose logP. XlogP is an atom additive method for logP calculations that classifies atoms by their hybridisation states and their neighbouring atoms. It also includes correction factors for some intramolecular interactions (Wang *et al.*, 1997). ClogP is the original (Hansch and Leo, 1979) model for logP determinations using their fragments and corrections. It warns when contributions of certain groups are not known. Ghose logP is another atomic contribution method (Ghose and Crippen, 1985; Gombar and Enslein, 1996).

The regression methods for measuring logP are good for calculating logP for small organic molecules but they fail when it comes to complicated drug structures falling

outside their training set. LogP has to be measured for a large number of compounds forming the training set, then the logP for compounds with similar structure can be predicted. There are a number of problems with these methods which include the actual measuring of logP values to begin with and the limitations of the training set (Mannhold *et al.*, 1995; Basak and Grunwald, 1995).

The theoretical methods have potential advantages over other methods that include: avoiding the use of additive fragments, the calculation of a large number of descriptors or the measurement of logPs for a training set. The solvation free energy approach can serve as a useful tool for rank ordering of compounds (Lombardo *et al.*, 1996). These methods for computing partition coefficients are direct simulation of solute in water and organic solvent. Once the free energy of solvation in aqueous and organic media has been determined it would be a simple matter to compute logP. These methods can be carried out using molecular dynamics and Monte Carlo simulations, but they are computer intensive and therefore usually impractical (Reynolds, 1995). Variations on the general theme include computing the free energy change for transferring a solute from aqueous to organic solutions using a continuum solvation model. This is usually far less computer intensive and gives reasonable estimations of solution free energies. Most of these methods use an organic phase other than octanol, from which an octanol water partition coefficient may be extrapolated by linear regression. The advantages of such methods are that they could be used to calculate relative logPs far more accurately than fragment based methods (Reynolds, 1995). Examples of theoretical methods include, those used to model brain-blood barrier permeability (Lombardo *et al.*, 1996; Klopman *et al.*, 1997).

3.3.2 MATERIALS AND METHODS

3.3.2.1   MEASURED LOGP

LogP was measured by potentiometric titration carried out using the Sirius equipment by Dr N Bonham at OSI Pharmaceuticals.

To measure the logP values, the aqueous pK_a values of the samples were measured as described in section [3.2.2]. The apparent pK_a (p_sK_a) values of the sample shifted in an upwards direction for acidic groups and downwards for basic groups. A weak acid is able to set up an equilibrium as the ions (anion and cation) and as the neutral molecule in the aqueous environment. The partition of the neutral molecule would be favoured over the ions into an organic phase. This would result in an increase in the equilibrium towards the neutral molecule as predicted by Le Chatelier's principle, resulting in a decrease in the available ions; which would then cause a shift in the potentiometric titration curve (see figure 3.3). For a given ratio of water to octanol, the size of the shift increased as logP increased. Multiple titrations were carried out with increasing volumes of octanol in subsequent titrations. The data from the titrations was combined to create a multiset, the shift in the pK_a was fitted to a model using the difference plot and used to determine logP.
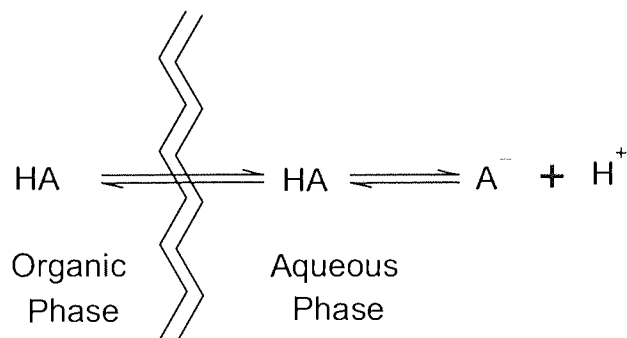
Figure – 3.3 Equilibrium between ionised and unionised species in aqueous and organic phases.

3.3.2.2   HPLC DETERMINATION OF LOGP

Some of the quinolones were analysed by HPLC to obtain retention times for these compounds at various concentrations of organic modifier (acetonitrile). Not all the quinolones were run because some of the compounds had very long retention times at the lower percentages of acetonitrile. Capacity factors (K) were calculated from the retention times (See section 2.8.3).

3.3.2.3 CALCULATED LOGPS

All calculations were performed using Microsoft Excel 97, ClogP from Biobyte V2.00, ChemX-3D and Tsar from Oxford Molecular Ltd, Oxford, UK and CS ChemOffice from CambridgeSoft, Cambridge, USA.

Structures for quinolones were constructed using the SMILES notation (See appendix A2). The structures required for the Tsar software were constructed using ChemX-3D. The structures were imported into Tsar, where they were aligned and underwent COSMIC energy minimisation, before Ghose logP was determined.

Moriguchi logP values were calculated using MS Excel 97 by applying the regression equation 3.15. CX is the total number of carbons and halogens, NO the total number of nitrogens and oxygens, PRX is a proximity factor, UB total number of unsaturated bonds, POL is a polarity factor, RNG is the number of aromatic rings and NO2 is the total number of NO_2 (Moriguchi *et al.*, 1992).

EQUATION 3.15

$$logP = 1.244(CX)^{0.6} - 1.017(NO)^{0.9} + 0.406PRX - 0.145(UB)^{0.8}$$
$$+0.268POL - 0.392RNG + 0.474NO2 - 1.041$$

The Moriguchi method is an easy method to apply although problems were experienced with the PRX and POL parameters, the calculation of these is rather ambiguous. The PRX parameter is known as the proximity parameter. The PRX parameter accounts for the proximity of nitrogen or oxygen atoms connected to each other through carbon, sulphur or phosphorus atoms. The POL parameter accounts for the number of aromatic polar substituents found within a molecule, the upper limit for this parameter is set to a value of 4 (Moriguchi *et al.*, 1992). Examples of Moriguchi logP calculations can be found in appendix A4.

Calculated logPs (Ghose LogP, ClogP, and Moriguchi logP) and where possible measured logP values were collated and compared.

3.3.3 RESULTS AND DISCUSSION

3.3.3.1   MEASURED LOGP

Measured logPs using the Sirius equipment correlated well with those reported in the literature by (Ross and Riley, 1992). As well as measured logPs, data was obtained for logD at pH 3.0 which was the mobile phase pH and pH 7.4, which represented the physiological pH (see table 3.3).

Quinolone	LogP	LogD at pH 3.0	LogD at pH 7.4	SD	Literature logP
BMS-284756-01	0.086	0.571	0.081	0.08	N/A
Cinoxacin	2.18	2.945	2.007	0.01	N/A
Flumequine	1.504	1.504	0.52	0.018	0.97
Gatifloxacin	-0.373	-0.473	-0.388	0.086	N/A
Levofloxacin	-0.118	-0.421	-0.209	0.058	N/A
Norfloxacin	-1.03	-4.353	-1.088	0.052	0.042
Ofloxacin	-0.165	-0.692	-0.265	0.071	0.318
Sparfloxacin	1.18	2.215	1.14	0.04	N/A
Ciprofloxacin	-0.379	-0.305	-0.416	0.065	-1.70
Methyl-Ciprofloxacin	0.334	-0.605	0.068	0.033	0.15
Ethyl-Ciprofloxacin	0.581	-0.732	0.392	0.027	0.53
Propyl-Ciprofloxacin	1.127	-0.675	0.951	0.029	1.07
Butyl-Ciprofloxacin	1.693	-0.567	1.502	0.017	1.54
Pentyl-Ciprofloxacin	2.251	0.038	2.056	0.028	2.06
Nalidixic Acid	1.15	1.119	-0.103	0.012	1.87
Fluorescein	3.701	3.678	0.003	0.018	N/A
Enoxacin	-1.00	-4.394	-1.261	0.058	-2.15

Table 3.3 – Measured logPs obtained from Sirius equipment as well as logD at pH 3.0 and 7.4. Literature logP were obtained from in-house literature from Farmacia y Technologia Farmaceutica, Valencia, Spain and Ross *et al.*, (1993); Ross and Riley, (1993)

The logP and logD data was used to compare with logP measurements determined using HPLC techniques as well as computed values.

3.3.3.2 LOGP DETERMINATION USING HPLC

The logarithm of the capacity factor K (See section 2.8.3) was calculated for different percentages of acetonitrile present in the mobile phase. The correlation between log$K$ and % acetonitrile showed a second order polynomial fit (see figure 3.4). Although there were only three data points for each compound, a good correlation was observed (see table 3.4).
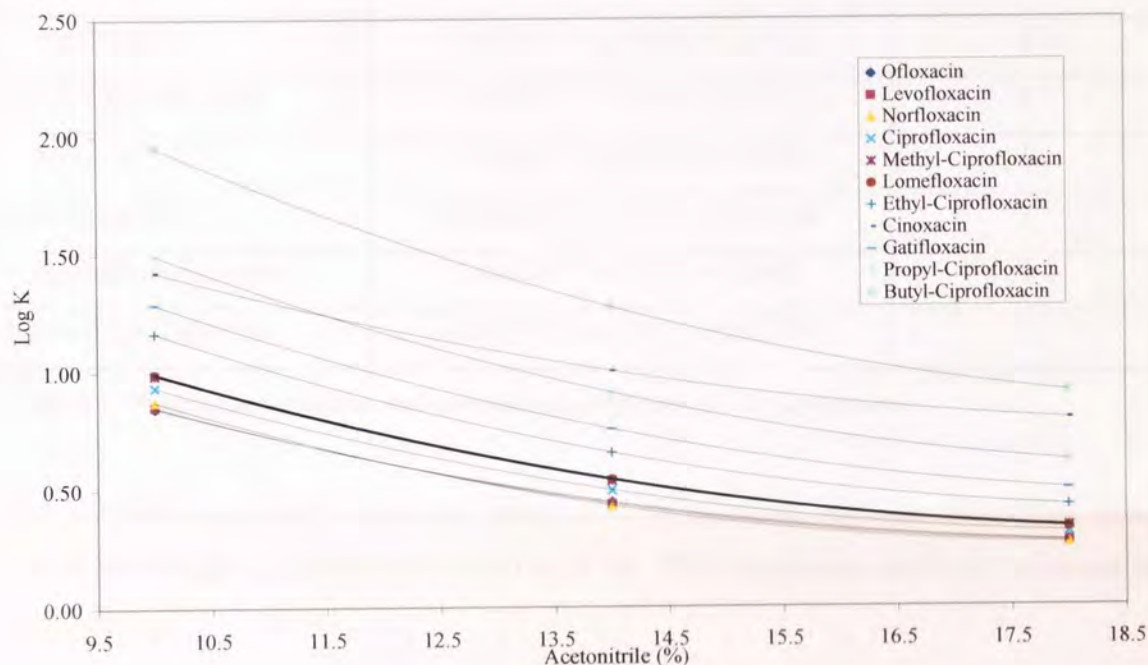
Figure 3.4 – The relationship between % acetonitrile in the mobile phase and log$K$.

As the retention time for the quinolones increased with the lower percentage of acetonitrile in the mobile phase there was a change in the peak shape. The peaks became broader with increased tailing.

Quinolone	Regression Equation	Correlation Coefficient r^2
Ofloxacin	$0.0073x^2 - 0.2767x + 2.8836$	1
Levofloxacin	$0.0078x^2 - 0.2917x + 2.9902$	1
Norfloxacin	$0.0088x^2 - 0.3234x + 3.2258$	1
Ciprofloxacin	$0.0081x^2 - 0.3043x + 3.1714$	1
Methyl-Ciprofloxacin	$0.0079x^2 - 0.3018x + 3.2198$	1
Lomefloxacin	$0.0076x^2 - 0.2963x + 3.1921$	1
Ethyl-Ciprofloxacin	$0.0088x^2 - 0.339x + 3.6756$	1
Cinoxacin	$0.0068x^2 - 0.2677x + 3.426$	1
Gatifloxacin	$0.0086x^2 - 0.3397x + 3.8246$	1
Propyl-Ciprofloxacin	$0.0092x^2 - 0.367x + 4.2486$	1
Butyl-Ciprofloxacin	$0.0101x^2 - 0.4132x + 5.0779$	1

Table 3.4 - Regression equations and correlation coefficient (r^2) for quinolones.

The parabolic regression equations were used to calculate $\log K_o$, a theoretical point where percentage of acetonitrile would be 0 %. This value was taken as a measure of lipophilicity.

The correlation of logP with $\log K_o$ was investigated (see figure 3.5). There were a number of outliers present (see figure 3.5), which could be explained by the method used to determine $\log K_o$. The quinolones norfloxacin, ofloxacin, levofloxacin, gatifloxacin and ciprofloxacin have very similar, short retention times and, when calculating K factors, the differences between them are very small, thereby the errors are increased.
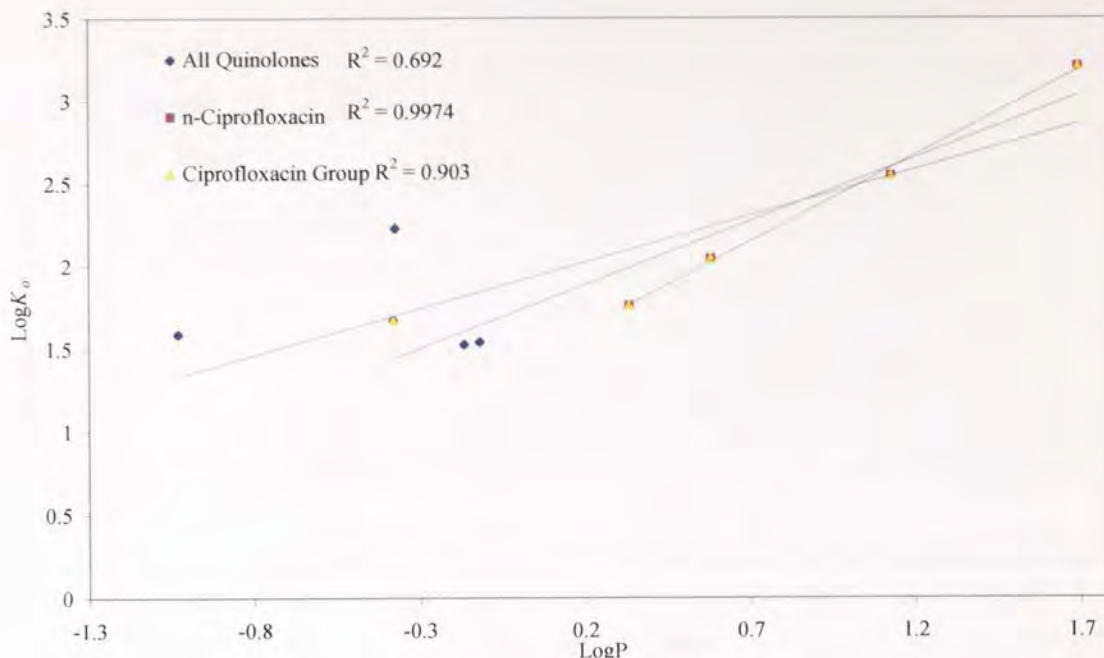
Figure 3.5 – Correlations determined between measured (Sirius) logP and logK_o.

A weak correlation was present between measured logP using the Sirius equipment and logK_o. The ciprofloxacin family produces a good correlation ($r^2 = 0.903$) and when ciprofloxacin, the parent molecule, was removed from the data set the correlation increased ($r^2 = 0.9974$). This can be explained by the fact that, for a homologous series of compounds, when the hydrogen is removed and replaced by a methyl group, there is a large increase in logP. With the addition of subsequent methyl groups the change is not as profound. This appears to hold true for the measured logP and logD values. This phenomenon is called a first-element effect and seldom occurs in homologous series with low lipophilicity components, this was also observed by Merino *et al*, (1995) for a homologous family of *n*-alkyl norfloxacin. However, for the logK_o, which was determined using HPLC the opposite is seen, with the addition of the first methyl group a change not as large as expected is observed (see figure 3.6).

With the removal of the hydrogen and the addition of a methyl group, the secondary amine is changed to a tertiary amine. This results in a change in hydrogen-bonding characteristics as well as increasing the hydrocarbon chain length. With subsequent additions of methyl groups, hydrogen-bonding is constant.
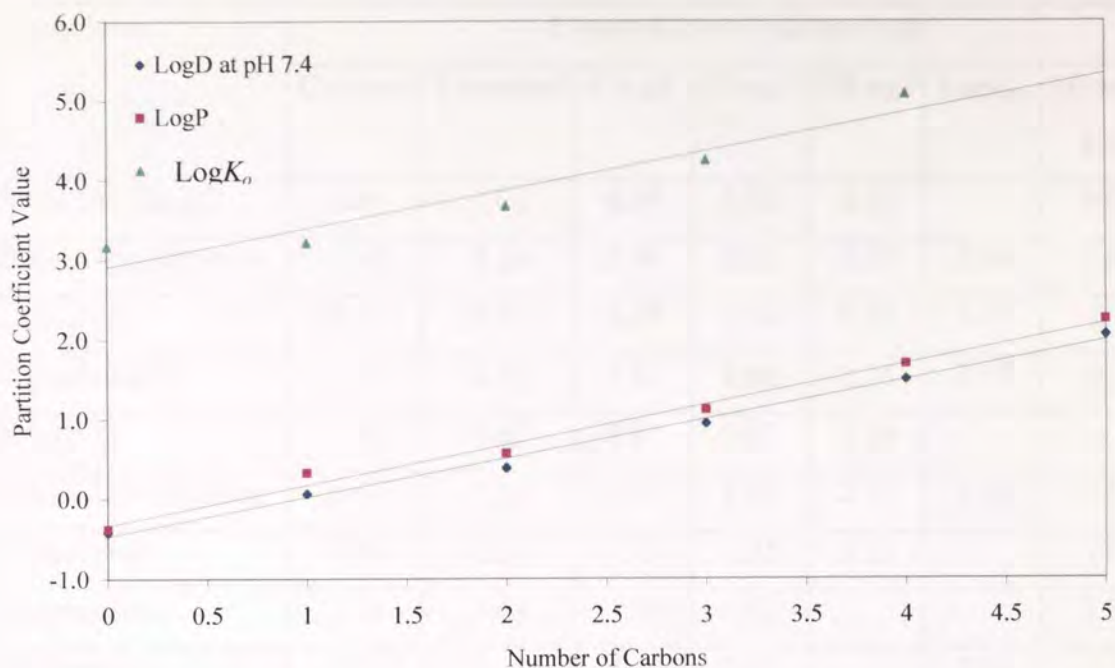
Figure 3.6 - Number of additional methyl groups added to ciprofloxacin parent molecule and relationship with logK_o, logP and logD.

3.3.3.3 COMPUTATIONAL LOGP

The logP data generated using the different theoretical methods was compared with the measured logP values (see table 3.5).

The Crippen and Viswanad logPs were determined using the CS ChemOffice software, both of these logPs cross-correlated well with each other see figure 3.7.

There is good correlation between measured logP and logD at physiological pH. However there are three outliers; nalidixic acid, fluorescein and flumequine (see figure 3.8). This would be expected because nalidixic acid and flumequine are not zwitterionic and at physiological pH they predominately exist as cations, while the zwitterionic quinolones would exist as the zwitterion or the uncharged species. In either case they would on a macromolecular basis have an overall neutral charge as the species for logP determination did.

Quinolone	Lipophilicity Measure logP						
	Crippen	Viswanad	ClogP	GLogP	MLogP	LogK$_o$	Measured LogP
BMS 284756-01	3.64	3.95	**0.95**	3.23	4.34		0.086
Butyl-Ciprofloxacin	2.94	3.16	**0.89**	2.21	3.09	5.08	1.693
Cinoxacin	0.71	0.85	**1.48**	1.34	0.30	3.43	2.18
Ciprofloxacin	1.32	1.59	1.56	**0.64**	2.18	3.17	-0.379
Enoxacin	1.46	1.62	**0.91**	0.67	2.14		-1.00
Ethyl-Ciprofloxacin	2.04	2.29	-0.17	**1.35**	2.65	3.68	0.581
Flumequine	2.08	2.28	2.73	**1.81**	3.13		1.504
Fluoroscein	3.60	**3.68**	2.70	0.82			3.701
Gatifloxacin	1.51	1.75	**-0.71**	2.21		3.82	-0.373
Levofloxacin	1.35	1.53	**-0.90**	0.80		2.99	-0.118
Lomefloxacin	1.84	2.09	2.40	0.59			
Methyl-Ciprofloxacin	1.70	1.95	**-0.70**	1.00	2.42	3.22	0.334
Nalidixic Acid	1.63	1.73	1.32	**1.14**	2.84		1.15
Norfloxacin	**1.37**	1.53	1.73	1.25	1.89	3.23	-1.03
Ofloxacin	1.35	1.53	**-0.90**	0.59	2.05	2.88	-0.165
Pentyl-Ciprofloxacin	3.36	3.55	1.42		**2.57**		2.251
Propyl-Ciprofloxacin	2.52	2.76	0.36	**1.81**	2.87	4.25	1.127
Sparfloxacin	**1.31**	1.77	-1.06	0.59	2.00		1.18

Table 3.5 - Calculated logPs determined using methods by Crippen, Viswanad, Ghose, Moriguchi and ClogP as well as measured logP (logK$_o$) determined using HPLC. Entries made in bold are closest to the measured logP values. Measured logP values taken from table 3.3.

Although the different methods for calculating logP cross correlate with each other, these methods show very poor correlations with actual measured logPs. The poorest correlation is provided by the Moriguchi logP. The logK$_o$ provided a better measure of logP than the calculated values (see table 3.6).
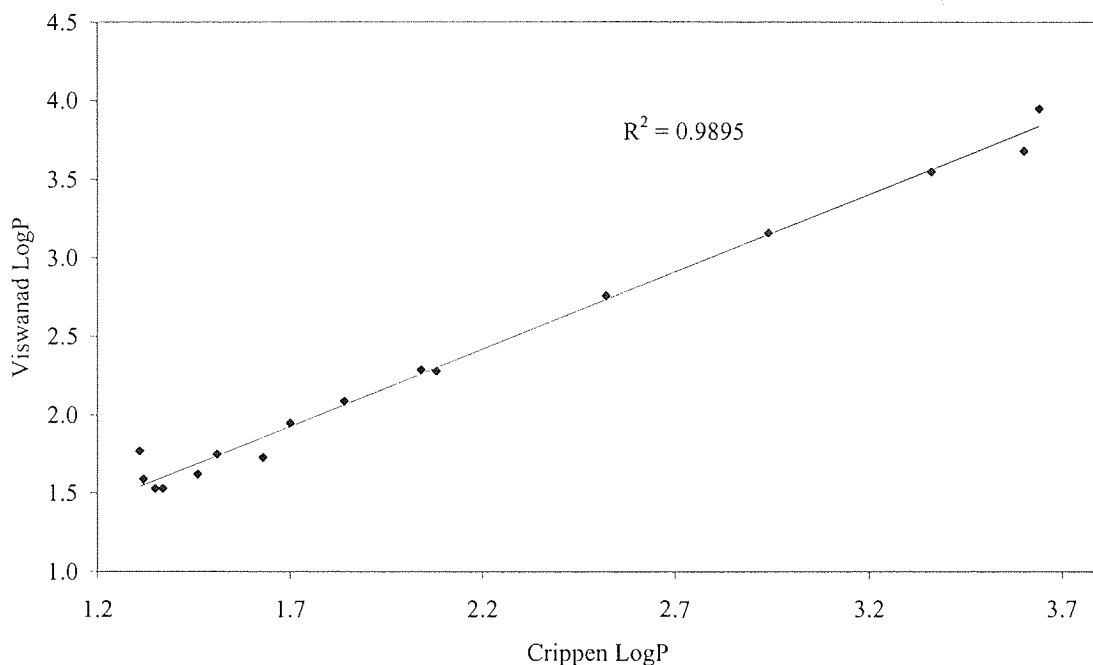
Figure 3.7 - Correlation of calculated logPs determined using Crippen and Viswanad methods.

It was clear that the different methods could not predict absolute logP values for the quinolones. The rank order obtained for the logP based on the different methods was compared. All the methods were able to accurately predict the rank order for the *n*-alkyl-ciprofloxacin family. However, with the other quinolones they could not accurately predict the rank order (see table 3.8). A correlation greater than 0.48 indicates a significant result (P<0.05).

	Measured LogP	Crippen	Viswanad	ClogP	Ghose LogP	Moriguchi LogP	LogK_o
Measured LogP	1.00						
Crippen	0.50	1.00					
Viswanad	0.48	1.00	1.00				
ClogP	0.43	0.33	0.29	1.00			
Ghose LogP	0.04	0.55	0.56	0.05	1.00		
Moriguchi LogP	-0.06	0.81	0.82	0.07	0.67	1.00	
LogK_o	0.58	0.83	0.82	0.21	0.87	0.52	1.00

Table 3.6 – LogP correlation matrix for different methods.

An interesting observation was made with the ClogP software, which could give a different predicted logP value depending on the SMILES notation used for the compound (see table 3.7). For example with ethyl-ciprofloxacin two logP values were

generated, one for the compound enrofloxacin, which is a generic name for ethyl-ciprofloxacin, and one could be generated for ethyl-ciprofloxacin. Based on this evidence, when using such software it would be prudent to enter all the structure, using consistent SMILES notation.
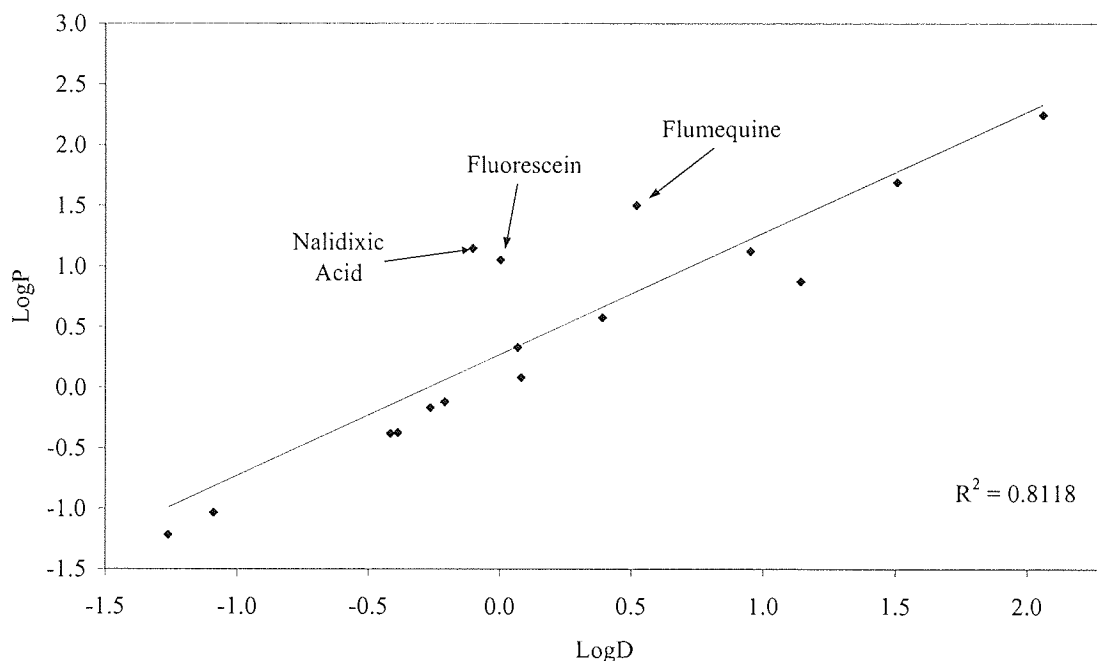
Figure 3.8 – Correlation between measured logP and logD at pH 7.4.

Quinolone	SMILES	ClogP
Enrofloxacin	O=C2C1=CC(F)=C(N4CCN(CC)CC4)N=C1N(C3CC3)C=C2C(O)=O	-0.99
Ethyl-Ciprofloxacin	O=C1C(C(O)=O)=CN(C4CC4)C2=C1C=C(F)C(N3CCN([CH2]C)CC3)=C2	0.27

Table 3.7 – Different logP values were produced for ethyl-ciprofloxacin using 2 different SMILES notations, one of which the software recognises as enrofloxacin.

With the current methods available for calculating logP, severe limitations were seen with zwitterionic compounds and ionised molecules. For many such molecules, ClogP cannot calculate a logP. The Moriguchi method for calculating logP is a rule-based system, thereby it always give a value for logP. This method loses accuracy by giving a broader coverage. Although Moriguchi showed that his model was comparable with others, his findings could not be reproduced with the quinolones (Moriguchi *et al.*, 1992; Moriguchi *et al.*, 1994). With all the methods used for calculating logP the

HPLC measured logP (logK_o) provided the best correlation with the measured logP with the Moriguchi logP being the weakest method used (see table 3.4).

The zwitterionic form predominates at the isoelectric point near physiological pH rather than the nonionic form. Maximum partitioning into the lipid phase occurs when an uncharged species is present in commensurable concentration relative to the zwitterionic form (see section 4.3.6). The true partition coefficient of these compounds would have to be calculated at the isoelectric point. The introduction of a second fluorine atom, decreases the lipophilicity of the quinolones, this brings to attention the existence of a specific electronic interaction of the 8-fluoro group with the quinolone ring. The presence of an oxazine ring anellated to the quinolone system as in ofloxacin decreases the lipophilicity. The lipophilicity of these molecules governs the ability to pass through the bacterial outer membrane and thereby exert antibacterial activity. For compounds of relatively high lipophilicity the phospholipid membrane is considered to be the route of transport (Takacs-Novak *et al.*, 1992).

Co-administration of the quinolones with antacids has also been implicated in a reduction in antimicrobial activity in urine. This reduction in activity has been attributed to the high concentration of Mg^{2+} in the urine. The presence of Mg^{2+} or Ca^{2+} resulted in a decrease in the apparent partition coefficient of lomefloxacin. It is necessary to assume that the metal-ion complex does not partition into the octanol phase and that complexation with the zwitterionic form of drug is much greater than the complexation with the cationic species. The decrease in bioavailability and reduced antimicrobial activity observed in the presence of metal ions may be explained on the basis of a decrease in lipophilicity of the complex compared with the free drug. This does not preclude metal-ion facilitated transport across cell membranes which may occur in biological systems. Although a compound may have no overall charge, it can still have local charges, which may lead to different affinities to transport systems in the body, and that minor changes in pH around the isoelectric point can have significant effects on charge (Ross *et al.*, 1993; Ross and Riley., 1993; Sorgel and Kinzig, 1993).

Different measures of Lipophilicity

Log D pH 7.4	LogP	Crippen Log P	Viswanad Log P	ClogP	GlogP	Moriguchi logP	LogK₀
Enoxacin	Enoxacin	Cinoxacin	Cinoxacin	Levofloxacin	Ofloxacin	Cinoxacin	Ofloxacin
Norfloxacin	Norfloxacin	Sparfloxacin	Levofloxacin	Ofloxacin	Lomefloxacin	Gatifloxacin	Levofloxacin
Ciprofloxacin	Ciprofloxacin	Ciprofloxacin	Norfloxacin	Methyl-Ciprofloxacin	Sparfloxacin	Sparfloxacin	Ciprofloxacin
Gatifloxacin	Gatifloxacin	Levofloxacin	Ofloxacin	Ethyl-Ciprofloxacin	Ciprofloxacin	Levofloxacin	Methyl-Ciprofloxacin
Ofloxacin	Ofloxacin	Ofloxacin	Ciprofloxacin	Cinoxacin	Enoxacin	Ofloxacin	Norfloxacin
Levofloxacin	Levofloxacin	Norfloxacin	Enoxacin	Propyl-Ciprofloxacin	Levofloxacin	Enoxacin	Cinoxacin
Nalidixic Acid	Nalidixic Acid	Enoxacin	Nalidixic Acid	Nalidixic Acid	Methyl-Ciprofloxacin	Ciprofloxacin	Ethyl-Ciprofloxacin
Methyl-Ciprofloxacin	BMS 284756-01	Gatifloxacin	Gatifloxacin	Sparfloxacin	Nalidixic Acid	Nalidixic Acid	Gatifloxacin
BMS 284756-01	Methyl-Ciprofloxacin	Nalidixic Acid	Sparfloxacin	Butyl-Ciprofloxacin	Norfloxacin	Norfloxacin	Propyl-Ciprofloxacin
Ethyl-Ciprofloxacin	Ethyl-Ciprofloxacin	Methyl-Ciprofloxacin	Methyl-Ciprofloxacin	Enoxacin	Cinoxacin	Methyl-Ciprofloxacin	Butyl-Ciprofloxacin
Flumequine	Sparfloxacin	Lomefloxacin	Lomefloxacin	Gatifloxacin	Ethyl-Ciprofloxacin	Lomefloxacin	
Butyl-Ciprofloxacin	Propyl-Ciprofloxacin	Ethyl-Ciprofloxacin	Flumequine	Pentyl-Ciprofloxacin	Flumequine	Ethyl-Ciprofloxacin	
Cinoxacin	Flumequine	Flumequine	Ethyl-Ciprofloxacin	Ciprofloxacin	Propyl-Ciprofloxacin	Propyl-Ciprofloxacin	
Pentyl-Ciprofloxacin	Butyl-Ciprofloxacin	Propyl-Ciprofloxacin	Propyl-Ciprofloxacin	Flumequine	Gatifloxacin	Butyl-Ciprofloxacin	
	Cinoxacin	Butyl-Ciprofloxacin	Butyl-Ciprofloxacin	Norfloxacin	Butyl-Ciprofloxacin	Pentyl-Ciprofloxacin	
	Pentyl-Ciprofloxacin	Pentyl-Ciprofloxacin	Pentyl-Ciprofloxacin	BMS 284756-01	BMS 284756-01	BMS 284756-01	
		BMS 284756-01	BMS 284756-01	Lomefloxacin	Pentyl-Ciprofloxacin		

Table 3.8 – Rank order of quinolones based on lipophilicity (low to high) for the different methods used to determine logP. Enoxacin, norfloxacin and ciprofloxacin are in different colours in-order to aid visualisation of the rank order.

It must be remembered that a complex interplay exists between the different physicochemical factors. Molecular properties other than overall hydrophobicity are required to help predict the absorption potential of compounds, such as hydrogen bonding potential, percentage polar surface area, flexibility of molecule and molecular volume (Ungell *et al.*, 1998).

3.4 MOLECULAR MODELLING

3.4.1 INTRODUCTION

Molecular modelling allows the exploration of molecules, when actual laboratory investigations maybe inappropriate, impractical or even impossible. The mathematical methods which computational chemistry uses can be split into two categories, molecular mechanics and quantum mechanics. Molecular mechanics applies classical Newtonian physics to molecular nuclei and to the large part ignores electrons. While quantum mechanics relies on the Schrödinger equation to describe a molecule with explicit treatment of the electronic structure. Quantum mechanics can further be subdivided into *ab initio* and semi-empirical methods.

The quinolones underwent molecular modelling to generate descriptors. These descriptors were then used to determine if there were any relationships between the quinolones and determine cellular permeability.

3.4.2 MATERIALS AND METHODS

CS ChemOffice version 5.0 by CambridgeSoft was used to calculate the physical parameters which include logP (Crippen and Viswanad), molecular refractivity, dipole moments and energies of formation *in vacuo*. A number of surface area measures were also computed including van der Waals solvation area, Connolly surface area and the area accessible to a water molecule (Suzuki and Kudo, 1990). Charge calculations for carboxylic acid group and ionisable nitrogen were also carried out. Semi-empirical methods using MOPAC were used to calculate the above parameters.

Molecular mechanical methods were used mainly because they are less computer intensive. The potential energy surface was used to calculate geometrical optimisations and physical properties such as charge, dipole moment and heat of formation. SPSS version 9 was used to carry out the cluster analysis.

3.4.3 RESULTS AND DISCUSSION

3.4.3.1 RELATIONSHIP BETWEEN PERMEABILITY AND LIPOPHILICITY

A sigmoidal relationship exists between cellular permeability (see section 4.3.5) and logD at pH 7.4 for the quinolones studied (see figure 3.9).

There is a correlation between the hydrophobicity of a drug and its potential to be transported across the intestinal barrier. Increasing the hydrophobicity of a drug results in a higher permeability. However, these results have indicated that when logP exceeds more than 2, a sigmoidal curve operates for these quinolones. Ungell *et al.*, (1998) concluded that a bell-shaped curve operates, when logP exceeds more than 3.5, showing that increased hydrophobicity does not necessarily increase the ability of a molecule to be absorbed. A number of authors concluded (Merino *et al.*, 1995; Bermejo *et al.*, 1999) that the relationship between logD and the cellular permeability forms a sigmoidal curve.

The permeability of compounds with a positive logP value depends strongly on lipophilicity, probably due to the increasing contribution of transcellular diffusion to the overall transport. This was in accordance with the concept of the existence of a threshold lipophilicity required for passive diffusion through the endothelium (Jaehde *et al.*, 1993). This threshold lipophilicity would help explain the sigmoidal shape of the relationship between cellular permeability P_{app} and logD as found in figure 3.8. Based on these data the limiting value appears to be a logD of 0.2. Since paracellular transport mainly depends on molecular size and charge, it can be assumed that the paracellular permeability is unlikely to differ markedly among the individual quinolones (Jaehde *et al.*, 1993).
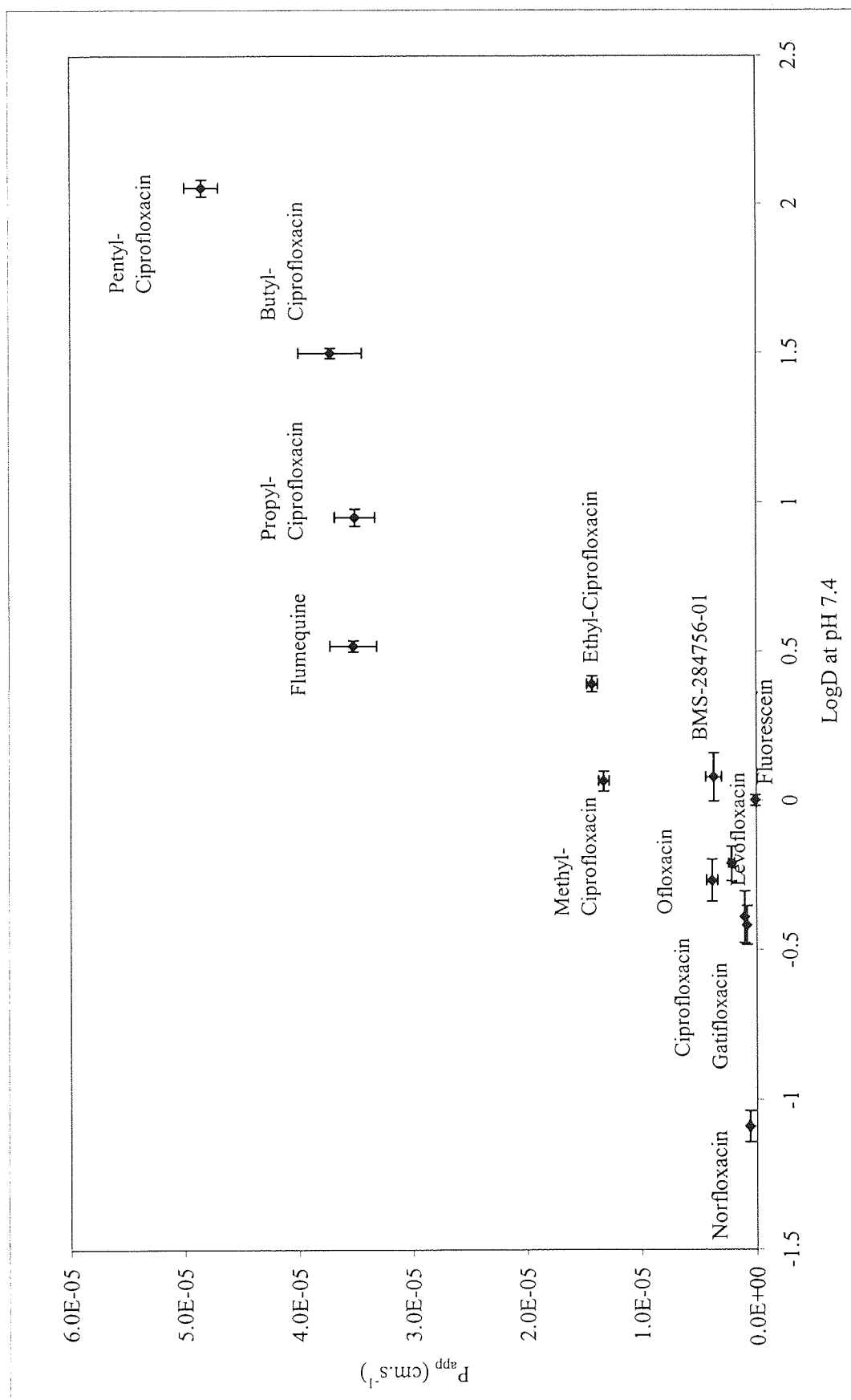
Figure 3.9 – Correlation between logD at pH 7.4 and the cellular permeability of the quinolones

The barrier that opposes the penetration of any passively absorbed substance across the gut wall is made up not merely of lipoidal membrane lining the surface of the *microvilli*, but also its external aqueous microenvironment. From a diffusional view-point, the aqueous microenvironment does not seem to behave like the free aqueous luminal fluid, because its resistance to solute diffusion is increased. Unstirred water layers are formed whenever any lipoidal barrier, either natural or artificial, comes in contact with an aqueous solution. If the lipophilicity of a molecule becomes too high, then the unstirred water layer will present an increased barrier to transport (Merino *et al.*, 1997). The cell membrane can also behave as an additional barrier to the transport of highly lipophilic compounds, because partitioning into the cellular membrane occurs and the compound then is unable to partition back into the aqueous environment of the cell.

Compounds with a low logD usually take the paracellular pathway across the cellular barrier; if these compounds are also of a large size, this route is not available and very low levels of cellular permeability are observed. The quinolones cover a relatively small molecular weight window which is generally larger than the paracellular cut-off, which results in them being excluded mostly from the paracellular pathway. Due to this their transport primarily appears to be based on their lipophilicity.

3.4.3.2   MOLECULAR MODELLING DESCRIPTORS

Significant cross-correlation of surface area measurements occurred (see table 3.9), therefore in any in-depth analysis of only one of the terms would be required. The compounds are similar in structure and therefore the charges found on the carboxylic moiety and ionisable nitrogen were of limited value, as where the energies of formation (see appendix A5).

It was found that in most cases only one descriptor in each category was useful because the other descriptors would cross correlate with it.

The quinolone structures underwent energy minimisation using COSMIC minimisation, they were found to be in similar conformations with the 7-piperazinyl ring planar and the substituent rings or groups perpendicular to the rings (see figure 3.10a to 3.10c).

	VDW solvation area	Connolly surface area	1.4 Å surface area	H₂O exclusion area	DMSO exclusion surface area
VDW solvation area	1				
Connolly surface area	0.993	1			
1.4 Å surface area	0.992	0.998	1		
H₂O exclusion area	0.985	0.991	0.996	1	
DMSO exclusion surface area	0.987	0.989	0.995	0.998	1

Table 3.9 – Correlation matrix showing cross-correlation of different surface measures.
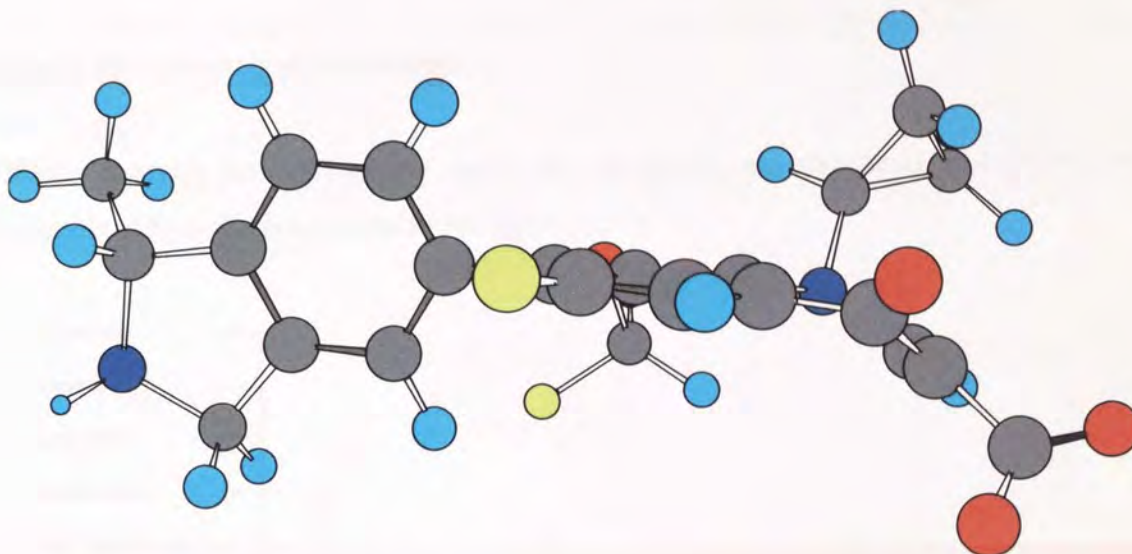
Figure 3.10a – Structure of BMS-284756-01.
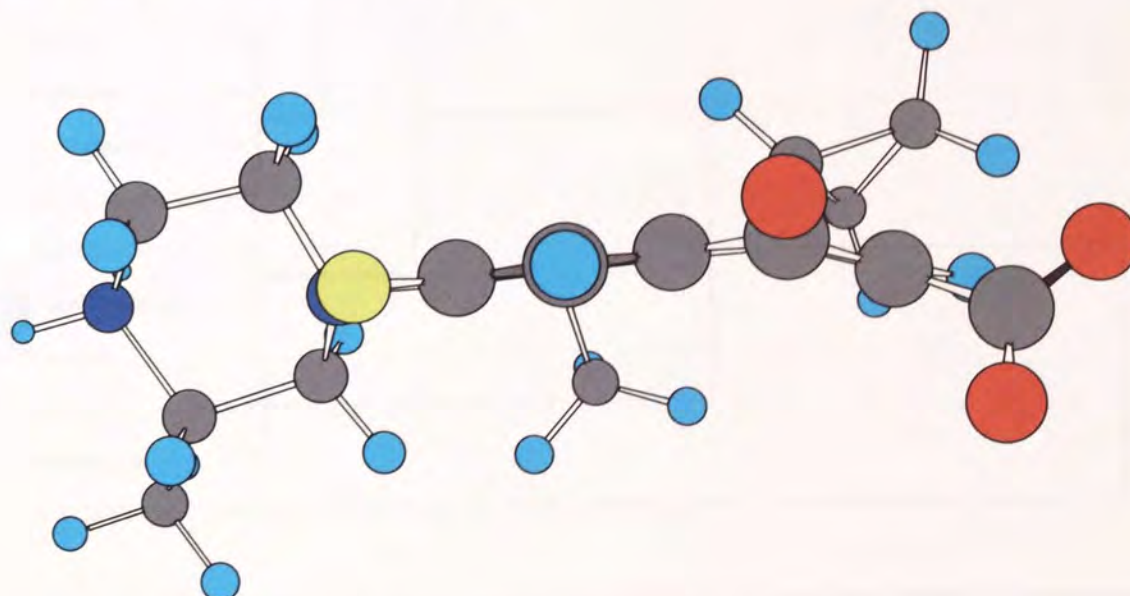
Figure 3.10b – Structure of gatifloxacin.
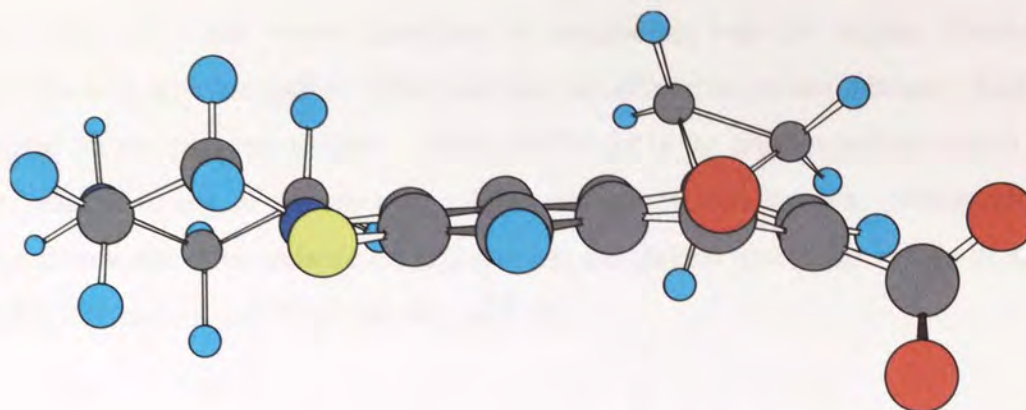
Figure 3.10c – Structure of ciprofloxacin.

Cluster analysis was carried out using the calculated and measured descriptors (see appendix A5) as the components (see figure 3.11).
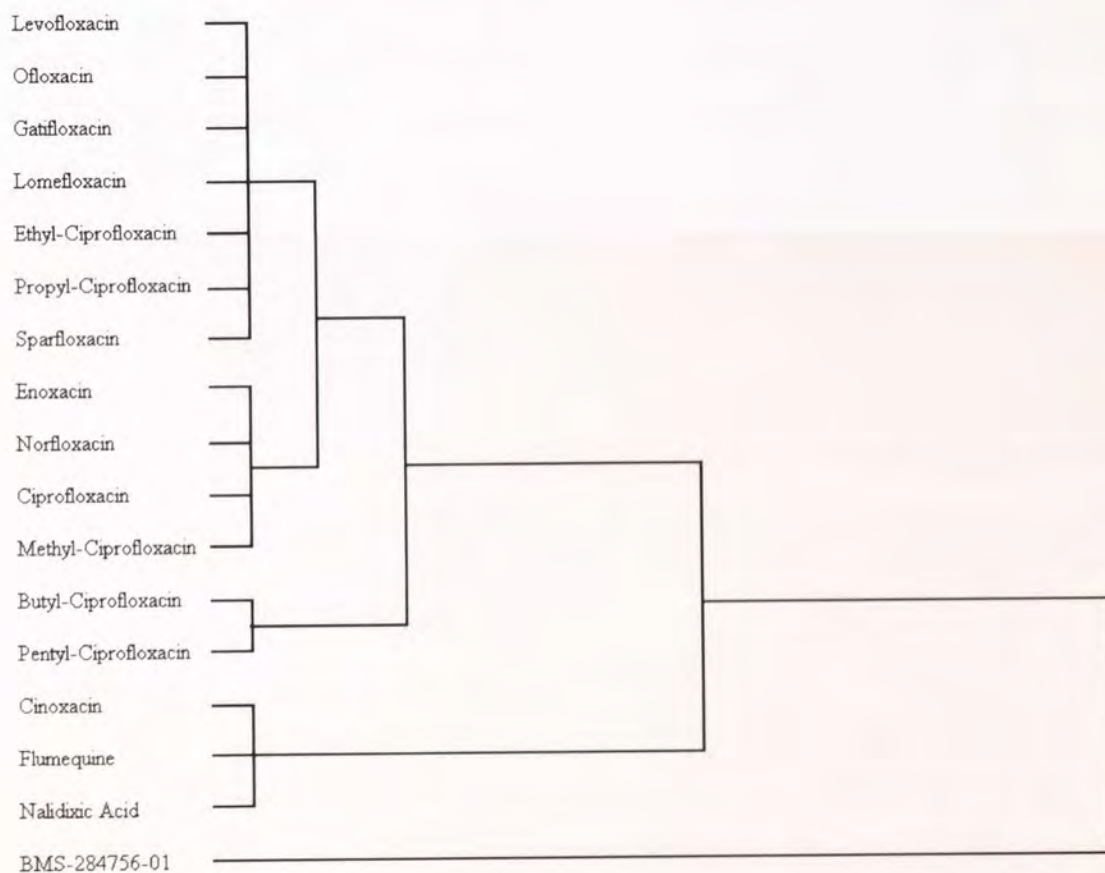
Figure 3.11 – Dendrogram of cluster analysis carried out on quinolones based on parameters calculated.

The cluster analysis separated the quinolones into distinct groups. The non-zwitterionic compounds can be found in a group on their own (cinoxacin, flumequine and nalidixic

acid). The butyl- and pentyl-ciprofloxacin compounds with the highest lipophilicity were also in a separate group. Ofloxacin and levofloxacin are neighbours which is as expected for the two enantiomers. BMS-284756-01 is the only quinolone which is the least 'related' to any of the other quinolones and appears on its own. Structurally it is different from the other quinolones and also has the highest molecular weight of 426.42, a logP 0.086 and pK_{a1} of 5.56 and pK_{a2} of 8.78.

The complete set of data used to construct the dendrogram and calculated surface measures can be found in appendix A5. This group of compounds was found to have a very limited set of physicochemical properties that did not provide enough variation for adequate modelling to be performed. A number of the calculated descriptors also cross-correlated with each other.

CHAPTER 4 QUINOLONE FLUX

4.1 SUMMARY

To verify if the cells were confluent and ready for transport experiments they were visually inspected using light microscopy and scanning electron microscopy. Light microscopy showed that cells grown in flasks formed confluent monolayers and scanning electron microscopy revealed the presence of *microvilli*. The duration of the transport experiments was also assessed, initially these experiments were run for 90 minutes, the transport was found to be linear over this time scale and based on this, the length of the transport experiments was reduced to 40 minutes. The reduced time interval would still provide enough data points to calculate the apparent cellular permeability (P_{app}). The role of fluorescein as a paracellular marker was also investigated, it was found that this compound showed polarised flux, with the basolateral-to-apical transport being significantly greater than the apical-to-basolateral transport. Based on this finding the use of fluorescein as a paracellular marker was questionable and TEERs were instead used to measure the integrity of the cellular monolayers.

Bi-directional fluxes of the quinolones were investigated and it was found that for all quinolones except BMS-284756-01, the basolateral-to-apical flux was greater than the apical-to-basolateral flux. This finding was indicative of the involvement of an active basolateral-to-apical secretion mechanism. BMS-284756-01 is considerably different from the other quinolones studied, it contains five ring structures and has the highest molecular weight of 426.42. The effects of different pH environments in the donor chamber were also investigated to mimic those found in the physiological environment. The pH was reduced to 5.5 to simulate the acidic microclimate, and raised to 8.5 as found in the lower regions of the gastrointestinal tract. The flux of the quinolones was affected with the change in pH, which could be related to the ionisation state of the quinolones. The antimicrobial activity of these quinolones was determined by measuring minimum inhibitory concentrations MICs, these were found to be in-line with those found in the literature Vancebryan *et al*, (1990) and Kidwai *et al*, (1998).

4.2 MATERIALS AND METHODS

The materials and methods used in this chapter have previously been described in chapter 2. The duration of the transport studies was 90 minutes rather than 40 minutes as stated in chapter 2.

4.3 RESULTS AND DISCUSSION

4.3.1 VISUAL INSPECTION OF CACO-2 CELLS

4.3.1.1 LIGHT MICROSCOPY

The following series of photographs (figures 4.1a to 4.1e) show Caco-2 cells, passage 31, grown in 75cm^2 flasks over a period of 5 days. All photographs were taken at x100 magnification. The cells can be seen to becoming confluent over the 5 days.
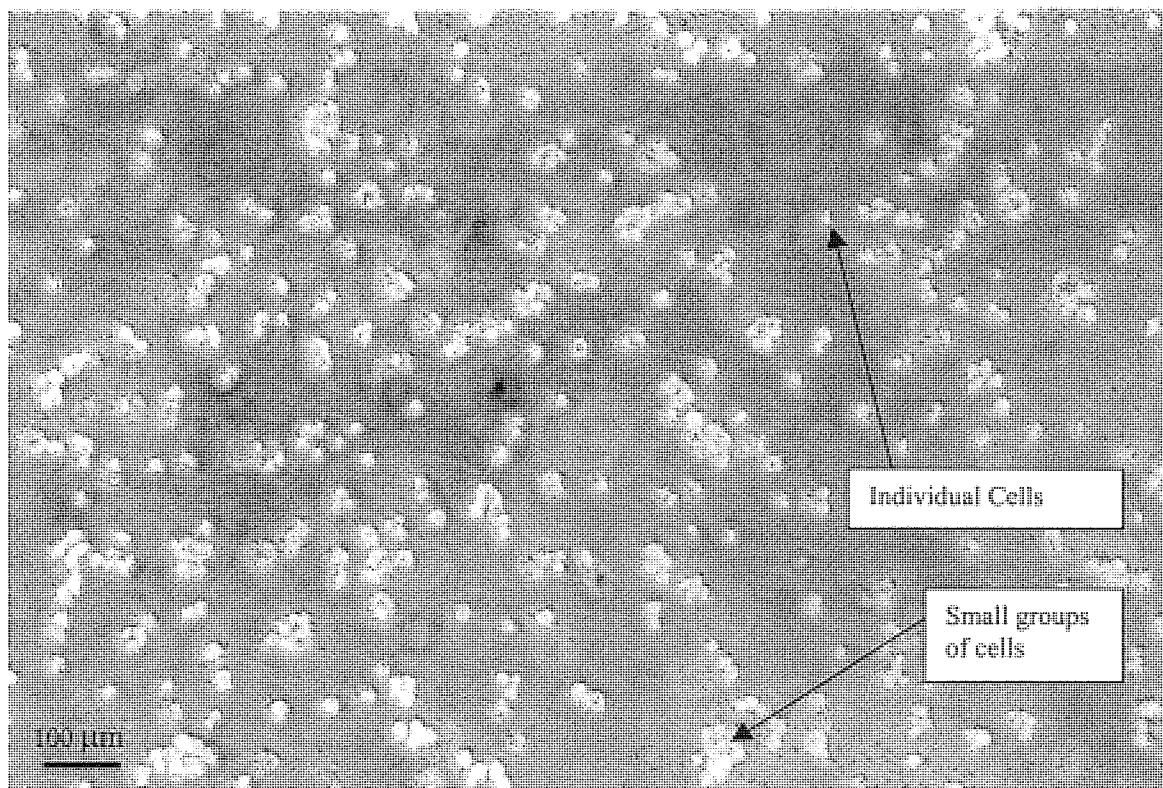
Figure 4.1a - Image of Caco-2 cells at day 0. A large number of individual and small groups of cells can be observed.
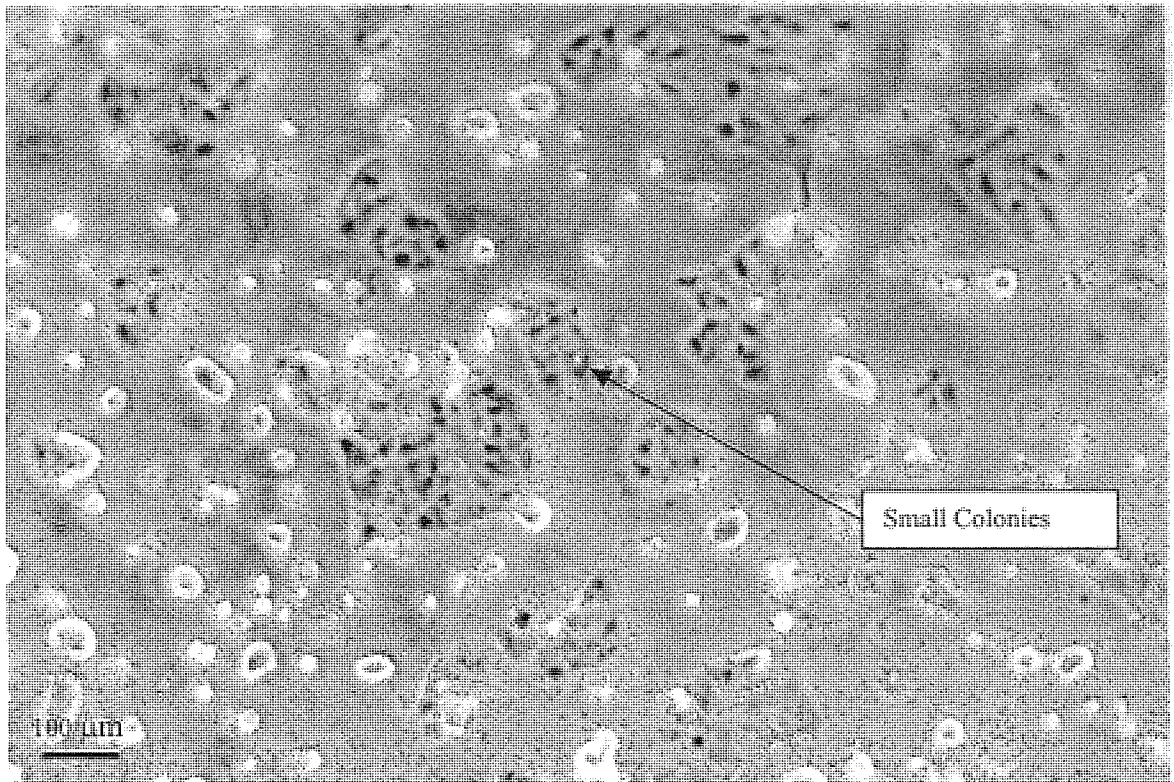
Figure 4.1b -Image of Caco-2 cells at day 1. The cells have started to form small colonies.
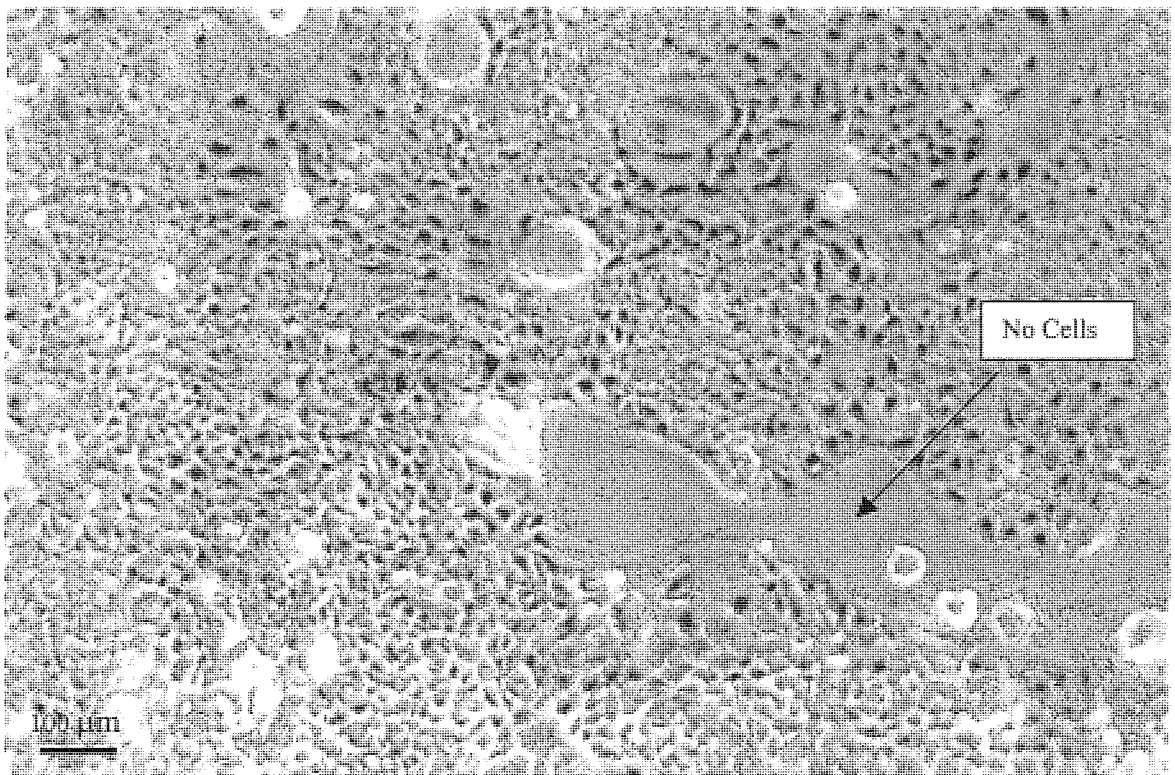
Figure 4.1c - Image of Caco-2 cells day 3. There has been a rapid period of growth over the last 24 hours, a number areas containing no cells are still visible.
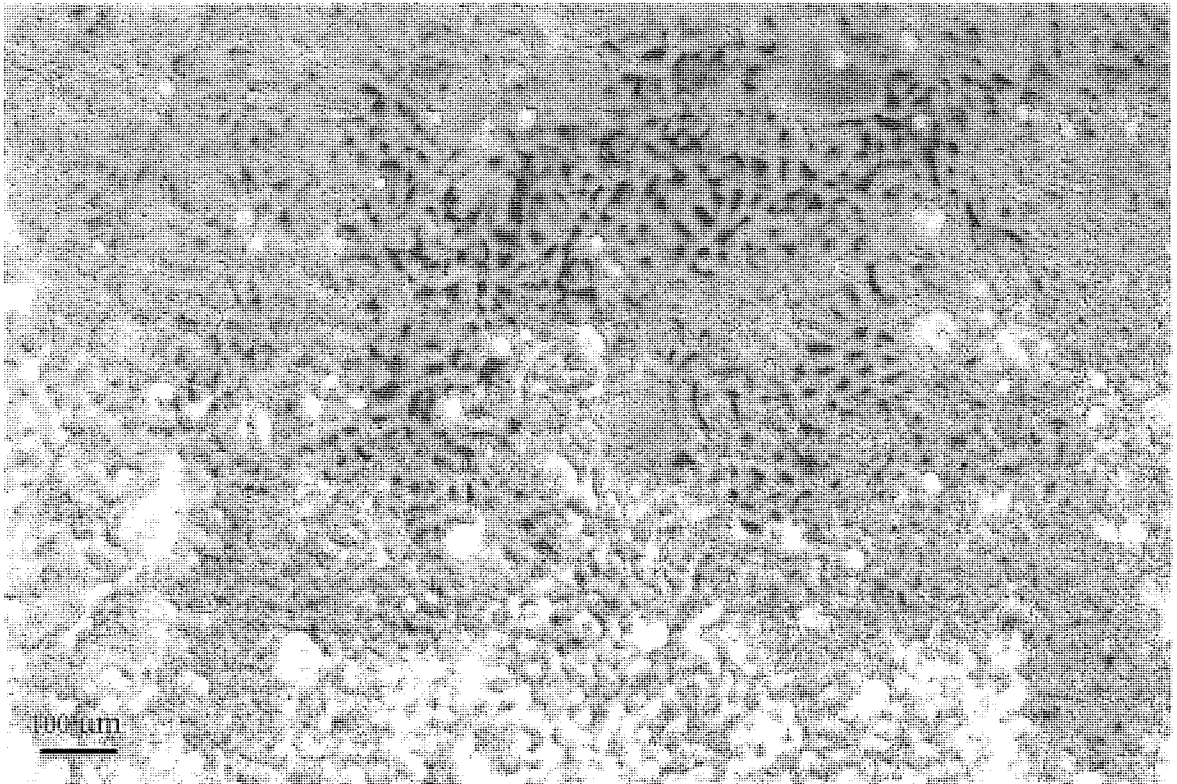
Figure 4.1d - Image of Caco-2 cells day 4. The cells have formed a confluent monolayer. However, small pockets of non-confluent cells are still present.

Dome Formations
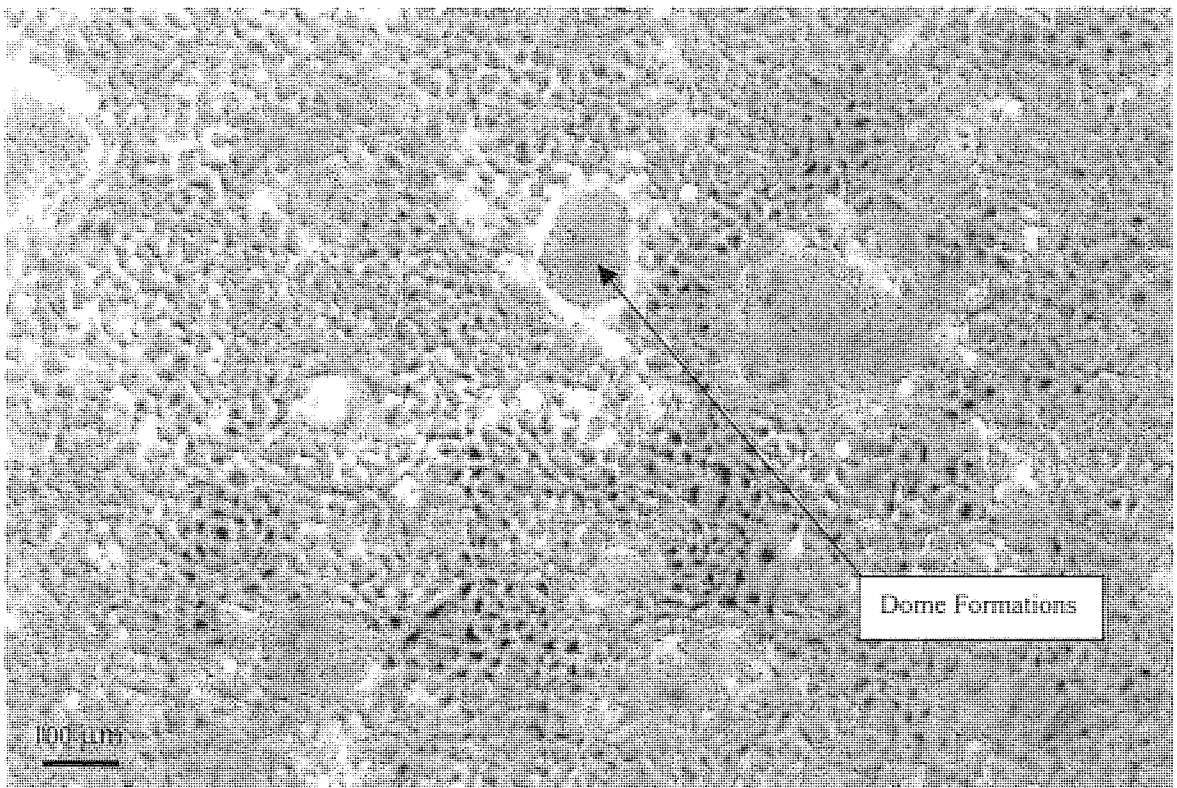
Figure 4.1e – Image of Caco-2 cells day 5, seeded on flasks. The cells are completely confluent and ready for experiments.

The cells grew well in flasks and reached confluence by day 5, which was consistent with reports in the literature. The cells showed a uniform distribution interdispersed with dome like formations (See figures 4.1a - e), (Pinto *et al.*, 1983). It was found that if the cells were passaged before they were fully confluent (~80 % to 90 % confluence), a very good single cell suspension was produced.

4.3.1.2   SCANNING ELECTRON MICROSCOPY SEM

Scanning electron microscopy was performed to visually confirm the presence of the brush-border *microvilli* on the cell surface (see section 2.5). The previous use of light microscopy had confirmed that the cells were confluent. The cells were passage number 39 and 26 days post-seeding.
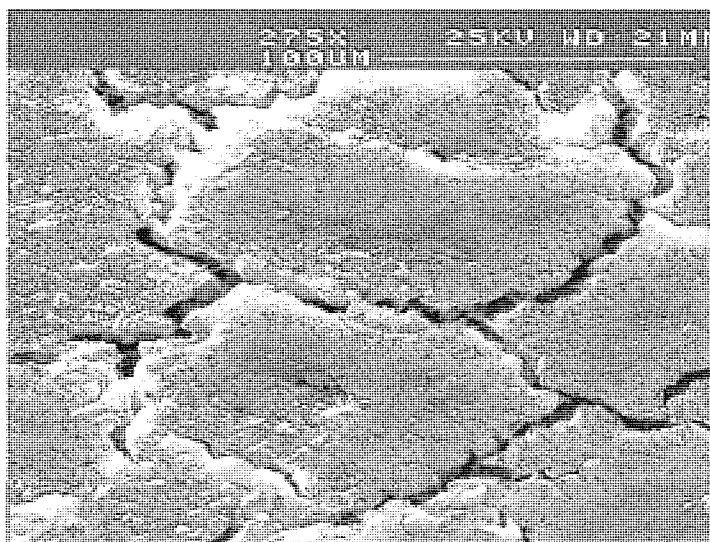
Figure 4.2a – The surface of the insert which had cracked under the fixing procedure.
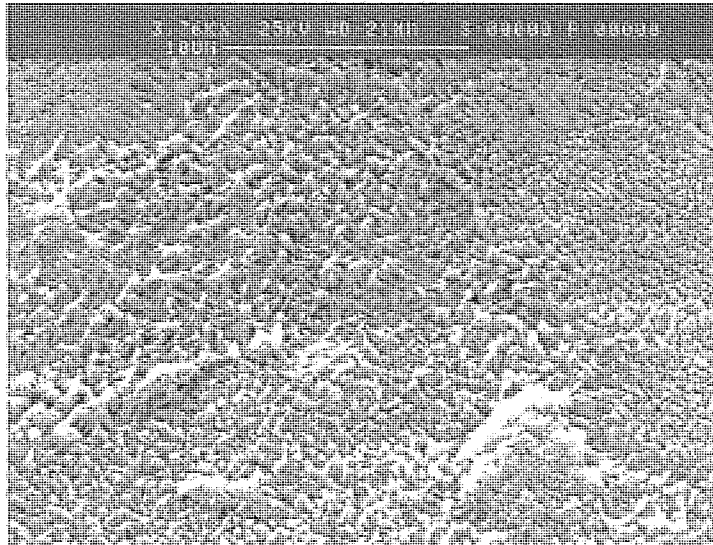
Figure 4.2b - Different densities of caco-2 cells can be clearly seen on the surface of the insert.
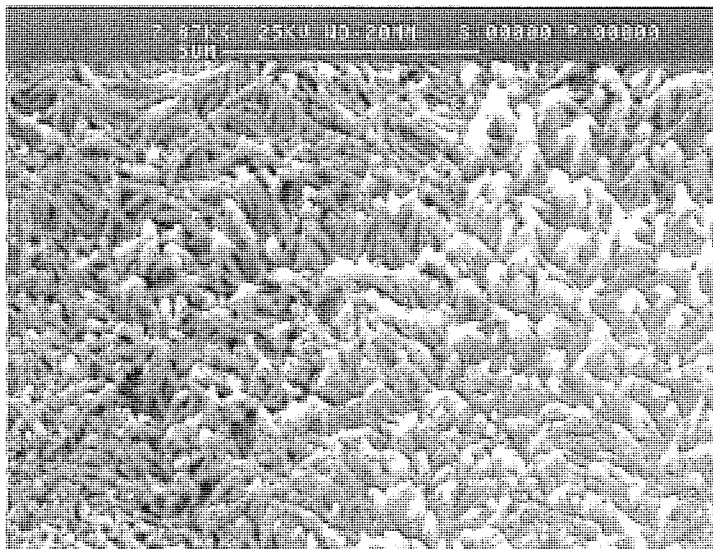
Figure 4.2c -At this extremely high magnification, the *microvilli* can be seen.
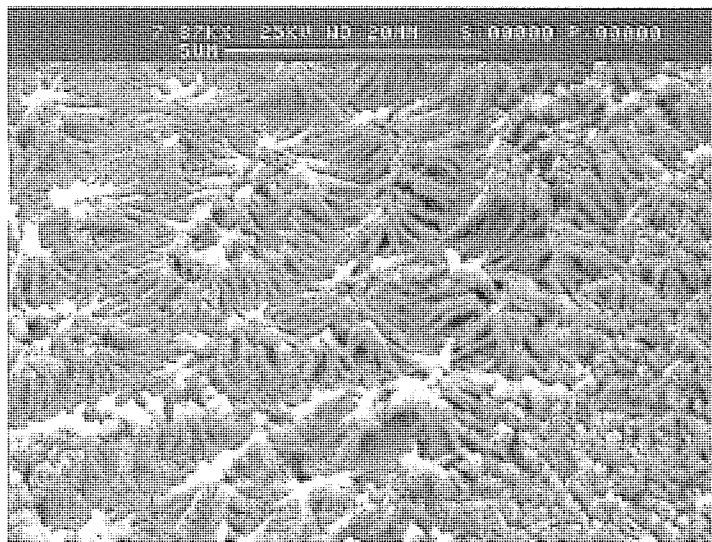
Figure 4.2d - At this extremely high magnification, the *microvilli* **can be seen.**

The cells were visually inspected for confluence and the scanning electron microscopy showed that the cells were well differentiated displaying *microvilli*.

4.3.2 DURATION OF TRANSPORT STUDIES

It was necessary to determine the optimum duration of the transport experiments and whether the support membrane for the cells had any significant inhibitory effect on the transport of compounds.

The transport of the quinolones was investigated through blank Costar inserts without the presence of cells; this was carried out to determine if the inserts themselves in any way behaved as a significant barrier to quinolone flux. Three quinolones, methyl-ciprofloxacin, propyl-ciprofloxacin and ofloxacin of varying lipophilicity were chosen (see table 3.2) together with D-[1-^{14}C]mannitol (1 mM) and fluorescein (10 μg.mL^{-1}), which were used as paracellular markers. Figure 4.3 shows that there was no significant difference in the transport of the five compounds across the inserts. Transport was linear for the first 30 to 40 minutes for all five compounds neglecting the first time point, the first time point can be neglected because a short lag period is present before steady state flux occurs. As a significant percentage of the compound traverses from the apical compartment into the basolateral compartment, sink conditions in the

basolateral compartment were lost and transport slowed, this occurred at approximately 50 minutes, with approximately 40 % of the compound in the donor compartment being transported.
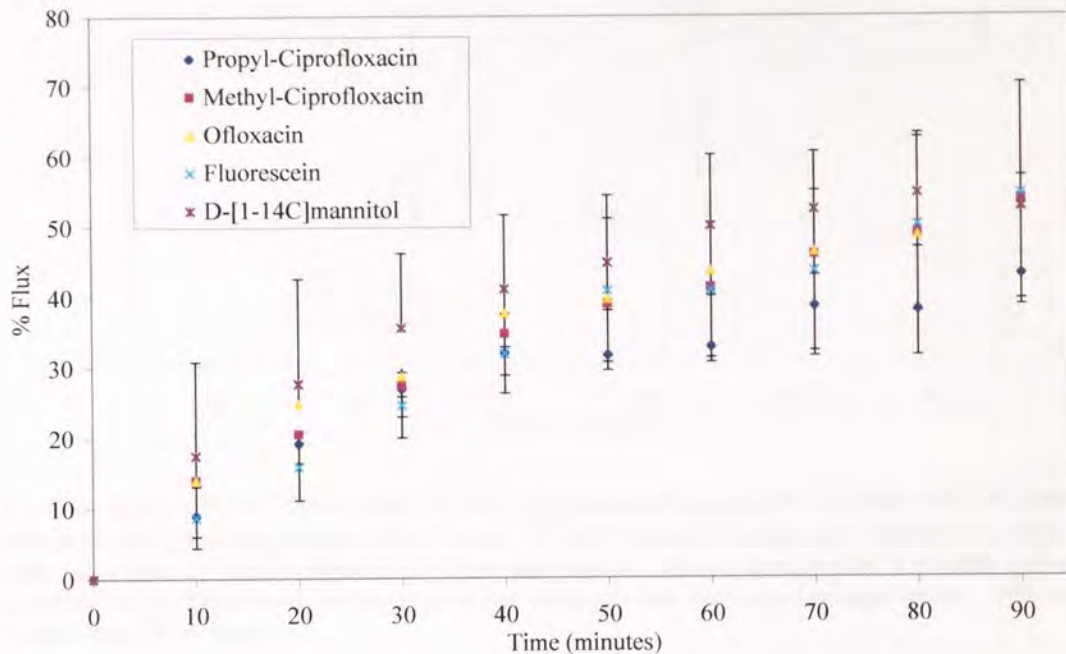
Figure 4.3 – Transport of D-[1-^{14}C]mannitol (1 mM), fluorescein (10 µg.mL^{-1}), ofloxacin (10 µM), methyl-ciprofloxacin (10 µM) and propyl-ciprofloxacin (10 µM) through inserts (n=3) without the presence of cells. The flux of each compound is expressed as the amount transported from the apical-to-basolateral compartment as a percentage of the compound in the apical compartment.

With transport experiments, such large variations are unusual. However, in this case, there was no cellular membrane present act to act as a barrier, as soon as the transport solution was placed in the apical compartment, it immediately started to diffuse into the basolateral compartment. There was no significant difference observed between the five compounds being studied, the transport was rapid and similar for all five compounds. There was no significant difference between the compounds for any one given time point (*e.g.* P=0.393, at 20 minutes). It can be concluded that the membrane support itself provided very little resistance to the transport of compounds.

On further investigation of the time period of 10 to 40 minutes it was found that transport for all five compounds was linear over this time frame (see figure 4.4).
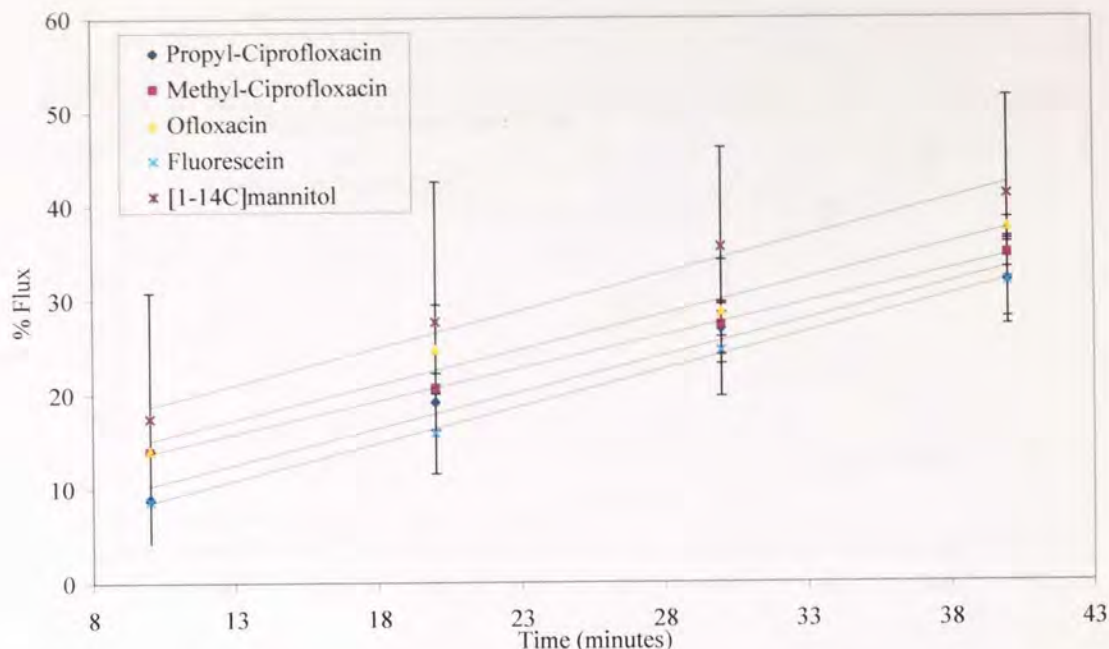
Figure 4.4 – Flux of D-[1-^{14}C]mannitol (1 mM), fluorescein (10 µg.mL^{-1}), ofloxacin (10 µM), methyl-ciprofloxacin (10 µM) and propyl-ciprofloxacin (10 µM) through inserts (n=3) without the presence of cells. The flux of each compound is expressed as the amount transported from the apical-to-basolateral compartment as a percentage of the compound in the apical compartment. This figure is an enlargement of figure 4.3.

The transport of ofloxacin (10 µM) and methyl-ciprofloxacin (10 µM) was measured through Caco-2 cells over a time period of 90 minutes; samples were taken every 10 minutes. Although the transport of both quinolones across blank inserts was similar, the transport of ofloxacin through Caco-2 cells was much lower than that for methyl-ciprofloxacin (see figure 4.5). This is reflected in their relative lipophilicities (logP for methyl-ciprofloxacin is 0.334 and for ofloxacin is –0.165). These findings showed that it would be possible to reduce the duration of the transport experiment from 90 minutes to 40 minutes. Transport over this time period would be linear and more transport experiments could be run with the reduced time, to make sure that an adequate number of data points were present, sampling interval was reduced from 10 minutes to 5 minutes. The amount of compound transported within this reduced time period from one compartment to the next would also be reduced; this would help to maintain sink conditions.
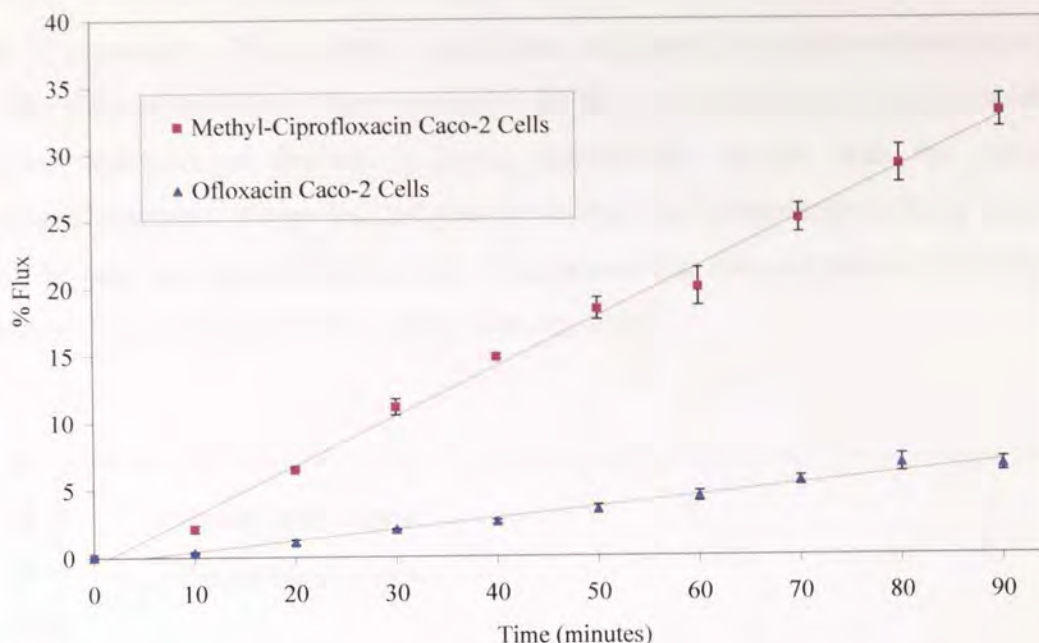
Figure 4.5 – The transport of ofloxacin (10 μM) and methyl-ciprofloxacin (10 μM) across Caco-2 cells passage 31 to 39 used 21 to 28 days post seeding (n=3). The transport of each compound was expressed as the amount transported from the apical-to-basolateral compartment as a percentage of the compound in the apical compartment.

To reduce the experimental time further, however, would cause problems, such as sampling and maintaining temperature as the frequency of sampling would have to be increased.

4.3.3 USE OF PARACELLULAR MARKERS

Fluorescein was used as a paracellular marker by Jaehde *et al*, (1993) for quinolone transport across the blood-brain-barrier. It was hoped that this compound could also be used for Caco-2 cells since it could be easily assayed and was not radioactive. Therefore the experimental procedure would be simpler without the presence of radiolabelled compounds because of the simplified sample handling and disposal requirements.

The average apparent permeability of fluorescein was P_{app} $1.16 \times 10^{-7} \pm 4.12 \times 10^{-8}$ cm.s^{-1} in the apical-to-basolateral directions and P_{app} $1.61 \times 10^{-7} \pm 6.13 \times 10^{-8}$ cm.s^{-1} (see figure 4.6). The apparent apical-to-basolateral permeability of D-[1-^{14}C]mannitol was

$2.75 \times 10^{-7} \pm 2.77 \times 10^{-8}$, therefore the P_{app}s for fluorescein were comparable to those for D-[1-^{14}C]mannitol. There was a significant difference in apical-to-basolateral and basolateral-to-apical flux of fluorescein ($P < 0.0001$ two-tailed t-test). With basolateral-to-apical transport of fluorescein being significantly greater than the apical-to-basolateral transport, it was decided that for further work fluorescein sodium would no longer be used as a paracellular marker. It appeared that this compound itself might be subjected to some form of active efflux from the cells.
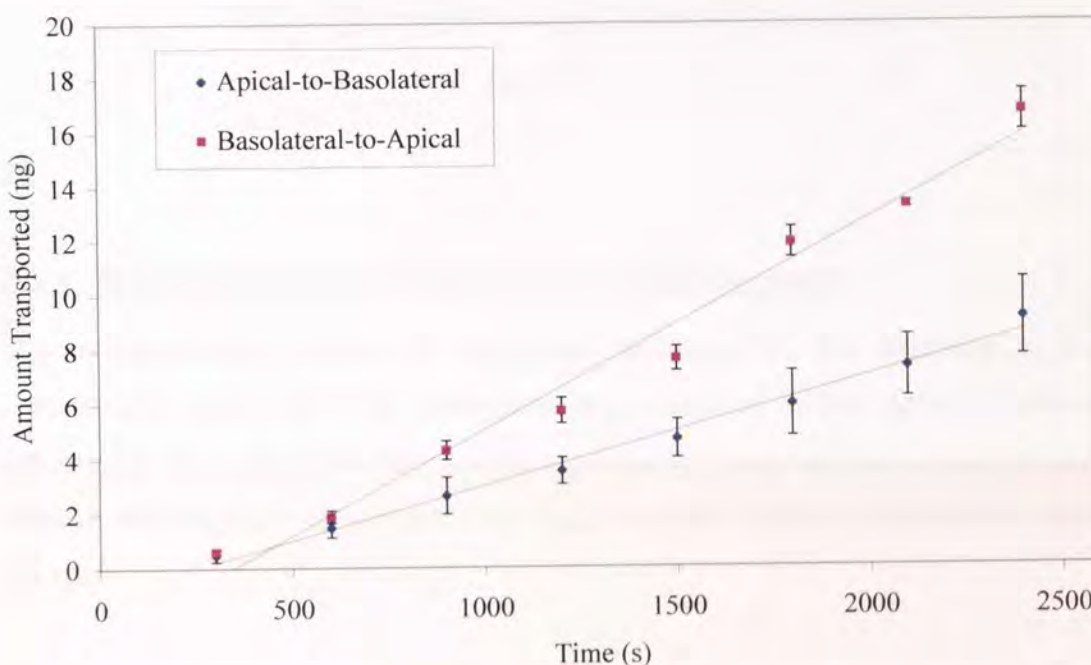
Figure 4.6 – The transport of fluorescein 10 μg.mL^{-1} across Caco-2 cells passage number 66, 22 to 24 days post-seeding (n=3).

Based on these findings the suitability of fluorescein, as a paracellular marker is questionable. Jaehde *et al.*, (1993) used fluorescein sodium as a paracellular marker while studying the flux of quinolones through a cellular model of the blood-brain-barrier in the apical-to-basolateral direction. However, they did not observe basolateral-to-apical flux and therefore may not be aware of any efflux mechanism present in the cellular model he was using. The use of fluorescein as a paracellular marker is not appropriate; this compound itself may be subject to a form of active secretion and could therefore compete with transporter the quinolones may potentially use.

4.3.4 TEERS

The TEERs for transport experiments were in the range of 400-600 $\Omega.cm^2$, these values are comparable to those found in the literature (Walter and Kissel, 1995) and (Artursson *et al.*, 1993). The TEER for the blank inserts was $126 \pm 4 \Omega$ this value was subtracted from all measured TEERs before they were multiplied by the area of the inserts (4.71 cm^2) (see equation 4.1).

EQUATION 4.1

$$TEER = [(Average Measured TEER) - (126 \pm 4)] \times 4.71$$
$$\Omega.cm^2$$

4.3.5 BIDIRECTIONAL TRANSPORT OF QUINOLONES

The transport of a number of quinolones belonging to the homologous *n*-alkyl ciprofloxacin family and other quinolones, was measured in both apical-to-basolateral and basolateral-to-apical directions. The experiments were run over a time period of 40 minutes, and the apparent permeability (P_{app}) was taken over the steady-state period of transport.

The quinolones were run in the basolateral-to-apical direction to investigate if there was any difference in the transport in different directions, *i.e.* the possibility of an efflux mechanism. The homologous family of *n*-alkyl ciprofloxacin showed an increase in transport with the addition of each methyl group (see figure 4.7).

In all cases, basolateral-to-apical flux was significantly greater than apical-to-basolateral flux ($P<0.05$; see figure 4.7). If the quinolones belonging to the *n*-alkyl ciprofloxacin family were passively transported, then the transport in the basolateral-to-apical and apical-to-basolateral directions would be the same. However, this was not the case for this series of compounds. Based on these findings, the apical-to-basolateral and basolateral-to-apical transport of a group of quinolones not belonging to this *n*-alkyl ciprofloxacin family was also investigated. (See figure 4.8).
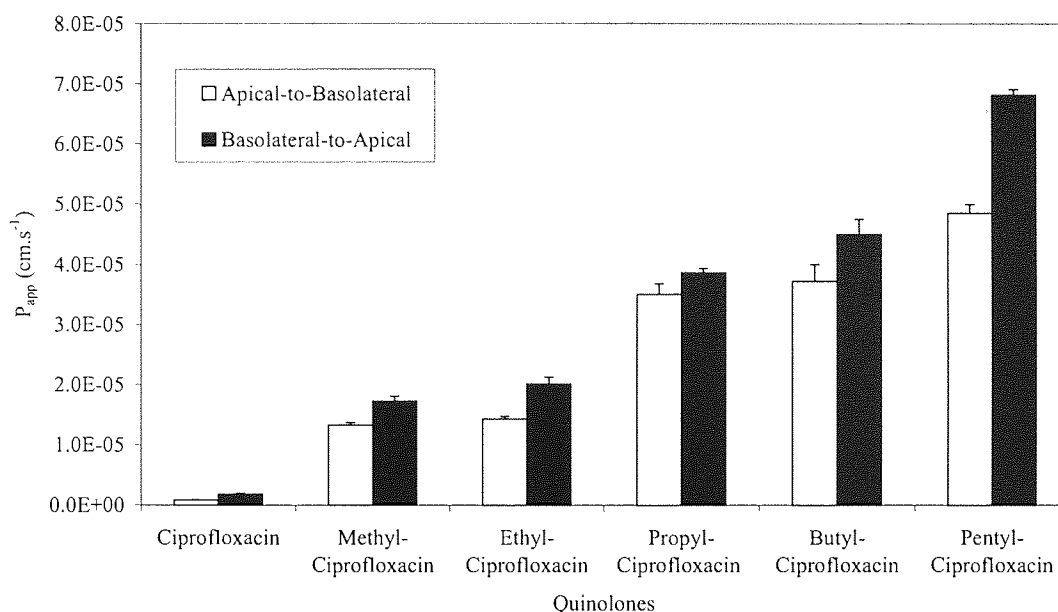
Figure 4.7 - The flux of *n*-alkyl ciprofloxacin homologous family (all at 10 μM) in both apical-to-basolateral and basolateral-to-apical directions. The Caco-2 cells used were passage number 33 to 64 (n=3), 21 to 28 days post seeding.

A summary of the ratio of basolateral-to-apical to apical-to-basolateral based on figures 4.7 and 4.8 is provided in table 4.1.

In all cases except BMS-284756-01, basolateral-to-apical flux was significantly greater than apical-to-basolateral (P<0.05). BMS-284756-01 did show greater basolateral-to-apical transport than in the apical-to-basolateral direction (see figure 4.8), this was not found to be significant (P=0.085). This is most likely due the variability present in the apical-to-basolateral transport. The P_{app}s for BMS-284756-01 are $3.73 \times 10^{-6} \pm 6.9 \times 10^{-7}$ cm.s^{-1} in the apical-to-basolateral direction and $4.91 \times 10^{-6} \pm 5.72 \times 10^{-7}$ cm.s^{-1} in the basolateral-to-apical direction. These data give an indication that there may be the presence of an active efflux mechanism, which would explain the basolateral-to-apical flux being greater than the apical-to-basolateral flux for a number of quinolones.

At this point, it would be pertinent to explain that for a purely passive process the apical-to-basolateral flux should be the same as basolateral-to-apical flux as observed for D-[1-^{14}C]mannitol and [^{3}H]testosterone (see section 5.3.2.2.2), unless an active transport mechanism is involved in either direction.
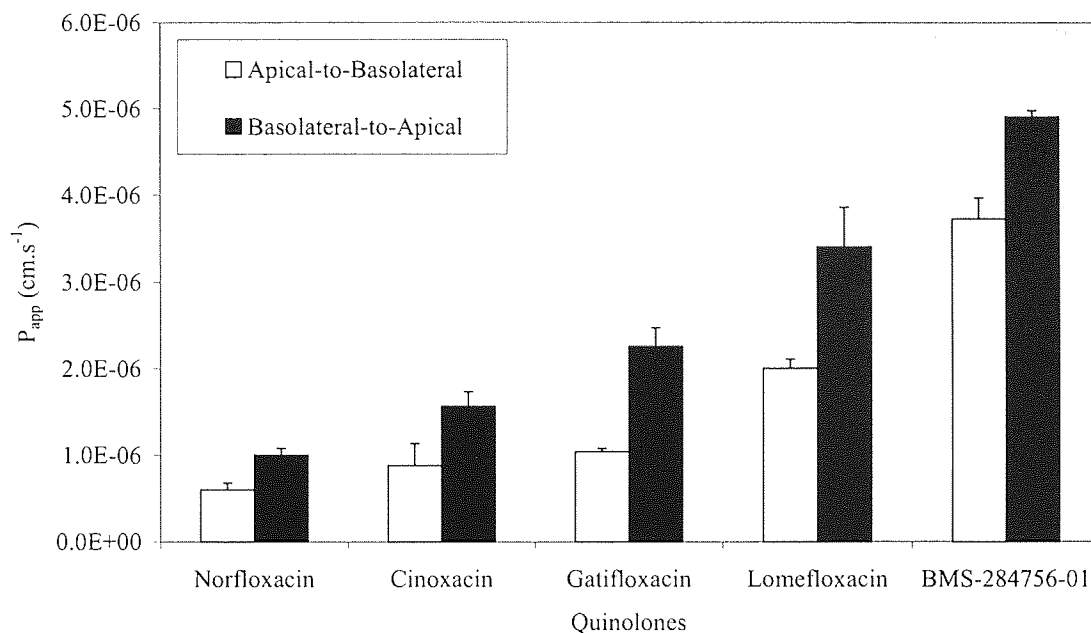
Figure 4.8 – The flux of a number of quinolones (10 µg.mL^{-1}) in both apical-to-basolateral and basolateral-to-apical directions. The Caco-2 cells used were passage number 33 to 64 (n=3), 21 to 28 days post seeding.

Quinolone	Ratio (basolateral-to-apical/apical-to-basolateral)	SD
Norfloxacin	1.66	0.25
Cinoxacin	1.77	0.54
Gatifloxacin	2.16	0.22
Lomefloxacin	1.70	0.24
Levofloxacin	1.32	0.15
BMS-284756-01	1.32	0.29
Ofloxacin	1.51	0.20
Ciprofloxacin	2.17	0.21
Methyl-Ciprofloxacin	1.30	0.07
Ethyl-Ciprofloxacin	1.41	0.09
Propyl-Ciprofloxacin	1.10	0.06
Butyl-Ciprofloxacin	1.21	0.11
Pentyl-Ciprofloxacin	1.41	0.05
Flumequine	1.14	0.13

Table 4.1 – Summary of ratio of (basolateral-to-apical/apical-to-basolateral) for quinolones.

The greater basolateral-to-apical flux than the apical-to-basolateral suggests the involvement of an active efflux process. Since this process operates in the basolateral-to-apical direction *i.e.* in nature it would secrete compounds into the luminal space, it will therefore be referred to as an active secretion process.

The flux of quinolones through Caco-2 cells shows a marked asymmetry with basolateral-to-apical flux being greater than apical-to-basolateral flux indicating that an active secretion mechanism may be present. This potential active secretion mechanism will be investigated in detail in chapter 5.

As stated in section 3.2, the permeability of the quinolones can be affected by the charge carried by the quinolone. The quinolones are zwitterionic compounds and therefore provide the opportunity to study the transport of different charged species by varying the pH of the transport medium. This will help determine the importance of charge if either of the ionic species or neutral molecules shows increased transport.

4.3.6 THE INFLUENCE OF DONOR pH

A number of the quinolones are zwitterionic compounds therefore their charge can be affected by the environment. A small representative group was used to investigate the effects of adjusting the pH. The apical pH was adjusted to 5.5 representing the acidic microclimate, and 8.5 representing the pH found in lower region of the intestine. The receiver phase was kept at pH 7.4.

Maximum permeability for propyl-ciprofloxacin was observed in the basolateral-to-apical direction. In the apical-to-basolateral directions maximal permeability occurs at pH 7.4 with it dropping off at pH 5.5 and the minimum occurring at pH 8.5. With flumequine maximum transport occurs at pH 5.5 in the apical-to-basolateral direction, followed by basolateral-to-apical transport at pH 7.4 and apical-to-basolateral at pH 7.4. The lowest level of transport occurred at pH 8.5, at this pH the apparent permeability for flumequine was lower than the lowest observed for propyl-ciprofloxacin (see figure 4.9).

The different permeabilities shown by propyl-ciprofloxacin and flumequine reflect their ionisation state at the pH studied. Propyl-ciprofloxacin, being zwitterionic at physiological pH, predominately exists as an overall neutral molecule (67 %, table 4.2) and therefore shows maximum permeability in this form.

129
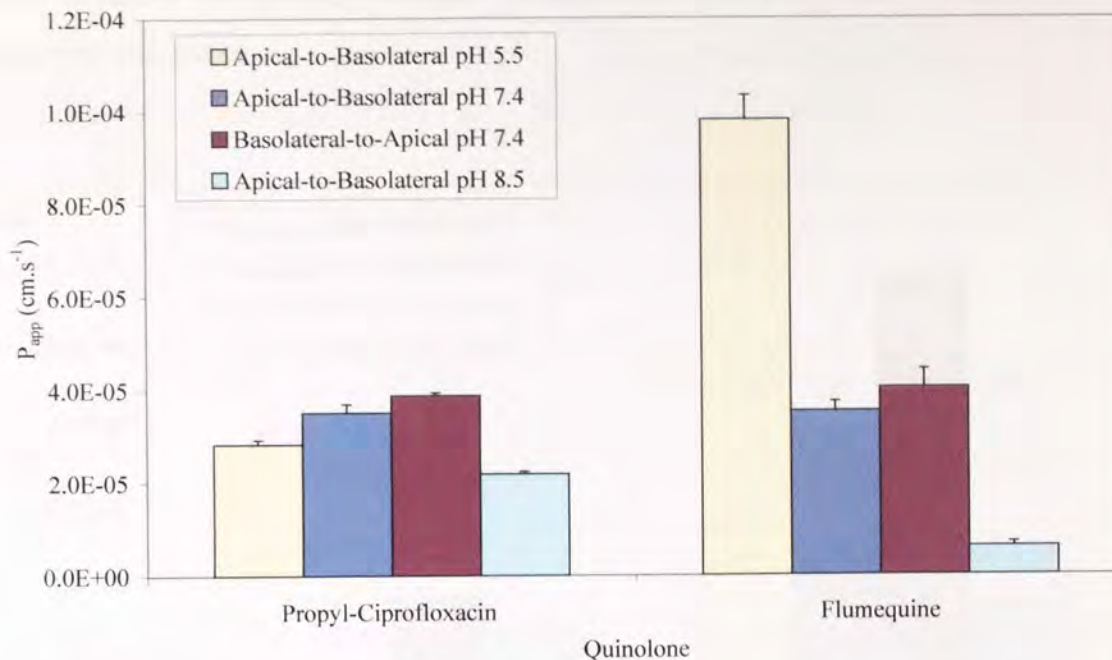
Figure 4.9 – The effect of adjusting the apical pH on the transport of propyl-ciprofloxacin and flumequine (10 μM) flux through Caco-2 cells passage 66 to 68 (n=3), 21 to 28 days post seeding.

These data correlate well with the pK_a data for these four compounds. Flumequine (pK_a of 6.47) is not zwitterionic and is a weak acid, at high pH it shows low cellular permeability because it would be in an ionised form (see table 4.2). At pH 5.5 over 90 % of flumequine is in the unionised form as the pH increases the presence of this unionised species decreases, at pH 8.5 there is only 0.92 % left in the unionised form while the remainder is present as the anion. The transport of the neutral form across the lipophilic intestinal membrane would be favoured to that of the charged anion.

The transport for the zwitterionic compounds (propyl-ciprofloxacin and ofloxacin) was lowest at acidic and alkaline pH and was greatest at pH 7.4. This pH is close to the isoelectric point for these compounds (see section 3.2.3); at this pH they predominately exist as an overall neutral species. Ciprofloxacin, which is also a zwitterion, showed maximum transport at pH 8.5. At this pH, over 56 % of ciprofloxacin would exist as the anion, therefore the ciprofloxacin anion showed the greatest permeability. This was a surprising finding, since it would be expected that the neutral molecule would have shown maximum transport. A possible explanation for this observation is that, ciprofloxacin shows a relatively low transport when compared to the other quinolones

and therefore the greater transport observed at pH 8.5 could be attributed to experimental errors.
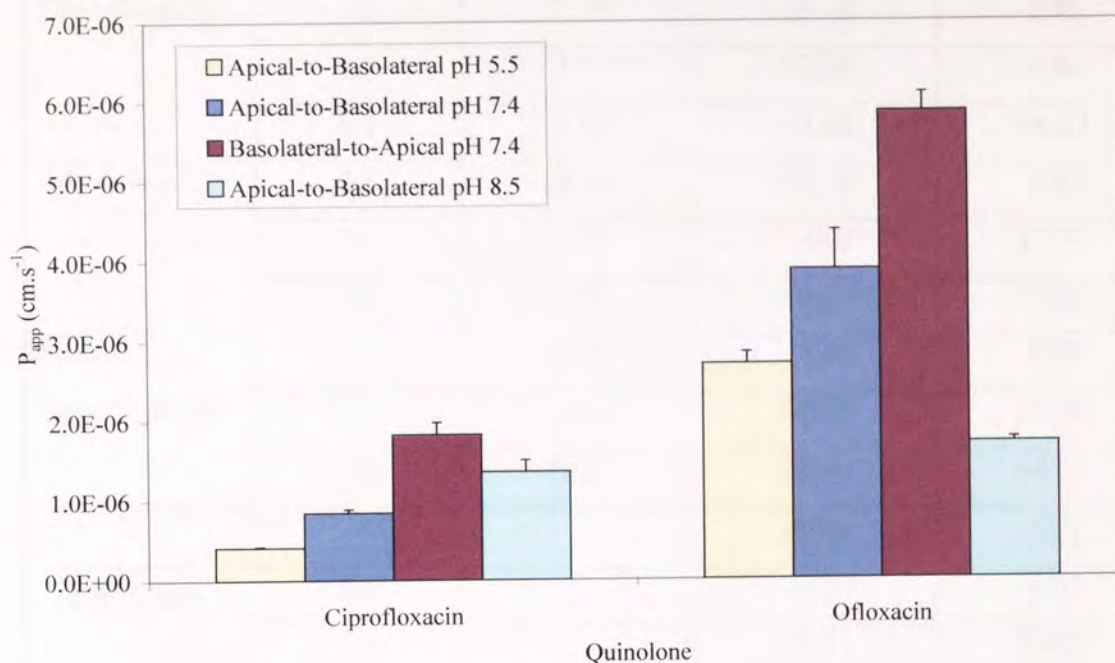
Figure 4.10 – The effects of adjusting the apical pH on the flux of ciprofloxacin and ofloxacin (10 µM) flux through Caco-2 cells passage 66 to 68 (n=3), 21 to 28 days post seeding.

In general, the transport of the neutral species is the highest. However, there are reports in the literature where the transport of the cationic species has been demonstrated to be favoured, because of interactions between negatively charged membrane phospholipids and the cation.

Quinolone	pH	% of each species present		
		$[H_2A^+]$	$[HA^\pm]$	$[HA^-]$
Ciprofloxacin	5.5	77.19	22.78	0.03
	7.4	3.73	87.34	8.94
	8.5	0.15	43.64	56.22
Ofloxacin	5.5	76.34	23.59	0.07
	7.4	3.22	79.08	17.70
	8.5	0.08	26.17	73.75
Propyl-Ciprofloxacin	5.5	83.92	15.99	0.09
	7.4	4.43	66.99	28.58
	8.5	0.08	15.68	84.23
			$[HA]$	$[A^-]$
Flumequine	5.5		90.32	9.68
	7.4		10.51	89.49
	8.5		0.92	99.08

Table 4.2 – Ionic composition of the quinolones, at three pH values, 5.5, 7.4 and 8.5. The percentages of each species present at different pH values was calculated using equations 3.8, 3.9, 3.11, 3.12 and 3.13.

Iseki *et al.*, (1992) observed that the rat intestinal brush-border membrane vesicles uptake of enoxacin, a zwitterionic quinolone, was higher at pH 5.5 than 7.4. It was concluded that the binding of the cationic form appeared to play a role in the process of intestinal absorption because pH in the vicinity of the intestinal epithelial cells is weakly acidic and proton-rich. This could be due to interactions between the negatively charged phospholipids and the cationic species present at pH 5.5 (Iseki *et al.*, 1992). This finding is contradictory to that seen with ofloxacin and propyl-ciprofloxacin with Caco-2 cells where the neutral species present at pH 7.4 showed the greatest transport and for ciprofloxacin, the anion showed the greatest transport. In conclusion, the apical-to-basolateral transport of the quinolones is not solely a passive process based upon the ionisation, it appears that some form of multifactorial transport maybe involved.

4.3.7 MICROBIOLOGICAL ACTIVITY

E.coli DC0 and *Staphylococcus aureus* NCTC6751, both Gram negative organisms, were used in the determination of minimum inhibitory concentrations for the quinolones. It was hoped that the MIC could be used, together with physicochemical properties measured in chapter 3, to aid the prediction of cellular permeability for the quinolones.

Quinolone	*E.coli* MIC ($\mu g.mL^{-1}$)	*Staphylococcus aureus* MIC ($\mu g.mL^{-1}$)
Cinoxacin	>128	>128
Ciprofloxacin	0.5	0.5
Methyl-Ciprofloxacin	1	0.5
Ethyl- Ciprofloxacin	2	0.25
Propyl-Ciprofloxacin	2	0.5
Butyl-Ciprofloxacin	2	1
Enoxacin	4	2
Flumequine	32	4
Lomefloxacin	4	2
Nalidixic Acid	>128	>128
Norfloxacin	4	1
Ofloxacin	2	0.5
Sparfloxacin	0.5	0.125

Table 4.3 - MICs for quinolones based on *E.coli* and *S. aureus*.

Both organisms showed similar sensitivities to the quinolones (see table 4.3). The older quinolones such as nalidixic acid and cinoxacin show the least activity. Sparfloxacin and the *n*-alkyl ciprofloxacin family of compounds show highest activity. *Staphylococcus aureus* was able to distinguish between the homologous *n*-alkyl ciprofloxacin family. There was no correlation between the MICs and logP or P_{app}, this is likely because the effectiveness of the quinolone is probably based on a number of

different factors such as binding affinity to target, rather than solely its affinity to cross the bacterial membrane.

4.3.8 DISCUSSION

Initial work to investigate the duration of the transport studies revealed that the duration could be reduced from 90 minutes to 40 minutes. Thus allowing the maintenance of sink conditions.

Fluorescein sodium was investigated as a paracellular marker. It was found that this compound also showed greater basolateral-to-apical transport than apical-to-basolateral. This compound shows good potential as a cheap and easy to use paracellular marker. However, before it can routinely be used for this purpose, the transport needs to be fully characterised. This is outside the scope of this project.

The work in this chapter showed that the transport of quinolones was not an entirely passive process. The basolateral-to-apical transport was greater than the apical-to-basolateral transport indicating the presence of an active secretion mechanism. Even though there is a greater basolateral-to-apical transport than apical-to-basolateral, the basolateral-to-apical transport follows the same lipophilicity trends as observed for the apical-to-basolateral transport. Indicating that the transport is dependent on lipophilicity with some form of active transport. This finding shifted the emphasis within this project to identify the nature of this active secretion mechanism (see chapter 5).

CHAPTER 5 ACTIVE TRANSPORT

5.1 SUMMARY

This chapter investigates the mechanisms involved in the active uptake and secretion of quinolones in Caco-2 cells.

Competing quinolones (norfloxacin 100 μM) appeared to decrease apical-to-basolateral flux of gatifloxacin (10 μM), suggesting a possible competing mechanism. The apical-to-basolateral flux of gatifloxacin was inhibited significantly by norfloxacin 100 μM, while sodium azide 15 mM with 2-deoxy-D-glucose 50 mM had no significant effect. There was no significant difference in the apparent apical-to-basolateral permeability of ciprofloxacin and norfloxacin at 10 μM and 100 μM concentrations.

The metabolic inhibitor combination of sodium azide, with 2-deoxy-D-glucose and 2,4-dinitrophenol, had significant inhibitory effects on the basolateral-to-apical secretion of gatifloxacin. However, active secretion could not be abolished.

The effects of reduction in temperature led to a decrease in transport of gatifloxacin in both apical-to-basolateral and basolateral-to-apical directions, which was most probably due to a loss in membrane fluidity. Even at the reduced temperature of 2°C the basolateral-to-apical transport was significantly greater than the apical-to-basolateral.

The donor concentration of two quinolones, butyl-ciprofloxacin and gatifloxacin were varied to find the affinity for an active transport mechanism. However, the plots of rate of transport versus concentration of quinolone showed that transport appears to be passive.

It was found that norfloxacin (100 μM) and ofloxacin (100 μM) competitively inhibited basolateral-to-apical flux of gatifloxacin.

The effects of the ionic inhibitors, probenecid, cimetidine and DIDS were investigated on the basolateral-to-apical transport of gatifloxacin. Probenecid was found to have an

inhibitory effect on the basolateral-to-apical transport of gatifloxacin. However, cimetidine had no effects on active secretion. DIDS, an organic anion exchange inhibitor, was found to only have a partial effect.

The work in section 4.3.3 revealed that fluorescein was subject to basolateral-to-apical secretion. Therefore, its effects on basolateral-to-apical transport of quinolones was also investigated. It was found that this compound had no significant inhibitory effect on the basolateral-to-apical flux of the quinolones at the concentration (10 $\mu g.mL^{-1}$) used as a paracellular marker.

Ofloxacin and levofloxacin are isomers and although differences in secretion between the two isomers have been reported in the literature (Rabbaa *et al.*, 1997), these could not be found between (S) isomer and racemic mixture *in vitro*.

The PgP and anion inhibitor, verapamil, at a concentration of 400 μM was able to completely abolish the basolateral-to-apical secretion of gatifloxacin. This result indicates the involvement of PgP in the active basolateral-to-apical secretion of gatifloxacin as well as some other efflux mechanism.

The major focus of the work in this chapter was the characterisation of the basolateral-to-apical secretion of the quinolones.

5.2 APICAL-TO-BASOLATERAL FLUX

5.2.1 INTRODUCTION

It appears from the data in section 4.3.5 and from findings by a number of authors including Griffiths *et al.*, (1993), Griffiths *et al.*, (1994) and Cavet *et al.*, (1997b), that the quinolones may be subject to active uptake and secretion. Therefore, it would be prudent to investigate any possible active uptake mechanism. Work was carried out on a smaller group of quinolones. Ciprofloxacin and norfloxacin two well studied quinolones together with gatifloxacin, a new quinolone were the major focus of the work. Currently, there is very little known about gatifloxacin, which does have some

structural similarity to ciprofloxacin. Thus it may serve an useful model to compare and contrast transport profiles with those of earlier quinolones such as ciprofloxacin and norfloxacin.

5.2.2 RESULTS AND DISCUSSION

5.2.2.1 EFFECTS OF CONCENTRATION ON APICAL-TO-BASOLATERAL FLUX

Active transport systems are prone to saturation at high substrate concentrations. Therefore, if quinolones undergo active transport in the apical-to-basolateral direction, the apparent permeability over a range of concentrations should be different.

The influence of concentration on apical-to-basolateral flux of ciprofloxacin and norfloxacin was investigated, these were transported across Caco-2 cells at 10 μM and 100 μM concentrations (see figure 5.1). If active uptake was present, there should be differences in the P_{app} s as concentration increased.

Initially all the quinolones were used at 10 μM, the concentration used by a number of authors (Cavet *et al.*, 1997b; Griffiths *et al.*, 1994; Jaehde *et al.*, 1993). To determine if an active uptake mechanism was present, which could be saturable, the concentration of the quinolone was increased to 100 μM. According to Jaehde *et al.*, (1993), if a transporter were present, at higher concentrations it would become saturated and this would be observable from the apparent permeability. Jaehde *et al.* (1993) found that there was no significant difference in the P_{app} for the quinolones at different donor concentrations with apical-to-basolateral flux across the blood-brain-barrier.

There was no significant difference between the two concentrations of quinolones (Ciprofloxacin P=0.058 and norfloxacin P=0.413). These data suggests that there was no active uptake present for ciprofloxacin and norfloxacin in the Caco-2 cell model used here. If there was an active uptake mechanism, a difference may have been observed.
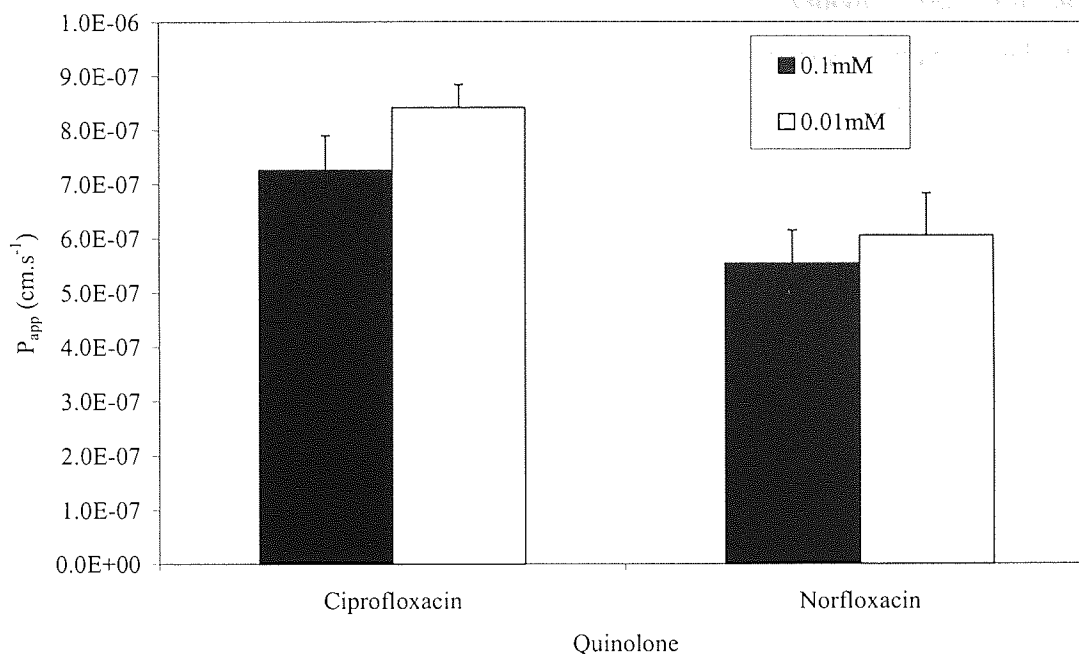
Figure 5.1 – The permeability P_{app} for ciprofloxacin and norfloxacin apical-to-basolateral, at 0.01 mM (10 μM) and 0.1 mM. Caco-2 cells were passage number 53 to 66, 21 to 28 days post seeding, n=3, TEER 626 ± 40 Ω.cm².

5.2.2.2   USE OF INHIBITORS

The two different concentrations of ciprofloxacin and norfloxacin used (10 μM and 100 μM) did not show any differences in the apparent permeability. Since concentration had no effect, a different approach was taken. Active transport processes are usually dependent on cellular ATP. Compounds such as sodium azide with 2-deoxy-D-glucose can be used to deplete energy stores and thereby, can inhibit active transport mechanisms.

A combination of sodium azide (15 mM) and 2-deoxy-D-glucose (50 mM), and verapamil (100 μM) were used as potential inhibitors of apical-to-basolateral flux. Verapamil (100 μM) has been suggested by a number of authors (Kusuhara *et al.*, 1998; Burton *et al.*, 1996; Anderle *et al.*, 1998) as an inhibitor of PgP, an apical membrane transporter protein. This transporter moves compounds from within the cell to the apical side. The rationale for using this inhibitor when studying apical-to-basolateral transport was that the quinolone flux in the presence of the inhibitor may be increased.

This would be indicative of basolateral-to-apical PgP involvement. Sodium azide is a potent ATP depleter, and was used in combination with 2-deoxy-D-glucose, which was used to replace glucose as an energy source. Additionally, if quinolones do use a specific transporter, they should compete with each other for it and, thereby, the addition of a competing quinolone to the apical compartment should reduce the transport of the quinolone of interest.

Figure 5.2 shows that norfloxacin (100 µM) appears to compete with gatifloxacin (10 µM) apical-to-basolateral flux by significantly reducing it by 40 % ($P<0.05$). Verapamil (100 µM) does not cause any significant change in transport ($P=0.114$). The combination of sodium azide (15 mM) and 2-deoxy-D-glucose (50 mM) cause an increase in apical-to-basolateral flux ($P<0.001$), this could result from the possible inhibition of a basolateral-to-apical mechanism, which would have led to the under-estimation of the original apical-to-basolateral flux.

Norfloxacin (100 µM) caused a significant reduction in the permeability of gatifloxacin (10 µM). Since norfloxacin is also a quinolone, a possible interpretation of these data is that it is competing with an active uptake mechanism available to gatifloxacin.

This study found that the apical-to-basolateral transport of gatifloxacin, a new quinolone, was unaffected by verapamil. However, it was also observed that norfloxacin (100 µM) reduced the flux of gatifloxacin (10 µM) apical-to-basolateral ($P<0.05$), by 35 %. Both norfloxacin and gatifloxacin have similar physicochemical properties (see sections 3.2.3 and 3.3.3) and therefore could, potentially, use the same transporter, and compete with each other for it

Based on these results and data from section 4.3.5, apical-to-basolateral transport of these quinolones appears to be dependent on lipophilicity and therefore is probably largely passive in nature. However, competition between different quinolones does occur, suggesting the involvement of an active transport mechanism that has a small effect. This is probably swamped by the much larger passive flux.
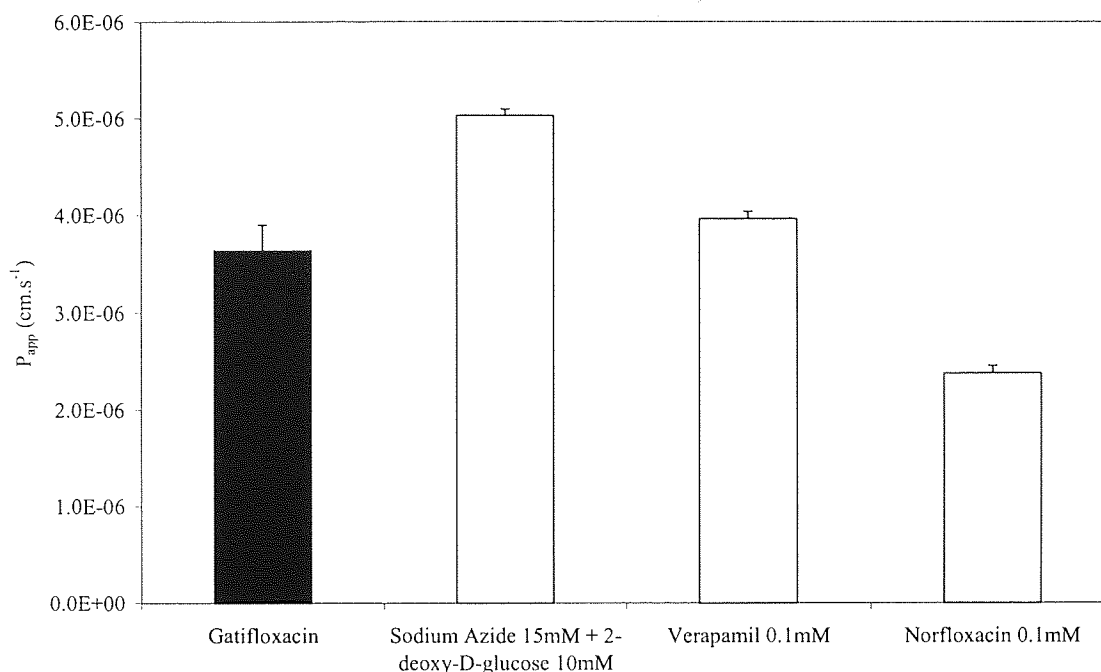
Figure 5.2 – The flux of gatifloxacin (10 µM) in apical-to-basolateral direction in the presence of a sodium azide (15 mM) and 2-deoxy-D-glucose (50 mM), verapamil (100 µM) and norfloxacin (100 µM). The cells were passage number 54, used between 21 and 28 days post seeding, TEER 611 ± 61 $\Omega.cm^2$. All transport studies were conducted in the apical-to-basolateral directions.

Mixed findings have been reported in the literature for the active apical-to-basolateral transport of quinolones. Rabbaa *et al*, (1997) used the rat intestinal model and found that the absorption of ofloxacin enantiomers appeared to involve active transport using an unknown transporter. Sasabe *et al.*, (1997) studied the hepatic uptake of quinolones using grepafloxacin and also found that the uptake of grepafloxacin within the liver was an active process. The uptake was estimated to be about 80 % *in vivo* during the first-pass through the liver. The uptake of grepafloxacin was temperature- and concentration-dependent and was substantially reduced in the presence of sodium azide. Sasabe *et al*, (1997) concluded that the hepatic uptake of grepafloxacin was by a sodium-independent, carrier-mediated, active transport system.

Cormet *et al.*, (1997a) showed that the uptake of sparfloxacin across Caco-2 cell brush-border membranes in the apical-to-basolateral direction does not require energy and occurs by both passive diffusion and non-specific binding as supported by kinetic and competition experiments. The uptake process was found to be insensitive to metabolic inhibitors and no inhibition was observed when the transport was carried out in the presence of competitors findings contradictory to those seen with this Caco-2 cell model.

5.3 BASOLATERAL-TO-APICAL FLUX

5.3.1 INTRODUCTION

Bi-directional fluxes of the quinolones had revealed that the basolateral-to-apical flux was significantly greater than the apical-to-basolateral flux for all the quinolones studied except BMS-284756-01 (the basolateral-to-apical flux of BMS-284756-01 was greater than the apical-to-basolateral, however it was not statistically significant; see section 4.3.5).

In humans, the quinolones show a significant level of faecal elimination, even after intravenous administration (Rabbaa *et al.*, 1996). This elimination could be due to gastrointestinal secretion or secretion into bile. However, substrates for the sodium-independent liver bile acid transporter were tested for their ability to inhibit ciprofloxacin secretion. Ciprofloxacin secretion was maintained in the presence of taurocholate and bromosulphophthalein indicating that biliary secretion was not a major contributor and it was thus possible that quinolone secretion was mediated by an unidentified multidrug resistance mechanism as discussed by Cavet *et al.*, (1997a) for ciprofloxacin secretion in Caco-2 cells. Clinical studies carried out with patients with renal failure demonstrated a less pronounced decrease in ciprofloxacin total clearance than could have been expected from creatinine clearance values. This suggests the existence of a compensatory mechanism for ciprofloxacin's renal elimination. The overall net intestinal clearance of ciprofloxacin in nephrectomised rats was significantly greater than in control groups. Renal failure did not alter the biliary excretion of ciprofloxacin, however, intestinal secretion was increased in a compensatory manner. The mechanism underlying the increased intestinal elimination of ciprofloxacin in renal failure was not identified (Dautrey *et al.*, 1999). In conclusion, an unknown intestinal transporter must exist which is able to compensate for the renal insufficiencies.

5.3.2 RESULTS AND DISCUSSION

5.3.2.1   METABOLIC INHIBITORS

A number of strategies can be used to determine whether an active secretion process is present. As stated earlier, most active processes rely on ATP as a source of energy, therefore, if cellular ATP is depleted, the active process cannot occur. Active transport involves the binding of specific substrates to membrane-located proteins. The energy can be supplied in two ways, one involves a coupled transport process whereby a second substrate is transported (symport or antiport) down its concentration gradient releasing energy (*e.g.* glucose and amino acid symport system with Na^+). The second is where the substrate binds to a transporter protein (pump), with energy being released from the hydrolysis of ATP. The transporter protein is then phosphorylated resulting in a conformational change in the pump bringing the active site with its ligand to the other side of the membrane and thus translocation into the cell (*e.g.* K^+ ATPase) (Karali *et al.*, 1989). Active transport processes are inhibitable by metabolic inhibitors, such as 2, 4-dinitrophenol (DNP) and sodium azide and require molecular oxygen. Substrate analogues of the transported compound can also inhibit transport by competing for the active site on the transporter. The temperature gradient is also higher than that for passive processes (Karali *et al.*, 1989).   Therefore any active secretion process dependent on energy in the form of ATP, is susceptible to metabolic inhibitors such as sodium azide and 2,4-dinitrophenol.

5.3.2.1.1   SODIUM AZIDE AND 2-DEOXY-D-GLUCOSE

The classical metabolic inhibitor sodium azide (15 mM) with 2-deoxy-D-glucose (50 mM) was used to observe effects on basolateral-to-apical efflux of gatifloxacin. Sodium azide acts to inhibit ATP by interfering with oxidative phosphorylation by inhibiting electron-flow in cytochrome oxidase, a key step in the ATP energy cycle (Stryer, 1988). The glycolytic pathway degrades glucose to generate ATP, therefore, the substitution of 2-deoxy-D-glucose for glucose prevents this from occurring.

This combination had a significant effect on inhibiting the basolateral-to-apical efflux of gatifloxacin 10 µM (P<0.005, see figure 5.3).
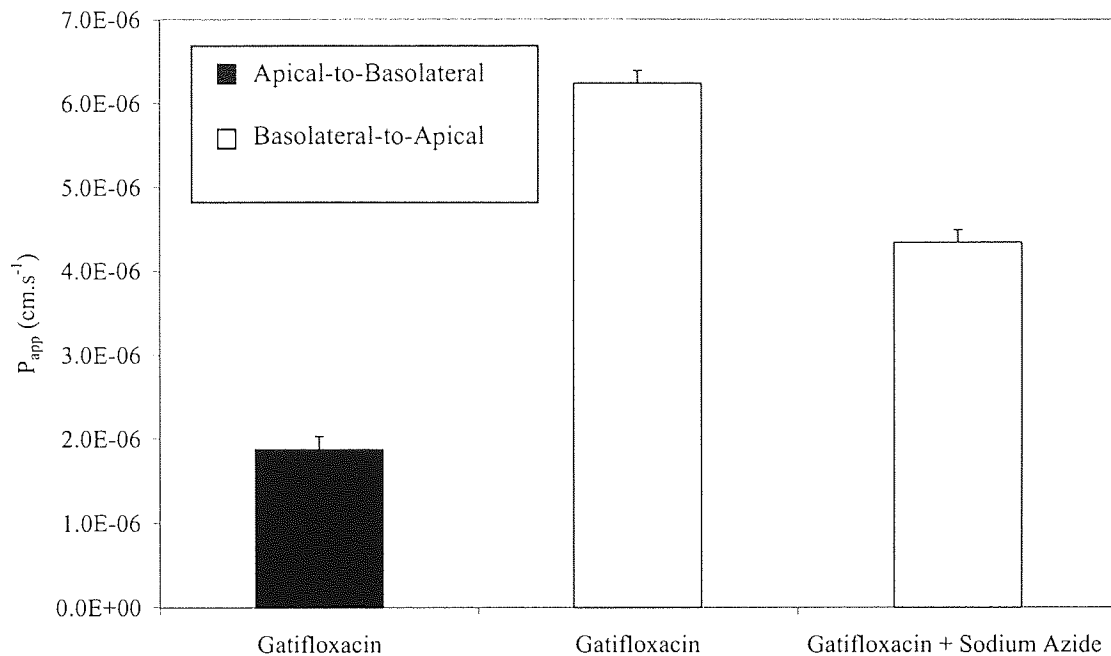
Figure 5.3 – The effects of sodium azide (15 mM) and 2-deoxy-D-glucuse (50 mM) on the basolateral-to-apical flux of gatifloxacin (10µM). The cells used were passage number 42, 21 to 28 days post seeding, n=3, TEER 781 ± 53 Ω.cm^2.

The combination of sodium azide (15 mM) with 2-deoxy-D-glucose (50 mM) caused a significant decrease in the basolateral-to-apical secretion of gatifloxacin (10 µM).

Griffiths *et al.*, (1993) also found that the net secretion of ciprofloxacin was abolished by the combination of sodium azide and 2-deoxy-D-glucose, implying a dependence upon cellular metabolism.

The present experiments conducted with gatifloxacin (10 µM), support these findings, in the presence of a combination of sodium azide and 2-deoxy-D-glucose, basolateral-to-apical flux was significantly reduced (P<0.005). Griffiths *et al.*, (1993) concluded that ciprofloxacin secretion was thus mediated by an active transport system, whether this represents a novel active secretion system of a yet unidentified physiological substrate remains to be elucidated. However, the basolateral-to-apical transport in this study was still greater than the apical-to-basolateral transport. This could result from an incomplete depletion of cellular energy stores.

5.3.2.1.2   2,4-DINITROPHENOL

The basolateral-to-apical transport studies carried out in the presence of sodium azide with 2-deoxy-D-glucose had led to a decrease in the basolateral-to-apical secretion of gatifloxacin (see section 5.3.2.1.1). However, this secretion was not completely abolished perhaps due to incomplete depletion of ATP. Therefore, in addition to sodium azide, the metabolic inhibitor 2,4-dinitrophenol (1 mM) was also investigated. This inhibitor uses a different mechanism to inhibit ATP, by uncoupling oxidative phosphorylation, it carries protons across the inner mitochondrial membrane, thereby, these protons are not available to ATPase and ATP is not formed (Stryer, 1988).

The inhibitory effects of 2,4-dinitrophenol were investigated on the basolateral-to-apical secretion of norfloxacin as well as of gatifloxacin. This would help to determine whether individual quinolones used different mechanisms of secretion, or whether the secretory mechanism could be used by a number of quinolones; that is, the secretion process maybe a class effect or else is limited to quinolones with close physicochemical properties.

The basolateral-to-apical flux of norfloxacin (10 μM) was significantly greater than the apical-to-basolateral flux ($P<0.0001$), indicating the presence of active secretion (see figure 5.4). With the addition of 2,4-dinitrophenol, the flux in the basolateral-to-apical direction was significantly reduced ($P<0.0001$). 2,4-Dinitrophenol had no significant effect on apical-to-basolateral flux ($P=0.438$, see figure 5.4).

These data demonstrate that the basolateral-to-apical flux for norfloxacin could be inhibited by 2,4-dinitrophenol. The effects of 2,4-dinitrophenol on gatifloxacin flux were then investigated to determine if a similar mechanism of transport was involved.

As found with norfloxacin, the basolateral-to-apical flux of gatifloxacin was significantly greater than the apical-to-basolateral flux ($P<0.001$, see figure 5.5). With the addition of 2,4-dinitrophenol, there was a slight reduction in the basolateral-to-apical flux of gatifloxacin which was not significant ($P=0.093$). As with norfloxacin, 2,4-dinitrophenol had no significant effect on the apical-to-basolateral flux of gatifloxacin ($P=0.815$; see figure 5.5).
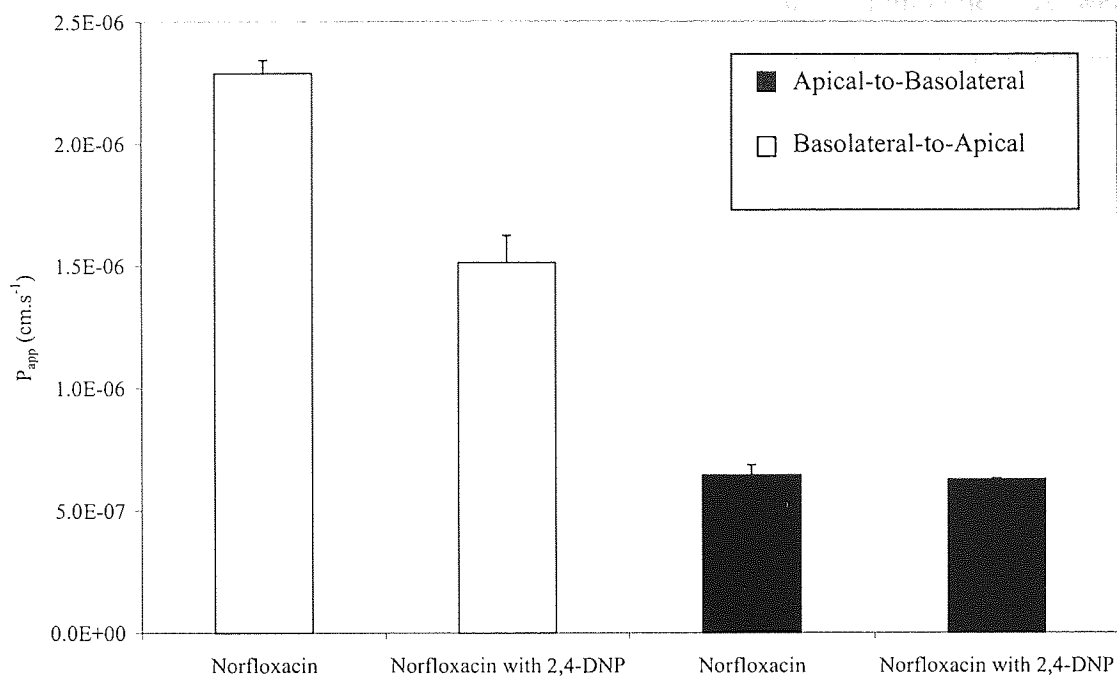
Figure 5.4 – The effects of 2,4-dinitrophenol (1 mM) on the apical-to-basolateral and basolateral-to-apical flux of norfloxacin (10 μM), the cells were passage number 45 and were used between 21 to 28 days post seeding, n=3, TEER 792 ± 122 $\Omega.cm^2$.
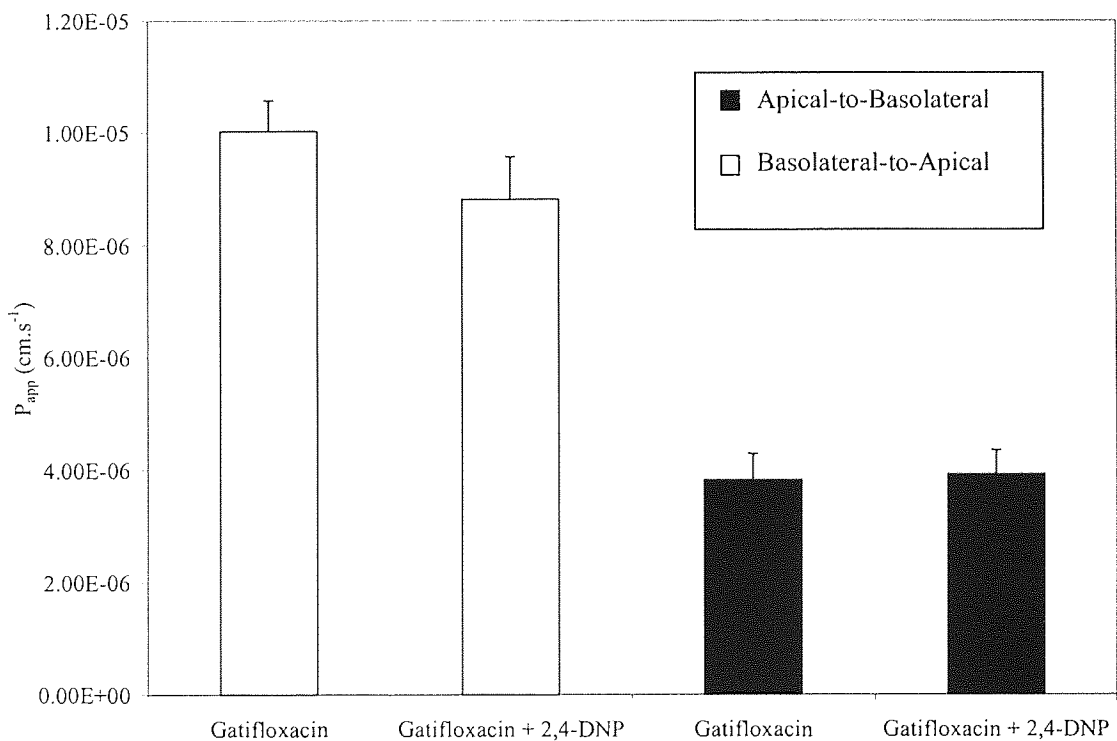
Figure 5.5 – The effects of 2,4-dinitrophenol (1 mM) on the apical-to-basolateral and basolateral-to-apical flux of gatifloxacin (10 μM), the cells were passage number 59 and were used between 21 to 28 days post seeding, n=3, TEER 813 ± 45 $\Omega.cm^2$.

The effects of 2,4-dinitrophenol (1 mM) on the inhibition of quinolone flux were investigated using norfloxacin (10 μM) and gatifloxacin (10 μM). 2,4-Dinitrophenol had no effect on the apical-to-basolateral flux of either quinolone. However, it did have a reducing effect on basolateral-to-apical flux of gatifloxacin and a significant effect on norfloxacin flux. The different levels of inhibition could be due to different levels of passive transcellular flux or different affinities for the transporter involved. The greater basolateral-to-apical transport than the apical-to-basolateral transport even in the presence of 2,4-dinitrophenol could result from the presence of more than one mechanism involved in the basolateral-to-apical transport of the quinolones. The 2,4-dinitrophenol could be knocking out the ATP-energy-dependent component however another mechanism may still be active.

Cormet-Boyaka *et al.*, (1998) also found that ATP depletion did not entirely inhibit basolateral-to-apical secretion of quinolones-as found here with 2,4-dinitrophenol on norfloxacin and gatifloxacin secretion. This lack of complete inhibition of the basolateral-to-apical secretion could result from the incomplete depletion of ATP using 2,4-dinitrophenol (Cormet-Boyaka *et al.*, 1998).

The metabolic inhibitors sodium azide with 2-deoxy-D-glucose and 2,4-dinitrophenol were able to decrease basolateral-to-apical secretion of gatifloxacin and norfloxacin to various degrees (see section 5.3.2.1.1 and 5.3.2.1.2). In conclusion, there is an unknown mechanism present in the Caco-2 cells which is affected by compounds which deplete cellular stores of ATP. The depletion does not lead to a complete cessation of the basolateral-to-apical secretion. This could result from incomplete abolishment of cellular energy stores or the quinolones could be using a combination of transport mechanisms in the basolateral-to-apical direction, such as passive transcellular as well as facilitated transport mechanism which may or may not be dependent on ATP.

5.3.2.2   EFFECT OF TEMPERATURE ON TRANSPORT

The secretion of quinolones could not be completely inhibited using the metabolic inhibitors therefore another approach was investigated. Temperature also has a role to

play in energy-dependent processes and, at a reduced temperature, active transport processes can be inhibited.

A number of authors (Cogburn *et al.*, 1991; Inui, 1992) have mentioned that a reduction in temperature to 4°C will result in the abolishment of active mechanisms. However, it is not entirely clear whether this is because of a reduction in the fluidity of the cellular membrane or inhibition of the active secretion mechanism.

5.3.2.2.1 GATIFLOXACIN FLUX AT 2°C AND 37°C

The effects of reducing the temperature for gatifloxacin (10 μM) transport over 40 minutes through Caco-2 cells was observed. There was a significant decrease in flux in both apical-to-basolateral and basolateral-to-apical directions as temperature was reduced from 37°C to 2°C (see figure 5.6).

The reduction in temperature from 37°C to 2°C had a significant effect on both apical-to-basolateral and basolateral-to-apical flux of gatifloxacin (10μM). However, the basolateral-to-apical flux was higher than the apical-to-basolateral, transport event at 2°C. The basolateral-to-apical P_{app} at 2°C for gatifloxacin was $5.81 \times 10^{-8} \pm 2.29 \times 10^{-9}$ $cm.s^{-1}$ while the apical-to-basolateral P_{app} was $2.43 \times 10^{-8} \pm 6.23 \times 10^{-10}$ $cm.s^{-1}$. It was interesting to observe that the ratio of basolateral-to-apical to apical-to-basolateral flux was similar for both temperatures (see table 5.1).

Cormet *et al.*, (1997b), found that the uptake of sparfloxacin by Caco-2 cells monolayers at 4°C was very slow and did not reach a plateau during the 60 minutes during which the experiment was run.

At 2°C, the transport of gatifloxacin was reduced substantially (80-fold). However, the basolateral-to-apical transport was significantly greater than the apical-to-basolateral transport. Although, at this reduced temperature, energy-dependent processes should have been retarded, this may not have occurred or the passive transport in the basolateral-to-apical direction was greater than in the apical-to-basolateral direction due to the morphological differences at each cellular surface. In order to better understand

the processes involved in the bi-directional transport of gatifloxacin at 2°C, a comparison was required using compounds which did not undergo active transport, *i.e.* D-[1-^{14}C]mannitol and [^{3}H]testosterone..
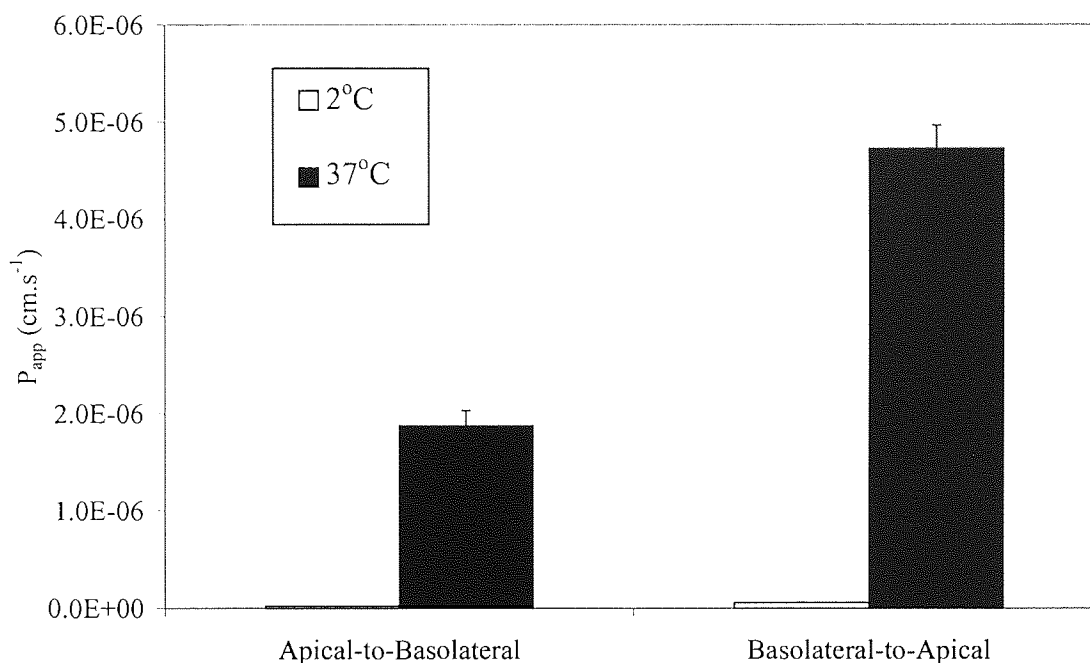
Figure 5.6 – The apical-to-basolateral and basolateral-to-apical flux of gatifloxacin at 2°C and 37°C. The cells were passage number 42 used 21 to 28 days post seeding, n=3, TEER 620 ± 76 Ω.cm^{2}.

5.3.2.2 [^{3}H]TESTOSTERONE AND D-[1-^{14}C]MANNITOL FLUX AT 2°C AND 37°C

The effects of change in temperature on gatifloxacin flux were compared with those of two other compounds. D-[1-^{14}C]Mannitol, the classical passively transported paracellular marker (Artursson *et al.*, 1993) and [^{3}H]testosterone a compound which undergoes passive transcellular transport (Nicklin *et al.*, 1992), were used to observe the effects of a change in temperature on paracellular and passive transcellular pathways.

The permeability of [^{3}H]testosterone (2 nM) at two different temperatures of 37°C and 2°C showed no significant difference in basolateral-to-apical and apical-to-basolateral flux at either temperature (figure 5.7), indicating transport occurred by passive means in both directions. However, when the temperature was reduced from 37°C to 2°C there was almost a 50 % drop in permeability in both directions. [^{3}H]Testosterone is a highly lipophilic molecule, which uses the transcellular route to traverse the cellular

membrane. As temperature was reduced the membrane permeability decreased because it became less fluid (Cogburn *et al.*, 1991). Cormet *et al.*, (1997a) noted that a decrease in sparfloxacin diffusion induced by a reduction of membrane fluidity related to phase transitions of lipid bilayers occurring in the range 10-30°C. The transport of [^{3}H]testosterone is largely controlled by the UWL and the viscosity of this layer at the reduced temperature could have a significant effect on the transport of [^{3}H]testosterone.
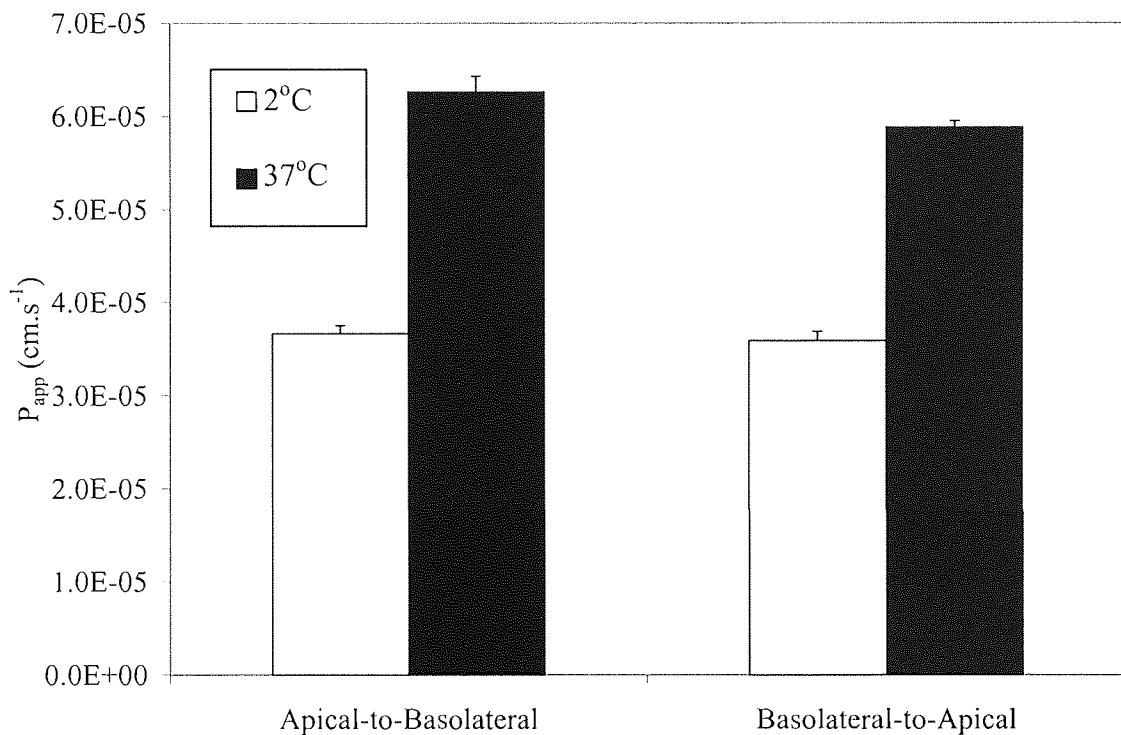
Figure 5.7 – **The permeation of [^{3}H]testosterone at 37°C and 2°C through Caco-2 cells, apical-to-basolateral and basolateral-to-apical directions. The cells were passage number 61 used 21 to 28 days post seeding, n=3, TEER 731 ± 36 Ω.cm^2.**

Cogburn *et al.*, (1991), found that compounds undergoing passive paracellular transport (fluorescein isothiocyanate, FITC showed a 2-fold decrease) were least sensitive to a reduction in temperature. However, compounds undergoing carrier-mediated transport (glucose showed a 10-fold decrease) showed the greatest changes in transport with changes in temperature and compounds undergoing passive transcellular transport (propranolol showed a 5-fold decrease) were affected to intermediate levels (Cogburn *et al.*, 1991).

Hidalgo *et al.*, (1989) assessed the effects of reduction of temperature to 4°C on the apical-to-basolateral transport of various compounds. The transport of the paracellular marker [^{14}C]inulin dropped below detectable levels at 4°C.

The permeability of D-[1-^{14}C]mannitol, the paracellular marker, through Caco-2 cells at 2°C and 37°C was also measured in apical-to-basolateral and basolateral-to-apical directions. As seen with [^{3}H]testosterone, there was a drop in cellular permeability at the lower temperature (see figure 5.8).
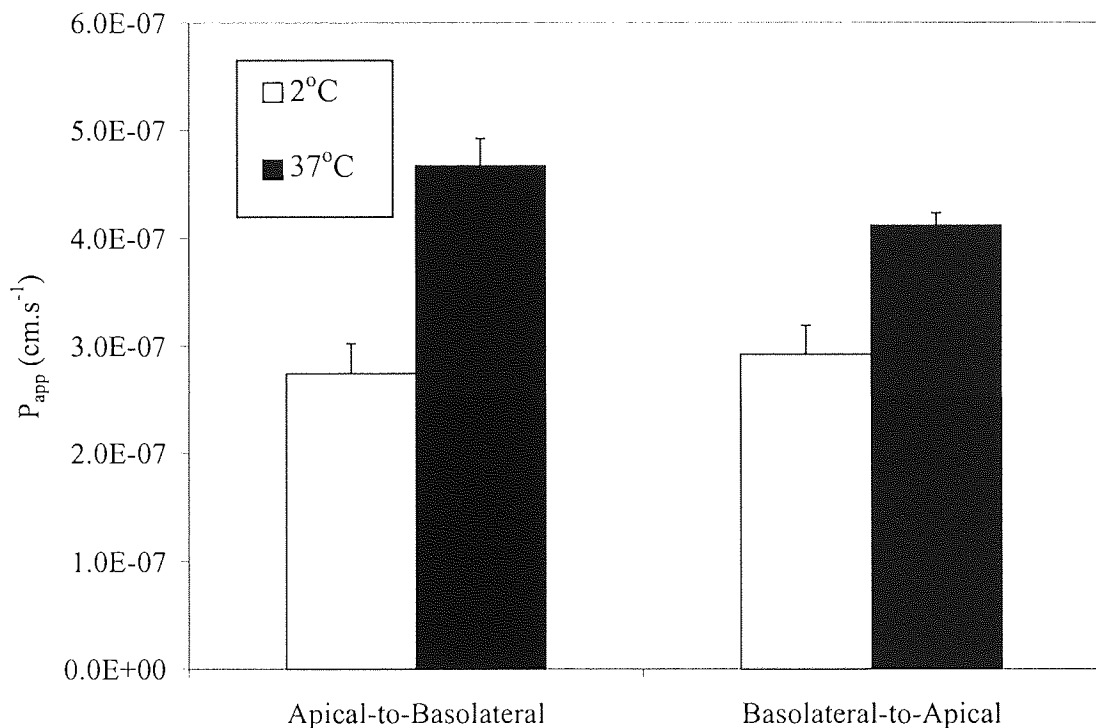
Figure 5.8 – The permeability of D-[1-^{14}C]mannitol (10 µM) in both apical-to-basolateral and basolateral-to-apical direction in Caco-2 cells passage number 61, used 21 to 28 days post seeding, n=3 TEER 731 ± 36 Ω.cm^{2}.

Transport of D-[1-^{14}C]mannitol at the reduced temperature should have been affected to a lesser extent than that seen with [^{3}H]testosterone. This is because the paracellular route would be less vulnerable to changes in temperature, unlike the transcellular route where, the fluidity of the membrane would decrease as temperature decreases. However, the reduction in the transport of both compounds at the reduced temperature was similar (table 5.1).

A large decrease in transport was observed as the temperature was reduced from 37°C to 2°C (80-fold) for gatifloxacin. This decrease was significantly larger than that observed for D-[1-^{14}C]mannitol and [^{3}H]testosterone. Therefore a different mechanism may be involved to that seen with D-[1-^{14}C]mannitol and [^{3}H]testosterone. At the reduced temperature the transcellular route may not be available to gatifloxacin leaving only the less favourable paracellular route.

The decrease in the transport of the transcellular marker [^{3}H]testosterone was not as high as expected. Since this compound is highly lipophilic with a logP of 3.32, the decrease in temperature from 37°C to 2°C should have had a similar reduction in transport as observed with gatifloxacin. A possible explanation for the lack of the substantial decrease could be that the logP of [^{3}H]testosterone is so high to begin with that it is beyond the optimal logP for transcellular transport *i.e.* it is on the downward slope of the logP versus permeability graph.

Based on the data obtained from the temperature experiments the following conclusions can be drawn. The permeability of both D-[1-^{14}C]mannitol and [^{3}H]testosterone in apical-to-basolateral and basolateral-to-apical directions was similar indicating that both compounds use passive routes of transport, the apical-to-basolateral/basolateral-to-apical ratios at 2°C and 37°C were close to unity. The very much lower permeability P_{app} for D-[1-^{14}C]mannitol suggest it uses the paracellular route this was consistent with its physicochemical properties; molecular weight of 180 kDa and low lipophilicity. The high P_{app} for [^{3}H]testosterone and its high molecular weight of 288.4 indicate that this compound utilises the passive transcellular route for transport.

Although transport in both directions decreases for D-[1-^{14}C]mannitol and [^{3}H]testosterone as temperature was reduced from 37°C to 2°C, the ratio of flux was almost unity (see table 5.1). The decrease in apical-to-basolateral flux was not significantly different from the decrease in basolateral-to-apical as temperature was reduced for D-[1-^{14}C]mannitol (P=0.100), this was the same for [^{3}H]testosterone (P=0.201). For both compounds transport was decreased by a factor of 1.4 to 1.71 with the reduction in temperature.

	Flux (Apical-to-basolateral/basolateral-to-apical)				Flux (37°C/2°C)			
	2°C	SD	37°C	SD	A-B	SD	B-A	SD
Gatifloxacin	0.418	0.0197	0.397	0.0385	77.414	6.7606	81.435	5.1646
D-[1-¹⁴C]Mannitol	0.940	0.1288	1.135	0.0688	1.703	0.1949	1.410	0.1363
[³H]testosterone	1.022	0.0372	1.065	0.0307	1.709	0.0607	1.640	0.0491

Table 5.1 – Various ratios calculated from gatifloxacin, D-[1-14C]mannitol and [3H]testosterone transport at 2°C and 37°C.

With gatifloxacin, a different story emerges. It has been established that the basolateral-to-apical transport of gatifloxacin contains an active component (see section 4.3.5). This active component also seems to be present at reduced temperatures, this was because the ratio of apical-to-basolateral/basolateral-to-apical at 2°C and 37°C was similar (P=0.448).

There are a number of possible explanations for the discrepancies observed for gatifloxacin flux at 37°C and 2°C. Firstly as temperature was reduced the transcellular route may no longer be available to gatifloxacin, due to the decrease in membrane fluidity. The routes available for transport may be just the passive paracellular route and the active secretory mechanism in the basolateral-to-apical direction. This would result in a very small flux in apical-to-basolateral and basolateral-to-apical directions, with the basolateral-to-apical flux being greater than the apical-to-basolateral flux, because of the presence of the additional secretory mechanism. Although active transporters such as the di-tri-peptide transporter are inhibited at reduced temperatures the effects on efflux mechanisms such as PgP are not known.

The data from gatifloxacin transport indicated that an active transporter must be involved. To characterise this transporter, information on the affinity of quinolones for it was sought.

5.3.2.3   EFFECT OF CONCENTRATION ON TRANSPORT

Active transport mechanisms such as PgP and the di-tri-peptide transporter may be affected by the concentration of substrate present (see section 1.6). With low concentrations of substrate, these active mechanisms can have significant effects; with higher concentrations passive diffusion will mask any active secretion mechanism. Butyl-ciprofloxacin showed a polarised transport, with the basolateral-to-apical transport being significantly greater than the apical-to-basolateral transport (see section 4.3.5). This higher basolateral-to-apical transport was seen for butyl-ciprofloxacin at a concentration of 10 µM. Therefore, the effects on basolateral-to-apical transport of butyl-ciprofloxacin in the concentration range 1 µM to 10 µM were investigated. Butyl-ciprofloxacin was used because it provided enough sensitivity on the HPLC

system (see section 2.8) to be detectable at concentrations lower than 10 μM in the donor phase.

Despite the appearance of polarised transport at 10 μM, there was no concentration-dependence at lower concentrations. As concentration of the quinolone increased in the basolateral compartment the rate of transport increased in a linear fashion, which was indicative of a passive process (see figure 5.9). If an active process had been present, then two components would have been visible, the graph would have shown the active component at the lower concentrations as a non-linear relationship between rate and concentration. As concentration increased a linear relationship would then be present, as the active transport mechanism becomes saturated (see section 1.6).

Since butyl-ciprofloxacin did not provide the affinity for the transporter, the experiment was repeated using gatifloxacin; the concentration range was changed to 5 μM to 3 mM as used by Cavet *et al.*, (1997a) for ciprofloxacin. The rationale for increasing the concentration range was that, these quinolones may have a very low affinity for the transporter involved in basolateral-to-apical flux. Gatifloxacin has a lower logP than butyl-ciprofloxacin therefore the passive transcellular transport for this quinolone should be less than that for butyl-ciprofloxacin. This lower passive transport should help to show any active transport present. However, as with butyl-ciprofloxacin linear concentration dependent transport was observed (figure 5.10), indicating that an active saturable mechanism was not present.

The two different quinolones, butyl-ciprofloxacin and gatifloxacin were used to investigate the capacity of a potential transporter. These two quinolones were at the different ends of physicochemical properties. Gatifloxacin has a logP of −0.373 and a molecular weight of 375.4 while butyl-ciprofloxacin has a logP of 1.693 and a molecular weight of 387.45.

Both compounds also showed basolateral-to-apical flux to be greater than apical-to-basolateral flux. However, affinity for a potential transporter for butyl-ciprofloxacin and gatifloxacin could not demonstrated. Based on these findings alone it appears that there was no active transport mechanism involved. However, earlier findings clearly

indicate that the basolateral-to-apical flux for a number of quinolones was greater than the apical-to-basolateral flux (see section 4.3.5).
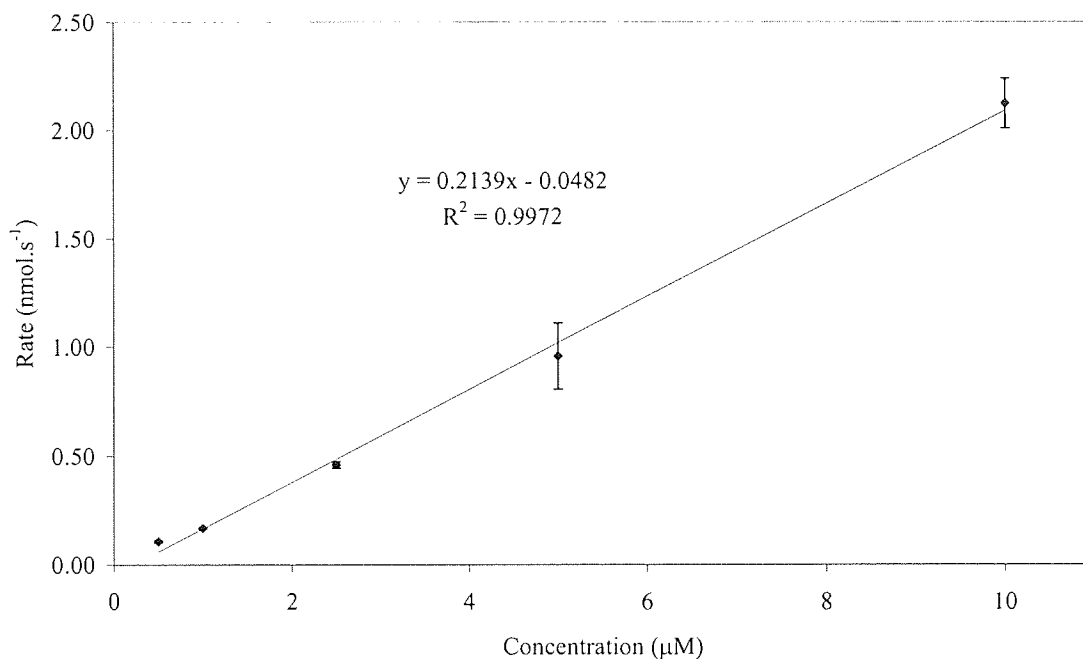
Figure 5.9 – Transport of butyl-ciprofloxacin basolateral-to-apical at different concentrations from 1 µM to 10 µM. The cells were passage 74 to 75, 21 to 28 days post seeding, n=3, TEER 398 ± 24 Ω.Cm².

Jaehde *et al.*, (1993) found that the permeability of ciprofloxacin across the blood-brain-barrier was independent of concentration and therefore it appeared that there was no saturable transport process involved. Our data using butyl-ciprofloxacin and gatifloxacin have produced similar results for basolateral-to-apical flux. However, this result is in direct contradiction of findings by other groups such as Cavet *et al*, (1997a) and Cormet *et al*, (1997a). A possible explanation for this observation is that the passive transport processes could have swamped the active component, (see equation 1.5). The term $K_d.C_d$ which describes the passive component could be significantly larger than the active component (see equation 1.4).
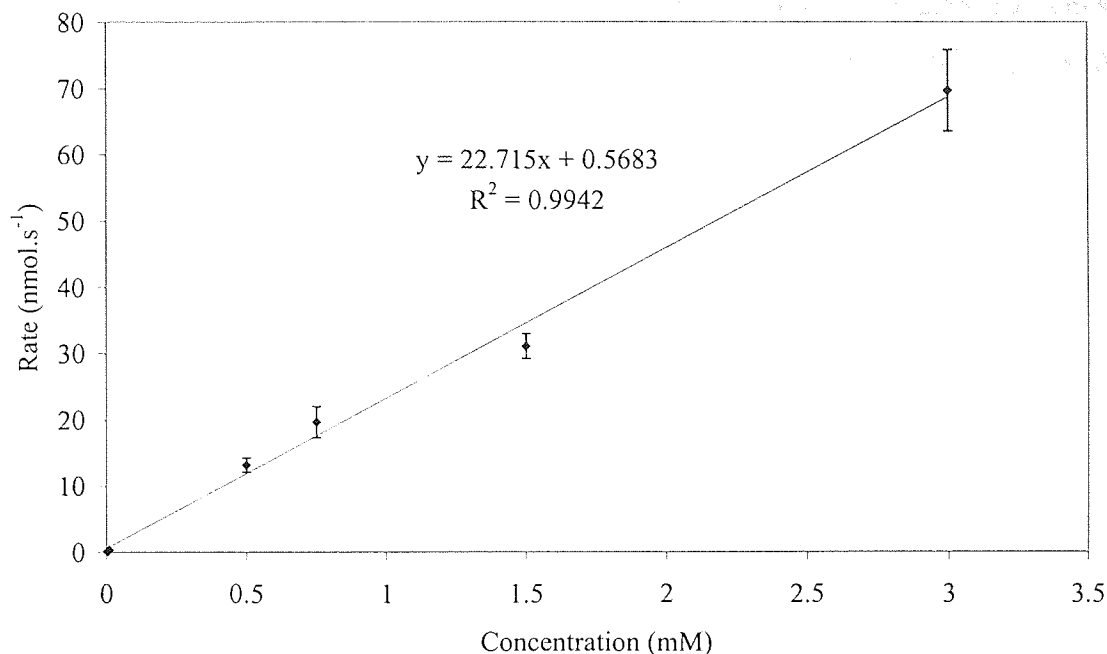
Figure 5.10 - The permeability of gatifloxacin basolateral-to-apical at concentrations from 5 µM to 3 mM. The cell were passage 50 to 51, 21 to 28 days post seeding n=3, TEER 686 ± 35 Ω.cm^2.

5.3.2.4   COMPETITION STUDIES WITH OTHER QUINOLONES

The affinity of the basolateral-to-apical secretory mechanism for two model quinolones butyl-ciprofloxacin and gatifloxacin had not be determined in the previous section. However, as earlier evidence supports the existence of an active mechanism, the next logical step would be to investigate the specificity of the transporter and determine if quinolones would compete with each other for it.

The flux of gatifloxacin was investigated in the presence of competing quinolones, which were ofloxacin, norfloxacin and ciprofloxacin. All four quinolones have relatively low lipophilicities with logP values, ciprofloxacin –0.416, ofloxacin 0.051, norfloxacin –0.118 and gatifloxacin –0.373, they also have similar pK_as (see section 3.2.3). These quinolones were chosen because they did not interfere with the HPLC analysis of gatifloxacin.

The basolateral-to-apical flux of gatifloxacin (10 μM) was $4.8 \times 10^{-6} \pm 2.58 \times 10^{-7}$ cm.s^{-1} and in the presence of ofloxacin (100 μM) this was reduced to $4.01 \times 10^{-6} \pm 1.73 \times 10^{-7}$ cm.s^{-1}.

Ofloxacin (100 μM) had a significant inhibitory effect (over 15 %) on the basolateral-to-apical flux of gatifloxacin (P=0.012). To verify the inhibitory effect of competition of ofloxacin with gatifloxacin, the effects of norfloxacin on the basolateral-to-apical secretion of gatifloxacin were investigated.

The transport of gatifloxacin in the basolateral-to-apical direction in the absence of norfloxacin was $4.23 \times 10^{-6} \pm 6.4 \times 10^{-8}$ cm.s^{-1}, while in the presence of norfloxacin (100 μM) this was reduced to $3.56 \times 10^{-6} \pm 1.78 \times 10^{-7}$ cm.s^{-1}. A concentration of norfloxacin (100 μM) caused a decrease in basolateral-to-apical flux of 10 μM of gatifloxacin, this decrease (approximately 15.8 %) in basolateral-to-apical flux was statistically significant (P=0.003).

The effects of norfloxacin, ciprofloxacin and ofloxacin competing with the basolateral-to-apical flux of gatifloxacin were investigated further by increasing the concentration of the competing quinolone. This was carried out to determine if the small levels of inhibition observed were a concentration-dependent phenomenon.

Norfloxacin (100 μM) had a significant inhibitory effect on the basolateral-to-apical flux of gatifloxacin (10 μM, P=0.016), norfloxacin (300 μM) although, still showing inhibition, did not have a significant effect (P=0.170, see figure 5.11). The reduced effect of the 300 μM concentration could be due to toxicity effects of the quinolones. However, concentrations higher than these have previously been used in the literature (Cormet *et al.*, 1997a).

The affects of ciprofloxacin were also explored on the inhibition of the basolateral-to-apical flux of gatifloxacin. At both 100 μM and 300 μM, ciprofloxacin had no significant effect on gatifloxacin basolateral-to-apical flux (P=0.172 for 100 μM and P= 0.198 for 300 μM respectively, see figure 5.12).
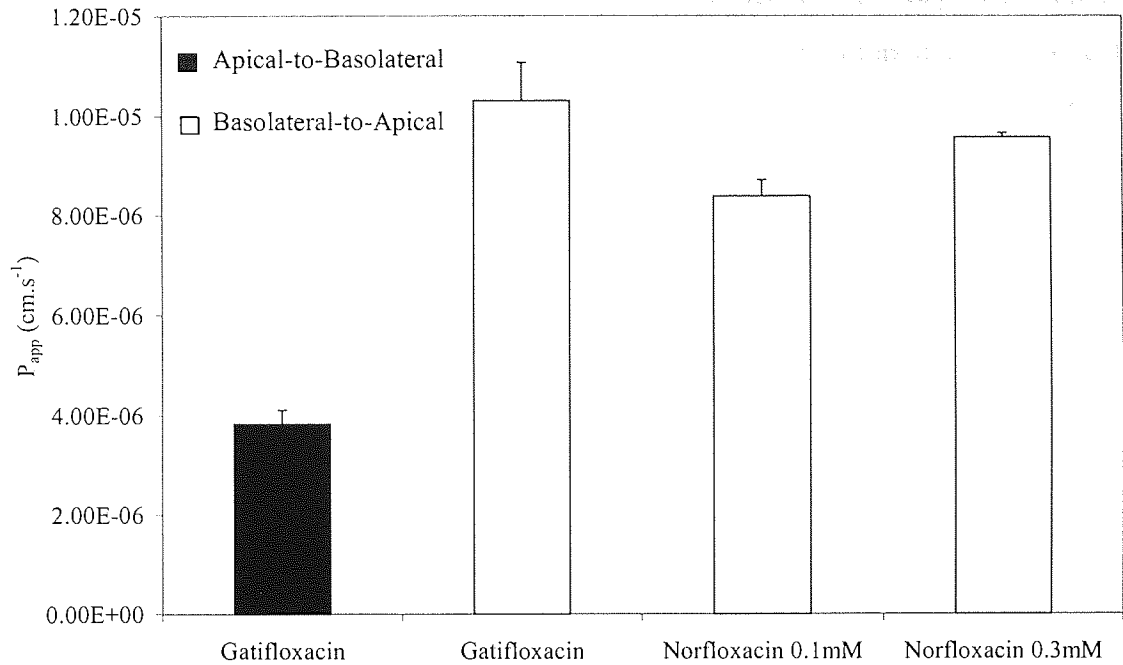
Figure 5.11 – The effects of norfloxacin (100 μM and 300 μM) flux on the basolateral-to-apical flux of gatifloxacin (10 μM). The cells were passage number 62, used between 21 to 28 days post seeding, n=3, TEER 754 ± 46 Ω.cm^2.
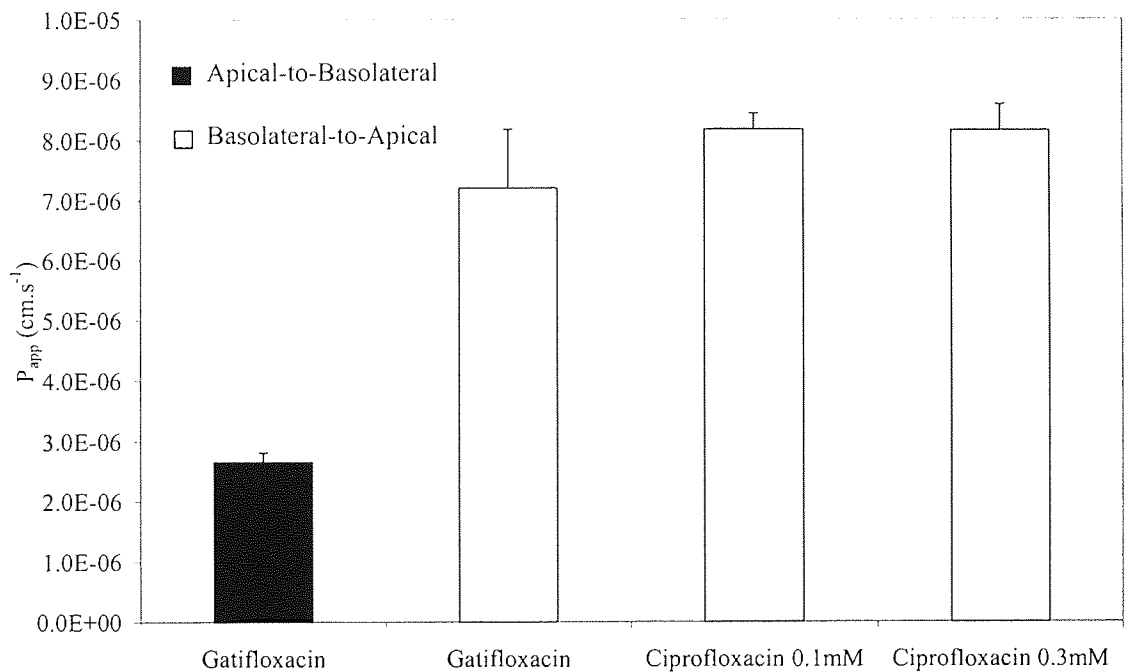
Figure 5.12 – The flux of gatifloxacin (10 μM) in the presence and absence of ciprofloxacin at concentration of (100 μM and 300 μM), the cells were passage number 65, used between 21 to 28 days post seeding, n=3, TEER 687 ± 37 Ω.cm^2.

Ofloxacin and norfloxacin (100 µM) both had a significant inhibitory effect on the basolateral-to-apical flux of gatifloxacin. However, neither compound was able to reduce basolateral-to-apical flux sufficiently to mirror apical-to-basolateral transport. At a higher concentration, norfloxacin 300 µM did not have a significant effect, neither did ciprofloxacin at 100 µM and 300 µM concentrations (see table 5.2).

Quinolone	% Inhibition of Gatifloxacin secretion	SD
Ofloxacin 100 µM	16.548	5.753
Norfloxacin 100 µM	18.669	1.557
Norfloxacin 300 µM	7.209	0.536
Ciprofloxacin 100 µM	-13.492	1.880
Ciprofloxacin 300 µM	-13.228	1.924

Table 5.2 – Percentage inhibition caused by competing quinolones.

Based on the results obtained from the competition studies for gatifloxacin with ofloxacin, norfloxacin and ciprofloxacin, a rank-order for the competing quinolones can be determined. Norfloxacin, followed by ofloxacin, caused the highest level of inhibition with ciprofloxacin having a surprising increase in basolateral-to-apical flux. Therefore, norfloxacin probably has a higher affinity for the putative transporter followed by ofloxacin while ciprofloxacin has the lowest (see table 5.2). The work in the previous section (section 5.3.2.3) was unable to find an active component in the basolateral-to-apical flux of gatifloxacin in the concentration range 5 µM to 3 mM. However, these experiments suggest that other quinolones are able to compete with gatifloxacin for basolateral-to-apical transport. This competition could not be proved to be concentration-dependent. Therefore, two possible conclusions could be drawn, firstly there is an active transport mechanism present which is sensitive to cross-competition between quinolones. Secondly some other physicochemical interaction occurs between the quinolones which results in the decreased transport.

Hunter and Hirst, (1997), found that a number of quinolones were capable of inhibition of both net secretions of ciprofloxacin and cellular accumulation across the basolateral cell surface. Cross-competition studies suggest that quinolones may compete for a

common carrier at the basolateral membrane. It was likely that the mechanism of transepithelial secretion involved a common accumulative transport at the basal membrane, followed by facilitated exit across the apical membrane (Hunter and Hirst, 1997).

Griffiths *et al.*, (1994), reported that ciprofloxacin and norfloxacin showed some degree of cross-competition indicating that a common secretory mechanism was present in the basolateral membranes. Varying degrees of competitive inhibition of ciprofloxacin (10 μM) basolateral-to-apical flux was seen with the addition of non-radiolabelled ciprofloxacin, as well as with other quinolones (Griffiths *et al.*, 1993).

Ito *et al.*, (1999), also observed that the flux of grepafloxacin and non-radiolabelled levofloxacin also decreased the flux of levofloxacin. Non-radiolabelled levofloxacin caused a concentration-dependent (100 μM to 500 μM) inhibition of radiolabelled levofloxacin flux from 20 to 50 %. Levofloxacin was actively secreted into urine in the isolated perfused rat kidney. The decrease in secretion of levofloxacin was caused by selective inhibition of the transport from cells to the lumen across the brush-border membrane (Ito *et al.*, 2000).

A number of groups have looked for competition between quinolones, using competition of the radiolabelled against the free compound or a with a different quinolone and have reported competition occurring, even if the identity of the mechanism involved could not be identified (Griffiths *et al.*, 1994; Cormet-Boyaka *et al.*, 1998).

The evidence so far points towards an active secretion mechanism which is affected, to some degree, by depletion of ATP and shows cross-competition with quinolones.

5.3.2.5   IONIC INHIBITORS

Results from section 5.3.2.4 have shown that competition occurred between quinolones for the basolateral-to-apical secretory process. The next step was to investigate which compounds are able to inhibit the mechanism involved in the secretion. Since the

quinolones are zwitterionic, they can potentially be transported by mechanisms involved in the transport of anions or cations or even both. Therefore compounds which inhibit ionic secretion were investigated.

The renal anion and cation transport systems are H^+-dependent organic antiport systems which would not be affected by the cellular depletion of ATP (Matsuo *et al.*, 1998). Organic ions are actively secreted into urine *via* the organic anion and or cation transport systems present in the proximal tubules therefore it would be logical to assess the effects of organic anion competition on quinolone flux to see if these transporters are implicated in the processes observed here.

It was postulated that the renal secretion of ciprofloxacin and other quinolones involves transport primarily *via* the renal organic anion transporter (Cavet *et al.*, 1997a; Yano *et al.*, 1997). Substrates of the renal transporters include cimetidine, probenecid and tetraethylammonium chloride. The apparent K_m for levofloxacin and grepafloxacin in the absence of any inhibitors in rat renal cortical slices were 13.9 and 6.2 mM respectively (Ito *et al.*, 1999). It is also known that ciprofloxacin may interact with the basolateral renal organic cation transporter; thus, ciprofloxacin may act as a bisubstrate for both organic anion and cation transporters, as it is a zwitterion (Cavet *et al.*, 1997a). At physiological pH, over 80 % of both ciprofloxacin and gatifloxacin are in the overall ionised species, with less than 20 % as the zwitterion (Ito *et al.*, 1999).

5.3.2.5.1 PROBENECID AS AN INHIBITOR OF EFFLUX

There are a number of classical inhibitors that would interfere with as anionic transporters. Probenecid (100 µM, see figure 5.13) is known to be an inhibitor of the anion transporter, it has a logP of 3.21. Probenecid was used because it is postulated by Jaehde *et al.* (1995) and Cao *et al.* (1992) that the quinolones may use the anion transporter, similar to the one found renally for the secretion of the quinolones. The affect of this compound was investigated on the basolateral-to-apical flux of ciprofloxacin and gatifloxacin.
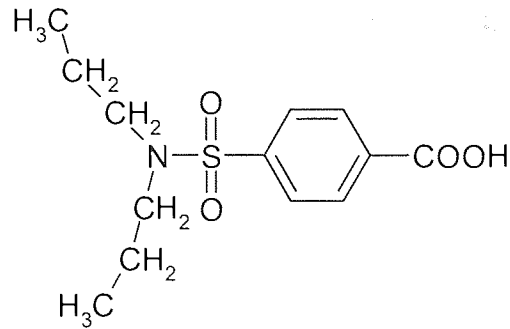
Figure 5.13 - Structure of probenecid

With the addition of probenecid (100 μM) to the transport experiments, the basolateral-to-apical flux of ciprofloxacin was significantly reduced (P=0.039 unpaired t-test). However, it is not entirely reduced to the apical-to-basolateral level of flux for ciprofloxacin (see figure 5.14).

Figure 5.14 – **The permeation of ciprofloxacin through Caco-2 cells apical-to-basolateral and basolateral-to-apical, as well as basolateral-to-apical transport in the presence of (100 μM) probenecid. Transport studies were performed on cells with a passage number 30, 21 to 28 days post seeding, n=3, TEER 764 ± 31 Ω.cm^2.**

To see if this interaction is a general property of quinolones, the effects of probenecid on gatifloxacin (10 μM) flux was assessed. Probenecid at two concentrations (100 μM and 500 μM) was used to observe the effect on the basolateral-to-apical flux of

gatifloxacin (10 μM). Previously, it had been shown that, like ciprofloxacin, the basolateral-to-apical flux of gatifloxacin was greater than the apical-to-basolateral flux (see section 4.3.5) as also shown in figure 5.15.

In contrast to ciprofloxacin, probenecid (100 μM) does not have any effects on the basolateral-to-apical flux of gatifloxacin (10 μM). However, probenecid (500 μM) had a significant inhibitory effect (P<0.001). The lack of probenecid (100 μM) having effect on the basolateral-to-apical flux could be due to differences in affinity for a potential transporter between ciprofloxacin and gatifloxacin, with gatifloxacin having a higher affinity for the transporter than ciprofloxacin. This area within the literature has a number of conflicting findings. However, it must be remembered a range of different models were used for much of this work. Cavet *et al.*, (1997a) had found that probenecid had no significant effect on the secretion of ciprofloxacin *in vitro*, a finding contradictory to that observed with this Caco-2 cell model.
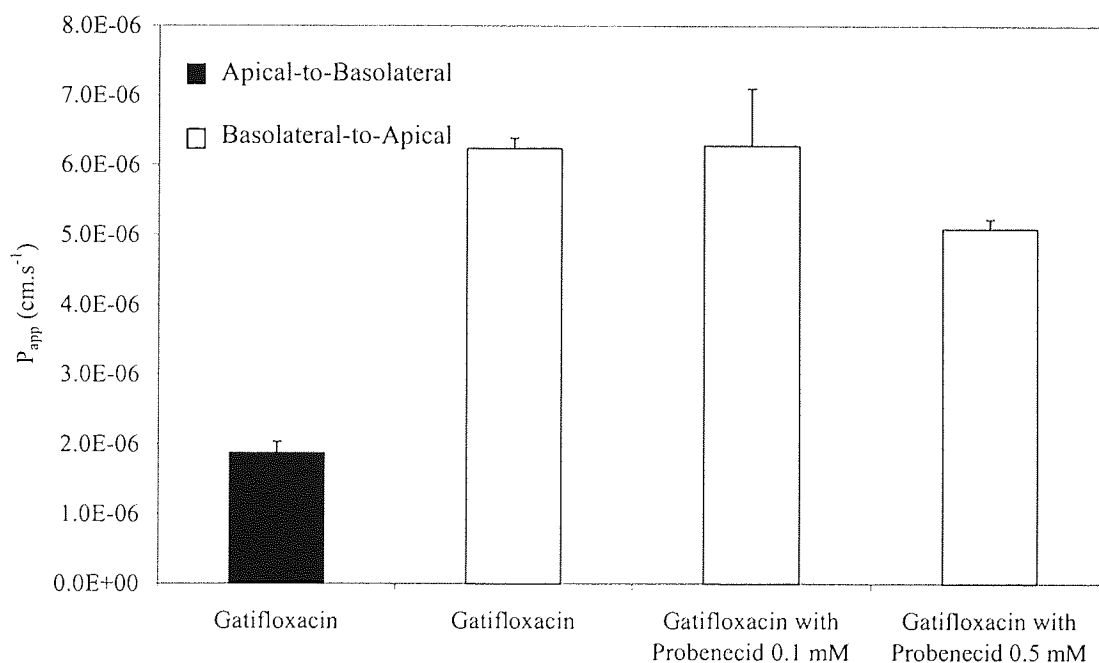
Figure 5.15 – The effects of probenecid (100 μM and 500 μM) on the basolateral-to-apical flux of gatifloxacin. Gatifloxacin (10 μM) apical-to-basolateral flux is included for comparison. The cells used were passage number 42, 21 to 28 days post seeding, n=3, TEER 840 ± 50 $\Omega.cm^2$.

Rabbaa *et al.*, (1996) found that, in rats, lomefloxacin was significantly secreted by the intestine and this was not reduced by probenecid, a substrate of the anionic transporter.

Cavet *et al.*, (1997a) also observed that the substrates of the three renal basolateral organic anion transport systems, sulphate, oxalate and thiosulphate at (10 mM) did not decrease ciprofloxacin secretion either.

Ooie *et al*, (1997) investigated the transport of fleroxacin across the blood-CSF barrier and showed that there appears to be an active transport of the quinolones from the CSF into the brain *via* the blood-CSF barrier. The quinolones were transported by the isolated choroid plexus *via* an organic anion transport system that was responsible for the efflux of β-lactams across the blood-CSF barrier. However, using the isolated choroid plexus, it was found that benzylpenicillin and probenecid inhibited the accumulation of fleroxacin in a concentration-dependent manner (Ooie *et al.*, 1997).

5.3.2.5.2 CIMETIDINE AS AN INHIBITOR OF EFFLUX

The anionic inhibitor produced a partial inhibition of two quinolones studied at two different concentrations. As mentioned before, the quinolones are zwitterionic therefore the cationic route of transport was next investigated.

Cimetidine is a cationic substrate for the renal transporter and would therefore interfere with possible cationic transport mechanisms the quinolones may utilise, it has a logP of 0.40 (see figure 5.16).
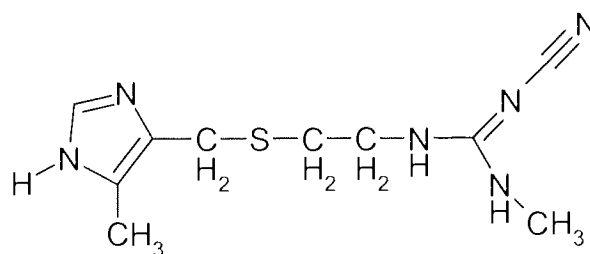
Figure 5.16 – Structure of cimetidine.

Cimetidine at either concentration (100 μM and 500 μM) did not have a significant inhibitory effect on basolateral-to-apical flux of gatifloxacin (10 μM, see figure 5.17). As with probenecid, there are mixed findings in the literature to whether cimetidine has an effect or not on secretion of quinolones. Ito *et al.*, (1999), found that cimetidine

(1mM) did not significantly influence the uptake of levofloxacin and grepafloxacin. In contrast, Yano *et al.*, (1997), found that a concentration of cimetidine 160 µM significantly reduced the clearance of levofloxacin in rats.

Investigations using kidney cell lines to investigate the role of the anion-exchange mechanisms in the secretion of quinolones have produced contradictory information. A number of authors have commented that the intestinal secretory mechanism involved in the secretion of quinolones may be similar to the renal tubular secretion (Cavet *et al.*, 1997a; Rabbaa *et al.*, 1997).
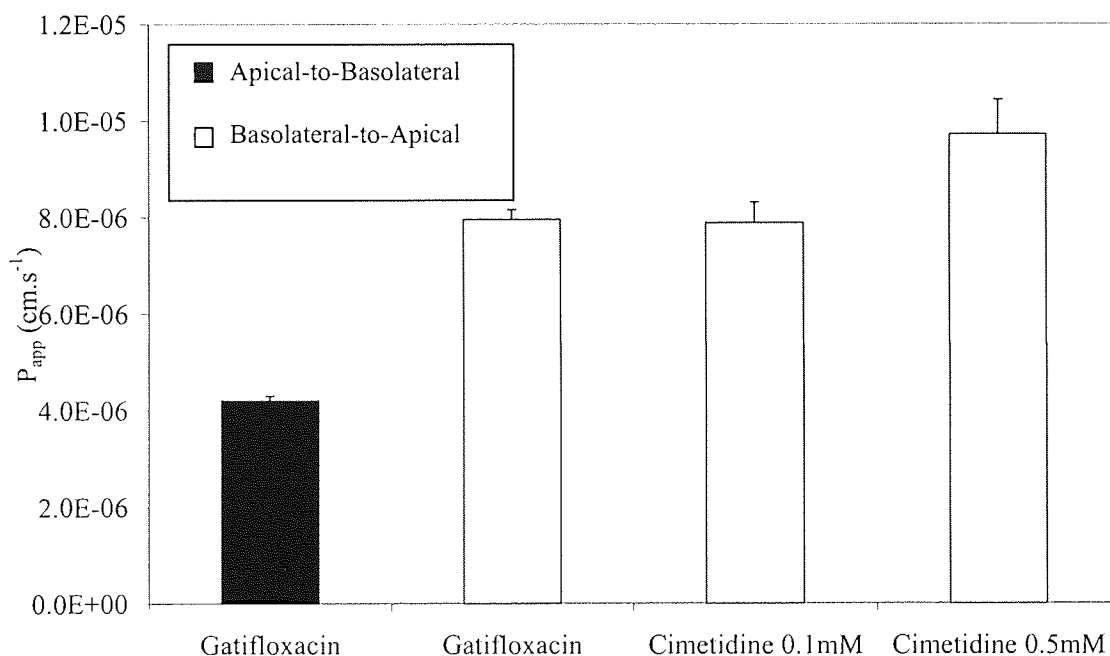
Figure 5.17 – The flux of gatifloxacin (10 µM) in the absence and presence of cimetidine (100 µM and 500 µM), cell were passage number 67, used between 21 and 28 days post seeding, n=3, TEER 676 ± 34 Ω.cm^2.

Matsuo *et al.*, (1998), also found that cimetidine and quinidine inhibited the basolateral-to-apical transcellular transport of levofloxacin without affecting cellular accumulation of levofloxacin. However, the cationic compound tetraethylammonium and the anionic drug *p*-aminohippurate (PAH) had no affect (Matsuo *et al.*, 1998; Ito *et al.*, 1999). Yano *et al.* (1997) also found that the urinary excretion rate of levofloxacin was significantly decreased by cimetidine. In conclusion, the renal secretion of levofloxacin was completely inhibited by cimetidine and the re-absorption fraction of levofloxacin

was not affected by cimetidine, tetraethylammonium, nor *p*-aminohippurate (Yano *et al.*, 1997). Ito *et al*, (2000) made similar observations for levofloxacin.

These findings are contradictory to those observed here with gatifloxacin, where cimetidine could not inhibit secretion. The comparison of different findings in the literature with those found for the gatifloxacin flux through Caco-2 cells, using cimetidine as an inhibitor of secretion, may not be valid. This is because different models are used and the secretion observed in the gastrointestinal tract may differ from that observed in the renal models.

5.3.2.5.3   DIDS AS AN INHIBITOR

Anionic and cationic compounds have been investigated to determine whether they have any effects on the basolateral-to-apical secretion of quinolones. DIDS, the organic anion exchange inhibitor, was investigated for its effects on the secretory process.
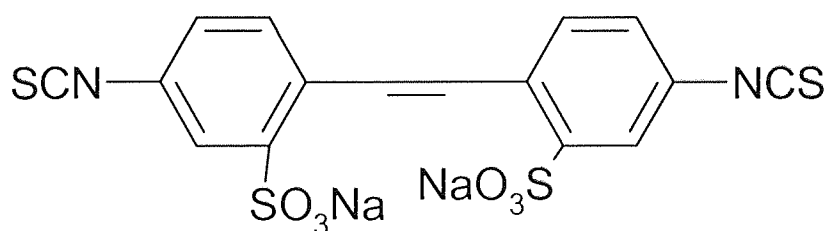
Figure 5.18 – Structure of 4,4'-diisothiocyanostilbene-2-2'-disulphonic acid.

The effects of 4,4'-diisothiocyanostilbene-2-2'-disulphonic acid DIDS (figure 5.18), an organic anion exchange inhibitor, was investigated on the basolateral-to-apical secretion of gatifloxacin (10 μM). DIDS is an irreversible covalent modifier having a reactive thiocynate group which modifies the lysine residues present on the transporter protein (Cavet *et al.*, 1997a).

It was found that DIDS (400 μM) had a significant inhibitory effect on the basolateral-to-apical flux of gatifloxacin ($P=0.013$, see figure 5.19).

Cavet *et al.*, (1997a) found that DIDS gave a concentration-dependent inhibition of ciprofloxacin transport. Net secretion of ciprofloxacin was significantly inhibited by

DIDS (400 µM). When DIDS was present in the apical compartment, there was no significant decrease in apical-to-basolateral or basolateral-to-apical flux. However, when DIDS was present in the basolateral compartment, it was able to inhibit basolateral-to-apical flux of ciprofloxacin (Cavet *et al.*, 1997a). The current work with gatifloxacin has also demonstrated that DIDS acts as an inhibitor for basolateral-to-apical secretion. However, the level of inhibition was much lower than that observed by (Cavet *et al.*, 1997a) for ciprofloxacin, this could be due to the differences between ciprofloxacin and gatifloxacin for the transporter as observed with probenecid.
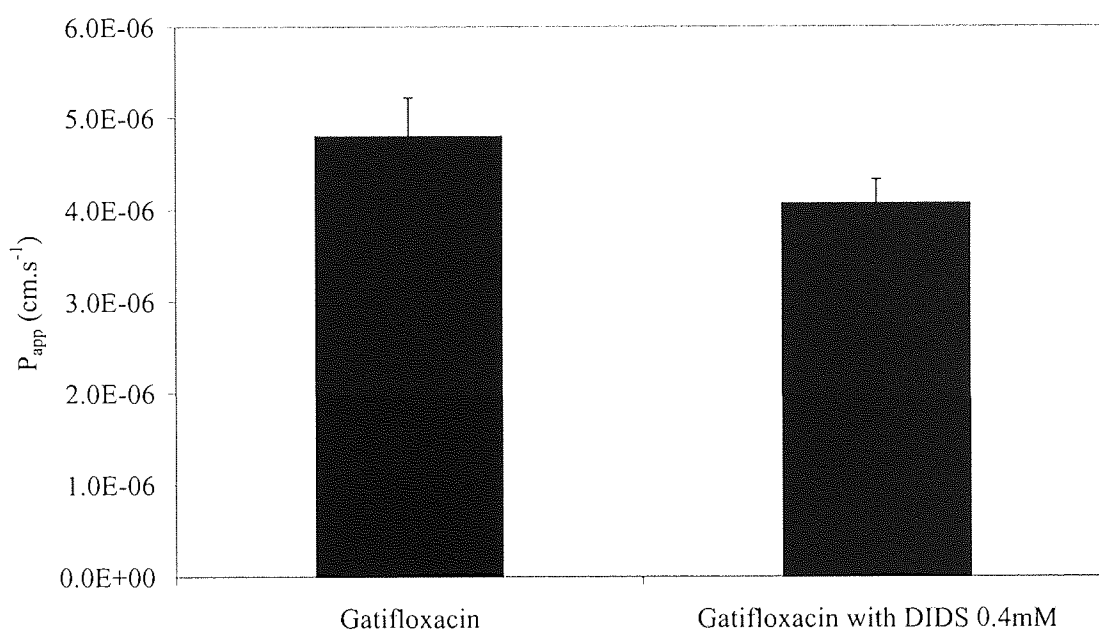
Figure 5.19 – The effects of DIDS (400 µM) on the basolateral-to-apical flux of gatifloxacin (10 µM). Cells passage number 40, 21 to 28 days post seeding, n=3, TEER 638 ± 32 Ω.cm^2 were used.

5.3.2.6   VERAPAMIL AS AN INHIBITOR OF EFFLUX

The work so far has indicated that the active basolateral-to-apical secretion can be inhibited by metabolic inhibitors, a reduction in temperature and probenecid. The literature indicates that PgP maybe implicated in the basolateral-to-apical secretion of the quinolones. Therefore an investigation into the role of PgP would be appropriate.
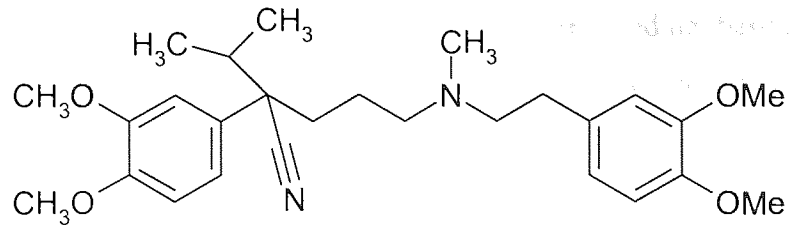
Figure 5.20 – Structure of verapamil

Verapamil was investigated as an inhibitor of basolateral-to-apical secretion of quinolones. It is a PgP inhibitor as well as a renal anion transport inhibitor (see figure 5.20)

Verapamil binds to PgP, however, it is not effluxed by PgP itself. It was used to investigate the involvement of PgP in the efflux of quinolones. Verapamil has a K_m of 1.5 µM for the PgP ATPase binding site (Stein, 1997).
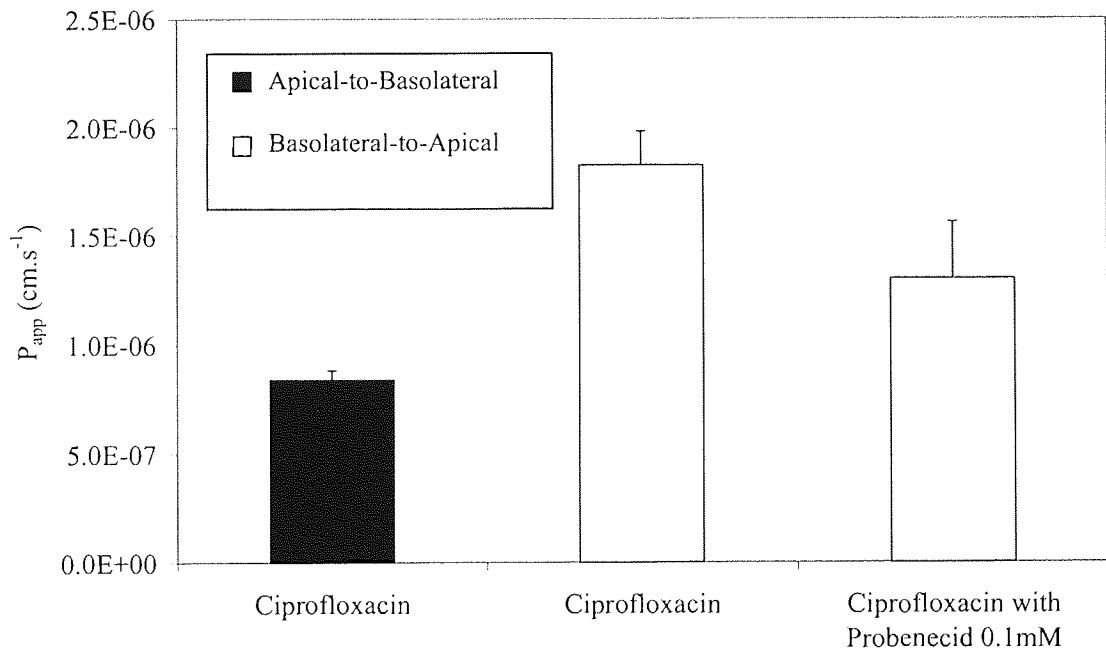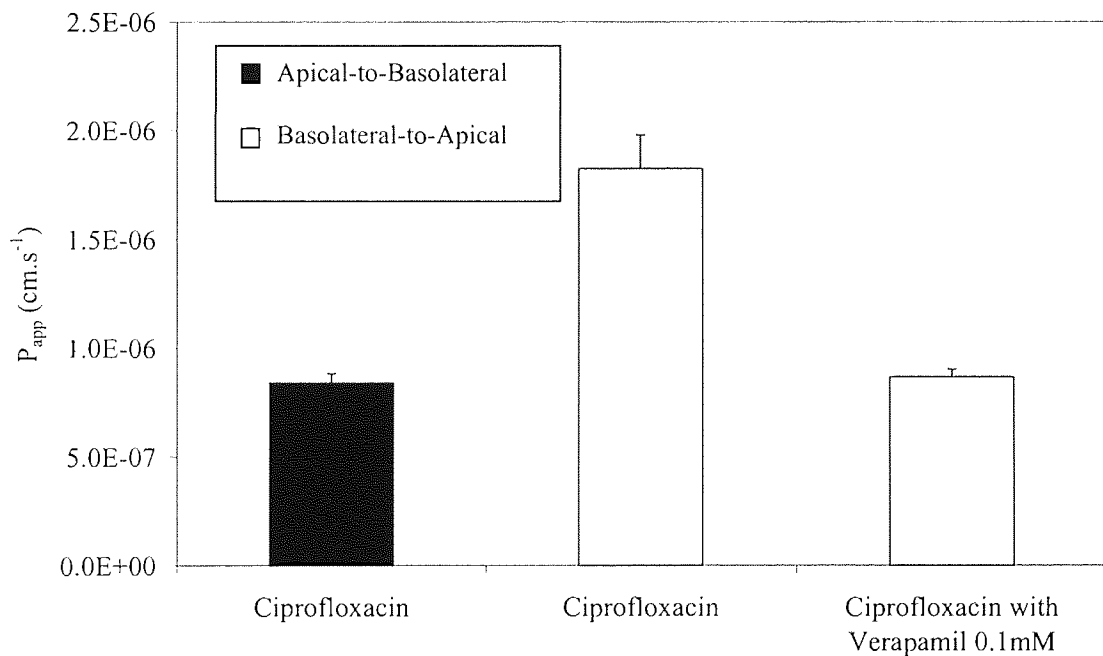

Figure 5.21 – The permeation of ciprofloxacin through Caco-2 cells apical-to-basolateral and basolateral-to-apical as well as basolateral-to-apical in the presence of verapamil (100 µM). Transport studies were performed on cells with a passage number 30, 21 to 28 days post seeding, n=3, TEER 764 ± 34 $\Omega.cm^2$.

Verapamil (100 µM) was able to bring basolateral-to-apical flux of ciprofloxacin into line with apical-to-basolateral flux, thereby abolishing the active secretion (see figure 5.21).

Hunter *et al.* (1993) observed that verapamil (100 μM) reduced net basolateral-to-apical transport of vinblastine a classical PgP substrate, and increased apical-to-basolateral transport at the same time to bring them in-line with each other.

The effects of verapamil on the basolateral-to-apical flux of gatifloxacin (10 μM) were also investigated, to compare with those on ciprofloxacin flux. The concentration of verapamil was adjusted from 0.1 mM through to 0.5 mM to investigate the presence of a concentration-dependent effect.
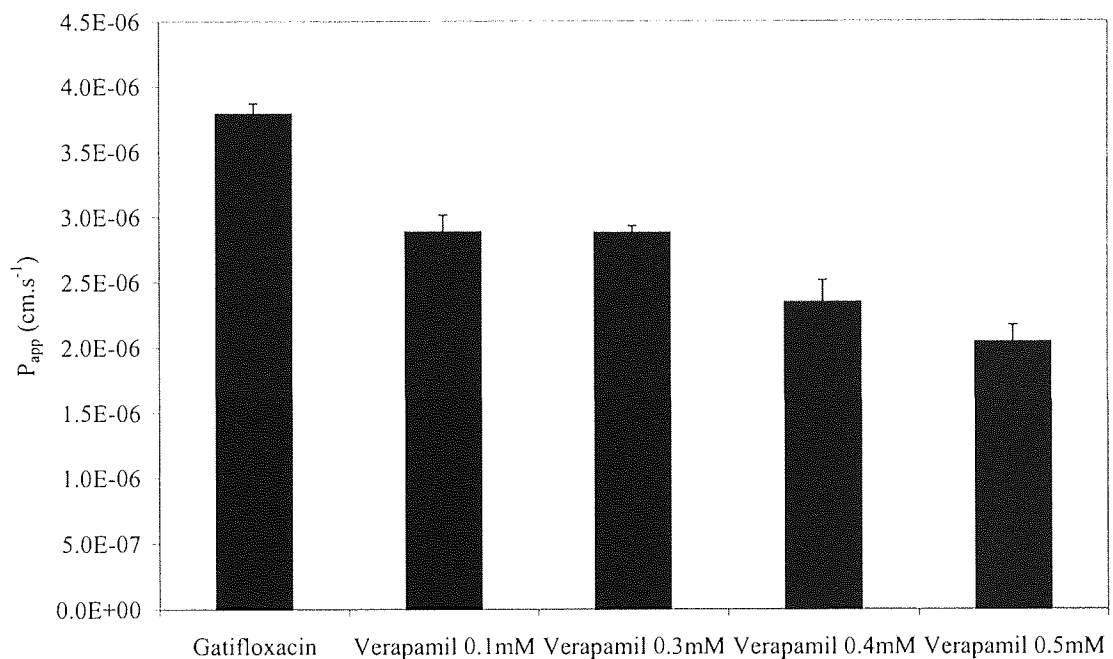
Figure 5.22 – The permeability of gatifloxacin (10 μM) basolateral-to-apical in the absence and presence of verapamil 100 μM through to 500 μM. The cells used were passage number 37 used 21 to 28 days post seeding, n=3, TEER 695 ± 45 Ω.cm².

Verapamil showed a concentration-dependent inhibitory effect on the basolateral-to-apical active secretion of gatifloxacin (see figure 5.22).

A concentration of verapamil (400 μM) was sufficient to reduce the basolateral-to-apical flux of gatifloxacin (10 μM) to the same level as apical-to-basolateral flux (see figure 5.23).

The toxicity of verapamil at various concentrations was accessed to see whether the inhibition observed was due to cellular death. A trypan blue stain was used to determine viable cells following exposure to verapamil (see section 2.3.2).
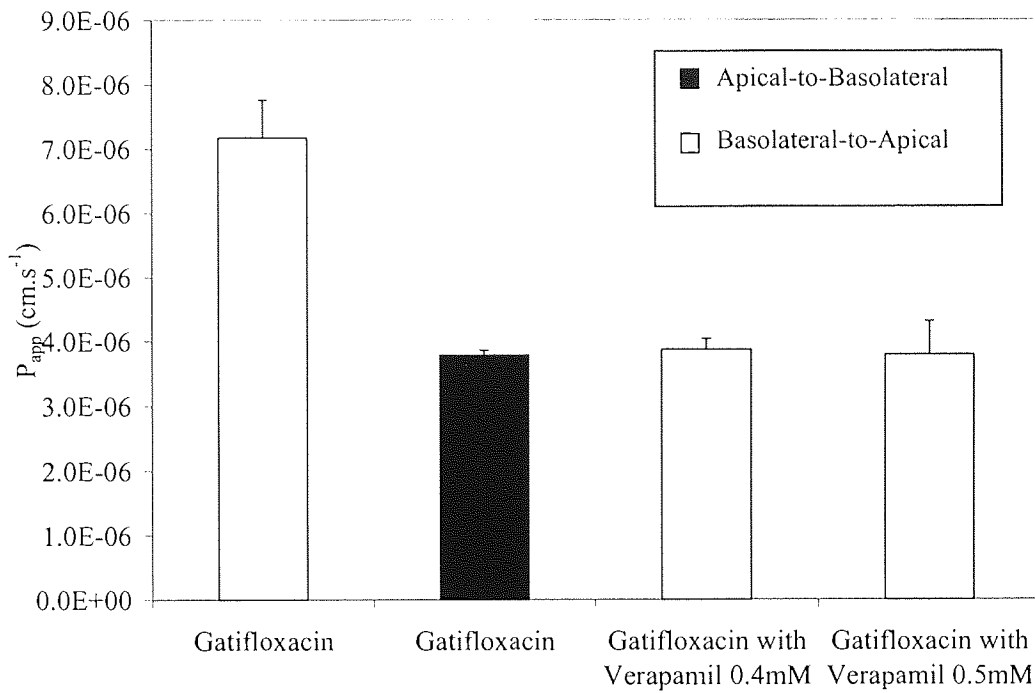
Figure 5.23 – The basolateral-to-apical flux of gatifloxacin In the presence of verapamil (400 μM and 500 μM). The cells were passage number 58, used between 21 to 28 days post seeding, n=3, TEER 770 ± 55 Ω.cm².

There was no significant difference between the percentage cells viable (P=0.307, ANOVA) between the different treatment groups (see figure 5.24). This indicated that a concentration of verapamil upto 500 μM was not toxic to cells, an observation in accordance with literature data (Cavet *et al.*, 1997a).

The present study shows that PgP is probably involved in the basolateral-to-apical secretion of quinolones. However, it may not be the sole mechanism of secretion. The intestine is capable of the transport of neutral as well as cationic drugs *via* the ATP-driven efflux pump PgP (Stein, 1997). Cavet *et al.*, (1997a), found that ciprofloxacin was secreted from the basolateral-to-apical solutions in Caco-2 cells. Verapamil, which is a substrate for the renal organic cation transporter and a competitive inhibitor of PgP was used to inhibit efflux of quinolones.
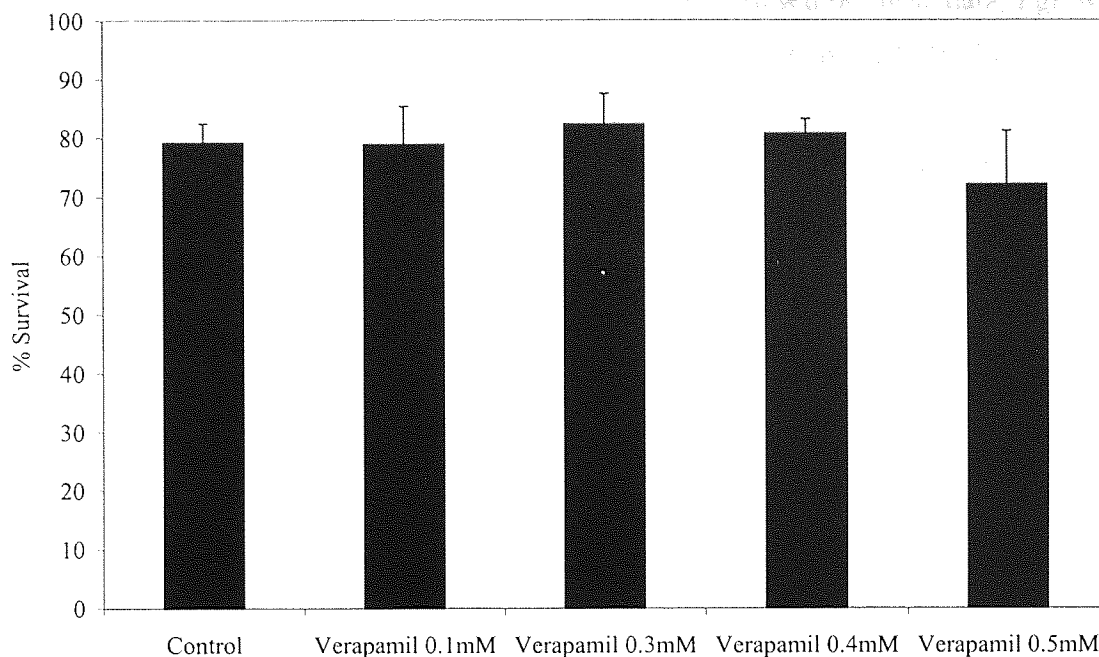
Figure 5.24 – The effects of verapamil on Caco-2 cells grown in 24-well plates, cells were exposed to verapamil (100 to 500 μM) for one hour, the cells were passage number 48, used 6 days after seeding, n=3.

Ito *et al.* (1999) found that quinidine, a PgP inhibitor, was able to inhibit the secretion of levofloxacin in a concentration-dependent manner and significantly inhibited uptake at 5 mM, in the pig kidney cell line LLC-PK$_1$. Unlike vinblastine, where a concentration of verapamil (100 μM) can cause a complete inhibition of flux, verapamil was not able to completely abolish the secretion of ciprofloxacin as found by Cavet *et al.* (1997a). It was not able to completely abolish the secretion of gatifloxacin (10 μM) in this Caco-2 cell model used here at 100 μM concentration either.

To identify the effects of PgP, Ito *et al.* (1997) studied the transport of levofloxacin in LLC-PK$_1$ and modified LLC-GA5-COL150 cells, which express a high level of PgP. The basolateral-to-apical flux of levofloxacin was greater than the apical-to-basolateral flux with both cell lines; however, the basolateral-to-apical flux with the modified cell line was significantly greater than the basolateral-to-apical flux in the LLC-PK$_1$ cells. These results indicated that levofloxacin was transported by a PgP-mediated transport system. Levofloxacin (3 mM) inhibited transport of cyclosporin A (5 μM) flux, therefore indicating that it has a lower affinity for the transporter than cyclosporin A. The transport of levofloxacin (3 mM) and quinidine (50 μM) in the modified cell-line,

was reduced to levels observed in the LLC-PK$_1$ cell line. Based on these data, PgP was implicated in the basolateral-to-apical secretion of quinolones (Ito *et al.*, 1997).

Cavet *et al.* (1997a) used MDCKI and II dog kidney epithelial cells to investigate the effects of PgP on the active efflux of quinolones. The MDCKII strain has a lower TEER than the MDCKI strain and a cationic selective pathway. Ciprofloxacin (10 μM) was not subject to basolateral-to-apical secretion, despite a substantial net secretion of vinblastine being observed. The PgP antibodies UIC2 or MRK16 had no significant effect on the secretory values for ciprofloxacin, however, there was a significant decrease in secretory vinblastine permeability measured concurrently. This indicates that PgP may not be involved in the active efflux of quinolones (Cavet *et al.*, 1997a).

Cormet-Boyaka *et al.* (1998) also found that the use of verapamil (100 μM) or progesterone during incubation of sparfloxacin in Caco-2 cells significantly increased the level of accumulation. These two inhibitors also induced an increase in the level of accumulation of vinblastine. Verapamil (100 μM) significantly reduced vinblastine flux but had only a marginal affect on the flux of sparfloxacin (Cormet-Boyaka *et al.*, 1998). It was also noted that the structural, chemical and uptake characteristics of sparfloxacin are in accordance with those of most PgP substrates (as mentioned in section 1.4.4.2). Sparfloxacin is a polycyclic molecule, has a high level of liposolubility and uptake occurs through passive diffusion through the apical membrane (Cormet-Boyaka *et al.*, 1998). Gatifloxacin secretion was also subject to inhibition by verapamil a PgP substrate.

With the current information available, it is difficult to determine whether verapamil is inhibiting gatifloxacin basolateral-to-apical secretion by blocking PgP, competing with quinolones for a organic cation transporter, or inhibiting an unknown transporter or a combination of these. However, it appears that PgP is involved in the basolateral-to-apical secretion of gatifloxacin to some degree. Whether this is applicable to the other quinolones studied is not clear.

5.3.2.7   FLUORESCEIN AS AN INHIBITOR OF EFFLUX

The effects of fluorescein sodium on the transport of quinolones were investigated in case this compound could interfere with the transport of the quinolones.

Fluorescein sodium has been used by Jaehde *et al.* (1993) as a possible paracellular marker. At physiological pH it has a logD of 0.003 and a molecular mass of 376.3. Because of these physicochemical properties, it shows very low cellular permeability (see section 4.3.3). The fluorescence intensity of fluorescein varies with pH. In acid solutions it can be protonated which results in a quenching of fluorescence (see figure 5.25).
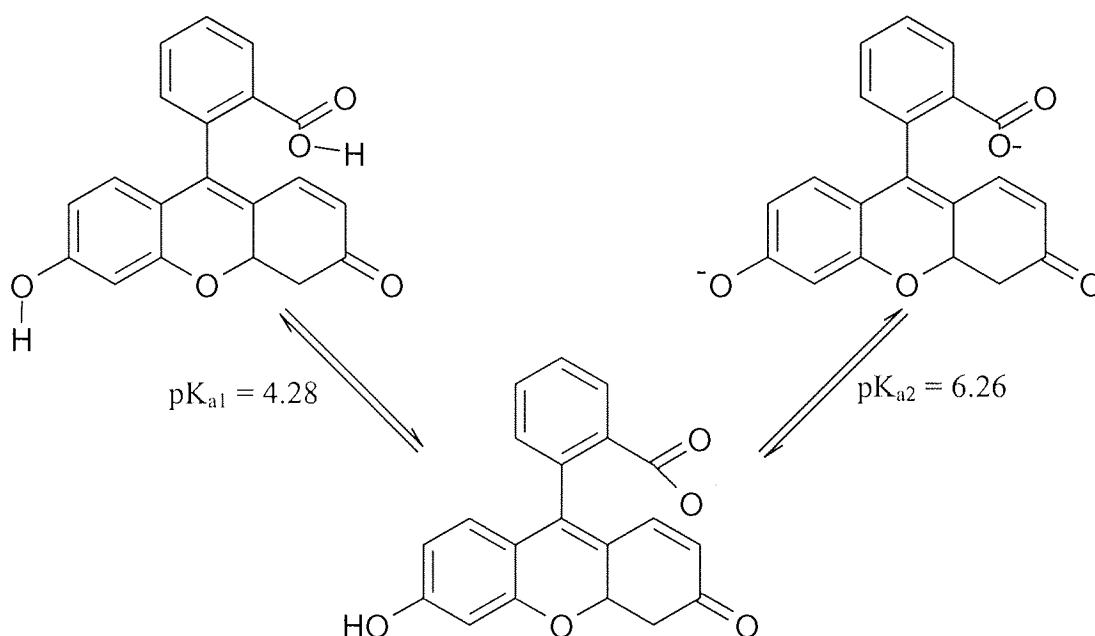
Figure 5.25 – Structure of fluorescein sodium, undergoing ionisation.

However, earlier work (see section 4.3.3) had shown that it was subject to active transport with the basolateral-to-apical flux being significantly greater than the apical-to-basolateral flux. There is no mention of it being a substrate for transport processes within the literature. As it could use potentially the same transporter as the quinolones for efflux, its effects on quinolone flux were investigated. In the initial experiments, it was used at a concentration of 10 μg.ml^{-1} (26.6μM), as used by Jaehde *et al.* (1993) in blood-brain-barrier models.

Concentrations of fluorescein ranging from 13 μM to 106 μM had no significant inhibitory effect on the basolateral-to-apical flux of gatifloxacin (see figure 5.26). Although fluorescein itself was subject to secretion in the basolateral-to-apical direction it does not interfere with the basolateral-to-apical secretion of gatifloxacin (10 μM).
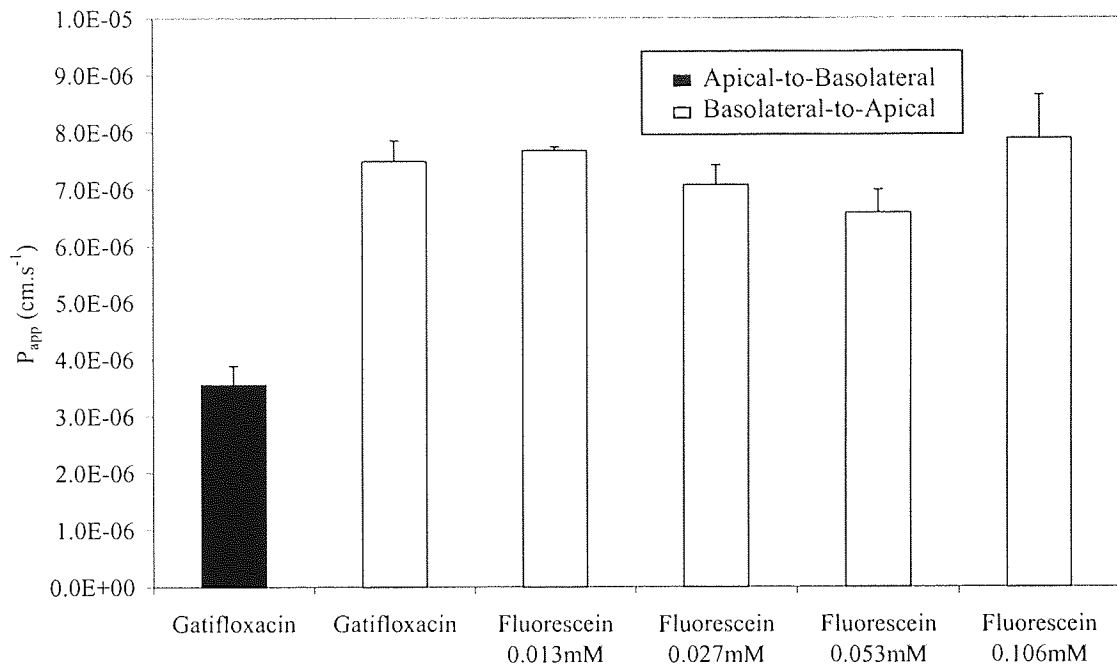
Figure 5.26 – The effects of various concentrations of fluorescein on the basolateral-to-apical flux of gatifloxacin (10 μM), the cell were passage number 68, used 21 to 28 days post seeding, n=3.

Since fluorescein was a substrate for an active efflux mechanism and itself does not interfere with quinolone flux at low concentration, its effects on gatifloxacin flux were investigated at a higher concentration (see figure 5.27).

Initial inspection of data for the higher concentrations of fluorescein showed that as concentration increased there was an inhibitory effect. Fluorescein (600μM and 100 μM) concentrations had no significant effect on gatifloxacin basolateral-to-apical flux only the 400 μM concentration had a significant inhibiting effect on basolateral-to-apical flux (P=0.006, see figure 5.27). Overall fluorescein had no significant inhibitory effect.
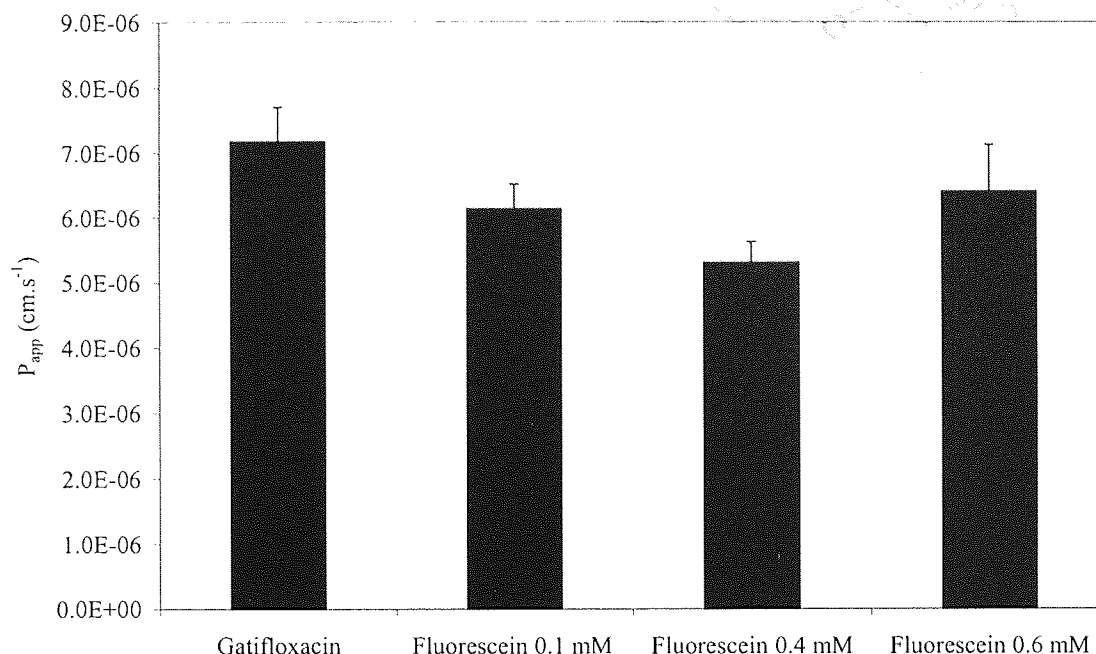
Figure 5.27 – The flux of gatifloxacin (10 µM) basolateral-to-apical in the absence and presence of fluorescein at various concentrations.

Jaehde *et al.* (1993) used fluorescein (10 $\mu g.ml^{-1}$) as a paracellular marker and found that the clearance of fluorescein across the blood-brain barrier was low, which would be expected for a hydrophilic molecule. They were not aware of active efflux of fluorescein itself (Jaehde *et al.*, 1993). There are few examples in the literature where fluorescein itself is used as a paracellular marker and based on the current findings it would have to be used with caution, as with any compound it may exert its own effects if included in a system. Prior to use, it is necessary to investigate whether it interacts with the cellular modelling being used or the transport of the compound being studied.

5.3.2.8   OFLOXACIN ISOMERS AND EFFLUX

Ofloxacin is a chiral quinolone, the S enantiomer is known as levofloxacin (see figure 5.28). The cellular flux of a racemic mixture of ofloxacin and the S enantiomer (levofloxacin) were compared to investigate any stereoselective dependence on the transport processes.

R-(+)-ofloxacin   S-(-)-ofloxacin

Figure 5.28 – Structures of two isomers of ofloxacin, R-(+)-ofloxacin and S-(-)-ofloxacin (levofloxacin).

Rabbaa *et al.*, (1997), observed that, in models using the rat intestine, the AUC for the R enantiomer was significantly greater (25 %) than the S isomer. The elimination of ofloxacin into bile favoured the S isomer (40 % more), which underwent stereoselective glucoronidation. The intestinal clearance of the R isomer was greater (17 %) than that of the S isomer. The S isomer shows greater antimicrobial activity being 8 to 128 times more active than the R isomer *in vitro*. The rate of elimination of the R isomer was greater (25 %) than that of the S isomer in models using intestinal segments. Rabbaa *et al.* (1997) demonstrated that the secretion observed in Caco-2 cells was approximately 50 % more than that seen with the racemic mixture. Elimination of the R-(+)-ofloxacin was predominant in the effluxes at all doses and was saturable up to 80 mg.kg^{-1}, elimination process was observed when the dose was increased (Rabbaa *et al.*, 1996; Rabbaa *et al.*, 1997).

The data showed no difference between ofloxacin racemic mixture and levofloxacin flux (see figure 5.29). This could be due to the fact that, although the pure S isomer was available, the pure R isomer was not and therefore the differences between them could not be determined. The passive transport process could also swamp any potential asymmetric carrier-mediated mechanism.

Figure 5.29 – Basolateral-to-apical and apical-to-basolateral flux of levofloxacin and ofloxacin (10 µM) through Caco-2 cells, passage number 70, used 21 to 28 days post seeding, n=3, TEER 615 ± 30 $\Omega.cm^2$.

Because there was no difference between the two enantiomers in their aqueous or lipid solubility, drug elimination should not be stereoselective if it involved only passive processes. The stereo-selectiveness infers that the intestinal secretion of ofloxacin was carrier-mediated, with the two optical isomers having different affinities for the receptor sites (Rabbaa *et al.*, 1996). Rabbaa *et al.*, (1996) also concluded that passive diffusion remains the predominant mechanism of intestinal elimination of ofloxacin.

The stereo-selective, carrier-mediated component is probably so small that it can not be detected in the racemic mixture. The model used can not provide sufficient sensitivity to show differences.

Quinolone	Sensitivity	Proposed mechanism	Models	Reference
Ciprofloxacin	Transport equivalent in apical-to-basolateral and basolateral-to-apical directions.	No active mechanism	Calu-3 cells	(Cavet et al., 1997b)
Ciprofloxacin	Sodium azide (15 mM) abolishes transport. Verapamil (100 µM) incomplete inhibition.	Unidentified mechanism.	Caco-2 cells	(Griffiths et al., 1993)
Ciprofloxacin	DIDS (400 µM) Verapamil (500 µM)	Unidentified multidrug resistance mechanism	Caco-2 cells	(Cavet et al., 1997a)
Levofloxacin	Cyclosporin A (5 and 10 µM) Quinidine (50 µM)	Involvement of PgP	LLC-PK$_1$	(Ito et al., 1997)
Levofloxacin	Grepafloxacin competed K_i 13.5 mM Quinidine (5 mM)	Transporter distinct from organic cation and anion transporter	Renal cortical slices	(Ito et al., 1999)
Levofloxacin	Grepafloxacin (100 µM) competed. Cimetidine (500 µM) decreased secretion.	Organic cation transport system.	Isolated perfused rat kidney.	(Ito et al., 2000)
Levofloxacin	Competition with unlabelled levofloxacin, ofloxacin, grepafloxacin and ciprofloxacin. Cimetidine (1 mM). Quinidine (1 mM).	Distinct renal transporter not H$^+$/organic cation antiport system.	LLC-PK$_1$	(Matsuo et al., 1998)
Levofloxacin	Cimetidine (160 µM)	Tubular secretion	In vivo rat clearance	(Yano et al., 1997)
Grepafloxacin	Levofloxacin competed K_i 4.7 mM	Transporter distinct from organic cation and anion transporter	Renal cortical slices	(Ito et al., 1999)
Sparfloxacin	Concentration dependent uptake (1-200 µM). Insensitive to sodium azide (15 mM).	Passive absorption	Caco-2 cells	(Cormet et al., 1997a)
Sparfloxacin	Verapamil (100 µM) Progesterone (100 µM) Insensitive to sodium azide (15 mM).	Involvement of PgP.	Caco-2 cells	(Cormet-Boyaka et al., 1998)

Table 5.3 – Summary of major literature findings regarding quinolone active secretion.

5.3.3 MODEL OF QUINOLONE TRANSPORT

A number of different sources, using different quinolones and different *in vitro* models have made observation on the transport of the quinolones. Their findings have been summarised in table 5.3.

The consensus is that the apical-to-basolateral transport is most likely a passive process with the basolateral-to-apical transport being an active process.

Based on the transport experiments conducted in this chapter, the following conclusions can be drawn. The apical-to-basolateral transport system was sensitive to competing quinolones. However, metabolic inhibitors showed no significant inhibitory effects on transport. With the data currently available, conclusions can not be drawn on the potential mechanism the apical-to-basolateral transport may involve.

The basolateral-to-apical active secretion mechanism is sensitive to energy depletion, shows competition with other quinolones and can be abolished by verapamil (see table 5.4).

Quinolone	Sensitivity	Inferred mechanism
Norfloxacin	2,4-dinitrophenol (1 mM).	Energy-dependent mechanisms
Ciprofloxacin	Probenecid (100 µM). Verapamil (100 µM) completely abolishes.	Anionic or PgP
Gatifloxacin	Probenecid (500 µM). DIDS (400 µM) Sodium azide (15 mM). Ofloxacin (100 µM). Norfloxacin (100 µM). Verapamil (400 µM) completely abolishes	Sensitive to competition. Energy-dependent Anionic inhibitor sensitivity PgP involvement

Table 5.4 – Summarised data from transport experiments

As stated earlier verapamil 400 µM was able to bring the basolateral-to-apical apparent permeability into line with the apical-to-basolateral permeability, thereby abolishing the active secretion. Verapamil is a substrate for PgP and therefore it appears that PgP plays a role in the secretion of quinolones, in conjunction with another efflux system which could be the anion exchange system.

CHAPTER 6 CONCLUSIONS

This chapter summarises the findings from the previous chapters and conclusions are drawn based on the data obtained.

A simple analytical HPLC method was developed for the determination of 14 quinolones. The general method used could be further adapted for other quinolones not as yet studied. The method proved to be robust and reliable. Detection of quinolones was possible down to 1 ng.ml^{-1} with a loop-volume of 50 μL for most of the quinolones (see section 2.8.2 and appendix A1).

Visual inspection of Caco-2 cells showed that they grew well and reached confluence within five days, the time-scale reported in the literature for such cells (Artursson, 1991). The SEM was able to reveal the brush-border on the cell surface and, at a sufficiently high magnification, *microvilli* were observed. These findings indicate that the cells were well differentiated and were, thereby, suitable for experiments to be conducted. The TEER was measured for monolayers before use and those that showed a greater than 100 Ω.cm^2 variation were rejected (see section 4.3.4).

Experiments conducted to measure quinolone flux through bare inserts revealed that the support membrane itself provided little resistance to quinolone flux. More importantly, the flux of a group of compounds with diverse physicochemical properties, from ofloxacin through to propyl-ciprofloxacin, logP ranging from –0.165 to 1.693 was similar.

Fluorescein sodium (10 μg.mL^{-1}) had been reported as a potential paracellular marker (Jaehde *et al.*, 1993). The flux of this compound was investigated in Caco-2 cells, while co-incubated with various quinolones. Concurrent use with the quinolones showed that the basolateral-to-apical flux of fluorescein was significantly greater than the apical-to-basolateral flux, indicating that fluorescein itself was subject to active secretion. The effects on the active secretion of quinolones in the presence of fluorescein were investigated. It was found this compound had no significant inhibitory effect on the

secretion of gatifloxacin. The effects of quinolones inhibiting the flux of fluorescein were not investigated.

The quinolones studied, on the most part, were zwitterionic except cinoxacin and flumequine. Therefore, the ionisation of the zwitterionic and non-zwitterionic compounds can be affected by the pH of the solvent. A small representative group: ofloxacin, ciprofloxacin and propyl-ciprofloxacin, all zwitterionic compounds, and flumequine, which is non-zwitterionic, were used to investigate the effects on cellular flux at pH 5.5, representing the acidic microclimate, as well as pH 8.5, which represented the pH in the lower intestine. It was found that the maximum level of flux occurred at pH 7.4, when the zwitterionic compounds were in the neutral form, this finding was contradictory to some reports in the literature where the cationic form showed maximum transport.

The microbiological activity of the quinolones was investigated using 2 test organisms. Similar trends in MICs were observed for the quinolones using both organisms. Both organisms were most sensitive to sparfloxacin followed by ciprofloxacin and the *n*-alkyl-homologous ciprofloxacin family with nalidixic acid and cinoxacin being the least active. Nalidixic acid and cinoxacin are both first-generation quinolones which, due to their low activity, are very rarely used in clinical therapy (Hooper and Wolfson, 1993).

The determination of lipophilicity of the quinolones using HPLC revealed a parabolic relationship between different percentages of acetonitrile and log$K$, this relationship theoretically should have been linear. However, the divergence from a linear relationship shows that the quinolones were interacting with the HPLC column to a greater extent than expected based solely on their lipophilicity. The classical sigmoidal relationship was observed between the cellular permeability P_{app} and LogD at pH 7.4. As the lipophilicity of the quinolone increases, the cellular permeability increased upto an optimal value. The different computational methods, as well as the two methods which measure logP, were compared and it was found that the absolute values between the methods were not comparable neither was the rank order, except for the *n*-alkyl ciprofloxacin family.

A model could not be constructed to relate the physicochemical properties of the quinolones to the cellular absorption. There were a number of reason for this. Firstly this series of compounds did not cover a broad enough range of physico-chemical properties. Secondly a number of the quinolones are zwitterionic which makes it difficult to predict physico-chemical properties such as logP. Finally the transport of these compounds was not a simple passive process, complex transport exists for these compounds which is not completely understood and is susceptible to changes in the local cellular environment. These factors thwarted a reliable prediction model at present.

Active apical-to-basolateral flux of quinolones was investigated and it was found that the concentration in the donor chamber had no significant effect on the apical-to-basolateral flux. However, it was found that norfloxacin (100 μM) significantly reduced the apical-to-basolateral flux of gatifloxacin (10 μM), while the metabolic inhibitor sodium azide had no inhibitory effect. There are references in the literature which indicate that the apical-to-basolateral flux of quinolones is an active process (Rabbaa *et al.*, 1997). Most of this work has been carried out using radiolabelled quinolones which, in this case, were not available. Uptake studies could not be performed using non-radiolabelled quinolones since their uptake could not be quantified using HPLC (see section 2.8.2). Based on the data available, it can be concluded that an unknown mechanism exists which is sensitive to competing quinolones.

Earlier data (see section 4.3.5) had suggested that the basolateral-to-apical flux of quinolones was also subject of active transport, in the form of an active secretion mechanism. Two quinolones, butyl-ciprofloxacin and gatifloxacin, were used to investigate the affinity of the transporter for quinolones. Unfortunately, neither compound revealed any affinity. This could occur because the lowest concentration of compound used already saturated the transporter. Conversely, the concentration of the quinolones was not high enough.

Active biological processes depend on energy in the form of cellular ATP. Cellular metabolism can be inhibited by compounds such as sodium azide and 2,4-dinitrophenol. Both metabolic inhibitors reduced basolateral-to-apical flux of the quinolones studied; the level of inhibition varied with the quinolone. However, it was not possible to

completely abolish the active secretion and bring basolateral-to-apical flux in line with apical-to-basolateral flux. This was also observed by a number of other authors (Griffiths *et al.*, 1993; Griffiths *et al.*, 1994). One possible reason for this lack of complete inhibition is that the method used to deplete energy could not completely deplete the cellular energy stores.

Another method of inhibiting an energy-dependent process is to decrease the temperature. The study using gatifloxacin found that both apical-to-basolateral as well as basolateral-to-apical flux were significantly reduced when the temperature was reduced from 37°C to 2°C. However, even at 2°C the basolateral-to-apical flux was greater than the apical-to-basolateral flux. The use of D-[1-^{14}C]mannitol and [^{3}H]testosterone showed that the flux of both of these passively transported compounds was reduced at the lower temperature. These findings question the validity of reducing temperature to inhibit active transport mechanisms. The reduction in temperature results in a decrease in the fluidity of the cellular membrane and hence a reduction in cellular flux and uptake, rather than inhibition of the active process. Another possible explanation is that the passive transport in the basolateral-to-apical direction is greater than that in the apical-to-basolateral direction because of the larger available surface area.

A number of literature sources (Jaehde *et al.*, 1995; Cavet *et al.*, 1997; Yano *et al.*, 1997; Ito *et al.*, 1999) have all suggested that quinolones undergo gastrointestinal secretion using a transporter related to the renal organic anion transporter. They have found that probenecid and cimetidine were able to inhibit active secretion in intestinal as well as renal models. In this present study, it was found that cimetidine (100 μM and 500 μM) had no inhibitory effect on the basolateral-to-apical flux of gatifloxacin. However, probenecid (100 μM) had a significant inhibitory effect on the basolateral-to-apical flux of ciprofloxacin (10 μM) which could also be demonstrated with gatifloxacin (10 μM) using probenecid (500 μM) as an inhibitor. These findings suggest that probenecid acts as an inhibitor of quinolone basolateral-to-apical transport and hence active secretion. However, different quinolones may have a different affinity for the transporter involved and, therefore, differences in the probenecid concentration were observed. DIDS (400 μM) also inhibited active secretion.

Based on the present data, it is suggested that gastrointestinal secretory mechanism for quinolones was affected by anionic inhibitors, and the transporter involved may show some relationship to the renal organic anion transporter.

The effects of competing quinolones on the basolateral-to-apical secretion of quinolones had mixed effects. It was found that ofloxacin (100 µM) and norfloxacin (100 µM) had an inhibitory effect on the secretion; however, ciprofloxacin (100 µM and 300 µM) showed no effect. As stated earlier, the quinolones could have different levels of affinity for the transporter involved and therefore they would show different amounts of competition.

Verapamil (400 µM) was found to completely abolish active secretion of gatifloxacin and verapamil (100 µM) was able to completely abolish the active secretion of ciprofloxacin basolateral-to-apical transport and bring it into line with apical-to-basolateral flux. Verapamil is a classical inhibitor for the PgP, an efflux mechanism implicated in the secretion of quinolones. However, it also inhibits the renal anion transporter. Based on these findings, the mechanism involved in the efflux of quinolones could be PgP or another transporter which is inhibited by verapamil. This transporter has not have been identified as yet.

It has been observed that ofloxacin, a racemic quinolone, shows different levels of biological activity between the two isomers as well as differences in elimination. The flux of levofloxacin, the S isomer of ofloxacin, was compared with the flux of the racemic mixture of ofloxacin. No difference was observable in flux in either direction between the S isomer and the racemic mixture. The pure R isomer was not available although this may have helped to show the differences, if any, between the secretion and uptake of the two forms of ofloxacin.

In conclusion, an active mechanism exists for the apical-to-basolateral flux of the quinolones the identity of which has not been determined at this time. The characteristics of this mechanism includes sensitivity to competing quinolones and ATP depleters.

The most likely mechanism of basolateral-to-apical secretion is PgP in combination with another mechanism, which may be the anionic transporter however, the presence of another unknown mechanism sensitive to verapamil cannot be ruled out. Although there are active mechanisms involved in the cellular flux of the quinolones, the major determinant in flux is lipophilicity. The active mechanism has a relatively small effect on transport in comparison to the passive lipophilicity based flux. For this group of compounds, the level of active efflux is so small that it would not have any clinical significance.

Further work involving a pure PgP inhibitor such as monoclonal antibodies and a pure anionic inhibitor would be required to determine if either mechanism is involved or as yet an unidentified mechanism is responsible for quinolone secretion. This would be aided by the use of radiolabelled quinolones to study uptake at the apical and basolateral membranes.

BIBLIOGRAPHY

Albert A and Serjeant EP (1983) *The Determination of Ionization Constants*. London, Chapman and Hall.

Aminimanizani A, Beringer P and Jelliffe R (2001) Comparative Pharmacokinetics and Pharmacodynamics of the Newer Fluoroquinolone Antibacterials. *Clinical Pharmacokinetics* **40**:169-187.

Anderle P, Niederer E, Rubas W, Hilgendorf C, SpahnLangguth H, Wunderli-Allenspach H, Merkle HP and Langguth P (1998) P-glycoprotein (P-gp) Mediated Efflux in Caco-2 Cell Monolayers: The Influence of Culturing Conditions and Drug Exposure on P-gp Expression Levels. *Journal Of Pharmaceutical Sciences* **87**:757-762.

Artursson P (1991) Cell Culture as Models for Drug Absorption Across the Intestinal Mucosa. *Critical Reviews in Therapeutic Drug Carrier Systems* **8**:305-330.

Artursson P and Hochman J (1994) Mechanisms of Absorption and Tight Junction Regulation. *Journal of Controlled Release* **29**:253-267.

Artursson P, Ungell AL and Lofroth JE (1993) Selective Paracellular Permeability In 2 Models Of Intestinal- Absorption - Cultured Monolayers Of Human Intestinal Epithelial-Cells and Rat Intestinal Segments. *Pharmaceutical Research* **10**:1123-1129.

Bain LJ and LeBlanc GA (1996) Interaction of Structurally Diverse Pesticides with the Human MDR1 Gene Product P-Glycoprotein. *Toxicology and Applied Pharmacology* **141**:288-298.

Basak SC and Grunwald. GD (1995) Estimation Of Lipophilicity From Molecular Structural Similarity. *New Journal Of Chemistry* **19**:231-237.

Bermejo M, Merino V, Garrigues TM, Delfina JMP, Mulet A, Vizet P, Trouiller G and Mercier C (1999) Validation Of A Biophysical Drug Absorption Model By The PATQSAR System. *Journal Of Pharmaceutical Sciences* **88**:398-405.

Berne RM and Levy MN (1993) *Physiology*. St Louis, London, Mosby Year Book.

Bieck PR (1993) *Colonic Drug Absorption and Metabolism*.

Blum RA (1992) Influence Of Renal Function On The Pharmacokinetics Of Lomefloxacin Compared With Other Fluoroquinolones. *American Journal of Medicine* **92**:18S-21S.

Burton PS, Conradi RA, Ho NFH, Hilgers AR and Borchardt RT (1996) How Structural Features Influence The Biomembrane Permeability Of Peptides. *Journal Of Pharmaceutical Sciences* **85/12**:1336-1340.

Cao CX, Silverstein SC, Neu HC and Steinberg TH (1992) J774 Macrophages Secrete Antibiotics *Via* Organic Anion Transporters. *Journal Of Infectious Diseases* **165**:322-328.

Cavet ME, West M and Simmons NL (1997a) Fluoroquinolone (Ciprofloxacin) Secretion By Human Intestinal Epithelial (Caco-2) Cells. *British Journal Of Pharmacology* **121**:1567-1578.

Cavet ME, West M and Simmons NL (1997b) Transepithelial Transport Of The Fluoroquinolone Ciprofloxacin By Human Airway Epithelial Calu-3 Cells. *Antimicrobial Agents & Chemotherapy* **41**:2693-2698.

Chen L, Chetty D and Chien Y (1999) A Mechanistic Analysis to Characterize Permeation Properties. *International Journal of Pharmaceutics* **184**:63-72.

Cogburn JN, Donovan MG and Schasteen CS (1991) A Model Of Human Small Intestinal Absorptive Cells. 1. Transport Barrier. *Pharmaceutical Research* **8**:210-216.

Conradi RA and Hilger AR (1992) The Influence Of Peptide Structure On Transport Across Caco-2 Cells. II. Peptide Bond Modification Which Results In Improved Permeability. *Pharmaceutical Research* **9/3**:435-439.

Cormet E, Huneau JF, Bouras M, Carbon C, Rubinstein E and Tome D (1997a) Evidence For A Passive Diffusion Mechanism For Sparfloxacin Uptake At The Brush-Border Membrane Of The Human Intestinal Cell-Line Caco-2. *Journal Of Pharmaceutical Sciences* **86**:33-36.

Cormet E, Huneau JF and Tome D (1997b) Sparfloxacin Binds To Rabbit Intestinal Brush-Border Membrane Vesicles By Ionic Interactions. *International Journal Of Pharmaceutics* **159**:127-130.

Cormet-Boyaka E, Huneau JF, Mordrelle A, Boyaka PN, Carbon C, Rubinstein E and Tome T (1998) Secretion Of Sparfloxacin From The Human Intestinal Caco-2 Cell Line Is Altered By P-Glycoprotein Inhibitors. *Antimicrobial Agents and Chemotherapy* **42**:2607-2611.

Daugherty AL and Mrsny RJ (1999) Transcellular Uptake Mechanisms Of The Intestinal Epithelial Barrier - Part One. *Pharmaceutical Science & Technology Today* **2**:144-151.

Dautrey S, Rabbaa L, Laouari D, Lacour B, Carbon C and Farinotti R (1999) Influence Of Renal Failure On Intestinal Clearance Of Ciprofloxacin In Rats. *Antimicrobial Agents and Chemotherapy* **43**:678-680.

Ding GH, Naora K, Nagasako S, Hirano H and Iwamoto K (1998) Excretion Of Ofloxacin Into Saliva In Rats With Renal Failure. *Journal Of Pharmacology and Experimental Therapeutics* **287**:31-36.

Dohgen M, Hayashi H, Yajima T and Suzuki T (1994) Stimulation Of Bicarbonate Secretion By Luminal Short-Chain Fatty Acids In The Rat And Human Colon In Vivo. *Japanese Journal of Physiology* **44**:519-531.

Emi Y, Tsunashima D, Ogawara K-I, Higaki K and Kimura T (1998) Role of P-Glycoprotein as a Secretory Mechanism in Quinidine Absorption from Rat Small Intestine. *Journal of Pharmaceutical Sciences* **87**:295-299.

Escribano E, Calpena AC, Garrigues TM, Freixas J, Domenech J and Moreno J (1997) Structure-Absorption Relationships Of A Series Of 6-Fluoroquinolones. *Antimicrobial Agents and Chemotherapy* **41**:1996-2000.

Franklin TJ and Snow. GA eds (1989) *Biochemistry of Antimicrobial Action*. London, Chapman and Hall.

Freshney IR (1994) *Culture of Animal Cells*. New York, Chichester, Wiley-Liss.

Ghose AK and Crippen GM (1985) Use Of Physicochemical Parameters In Distance Geometry And Related Three-Dimensional Quantitative Structure-Activity Relationships: A Demonstration Using Escherichia Coli Dihydrofolated Reductase Inhibitors. *Journal of Chemical Information and Computer Science* **28**:333-346.

Gombar VK and Enslein. K (1996) Assessment Of N-Octanol/Water Partition Coefficient: When Is The Assessment Reliable? *Journal Of Chemical Information And Computer Science.* **36**:1127-1134.

Grasset E, Pinto M, Dussaulx E, Zweibaum A and Desjeux J-F (1984) Epithelial Properties Of Human Colonic Carcinoma Cell Line Caco-2: Electrical Parameters. *American Journal of Physiology* **247**:C260-C267.

Greenwood D ed (1995) *Antimicrobial Chemotherapy*. Oxford University Press.

Griffiths NM, Hirst BH and Simmons NL (1993) Active Secretion Of the Fluoroquinolone Ciprofloxacin By Human Intestinal Epithelial Caco-2 Cell-Layers. *British Journal Of Pharmacology* **108**:575-576.

Griffiths NM, Hirst BH and Simmons NL (1994) Active Intestinal Secretion Of the Fluoroquinolone Antibacterials Ciprofloxacin, Norfloxacin and Pefloxacin - a Common Secretory Pathway. *Journal Of Pharmacology and Experimental Therapeutics* **269**:496-502.

Hansch C and Leo AJ (1979) Substituent Constants For Correlation. *Analysis in Chemistry and Biology*.

Herbette L (1999) Artists Impression Of Phospholipid Bilayer, Taken from Sirius Instrument Manual.

Hidalgo IJ, Raub TJ and Borchardt RT (1989) Characterization Of the Human-Colon Carcinoma Cell-Line (Caco-2) As a Model System For Intestinal Epithelial Permeability. *Gastroenterology* **96**:736-749.

Higgins CF, Callaghan R, Linton KJ and Rosenberg MF (1997) Structure Of Multidrug Resistance P-Glycoprotein. *Seminars in Cancer Biology* **8**:135-142.

Hooper DC and Wolfson JS eds (1993) *Quinolone Antimicrobial Agents*. American Society for Microbiology.

Hoskins J, Deherdt SV, Moore RE and Bumol TF (1993) The Development and Characterization Of Vinca Alkaloid-Resistant Caco-2 Human Colorectal Cell-Lines Expressing MDR-1. *International Journal Of Cancer* **53**:680-688.

Hugoi WB and Russell. AD eds (1998) *Pharmaceutical Microbiology*. Oxford, Blackwell Science.

Hunter J and Hirst BH (1997) Intestinal Secretion Of Drugs. The Role Of P-Glycoprotein And Related Drug Efflux Systems In Limiting Oral Drug Absorption. *Advanced Drug Delivery Reviews* **25**:129-157.

Hunter J, Hirst BH and Simmons NL (1993) Drug Absorption Limited By P-Glycoprotein-Mediated Secretory Drug Transport In Human Intestinal Epithelial Caco-2 Cell-Layers. *Pharmaceutical Research* **10**:743-749.

Ichikawa N, Naora K and Iwamoto K (1994) Comparative Study Of Permeability Into Rat Cerebrospinal Fluid Of The Quinolones: Dependency On Their Lipophilicities. *Biological and Pharmaceutical Bulletin* **17**:152-155.

Inui K, Yamamoto M and Saito H (1992) Transepithelial Transport Of Oral Cephalosporins By Monolayers Of Intestinal Epithelial Cell Line Caco-2 Cells-2: Specific Transport Systems In Apical And Basolateral Membranes. *Journal Of Pharmacology And Experimental Therapeutics.* **261/1**:195-201.

Iseki K, Hirano T, Fukushi Y, Kitamura Y, Miyazaki S, Takada M, Sugawara M, Saitoh H and Miyazaki K (1992) The pH Dependent Uptake of Enoxacin by Rat Intestinal Brush-border Membrane Vesicles. *Journal of Pharmacy and Pharmacology* **44**:722-726.

Iseki K, Hirano T, Tsuji K, Miyazaki S, Takada M, Kobayashi M, Sugawara M and Miyazaki K (1998) Ionic-Diffusion Potential-Dependent Transport Of A New Quinolone, Sparfloxacin, Across Rat Intestinal Brush-Border Membrane. *Journal Of Pharmacy and Pharmacology* **50**:627-634.

Ito T, Yano I, Tanaka K and Inui KI (1997) Transport Of Quinolone Antibacterial Drugs By Human P-Glycoprotein Expressed In A Kidney Epithelial Cell Line, LLC-PK1. *Journal of Pharmacology and Experimental Therapeutics* **282**:955-960.

Ito T, Yano I, Masuda S, Hashimoto Y and Inui K (1999) Distribution Characteristics Of Levofloxacin And Grepafloxacin In Rat Kidney. *Pharmaceutical Research* **16**:534-539.

Ito T, Yano I, Hashimoto Y and Inui K-i (2000) Transepithelial Transport Of Levofloxacin In The Isolated Perfused Rat Kidney. *Pharmaceutical Research* 17:236-241.

Jaehde U, Langemeijer MW, de Boer AG and Breimer DD (1992) Cerebrospinal Fluid Transport And Disposition Of The Quinolones Ciprofloxacin And Pefloxacin In Rats. *Journal of Pharmacology & Experimental Therapeutics* 263:1140-1146.

Jaehde U, Goto T, Deboer AG and Breimer DD (1993) Blood-Brain-Barrier Transport Rate Of Quinolone Antibacterials Evaluated In Cerebrovascular Endothelial-Cell Cultures. *European Journal Of Pharmaceutical Sciences* 1:49-55.

Jaehde U, Sorgel F, Reiter A, Sigl G, Naber KG and Schunack W (1995) Effect Of Probenecid On the Distribution and Elimination Of Ciprofloxacin In Humans. *Clinical Pharmacology & Therapeutics* 58:532-541.

Jim LK, El-Sayed N and Al-Khamis (1992) A Simple High Performance Liquid Chromatographic Assay For Ciprofloxacin In Human Serum. *Journal Of Clinical Pharmacy And Therapeutics* 17:111-115.

Kaatz GW, Seo SM and Ruble CA (1993) Efflux-Mediated Fluoroquinolone Resistance In Staphylococcus-aureus. *Antimicrobial Agents and Chemotherapy* 37:1086-1094.

Karali TT, Maewawa H, Okano T, Inui K and Hori R (1989) Gastrointestinal Absorption Of Drugs. *Critical Reviews in Therapeutic Drug Carrier Systems* 6:39-86.

Kidwai M, Misra P and Kumar R (1998) The Fluorinated Quinolones. *Current Pharmaceutical Design* 4:101-118.

Klopman G, Ding C and Macina. OT (1997) Computer Aided Olive Oil-Gas Partition Coefficient Calculations. *Journal Of Chemical Information And Computer Science.* 37:569-575.

Kusuhara H, Suzuki H and Sugiyama Y (1998) The Role of P-Glycoprotein and Canalicular Multispecific Organic Anion Transporter in the Hepatobiliary Excretion of Drugs. *Journal of Pharmaceutical Sciences* **87**:1025-1040.

Lennernas H (1998) Human Intestinal Permeability. *Journal of Pharmaceutical Sciences* **87/4**:403-410.

Leo A, Hansch C and Elkins D (1971) Partition Coefficients And Their Uses. *Chemical Reviews* **71**:525-616.

Liang R and Fei Y-J (1995) Human Intestinal H+/Peptide Cotransporter. Cloning, Functional Expression, And Chromosomal Localization. *Journal Of Biological Chemistry.* **270/12**:6456-6463.

Lipinski CA (1997) Computational Approach To Potential Absorption Problems: Analysis Of Human Data, In (4th International Conference On Drug Absorption), Edinburgh.

Lombardo F, Blake JF and Curatolo. WJ (1996) Computation Of Brain-Blood Partitioning Of Organic Solutes Via Free Energy Calculations. *Journal Of Medicinal Chemistry* **39**:4750-4755.

Lubasch A, Keller I, Borner K, Koeppe P and Lode H (2000) Comparative Pharmacokinetics of Ciprofloxacin, Gatifloxacin, Grepafloxacin, Levofloxacin, Trovafloxacin and Moxifloxacin after Single Oral Administration in Healthy Volunteers. *Antimicrobial Agents and Chemotherapy* **44**:2600-2603.

Lu S, Gough AW, Bobrowski WF and Stewart BH (1996) Transport Properties Are Not Altered Across Caco-2 Cells With Heightened TEER Despite Underlying Physiological And Ultrastructural Changes. *Journal Of Pharmaceutical Sciences* **85**:270-273.

MacAdam A (1993) The Effect Of Gastro-Intestinal Mucus On Drug Absorption. *Advanced Drug Delivery Reviews* **11**:201-220.

Mannhold R, Rekker RF and Sonntag C (1995) Comparative Evaluation Of The Predictive Power Of Calculation Procedures Of Molecular Lipophilicity. *Journal Of Pharmaceutical Sciences* **84/12**:1410-1419.

Matsuo Y, Yano I, Ito T, Hashimoto Y and Inui KI (1998) Transport Of Quinolone Antibacterial Drugs In A Kidney Epithelial Cell Line, LLC-PK1. *Journal Of Pharmacology and Experimental Therapeutics* **287**:672-678.

Mehta AC, Davis SH and Kay EA (1992) High Performance Liquid Chromatographic Determination Of Ciprofloxacin In Plasma. *Journal Of Clinical Pharmacy And Therapeutics* **17**:117-120.

Merino V, Freixas J, del Val Bermejo M, Garrigues TM, Moreno J and Pla-Delfina JM (1995) Biophysical Models As An Approach To Study Passive Absorption In Drug Development: 6-Fluoroquinolones. *Journal of Pharmaceutical Sciences* **84**:777-782.

Merino V, Martin-Algarra RV, Rocher A, Garrigues TM, Freixas J and Polache A (1997) Effects Of Ethanol On Intestinal Absorption Of Drugs. I. In Situ Studies With Ciprofloxacin Analogs In Normal And Chronic Alcohol-Fed Rats. *Alcoholism: Clinical & Experimental Research* **21**:326-333.

Mizuma T, Sakai N and Awazu S (1994) Na+-Dependent Transport of aminopeptidase-resistant sugar-coupled tripeptides in rat intestine. *Biochemical and Biophysical Research Communication* **203**:1412-1416.

Moriguchi I, Hirono S, Liu Q, Nakagome I and Matsushita Y (1992) Simple Method of Calculating Octanol/Water Coefficient. *Chemical Pharmaceutical Bulletin* **40(1)**:127-130.

Moriguchi I, Hirono S, Nakagome I and Hirano H (1994) Comparison Of Reliabilty Of Logp Values For Drugs Calculated By Several Methods. *Chemical Pharmaceutical Bulletin* **42(4)**:976-978.

Nicklin P, Irwin B, Hassan I, Williamson I and Mackay M (1992) Permeable Support Type Influences The Transport Of Compounds Across Caco-2 Cells. *International Journal Of Pharmaceutics* **83**:197-209.

Nightingale CH (1994) Pharmacokinetic And Pharmacodynamic Properties Of Quinolones, *A Contemporary Assessment of Quinolone Therapy* (Nightingale CH ed) pp 3-10, University of Wisconsin (USA).

Nouaille-Degorce B, Veau C, Dautrey S, Tod M, Laouari D, Carbon C and Farinotti R (1998) Influence Of Renal Failure On Ciprofloxacin Pharmacokinetics In Rats. *Antimicrobial Agents Chemotherapy* **42**:289-292.

Ooie T, Suzuki H, Terasaki T and Sugiyama Y (1996a) Characterization of the Transport Properties of a Quinolone Antibiotic, Fleroxacin, in Rat Choroid Plexus. *Pharmaceutical Research* **13**:523-527.

Ooie T, Suzuki H, Terasaki T and Sugiyama Y (1996b) Comparative Distribution Of Quinolone Antibiotics In Cerebrospinal Fluid And Brain In Rats And Dogs. *Journal Of Pharmacology and Experimental Therapeutics* **278**:590-596.

Ooie T, Terasaki T, Suzuki H and Sugiyama Y (1997) Kinetic Evidence For Active Efflux Transport Across The Blood-Brain Barrier Of Quinolone Antibiotics. *Journal Of Pharmacology and Experimental Therapeutics* **283**:293-304.

Othman S and Muti H (1988) Studies On The Adsorption And Solubility Of Nalidixic Acid. *International Journal Of Pharmaceutics* **41**:197-203.

Palm K and Luthman K (1996) Correlation Of Drug Absorption With Molecular Surface Properties. *Journal Of Pharmaceutical Sciences* **85/1**:32-39.

Palm K, Stenberg P, Luthman K and Artursson. P (1997) Polar Molecular Surface Properties Predict The Intestinal Absorption Of Drugs In Humans. *Pharmaceutical Research* **14**:568-571.

Pauletti GM, Gangwar S, Knipp GT, Nerurkar MM, Okumu FW, Tamura K, Siahaan TJ and Borchardt RT (1996) Structural Requirements For The Intestinal Absorption Of Peptide Drugs. *Journal of Controlled Release* **41**:3-17.

Pinto M, Robine-Leon S, Appay M-D, Kedinger M, Triadou N, Dussaulx E, Lacroix B, Simon-Assmann P, Haffen K, Fogh J and Zweibaum A (1983) Enterocyte-Like Differentiation And Polarization Of The Human Colon Carcinoma Cell Line Caco-2 In Culture. *Biology of the Cell* **47**:323-330.

Rabbaa L, Dautrey S, Colas-Linhart N, Carbon C and Farinotti R (1996) Intestinal Elimination of Ofloxacin Enatiomers in the Rat: Evidence of a Carrier-Mediated Process. *Antimicrobial Agents and Chemotherapy* **40**:2126-2130.

Rabbaa L, Dautrey S, Colas-Linhart N, Carbon C and Farinotti R (1997) Absorption Of Ofloxacin Isomers In The Rat Small Intestine. *Antimicrobial Agents and Chemotherapy* **41**:2274-2277.

Reece RJ and Maxwell A (1991) DNA Gyrase: Structure and Function. *Critical Reviews in Biochemistry and Molecular Biology* **26**:335-375.

Rekker RF and Laak AMT (1993) On The Reliability Of Calculated Log P-Values: Rekker, Hansch/Leo And Suzuki Approach. *Quantitative Structure Activity Relationships* **15**:152-157.

Reynolds CH (1995) Estimating Lipophilicity Using The GB/SA Continuum Solvation Model: A Direct Method For Computing Partition Coefficients. *Journal Of Chemical Information And Computer Science* **35**:738-742.

Ribadeneira MD and Aungst BJ (1996) Effects Of Structural Modifications On The Intestinal Permeability Of Angiotensin II Receptor Antagonists And The Correlation Of In Vitro, In Situ, And In Vivo Absorption. *Pharmaceutical. Research* **13/2**:227-233.

Rispal P, Grellet J, Celerier C, Breilh D, Dorian M, Pellegrin JL, Saux MC and Leng B (1996) Comparative Uptake Of Sparfloxacin And Ciprofloxacin Into Human THP 1 Monocytic Cells - Evidence For An Organic Anion Transport. *Arzneimittel-Forschung/Drug Research* **46**:316-319.

Ross DL, Elkinton S and Riley CM (1993) Physicochemical Properties Of The Fluoroquinolone Antimicrobials VI. Effect Of Metal Ion Complexation On Octan-1-ol Water Partitioning. *International Journal Of Pharmaceutics* **93**:131-138.

Ross DL and Riley CM (1990) Aqueous Solubilities Of Some Variously Substituted Quinolone Antimicrobials. *International Journal Of Pharmaceutics* **63**:237-250.

Ross DL and Riley CM (1992) Physicochemical Properties Of the Fluoroquinolone Antimicrobials.2. Acid Ionization-Constants and Their Relationship to Structure. *International Journal Of Pharmaceutics* **83**:267-272.

Ross DL and Riley. CM (1992) Physicochemical Properties Of The Fluoroquinolone Antimicrobials. III 1-Octanol/Water Partition Coefficients And Their Relationships To Structure. *International Journal Of Pharmaceutics.* **88**:379-389.

Ross DL and Riley. M (1993) Physicochemical Properties Of The Fluoroquinolone Antimicrobials V. Effect Of Fluoroquinolone Structure And pH On The Complexation Of Various Fluoroquinolone With Magnesium And Calcium Ions. *International Journal Of Pharmaceutics* **93**:121-129.

Rubas W and Cromwell MEM (1996) An Integrated Method To Determine Epithelial Transport And Bioactivity Of Oral Drug Candidates In Vitro. *Pharmaceutical Research.* **13/1**:23-26.

Ruelle P and Kesselring UW (1998) The Hydrophobic Effect. 1. A Consequence Of The Mobile Order In H-Bonded Liquids. *Journal of Pharmaceutical Sciences* **87/8**:987-997.

Russell AD and Chopra I (1996) *Understanding Antibacterial Action and Resistance.* Ellis Horwood

Sasabe H, Terasaki T, Tsuji A and Sugiyama Y (1997) Carrier-Mediated Hepatic Uptake Of Quinolone Antibiotics In The Rat. *Journal of Pharmacology & Experimental Therapeutics* **282**:162-171.

Sasabe H, Tsuji A and Sugiyama Y (1998) Carrier-Mediated Mechanism For The Biliary Excretion Of The Quinolone Antibiotic Grepafloxacin And Its Glucuronide In Rats. *Journal Of Pharmacology and Experimental Therapeutics* **284**:1033-1039.

Sherwood L (1997) *Human Physiology From Cell to Systems.* Wadsworth Publishing Company.

Shibl AM and Tawfik AF (1991) Determination Of Lomefloxacin In Biological Fluids By HPLC And A Microbiological Method. *Journal Of Clinical Pharmacy And Therapeutics* **16**:353-359.

Simanjuntak MT, Sato H, Tamai I, Terasaki T and Tsuji A (1991) Transport Of the New Quinolone Antibacterial Agents Of Lomefloxacin and Ofloxacin By Rat Erythrocytes, and Its Relation to the Nicotinic- Acid Transport-System. *Journal Of Pharmacobio-Dynamics* **14**:475-481.

Sorgel F, Granneman GR, Stephan U and Locke C (1992) Effect Of Cimetidine On The Pharmacokinetics Of Temafloxacin. *Clinical Pharmacokinetics* **22**:75-82.

Sorgel F and Kinzig M (1993) Pharmacokinetics of Gyrase Inhibitors, Part 1: Basic Chemistry and Gastrointestinal Disposition. *The American Journal of Medicine* **94/3A**:3A/44S-43A/55S.

Sorgel F, Naber KG, Jaehde U, Reiter A, Seelmann R and Sigl G (1989) Gastrointestinal Secretion Of Ciprofloxacin. Evaluation Of The Charcoal Model For Investigations In Healthy Volunteers. *American Journal of Medicine* **87**:62S-65S.

Stein WD (1997) Kinetics of Multidrug Transporter (P-Glycoprotein) and Its Reversal. *Physiological Reviews* 77:545-590.

Stryer L (1988) *Biochemistry.* 3rd Edition. Freeman and Company, New York..

Suzuki T and Kudo Y (1990) Automatic LogP Estimation Based On Combined Additive Modelling Methods. *Journal Of Computer Aided Molecular Design* 4:155-198.

Swaan PW, Stehouwer MC and Tukker. JJ (1995) Molecular Mechanism For The Relative Binding Affinity To The Intestinal Peptide Carrier. Comparison Of Three Ace-Inhibitors: Enalapril, Enalaprilat And Lisinopril. *Biochimica Et Biophysica Acta* 1236:31-38.

Takacs-Novak K, Jozan M, Hermecz I and Szaz G (1992) Lipophilicity Of Antibacterial Fluoroquinolones. *International Journal of Pharmaceutics* 79:89-96.

Tsuji A and Tamai I (1996) Carrier Mediated Intestinal Transport Of Drugs. *Pharmaceutical Research* 13:963-977.

Ueda K, Taguchi Y and Morishima M (1997) How Does P-Glycoprotein Recognise Its Substrate? *Seminars in Cancer Biology* 8:151-159.

Uematsu T, Kusajima H, Umemura K, Ishida R, Ohkubo H and Nakashima M (1993) A New Antimicrobial Quinolone (AM-1155) Analysed In Hair As An Index Of Drug Exposure And As A Time-Marker. *Journal of Pharmacy and Pharmacology* 45:1012-1014.

Ungell AL (1997) In Vitro Absorption Studies And Their Relevance To Absorption From The GI Tract. *Drug Development and Industrial Pharmacy* 23:879-892.

Ungell AL, Nylander S, Bergstrand S, Sjoberg A and Lennernas H (1998) Membrane Transport of Drugs in Different Regions of the Intestinal Tract of the Rat. *Journal of Pharmaceutical Sciences* 87/3:360-366.

Vance-Bryan K, Guay DR and Rotschafer JC (1990) Clinical Pharmacokinetics Of Ciprofloxacin. *Clinical Pharmacokinetics* **19**:434-461.

Vancebryan K, Guay DRP and Rotschafer JC (1990) Clinical Pharmacokinetics Of Ciprofloxacin. *Clinical Pharmacokinetics* **19**:434-461.

Walter E and Kissel T (1995) Heterogeneity In the Human Intestinal-Cell Line Caco-2 Leads to Differences In Transepithelial Transport. *European Journal Of Pharmaceutical Sciences* **3**:215-230.

Wang R, Fu Y and Lai. L (1997) A New Atom-Additive Method For Calculating Partition Coefficients. *Journal Of Chemical Information And Computer Science* **37**:615-621.

Werner U, Kissel T and Stuber. W (1997) Effects Of Peptide Structure On Transport Properties Of Seven Thyrotrophin Releasing Hormone (TRH) Analogues In A Human Intestinal Cell Line (Caco-2 Cells-2). *Pharmaceutical Research* **14/2**:246-250.

Wilson APR and Gruneberg RN eds (1997) *Ciprofloxacin: 10 years of clinical experience.* Maxim Medical, Magdalen Centre, The Oxford Science Park, Oxford.

Wilson CG and Washington N (1989) *Physiological Pharmaceutics Biological Barriers to Drug Absorption.* Ellis Horwood Limited, Chichester.

Wilson G, Hassan IF, Dix CJ, Williamson 1, Shah R, Mackay M and Artursson P (1990) Transport and Permeability Properties Of Human Caco-2 Cells - an Invitro Model Of the Intestinal Epithelial-Cell Barrier. *Journal Of Controlled Release* **11**:25-40.

Winiwarter S, Bonham NM, Ax F, Hallberg A, Lennernas H and Karlen A (1998) Correlation Of Human Jejunal Permeability (In Vivo) Of Drugs With

Experimentally And Theoretically Dervived Parameters. A Multivariate Data Analysis Approach. *Journal of Medicinal Chemistry* **41**:4939-4949.

Wright DH, Herman VK, Konstantinides FN and Rotschafer JC (1998) Determination Of Quinolone Antibiotics In Growth Media By Reversed- Phase High-Performance Liquid Chromatography. *Journal of Chromatography B Biomedical Sciences Applied* **709**:97-104.

Yano I, Ito T, Takano M and Inui K-i (1997) Evaluation of Renal Tubular Secretion and reabsorption of Levofloxacin in Rats. *Pharmaceutical Research* **14**:508-511.

Yee SY (1997) In Vitro Permeability Across Caco3 Cells (Colonic) Can Predict In Vivo (Small Intestinal) Absorption In Man - Fact Or Myth. *Pharmaceutical Research* **14**:763-766.

Zeller V, Janoir C, Kitzis MD, Gutmann L and Moreau NJ (1997) Active Efflux As A Mechanism Of Resistance To Ciprofloxacin In Streptococcus Pneumoniae. *Antimicrobial Agents and Chemotherapy* **41**:1973-1978.

APPENDIX A1 - HPLC

A1.1 HPLC CALIBRATION CURVES

The following are calibration curves for each of the quinolones studied, all calibrations curves show good linearity and at least four data points are present.

$y = 0.0165x + 0.0712$

$R^2 = 0.9765$
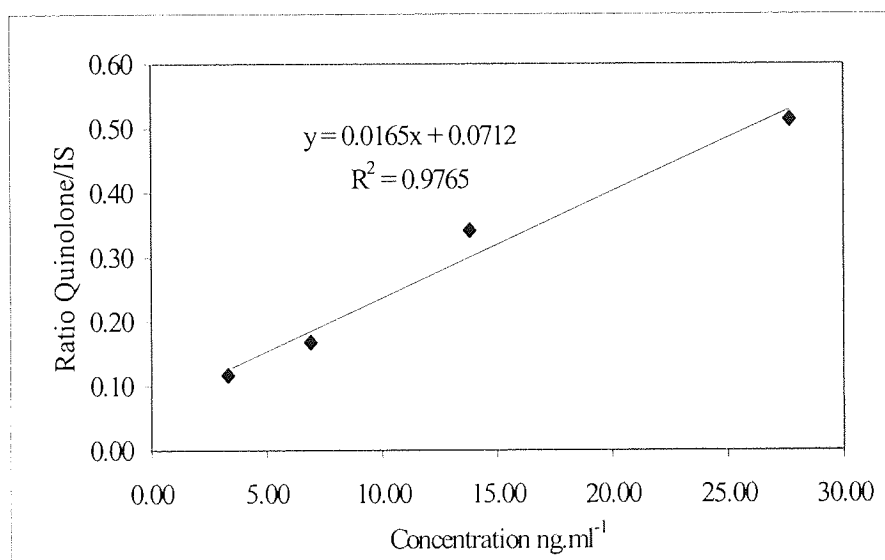
Figure A1.1 - BMS-284756-01

$y = 0.0594x - 0.0073$

$R^2 = 0.9981$
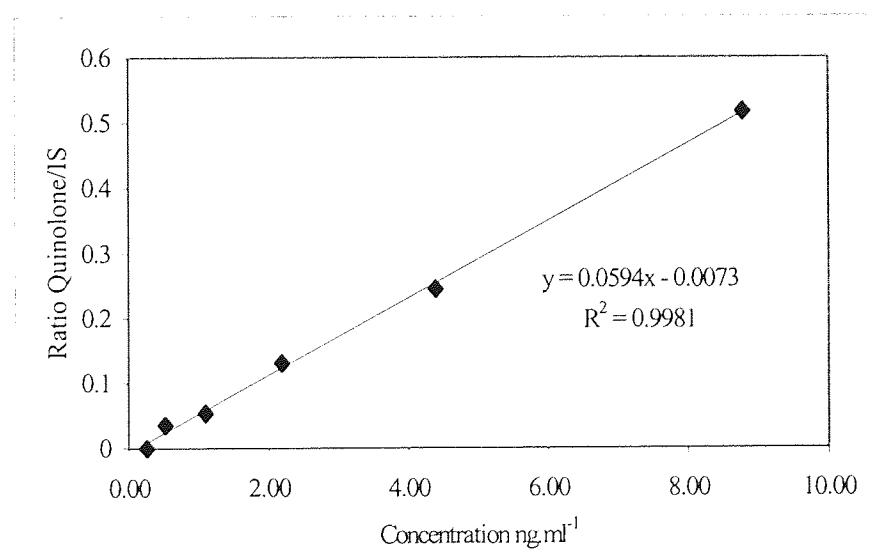
Figure A1.2 - Cinoxacin
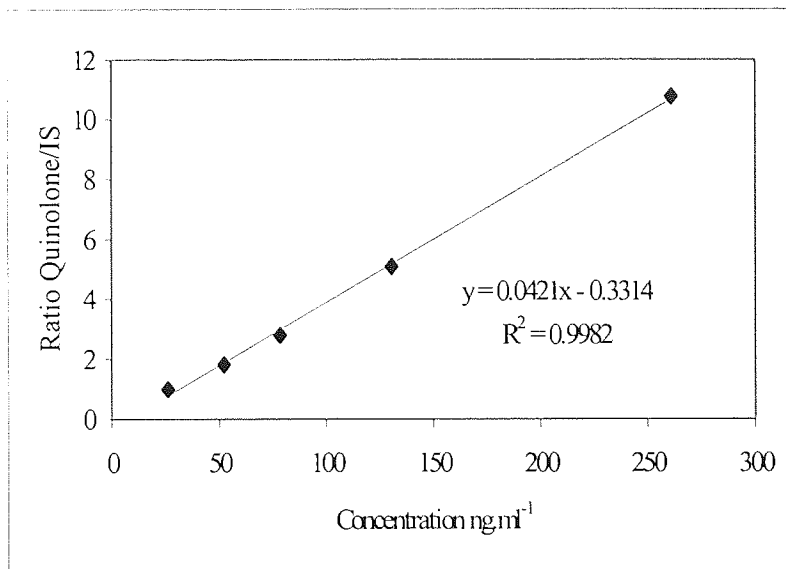
Figure A1.3 - Flumequine
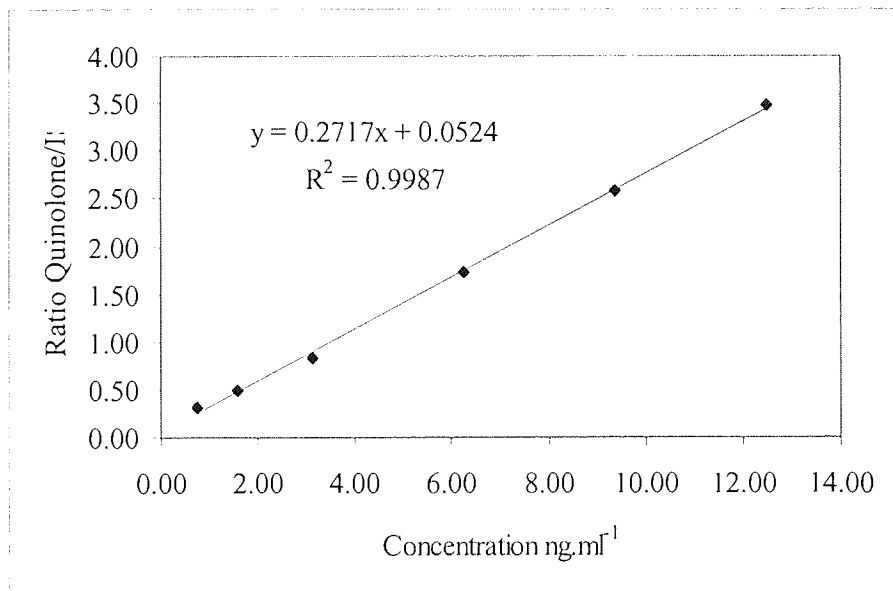
Figure A1.4 – Gatifloxacin
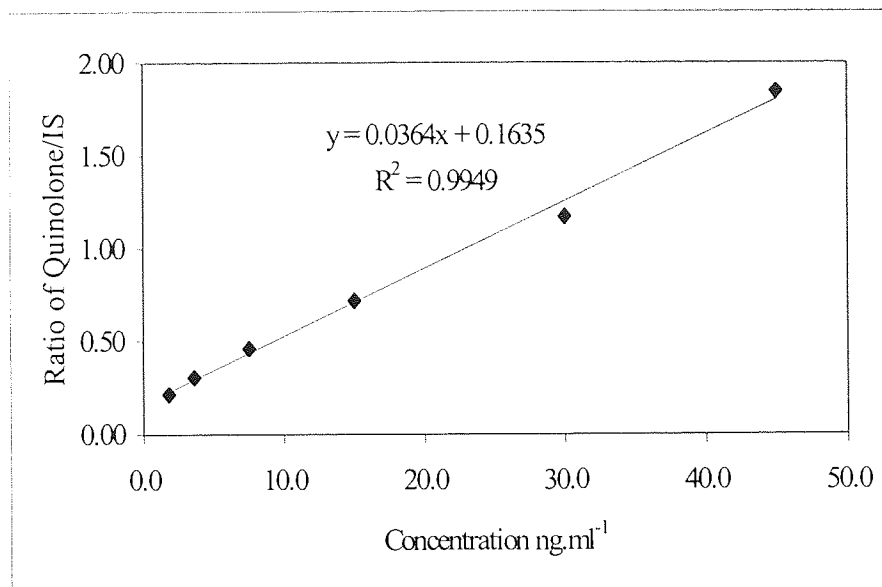
Figure A1.5 – Levofloxacin

$y = 0.0364x + 0.1635$

$R^2 = 0.9949$
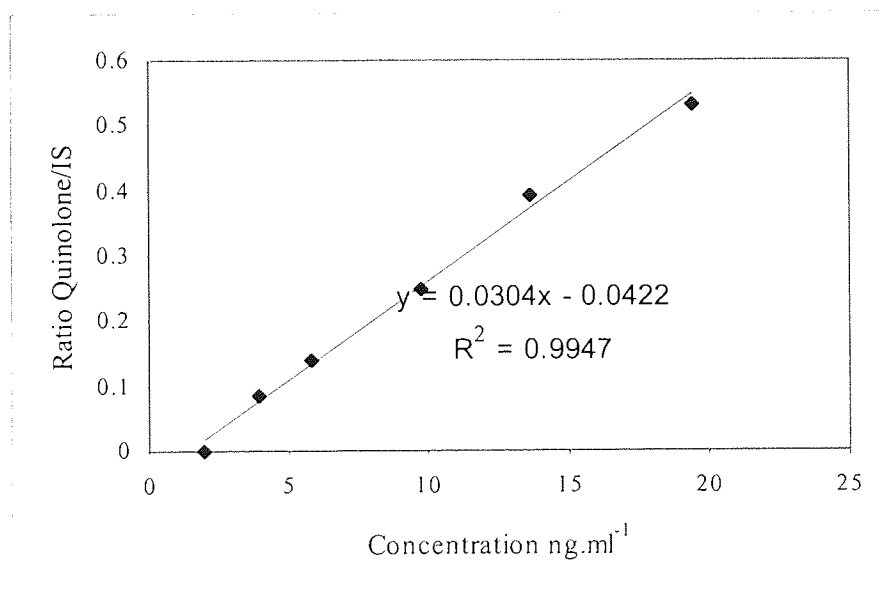
Figure A1.6 – Lomefloxacin

$y = 0.0304x - 0.0422$

$R^2 = 0.9947$
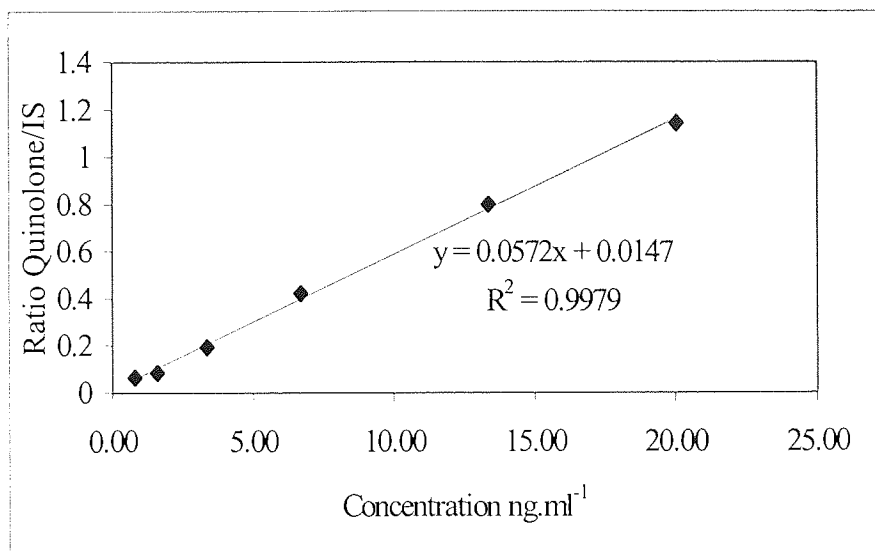
Figure A1.7 - Norfloxacin
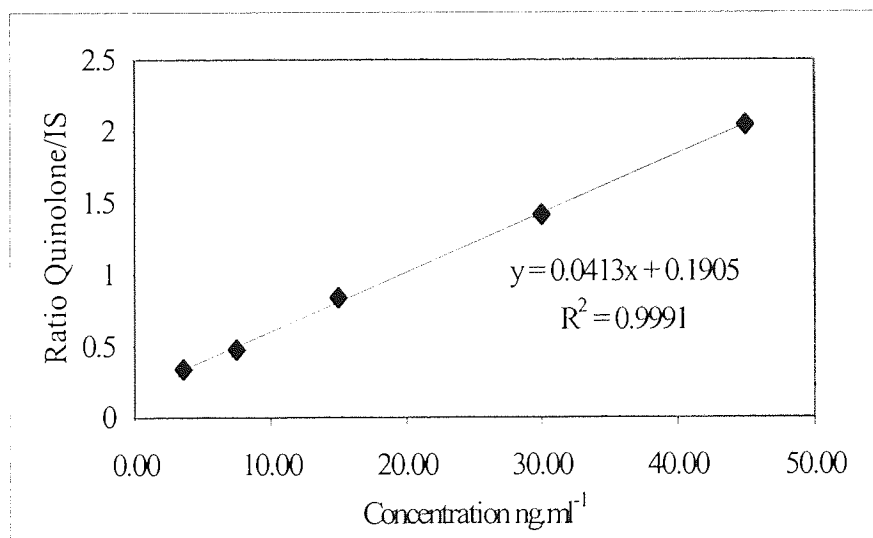
Figure A1.8 – Ofloxacin
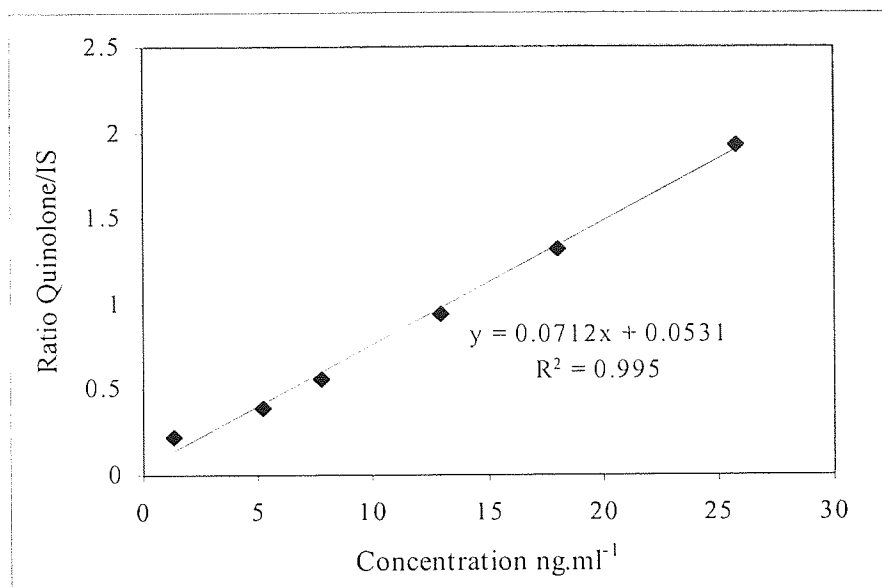
Figure A1.9 – Ciprofloxacin

$$y = 0.0712x + 0.0531$$
$$R^2 = 0.995$$
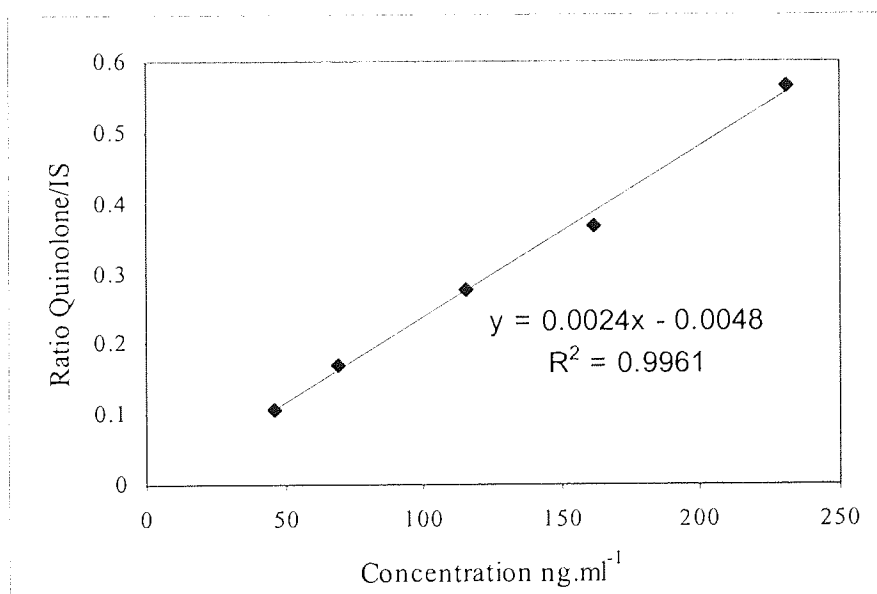
Figure A 1.10 - Methyl-Ciprofloxacin

$$y = 0.0024x - 0.0048$$
$$R^2 = 0.9961$$
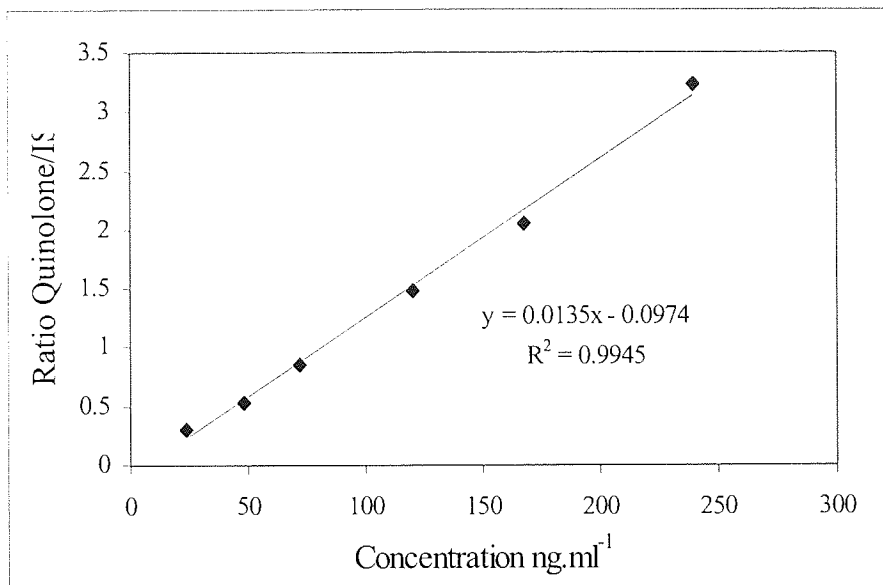
Figure A1.11 - Ethyl-Ciprofloxacin

The graph shows a plot of Ratio Quinolone/IS versus Concentration ng.ml^{-1} with the equation:

$$y = 0.0135x - 0.0974$$
$$R^2 = 0.9945$$
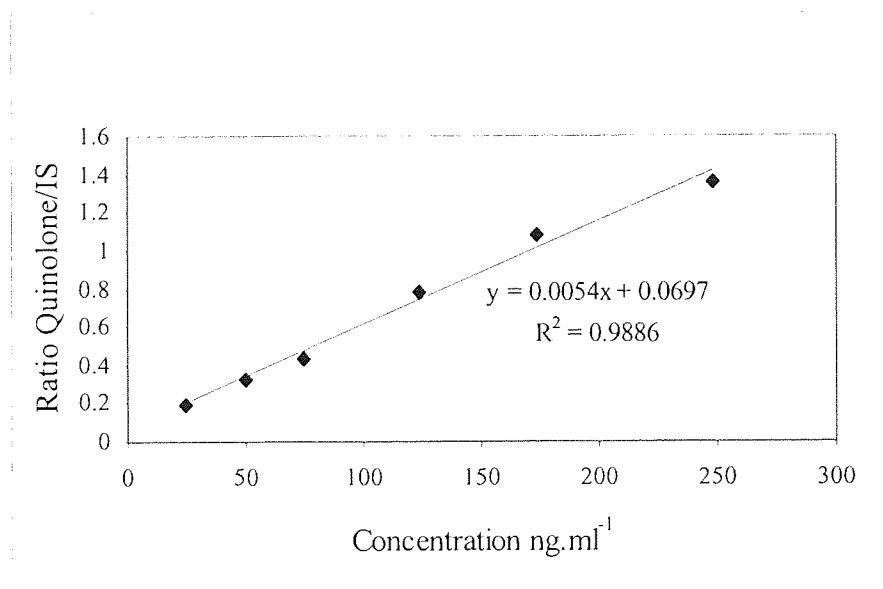
Figure A1.12 – Propyl-Ciprofloxacin

The graph shows a plot of Ratio Quinolone/IS versus Concentration ng.ml^{-1} with the equation:

$$y = 0.0054x + 0.0697$$
$$R^2 = 0.9886$$
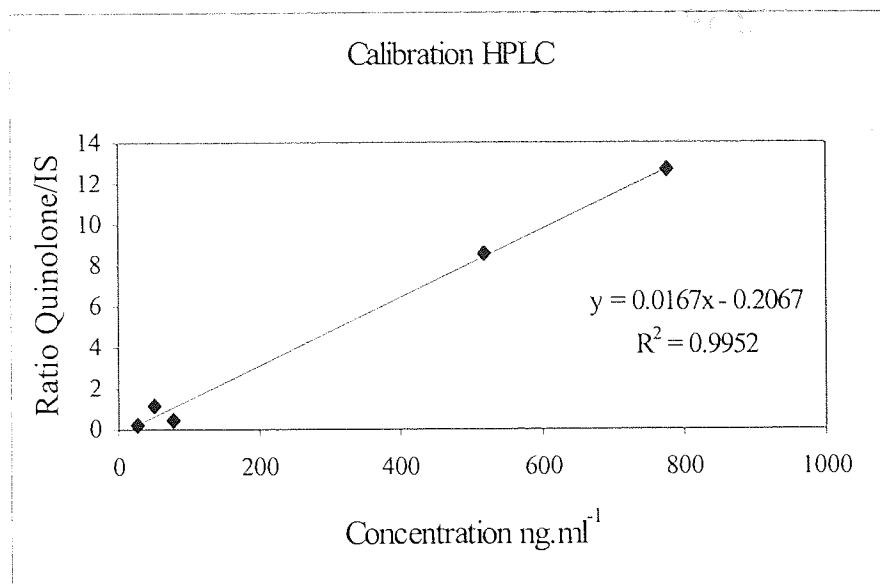
Figure A1.13 - Butyl-Ciprofloxacin
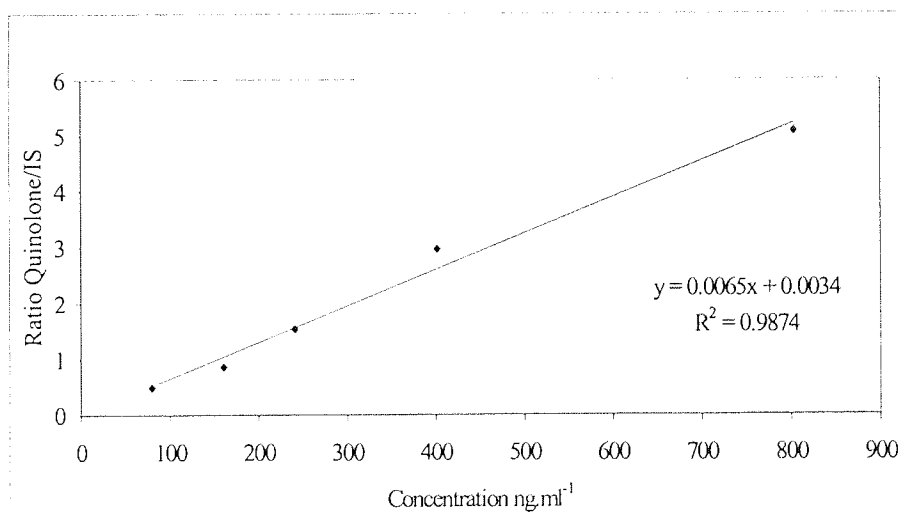
Figure A1.14 - Pentyl-Ciprofloxacin

A1.2 SAMPLE HPLC CHROMATOGRAPHS

The following are sample chromatographs for each of the quinolones assayed using HPLC.

P. NO	TIME	AREA	MK	IDNO	CONC	NAME
1	1.678	703271	E		5.9409	
2	2.38	46106			0.39	
3	2.535	256660	V		2.1712	
4	3.28	1983130			16.7764	
5	4.823	8781577	S		74.2884	
6	5.505	11523	T		0.0975	
7	5.752	14893	T		0.126	
8	5.928	24761	TV		0.2095	
	TOTAL	11820919			100	
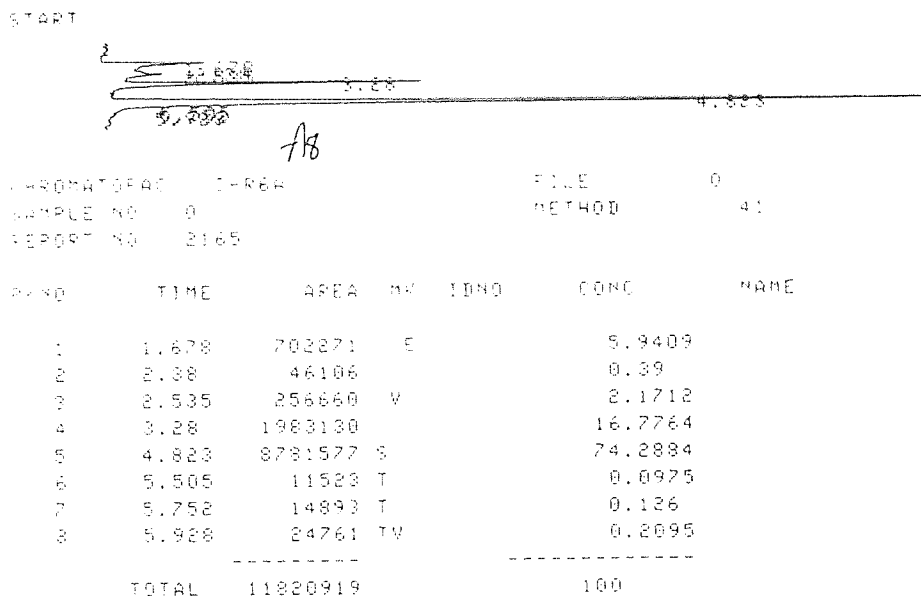
Figure A1.15 - BMS-284756-01

17·49 ng·ml⁻¹

	TIME	AREA			CONC	NAME
1	5.148	574250			24.9039	
2	5.993	1529535			75.0961	
	TOTAL	2004749			100	

Figure A1.16 - Cinoxacin

START

261·11ng.ml⁻¹

CHROMATOPAC   C-R6A   FILE   0
SAMPLE NO   0   METHOD   41

PKNO   TIME   AREA   MV IDNO   CONC   NAME

    1   3.167   572062   8.503
    2   4155663   91.4969
                       ---------   ----------
         TOTAL   100

Figure A1.17 - Flumequine

START

    1.21
    4.398   2.98

124·96ng.ml⁻¹

CHROMATOPAC   C-R6A   FILE   0
SAMPLE NO   0   METHOD   41
REPORT NO   5538

PKNO   TIME   AREA   MK IDNO   CONC   NAME

    1   1   161894   3.4537
    2   1.21   67920   V   1.4489
    3   2.98   3933827   83.92
    4   4.398   523952   V   11.1774
                       ---------   ----------
         TOTAL   4687593   100

Figure A1.18 - Gatifloxacin

```
START
```


44.99 ng.ml⁻¹

```
CHROMATOPAC    C-R6A              FILE          0
SAMPLE NO    0                    METHOD        41
REPORT NO    5845

PKNO     TIME       AREA   MK  IDNO      CONC        NAME

  1     1.267      32127                 0.9606
  2     1.865    2153166                64.3832
  3     4.62     1159004                34.6561
                 ---------             -------------
         TOTAL    3344297               100
```
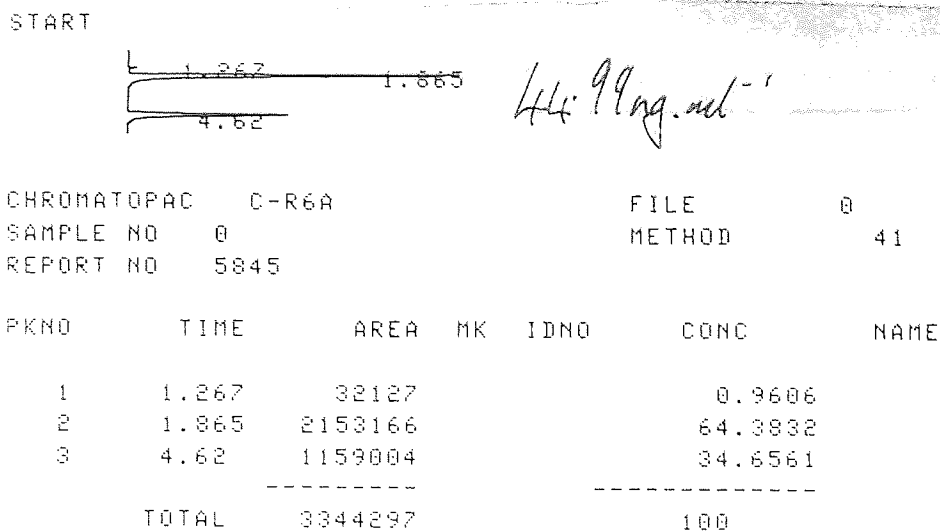
Figure A1.19 - Levofloxacin

180 ng.ml⁻¹

IS
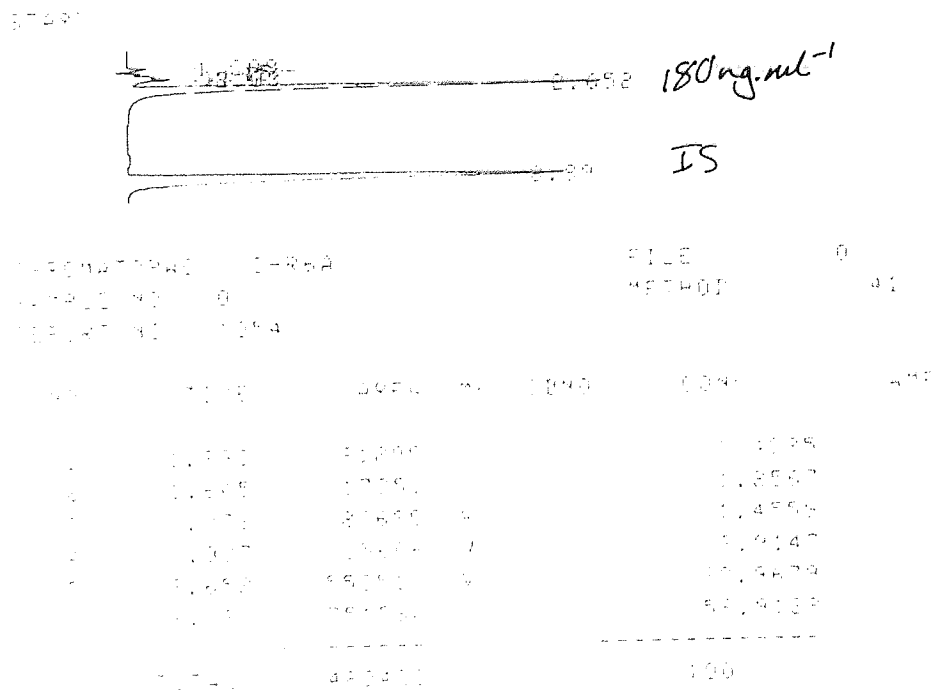
Figure A1.20 - Lomefloxacin

START

2.196

1.592 ng.ml⁻¹
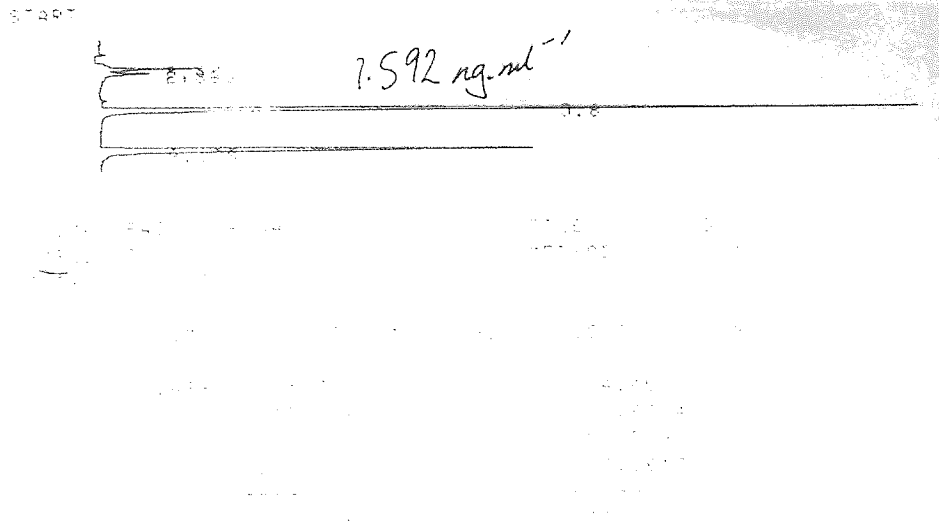
Figure A1.21 - Norfloxacin

START

1.182   1.755   *44.95 ng.ml⁻¹*

4.347

```
CHROMATOPAC    C-R6A                    FILE           0
SAMPLE NO    0                          METHOD           41
REPORT NO    5838

PKNO       TIME        AREA   MK   IDNO      CONC        NAME

    1      1.182      20643                  0.6013
    2      1.755     2297483                66.9209
    3      4.347     1115006                32.4778
                    ---------              ------------
           TOTAL     3433132                  100
```
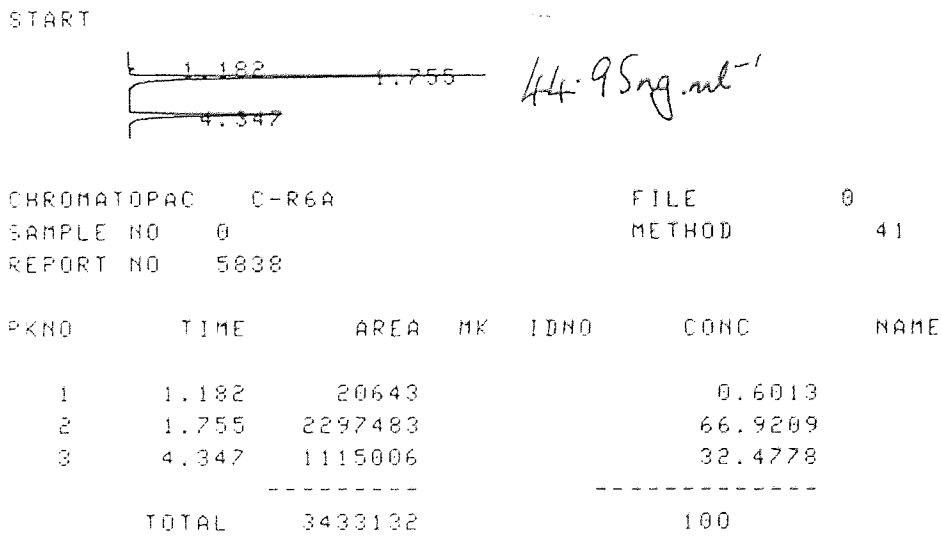
Figure A1.22 - Ofloxacin

START

1.377
2.122
4.87

11.02 ng.ml⁻¹
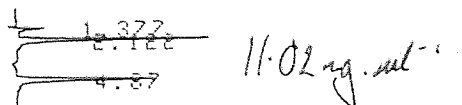
```
CHROMATOPAC    C-R6A              FILE          0
SAMPLE NO    0                    METHOD          41
REPORT NO    5608

PKNO      TIME        AREA   MK  IDNO      CONC        NAME

  1      1.377       88147                8.3615
  2      2.122      510787               48.4524
  3      4.87       455269               43.1861
                   ---------            -------------
         TOTAL     1054203                100
```

Figure A1.23 - Ciprofloxacin

230.69 ng.ml⁻¹
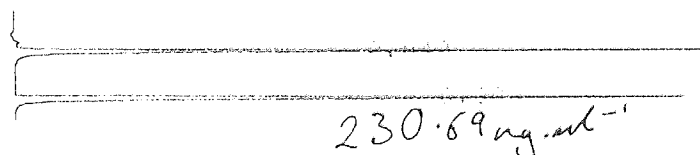
Figure A1.24 - Methyl-Ciprofloxacin

359. 1ng.ml⁻¹
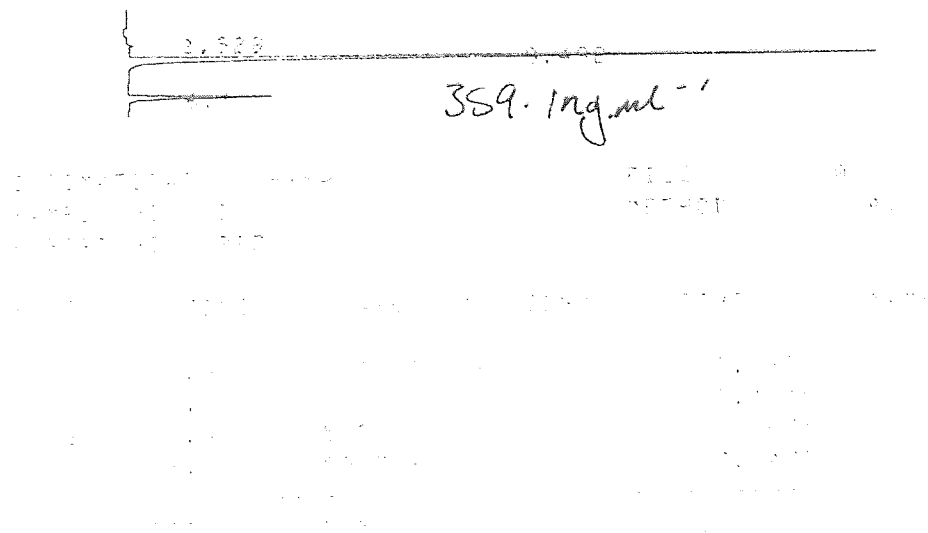
Figure A1.25 - Ethyl-Ciprofloxacin

248.2ng.ml⁻¹
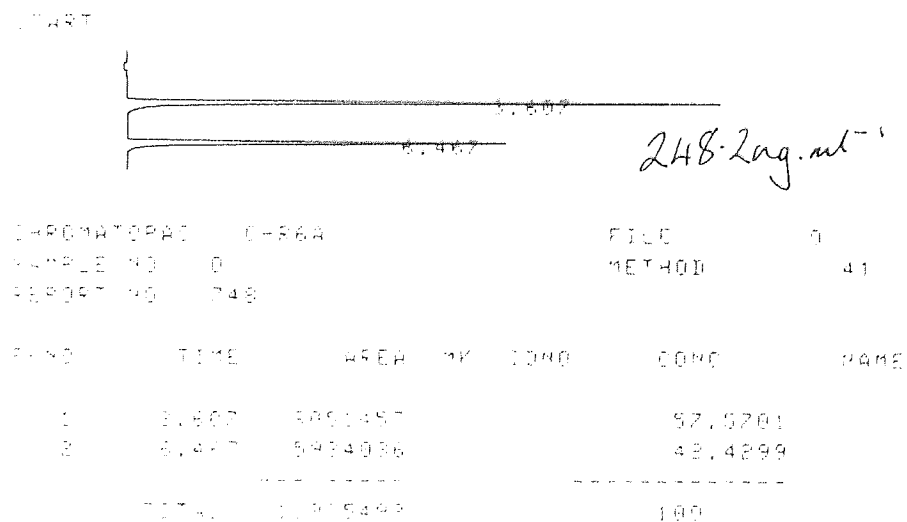
Figure A1.26 - Propyl-Ciprofloxacin

$778 \cdot 16 \, ng. \, ml^{-1}$
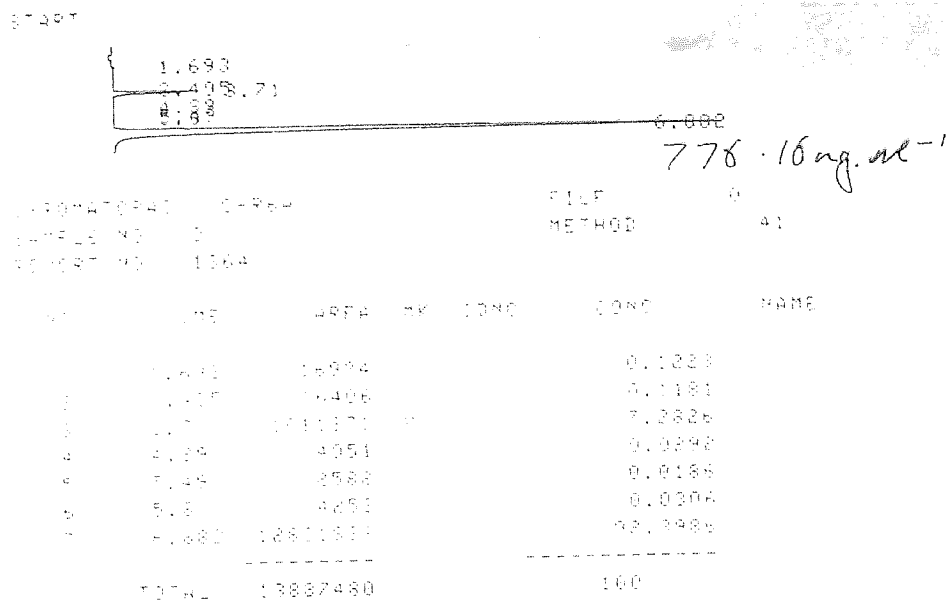
Figure A1.27 - Butyl-Ciprofloxacin

$40 \cdot 242 \, ng.$
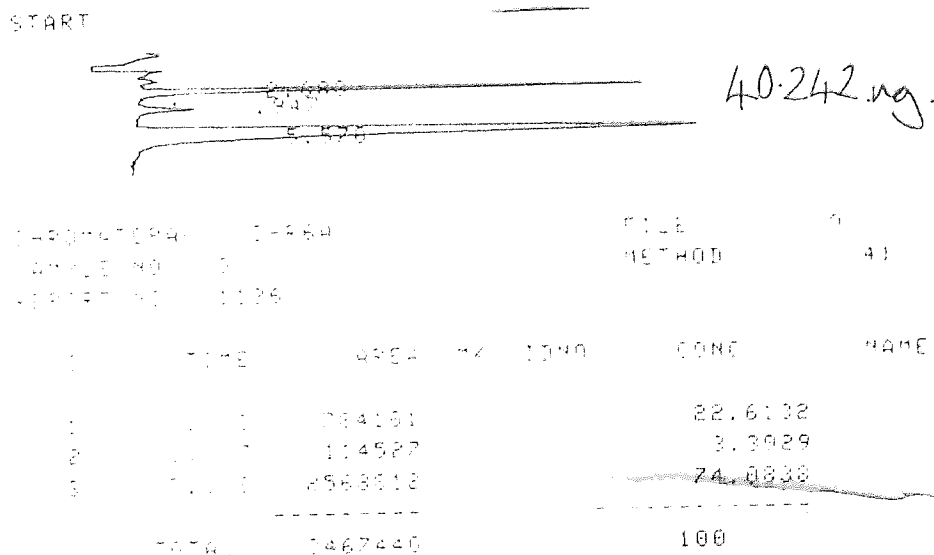
Figure A1.28 - Pentyl-Ciprofloxacin

APPENDIX A2 - SMILES

Quinolone	SMILES Structure
BMS 284756-01	O=C1C(C(O)=O)=CN(C4CC4)C2=C1C=C(F)C(C3=CC=C(C(C)NC5)C5=C3)=C2OC(F)F
Cinoxacin	O=C2C1=CC3=C(OCO3)C=C1N(CC)N=C2C(O)=O
Ciprofloxacin	O=C1C(C(O)=O)=CN(C4CC4)C2=C1C=C(F)C(N3CCN([H])CC3)=C2
Butyl-Ciprofloxacin	O=C1C(C(O)=O)=CN(C4CC4)C2=C1C=C(F)C(N3CCN(C[CH2]CC)CC3)=C2
Ethyl-Ciprofloxacin	O=C1C(C(O)=O)=CN(C4CC4)C2=C1C=C(F)C(N3CCN([CH2]C)CC3)=C2
Methyl-Ciprofloxacin	O=C1C(C(O)=O)=CN(C4CC4)C2=C1C=C(F)C(N3CCN(C)CC3)=C2
Pentyl-Ciprofloxacin	O=C1C(C(O)=O)=CN(C4CC4)C2=C1C=C(F)C(N3CCN(CCCCC)CC3)=C2
Propyl-Ciprofloxacin	O=C1C(C(O)=O)=CN(C4CC4)C2=C1C=C(F)C(N3CCN(CCC)CC3)=C2
Enoxacin	O=C2C1=CC(F)=C(N3CCN([H])CC3)N=C1N(CC)C=C2C(O)=O
Flumequine	O=C2C1=CC(F)=CC3=C1N(C(C)CC3)C=C2C(O)=O
Gatifloxacin	O=C1C(C(O)=O)=CN(C3CC3)C2=C1C=C(F)C(N4CC(C)NCC4)=C2OC
Levofloxacin	O=C2C1=CC(F)=C(N4CCN(C)CC4)C3=C1N([C@H](C)CO3)C=C2C(O)=O
Lomefloxacin	O=C2C1=CC(F)=C(N3CCN([H])C(C)C3)C(F)=C1N(CC)C=C2C(O)=O
Nalidixic Acid	O=C1C(C(O)=O)=CN(CC)C2=C1C=CC(C)=N2
Norfloxacin	O=C2C1=CC(F)=C(N3CCN([H])CC3)C=C1N(CC)C=C2C(O)=O
Ofloxacin	O=C2C1=CC(F)=C(N4CCN(C)CC4)C3=C1N(C(C)CO3)C=C2C(O)=O
Sparfloxacin	O=C1C(C(O)=O)=CN(C3CC3)C2=C1C(N)=C(F)C(N4C[C@H](C)N[C@H](C)C4)=C2F
Fluoroscein	OC1=CC2=C(C5(C4=CC=CC=C4C(O5)=O)C(C=CC(O)=C3)=C3O2)C=C1

APPENDIX A3 – SAMPLE CALCULATIONS

A3.1 D-[1-^{14}C]Mannitol

Sample calculation for D-[1-^{14}C]mannitol (10µM) transport.

		VD (µL)	VR (µL)	SAMPLE (µL)	VD CONC (µg.mL^{-1})	VD AMOUNT (ng)		
		1500	2600	150	1.93	2898.87		
Well	Time (s)	Vr Conc (ng.ml^{-1})	Amount removed (ng)	Amount in Vr (ng)	Cumalative Amount removed (ng)	Corrected Amount Vr (ng)	% Flux	Amount (g)
A01	300	2.23	3.34E-01	5.79E+00	0.00E+00	5.79E+00	0.20	5.79E-09
A02	600	2.61	3.91E-01	6.78E+00	3.34E-01	7.11E+00	0.25	7.11E-09
A03	900	2.93	4.39E-01	7.61E+00	7.25E-01	8.34E+00	0.29	8.34E-09
A04	1200	3.35	5.02E-01	8.70E+00	1.16E+00	9.87E+00	0.34	9.87E-09
A05	1500	3.66	5.49E-01	9.51E+00	1.67E+00	1.12E+01	0.39	1.12E-08
A06	1800	3.79	5.68E-01	9.84E+00	2.22E+00	1.21E+01	0.42	1.21E-08
A07	2100	4.06	6.09E-01	1.06E+01	2.78E+00	1.33E+01	0.46	1.33E-08
A08	2400	4.26	6.38E-01	1.11E+01	3.39E+00	1.45E+01	0.50	1.45E-08
B01	300	2.23	3.34E-01	5.79E+00	0.00E+00	5.79E+00	0.20	5.79E-09
B02	600	2.59	3.88E-01	6.72E+00	3.34E-01	7.06E+00	0.24	7.06E-09
B03	900	2.95	4.42E-01	7.66E+00	7.22E-01	8.38E+00	0.29	8.38E-09
B04	1200	3.24	4.86E-01	8.42E+00	1.16E+00	9.59E+00	0.33	9.59E-09
B05	1500	3.49	5.24E-01	9.08E+00	1.65E+00	1.07E+01	0.37	1.07E-08
B06	1800	3.67	5.50E-01	9.53E+00	2.17E+00	1.17E+01	0.40	1.17E-08
B07	2100	3.96	5.93E-01	1.03E+01	2.72E+00	1.30E+01	0.45	1.30E-08
B08	2400	4.34	6.51E-01	1.13E+01	3.32E+00	1.46E+01	0.50	1.46E-08
C01	300	2.20	3.30E-01	5.72E+00	0.00E+00	5.72E+00	0.20	5.72E-09
C02	600	2.60	3.90E-01	6.76E+00	3.30E-01	7.09E+00	0.24	7.09E-09
C03	900	2.83	4.24E-01	7.35E+00	7.20E-01	8.07E+00	0.28	8.07E-09
C04	1200	3.27	4.90E-01	8.50E+00	1.14E+00	9.64E+00	0.33	9.64E-09
C05	1500	3.49	5.24E-01	9.09E+00	1.63E+00	1.07E+01	0.37	1.07E-08
C06	1800	3.81	5.72E-01	9.91E+00	2.16E+00	1.21E+01	0.42	1.21E-08
C07	2100	4.38	6.57E-01	1.14E+01	2.73E+00	1.41E+01	0.49	1.41E-08
C08	2400	4.45	6.68E-01	1.16E+01	3.39E+00	1.50E+01	0.52	1.50E-08

Table A3.1 – Sample Calculation for D-[1-^{14}C]Mannitol transport.

A3.2 GATIFLOXACIN

Sample calculation for Gatifloxacin (10 μM)Transport

		Vd (μl)	Vr (μl)	Sample (μl)	Vd Conc (μg.ml^{-1})	Vd Amount (ng)		
		1500	2600	150	3.75	5625.00		
Well	Time (s)	Vr Conc (ng.ml^{-1})	Amount removed (ng)	Amount in Vr (ng)	Cumulative Amount removed (ng)	Corrected Amount Vr (ng)	% Flux	Amount (g)
A01	300	1.60	0.24	4.17	0.00	4.17	0.07	4.17E-09
A02	600	4.67	0.70	12.14	0.24	12.38	0.22	1.24E-08
A03	900	8.39	1.26	21.80	0.94	22.74	0.40	2.27E-08
A04	1200	12.25	1.84	31.85	2.20	34.05	0.61	3.41E-08
A05	1500	23.57	3.53	61.27	4.04	65.31	1.16	6.53E-08
A06	1800	27.39	4.11	71.22	7.57	78.79	1.40	7.88E-08
A07	2100	32.29	4.84	83.95	11.68	95.63	1.70	9.56E-08
A08	2400	37.06	5.56	96.37	16.52	112.89	2.01	1.13E-07
B01	300	1.46	0.22	3.79	0.00	3.79	0.07	3.79E-09
B02	600	4.86	0.73	12.63	0.22	12.85	0.23	1.29E-08
B03	900	9.73	1.46	25.30	0.95	26.24	0.47	2.62E-08
B04	1200	15.53	2.33	40.37	2.41	42.78	0.76	4.28E-08
B05	1500	26.15	3.92	67.99	4.74	72.72	1.29	7.27E-08
B06	1800	33.50	5.02	87.09	8.66	95.75	1.70	9.58E-08
B07	2100	29.53	4.43	76.79	13.68	90.47	1.61	9.05E-08
B08	2400	45.98	6.90	119.54	18.11	137.65	2.45	1.38E-07
C01	300	3.46	0.52	8.98	0.00	8.98	0.16	8.98E-09
C02	600	7.23	1.08	18.79	0.52	19.31	0.34	1.93E-08
C03	900	11.26	1.69	29.28	1.60	30.88	0.55	3.09E-08
C04	1200	16.97	2.55	44.13	3.29	47.43	0.84	4.74E-08
C05	1500	29.58	4.44	76.91	5.84	82.75	1.47	8.28E-08
C06	1800	31.17	4.68	81.03	10.28	91.31	1.62	9.13E-08
C07	2100	36.89	5.53	95.90	14.95	110.85	1.97	1.11E-07
C08	2400	47.79	7.17	124.26	20.48	144.74	2.57	1.45E-07

Table A3.2 – Sample calculation for gatifloxacin transport.

A3.3 FORMULAE USED

		Vd (μl) 1500	Vr (μl) 2600	Sample (μl) 150	Vd Conc (μg.ml⁻¹) 3.75	Vd Amount (ng) 5625.00		
Well	Time (s)	Vr Conc (ng.ml⁻¹)	Amount removed (ng)	Amount in Vr (ng)	Cumulative Amount removed (ng)	Corrected Amount Vr (ng)	% Flux	Amount (g)
A01	5	=C8/1000	=D8*$E$2	=(E8/$E$2)*$C$2	=E7+G7	=F8+G8	=(H8/$H$3)*100	=(H8/1000000000)/2.6
A02	10	=C9/1000	=D9*$E$2	=(E9/$E$2)*$C$2	=E8+G8	=F9+G9	=(H9/$H$3)*100	=(H9/1000000000)/2.6
A03	15	=C10/1000	=D10*$E$2	=(E10/$E$2)*$C$2	=E9+G9	=F10+G10	=(H10/$H$3)*100	=(H10/1000000000)/2.6
A04	20	=C11/1000	=D11*$E$2	=(E11/$E$2)*$C$2	=E10+G10	=F11+G11	=(H11/$H$3)*100	=(H11/1000000000)/2.6
A05	25	=C12/1000	=D12*$E$2	=(E12/$E$2)*$C$2	=E11+G11	=F12+G12	=(H12/$H$3)*100	=(H12/1000000000)/2.6
A06	30	=C13/1000	=D13*$E$2	=(E13/$E$2)*$C$2	=E12+G12	=F13+G13	=(H13/$H$3)*100	=(H13/1000000000)/2.6
A07	35	=C14/1000	=D14*$E$2	=(E14/$E$2)*$C$2	=E13+G13	=F14+G14	=(H14/$H$3)*100	=(H14/1000000000)/2.6
A08	40	=C15/1000	=D15*$E$2	=(E15/$E$2)*$C$2	=E14+G14	=F15+G15	=(H15/$H$3)*100	=(H15/1000000000)/2.6
B01	5	=C17/1000	=D17*$E$2	=(E17/$E$2)*$C$2	=E16+G16	=F17+G17	=(H17/$H$3)*100	=(H17/1000000000)/2.6
B02	10	=C18/1000	=D18*$E$2	=(E18/$E$2)*$C$2	=E17+G17	=F18+G18	=(H18/$H$3)*100	=(H18/1000000000)/2.6
B03	15	=C19/1000	=D19*$E$2	=(E19/$E$2)*$C$2	=E18+G18	=F19+G19	=(H19/$H$3)*100	=(H19/1000000000)/2.6
B04	20	=C20/1000	=D20*$E$2	=(E20/$E$2)*$C$2	=E19+G19	=F20+G20	=(H20/$H$3)*100	=(H20/1000000000)/2.6
B05	25	=C21/1000	=D21*$E$2	=(E21/$E$2)*$C$2	=E20+G20	=F21+G21	=(H21/$H$3)*100	=(H21/1000000000)/2.6
B06	30	=C22/1000	=D22*$E$2	=(E22/$E$2)*$C$2	=E21+G21	=F22+G22	=(H22/$H$3)*100	=(H22/1000000000)/2.6
B07	35	=C23/1000	=D23*$E$2	=(E23/$E$2)*$C$2	=E22+G22	=F23+G23	=(H23/$H$3)*100	=(H23/1000000000)/2.6
B08	40	=C24/1000	=D24*$E$2	=(E24/$E$2)*$C$2	=E23+G23	=F24+G24	=(H24/$H$3)*100	=(H24/1000000000)/2.6

Table A3.3 – Sample formulae used.

APPENDIX A4- MORIGUCHI LOGP CALCULATIONS

Quinolone	CX	NO	PRX	UB	HB	POL	RNG	Moriguchi logP
BMS 284756-01	24	6	5	9	1	3	1	4.344
Cinoxacin	12	7	4	6	1	2	1	0.295
Ciprofloxacin	17.5	6	2	6	1	4	1	2.182
Butyl-Ciprofloxacin	21.5	6	2	6	1	4	1	3.092
Ethyl-Ciprofloxacin	19.5	6	2	6	1	4	1	2.646
Methyl-Ciprofloxacin	18.5	6	2	6	1	4	1	2.416
Pentyl-Ciprofloxacin	22.5	6	2	6	1	4	1	3.309
Propyl-Ciprofloxacin	20.5	6	2	6	1	4	1	2.872
Enoxacin	15.5	7	4	6	1	4	0	2.140
Flumequine	14.5	4	2	6	1	3	0	3.126
Gatifloxacin	19.5	7	2	6	1	4	1	1.887
Levofloxacin	18.5	7	2	6	1	4	0	2.049
Lomefloxacin	17.5	6	2	6	1	4	0	2.574
Nalidixic Acid	12	5	4	6	1	2	0	2.218
Norfloxacin	16.5	6	2	6	1	4	0	2.333
Ofloxacin	18.5	7	2	6	1	4	0	2.049
Sparfloxacin	20	7	2	6	1	4	1	2.000
Fluoroscein	20	5	2	10	0	3	0	2.838

Table A4.1 – Moriguchi logP calclulations

APPENDIX A5 - CALCULATED PHYSICOCHEMICAL PROPERTIES

A5.1 NEUTRAL MOLECULES

	M_R Da	MR Viswanad $cm^3 mol^{-1}$	IP eV	Dipole M D	Dipole M COSMO D	Dipole M Ratio	ΔH_f in vacuo kcal mol^{-1}	ΔH_f COSMO kcal mol^{-1}	ΔH_f Difference kcal mol^{-4}
BMS 284756-01	444.41	110.98	9.013	5.163	8.889	0.581	-214.897	-246.034	-31.137
Cinoxacin	262.22	63.10	9.033	5.815	10.269	0.566	-127.231	-152.236	-25.004
Ciprofloxacin	331.34	87.94	8.829	6.972	12.053	0.578	-98.069	-127.690	-29.621
Butyl-Ciprofloxacin	387.45	107.11	8.769	7.260	12.508	0.580	-116.356	-145.327	-28.971
Ethyl-Ciprofloxacin	359.39	97.98	8.935	6.644	10.905	0.609	-102.755	-130.976	-28.221
Methyl-Ciprofloxacin	345.37	93.23	8.978	6.581	11.268	0.584	-100.434	-129.412	-28.978
Pentyl-Ciprofloxacin	401.47	111.71	8.766	6.656	11.269	0.591	-121.116	-149.076	-27.960
Propyl-Ciprofloxacin	373.42	102.51	8.761	6.651	10.782	0.617	-111.179	-139.169	-27.989
Enoxacin	320.32	83.95	8.889	5.858	9.909	0.591	-125.603	-153.240	-27.638
Enrofloxacin	359.40	96.45	8.797	6.273	10.173	0.617	-101.737	-129.977	-28.240
Flumequine	261.26	67.87	8.810	7.122	12.213	0.583	-140.582	-165.690	-25.107
Gatifloxacin	375.40	98.82	9.000	6.156	10.909	0.564	-131.256	-159.887	-28.632
Levofloxacin	361.38	94.94	8.979	6.401	10.895	0.588	-160.402	-189.775	-29.372
Lomefloxacin	351.35	90.11	9.056	4.163	7.628	0.546	-169.012	-195.554	-26.543
Nalidixic Acid	232.20	63.13	8.927	5.252	9.021	0.582	-95.177	-119.433	-24.257
Norfloxacin	319.34	85.48	8.806	7.030	11.764	0.598	-129.557	-158.389	-28.831
Ofloxacin	361.38	94.94	8.911	6.065	10.418	0.582	-160.559	-189.498	-28.939
Sparfloxacin	393.42	101.69	8.602	4.495	8.170	0.550	-143.999	-170.772	-26.772
Fluoroscein	332.30	88.50	9.098	5.156	7.980	0.646	-110.548	-132.756	-22.208

Table A5.1a – Molecular descriptors for neutral molecules

	VDW Solvation A²	Connolly Access A²	1.4A Mol Area A²	H₂O SolExcl V A³	Ovality 1.4A	Connolly Access A A²	2.5A Mol Area A²	DMSO SolExcl V A³	Ovality 2.5A
BMS 284756-01	174.636	639.105	364.305	337.909	1.553	847.046	847.046	375.428	1.421
Cinoxacin	116.529	436.911	223.275	183.786	1.428	623.218	223.627	194.699	1.377
Ciprofloxacin	141.984	529.692	290.261	259.588	1.473	729.849	288.198	277.980	1.399
Butyl-Ciprofloxacin	169.570	644.598	360.598	330.234	1.562	873.411	357.972	353.465	1.481
Ethyl-Ciprofloxacin	153.869	586.474	326.805	298.620	1.513	799.606	324.412	319.132	1.436
Methyl-Ciprofloxacin	147.347	553.799	306.905	279.571	1.484	758.626	304.796	298.475	1.411
Pentyl-Ciprofloxacin	175.487	667.538	376.358	346.821	1.577	866.853	372.786	372.638	1.489
Propyl-Ciprofloxacin	161.162	613.450	342.477	313.671	1.534	833.370	339.879	335.852	1.455
Enoxacin	135.987	509.137	278.065	250.901	1.445	703.960	275.721	268.624	1.369
Enrofloxacin	155.295	584.237	324.905	292.059	1.526	798.702	322.172	311.733	1.449
Flumequine	113.063	425.532	224.130	194.753	1.379	606.029	223.024	204.534	1.328
Gatifloxacin	152.484	575.376	323.767	305.843	1.475	780.008	320.622	328.564	1.392
Levofloxacin	148.832	568.038	314.859	288.371	1.492	774.421	312.304	310.670	1.408
Lomefloxacin	142.868	541.480	297.284	272.281	1.463	746.663	295.045	290.059	1.392
Nalidixic Acid	111.767	426.932	220.577	181.266	1.424	606.541	220.318	193.351	1.362
Norfloxacin	138.009	518.543	283.032	249.822	1.475	717.656	280.655	266.947	1.400
Ofloxacin	148.741	565.972	314.432	289.530	1.486	772.477	311.203	311.100	1.402
Sparfloxacin	158.249	600.432	335.092	303.854	1.533	811.683	331.646	330.279	1.435
Fluoroscein	140.456	505.428	270.888	239.167	1.454	703.053	268.504	256.916	1.374

Table A5.1b – Molecular descriptors for neutral molecules

	Charges cOH	cOOH COSMO	cOH Diff	coOH	coOH COSMO	coOH Diff	Ccooh	Ccooh COSMO	Ccooh Diff	N	N COSMO	Charges N Diff	0 eV	Polarisability α-XX COSMO	AU Diff
BMS 284756-01	-0.425	-0.560	-0.134	-0.305	-0.346	-0.041	-0.350	-0.451	-0.101	-0.125	-0.214	-0.088	341.523	0	-341.523
Cinoxacin	-0.387	-0.558	-0.171	-0.315	-0.340	-0.024	-0.235	-0.324	-0.089	0.000	0.000	0.000	199.822	0	-199.822
Ciprofloxacin	-0.417	-0.593	-0.176	-0.307	-0.345	-0.038	-0.330	-0.458	-0.128	-0.104	-0.192	-0.088	264.901	0	-264.901
Butyl-Ciprofloxacin	-0.417	-0.590	-0.173	-0.308	-0.346	-0.038	-0.330	-0.457	-0.127	-0.092	-0.115	-0.023	305.160	0	-305.160
Ethyl-Ciprofloxacin	-0.425	-0.593	-0.168	-0.306	-0.346	-0.040	-0.337	-0.448	-0.111	-0.095	-0.150	-0.055	288.869	0	-288.869
Methyl-Ciprofloxacin	-0.425	-0.602	-0.176	-0.305	-0.344	-0.039	-0.335	-0.455	-0.121	-0.091	-0.157	-0.066	279.530	0	-279.530
Pentyl-Ciprofloxacin	-0.425	-0.600	-0.174	-0.305	-0.345	-0.040	-0.335	-0.454	-0.119	-0.093	-0.139	-0.046	319.341	0	-319.341
Propyl-Ciprofloxacin	-0.425	-0.589	-0.164	-0.305	-0.347	-0.041	-0.335	-0.444	-0.109	-0.092	-0.150	-0.058	298.729	0	-298.729
Enoxacin	-0.416	-0.588	-0.172	-0.308	-0.345	-0.037	-0.328	-0.444	-0.116	-0.110	-0.188	-0.078	263.176	0	-263.176
Enrofloxacin	-0.421	-0.591	-0.170	-0.306	-0.345	-0.039	-0.328	-0.432	-0.104	-0.102	-0.154	-0.052	303.183	0	-303.183
Flumequine	-0.424	-0.596	-0.172	-0.304	-0.346	-0.041	-0.342	-0.462	-0.120	0.000	0.000	0.000	186.296	0	-186.296
Gatifloxacin	-0.427	-0.601	-0.174	-0.304	-0.346	-0.043	-0.337	-0.446	-0.109	-0.109	-0.193	-0.084	266.649	0	-266.649
Levofloxacin	-0.426	-0.600	-0.174	-0.305	-0.347	-0.042	-0.337	-0.454	-0.117	-0.094	-0.155	-0.061	262.601	0	-262.601
Lomefloxacin	-0.410	-0.586	-0.175	-0.311	-0.344	-0.034	-0.330	-0.450	-0.121	-0.105	-0.184	-0.078	263.197	0	-263.197
Nalidixic Acid	-0.420	-0.596	-0.175	-0.308	-0.344	-0.036	-0.338	-0.449	-0.111	-0.147	-0.205	-0.058	187.301	0	-187.301
Norfloxacin	-0.422	-0.596	-0.174	-0.307	-0.345	-0.038	-0.334	-0.457	-0.123	-0.115	-0.191	-0.076	265.511	0	-265.511
Ofloxacin	-0.427	-0.598	-0.171	-0.304	-0.347	-0.043	-0.336	-0.451	-0.115	-0.096	-0.154	-0.058	262.412	0	-262.412
Sparfloxacin	-0.406	-0.578	-0.172	-0.316	-0.345	-0.029	-0.334	-0.447	-0.112	-0.122	-0.180	-0.059	298.145	0	-298.145
Fluoroscein													211.045	0	-211.045

Table A5.1c – Molecular descriptors for neutral molecules

A5.2 ZWITTERIONIC MOLECULES

	Dipole M D	Dipole M COSMO D	Dipole M Ratio	ΔH_f in vacuo kcal mol^{-1}	ΔH_f COSMO Kcal mol^{-1}	ΔH_f Difference kcal mol^{-4}
BMS 284756-01	48.451	64.363	0.753	-122.406	-248.422	126.016
Ciprofloxacin	46.937	61.883	0.758	0.182	-131.233	131.415
Butyl-Ciprofloxacin	42.388	62.218	0.681	-17.959	-139.373	121.414
Ethyl-Ciprofloxacin	45.445	60.313	0.753	-7.413	-126.667	119.254
Methyl-Ciprofloxacin	47.556	61.363	0.775	0.951	-122.605	123.556
Pentyl-Ciprofloxacin	48.691	62.304	0.782	-23.626	-144.361	120.735
Propyl-Ciprofloxacin	48.163	62.301	0.773	-12.434	-134.011	121.577
Enoxacin	39.412	56.547	0.697	-32.442	-158.482	126.040
Enrofloxacin	46.673	60.647	0.770	-5.837	-124.207	118.370
Gatifloxacin	45.837	60.115	0.762	-39.474	-163.219	123.745
Levofloxacin	43.263	58.413	0.741	-64.475	-184.103	119.628
Lomefloxacin	43.898	58.584	0.749	-74.957	-199.653	124.696
Norfloxacin	46.862	60.823	0.770	-32.156	-162.516	130.360
Ofloxacin	46.281	60.350	0.767	-66.382	-186.378	119.996
Sparfloxacin	44.952	58.918	0.763	-57.038	-174.560	117.522

Table A5.2a – Molecular descriptors for zwitterionic form.

	VDW Solvation A^2	Connolly Access A A^2	1.4A Mol Area A^2	H_2O SolExcl V A^3	Ovality 1.4A
BMS 284756-01	175.960	653.547	366.344	333.322	1.576
Ciprofloxacin	142.615	533.137	291.513	260.126	1.479
Butyl-Ciprofloxacin	169.091	646.172	361.884	331.525	1.562
Ethyl-Ciprofloxacin	155.255	587.934	327.784	303.622	1.500
Methyl-Ciprofloxacin	148.548	559.683	309.015	281.252	1.489
Pentyl-Ciprofloxacin	175.489	669.331	377.072	348.068	1.576
Propyl-Ciprofloxacin	161.748	615.731	343.362	314.309	1.536
Enoxacin	136.516	507.636	277.536	251.645	1.440
Enrofloxacin	154.738	583.199	324.324	292.490	1.522
Gatifloxacin	153.166	578.901	325.025	306.374	1.479
Levofloxacin	144.591	549.735	306.545	291.170	1.443
Lomefloxacin	142.972	541.673	296.996	271.655	1.464
Norfloxacin	138.005	519.081	283.061	250.788	1.472
Ofloxacin	149.136	567.999	315.307	291.111	1.484
Sparfloxacin	158.413	599.914	335.289	304.861	1.531

Table A5.2b – Molecular descriptors for zwitterionic form.

225

	cO$_o$-	cO$_o$-COSMO	cO$_o$-Diff	coO-	coO-COSMO	coO-Diff	C$_{coo}$-	C$_{coo}$-COSMO	C$_{coo}$-Diff	N$^+$	N$^+$COSMO	N$^+$Diff
BMS 284756-01	-0.605	-0.775	0.169	-0.587	-0.772	0.184	0.558	0.950	-0.392	0.590	0.639	-0.049
Ciprofloxacin	-0.601	-0.781	0.180	-0.594	-0.775	0.181	0.557	0.653	-0.096	0.640	0.661	-0.021
Butyl-Ciprofloxacin	-0.601	-0.780	0.179	-0.595	-0.775	0.180	0.557	0.653	-0.096	0.570	0.567	0.003
Ethyl-Ciprofloxacin	-0.600	-0.779	0.178	-0.592	-0.777	0.185	0.558	0.655	-0.097	0.598	0.578	0.020
Methyl-Ciprofloxacin	-0.601	-0.777	0.176	-0.595	-0.775	0.180	0.557	0.650	-0.093	0.588	0.583	0.005
Pentyl-Ciprofloxacin	-0.601	-0.780	0.179	-0.595	-0.776	0.181	0.557	0.654	-0.097	0.562	0.560	0.002
Propyl-Ciprofloxacin	-0.601	-0.782	0.180	-0.595	-0.775	0.180	0.557	0.653	-0.096	0.570	0.566	0.004
Enoxacin	-0.598	-0.778	0.181	-0.585	-0.774	0.189	0.558	0.651	-0.093	0.654	0.665	-0.011
Enrofloxacin	-0.597	-0.776	0.180	-0.591	-0.774	0.183	0.556	0.650	-0.094	0.557	0.557	0.000
Gatifloxacin	-0.598	-0.779	0.181	-0.597	-0.775	0.178	0.559	0.654	-0.095	0.619	0.627	-0.009
Levofloxacin	-0.601	-0.783	0.182	-0.559	-0.774	0.215	0.557	0.654	-0.097	0.615	0.595	0.020
Lomefloxacin	-0.601	-0.777	0.176	-0.591	-0.775	0.184	0.559	0.653	-0.094	0.627	0.653	-0.026
Norfloxacin	-0.604	-0.776	0.172	-0.591	-0.774	0.183	0.557	0.651	-0.095	0.634	0.658	-0.024
Ofloxacin	-0.602	-0.782	0.180	-0.592	-0.773	0.181	0.557	0.653	-0.097	0.581	0.577	0.003
Sparfloxacin	-0.598	-0.778	0.181	-0.596	-0.774	0.178	0.561	0.654	-0.092	0.587	0.587	0.001

Table A5.2c – Molecular descriptors for zwitterionic form.